Development of Molecular Spur Gears

and

Toward the Stepwise Synthesis of a Molecular Borromean Link

Dissertation zur Erlangung
der naturwissenschaftlichen Doktorwürde
(Dr. sc. nat.)

vorgelegt der
Mathematisch-naturwissenschaftlichen Fakultät
der Universität Zürich

von

Derik Kent Frantz
aus den USA

Promotionskomitee
Prof. Dr. Jay S. Siegel (Vorsitz)
Prof. Dr. Kim K. Baldridge
Prof. Dr. Roger Alberto
Prof. Dr. Jean-Pierre Sauvage

Zürich, 2012

Die vorliegende Arbeit wurde von
der Mathematisch-naturwissenschaflichen Fakultät
der Universität Zürich im März 2012
als Dissertation angenommen

Promotionskomitee:

Jay S. Siegel, Vorsitz

Kim K. Baldridge

Roger Alberto

Jean-Pierre Sauvage

Universität Zürich
Zürich, Schweiz 2012

To Alan and Diane Richard

In memoriam:

Thelma I. Rineer (19 July 1940 – 17 January 2010)

W. Cary Quillin (16 April 1953 – 29 March 2009)

Acknowledgment

After completing a guest studentship, a master's degree, and now a doctoral dissertation, my time in Zurich—six years in total—is coming to an end. It is with bittersweet sentiment that I now reflect on all of the people who have made this tenure such a wonderful and enriching experience and to whom I must soon bid farewell.

I am most indebted to my research advisor, Jay Siegel. I first met him at a meeting in the summer of 2004, where I asked if he would be willing to take me on as an applicant for a Fulbright fellowship. He accepted and I began working under his supervision in January 2006. Graciously, he later accepted me into his group as a master's student and as a doctoral candidate. His enthusiasm in my projects never waned and he never ceased to motivate me, to challenge me, and to support me. He has always shown a deep and genuine interest in my professional development by encouraging me to develop my own creativity and perspective on chemistry, by sending me to international conferences, and by laying the foundation for my future career. I am truly grateful for all that he has done for me

I have enjoyed a fruitful collaboration with Kim Baldridge, whose unsurpassed ability to calculate structures and energies of complicated molecules provided inspiration for the spur gear project given in Section One of this thesis. In addition to the scientific collaboration, she has been a solid rock of support throughout my studies.

Nat Finney has also been a constant source of support and inspiration since I arrived in Zurich. He has always been excited to discuss chemistry and his encyclopedic knowledge of synthesis often helped me to overcome challenges in the laboratory. Special thanks go to David Reingold. As my undergraduate advisor at Juniata College, he introduced me to Prof. Siegel and forged my path to Zurich. I have been fortunate to develop friendships with professors Volkan Kısakürek and Ehud Landau, with whom I have, on multiple occasions, indulged in fun-filled evenings.

I am thankful to the NMR, MS, and crystallography groups and services. In particular, I want to thank Thomas Fox, who, as a scientific assistant in the Inorganic Chemistry Institute, was under absolutely no obligation to help me, but provided invaluable assistance with variable temperature NMR measurements. Simon Jurt and Nadja Bross have been incredibly helpful in solving problems that have arisen with NMR spectrometers. Laurent Bigler, Urs Stalder, and Jean-Christophe Prost have

expertly measured a multitude of MS spectra for me. I am grateful to Anthony Linden, and Sascha Blumentritt, who solved a critical crystal structure for my doctoral thesis and many structures in my master's work.

The secretarial staff in the OCI is second to none and has solved many, many problems for me. I thank Sarah Amman, Salomé Fässler, Christa Werner, Cornelia Moor, Marie-Therese Bohley, and Marianne Grima for their willingness to help with a variety of issues.

Of course, I have been surrounded by a team of excellent chemists whom I have regularly consulted for chemical advice and who have made the lab a great place to work. Rather than list a complete list of names with everyone I have enjoyed working with, I will highlight a few coworkers who have been especially instrumental in my personal and professional development: Silvia Rocha, who has been a great friend and colleague for many years; Simon Duttwyler, who is the best chemist I have met so far and who allowed a small portion of his brilliance to rub off on me; Yoshizumi Yasui, who mentored me when I arrived and initiated my early work; Jui-Chang (Swen) Tseng, who offered a treasure trove of practical advice; Roman Maag, with whom I have had many chemical discussions that led to many solutions; Arif Karim, who helped me immensely in my early years in Zurich; and Helen Seifert, who worked side-by-side with me over the past year on the Borromean link project.

In addition to those mentioned above, I have made close friends in the University of Zurich, in particular: Mike Packard, Anne Bowen, Anna Butterfield, Oliver Allemann, Becky Abramson, Eoin Quinlan, Anna Véron, Karla Arias, Paola Romanato, Davide Bandera, Michele Gatti, Jeremy Klosterman, Fabián Cuétara, Imke Schubert, Rolf Sigrist, Michael Löpfe, Ashley Sullivan, Mireille Vonlanthen, Benno Bischof, Daphne Diemer, Fitore Kasumaj, Yohann Potier, Celine Amoreira, Martin Mattarella, Fabienne Furrer, Dominic Tscherrig, Jérôme Ungricht, Xinjun Luan, Alexander Szentkuti, Michael Felber, Sebastian Imstepf, and Sara Da Ros.

I thank Cary Quillin,† James Ellerbee, Bruce Davie, Huw Davies, Olan Duran, André Mebold, and Tom Grieve, who have helped me properly organize my priorities in life.

I thank Helmut and David Papst for offering a place for me to stay when I first arrived in Zurich.

For their infinite and constant love and support, I thank my parents, Alan and Diane Richard, and the rest of my family.

I am especially grateful to Tilana Silva for her patience, compassion, dedication, and love, especially during the rough patches.

Finally, I wish to thank Jay Siegel, Kim Baldridge, Roger Alberto, and Jean-Pierre Sauvage, for their willingness to be part of my *Promotionskomitee*. Special thanks go to Robert Pascal for serving as an external reviewer.

ABSTRACT

Development of Molecular Spur Gears
and Toward the Stepwise Synthesis of a Molecular Borromean Link
by
Derik Kent Frantz
University of Zurich, 2012
Prof. Dr. Jay S. Siegel, Chair

Abstract of Section One

Molecular rotors, devices, and machines represent nanoscopic miniaturizations of macroscopic mechanical constructs. Among the most ubiquitous contrivances in machinery is the gear, which transfers rotational force from one axis to another or into translational motion. Dynamic gearing has been demonstrated in several molecules comprising sterically crowded, intermeshed molecular rotators that are held in a bent arrangement, a framework that resembles bevel gears. Holding two peripherally bladed gears side-by-side in a collateral orientation, the spur gear is the most common type of gear in macroscopic machinery. Dynamic gearing has yet to be demonstrated in molecular spur gears. Using a combination of molecular design, computation, synthesis, structural investigations, and dynamic NMR, Section One of this thesis aims at understanding the behavior of molecular spur gears based on triptycene.

Conformational analysis shows that steric interactions and strain, which drive the gearing behavior of molecular bevel gears, do not favor geared rotation in triptycene-based molecular spur gears. Instead, computational evidence indicates that van der Waals attractions favor gearing conformations and that hydrogen–hydrogen repulsion disfavors gear-clashed conformations in these systems, the net result being that geared rotation is preferred over gear slippage.

To experimentally test this prediction, a series spur gear derivatives of 4,4'-bis(triptycene-9-ylethynyl)-2,2'-bibenzimidazole were synthesized, including desymmetrized derivatives, which were expected to exhibit phase isomerism under conditions in which gear slippage is slow and geared rotation is fast. These phase

isomers were sought at low temperature using dynamic NMR experiments, but were not observed, most likely due to the low barriers to gear slippage (7–8 kcal/mol) that lie at the detection limit of this experimental method. X-ray crystallographic analysis of a molecular spur gear revealed a structure that closely matched the calculated structure of a gear-meshed conformation.

Abstract of Section Two

The Borromean link is a topological system in which three rings interlock in such a way that breakage of one of the rings allows the other two to separate. The link has been used for (at least) a millennium as a symbol of strength in unity and has fascinated knot theorists for over 130 years. As chemists began to generate catenanes and rotaxanes through statistical and directed pathways, the synthesis of a Borromean link quickly became a sort of "holy grail" of molecular topology. Since then, molecular Borromean links have been synthesized by DNA nanotechnology and directed assembly approaches, but a stepwise synthesis remains elusive. The critical step in the stepwise synthesis of a molecular Borromean link is the formation of a ring-in-ring complex that is templated with two units that serve as parts of the final, third ring. Previous attempts to form this interlocked structure by a threading approach have failed.

Two new strategies were attempted to overcome this problem and reach the desired synthetic intermediate. The first of these sought to introduce a pre-templated cap, which, upon coupling to a templated macrocycle, would serve as a cap to the second ring and a linear unit that is part of the third ring. Design and modeling indicated that thioketals would serve well as templating motifs and a synthesis of this construct was completed. The second strategy aimed at overcoming the problem of threading by introducing small, dumbbell-shaped molecules into the desired topological positions by an activated template method. Until this point, both methods have been unsuccessful in generating a templated, ring-in-ring complex, though there is room for much more experimentation. Another, highly symmetric, molecular Borromean link construct in which all of the templating linkers are thioketals was also envisioned. Initial synthesis of building blocks was successful.

ZUSAMMENFASSUNG

Development of Molecular Spur Gears
and Toward the Stepwise Synthesis of a Molecular Borromean Link

von
Derik Kent Frantz
Universität Zürich, 2012
Prof. Dr. Jay S. Siegel, Vorsitz

Zusammenfassung von Teil Eins

Molekulare Rotoren und Maschinen sind nanoskopische Abbilder der makroskopischen mechanischen Konstrukte. Zu den gängigsten Maschinenbauteilen gehört das Zahnrad, welches die Drehkraft von einer Achse zu anderen Achsen oder in translatorische Bewegung transferiert. Einige Moleküle, welche sterisch anspruchsvolle Rotatoren besitzen, weisen eine verzahnte Rotation auf. Solche Moleküle hatten bisher verwinkelte Rotationsachsen. Diese Ausrichtung der Rotatoren ist jener von Kegelzahnrädern sehr ähnlich. Im Gegensatz dazu haben Stirnzahnräder parallele Rotationsachsen, die häufigste Art von Zahnrädern, welche in makroskopischen Maschinen vorkommt. Dynamische verzahnte Rotation in molekularen Stirnzahnrädern konnte bis anhin noch nicht nachgewiesen werden. Mit einer Kombination aus molekularem Design, Berechnung, Synthese, Strukturaufklärung und dynamischen NMR Messungen wird in dieser Arbeit die Bestimmung des Verhaltens von molekularen Stirnzahnrädern, basierend auf Triptycen, untersucht.

Die Konformationsanalyse zeigt, dass sterische Wechselwirkungen und Spannung, welche das Verhalten von molekularen Kegelzahnrädern antreiben, verzahnte Rotation in Triptycen-basierten Stirnzahnrädern nicht bevorzugen. Stattdessen zeigen Computersimulationen, dass van der Waals-Anziehungen die verzahnte Konformationen begünstigen und Wasserstoff–Wasserstoff-Abstossungen das Energieniveau der unverzahnten Konformationen erhöhen. Dieses Ergebnis zeigt,

dass in solchen Systemen verzahnte Rotation gegenüber unverzahnter Rotation bevorzugt sein sollte.

Um diese Vorhersage experimentell zu prüfen, wurde eine Serie von Stirnzahnrädern, basierend auf 4,4'-Bis(tripytcen-9-ylethinyl)-2,2'-bibenzimidazol, synthetisiert. Diese beinhalteten auch desymmetrisierte Derivate, welche voraussichtlich Phasenisomerie aufweisen würden, unter Bedingungen, in denen verzahnte Rotation schnell und unverzahnte Rotation langsam geschieht. Die Phasenisomere wurden bei niedriger Temperatur durch dynamische NMR-Experimente nachzuweisen versucht, aber konnten nicht beobachtet werden, wahrscheinlich aufgrund der niedrigen Energiebarriere für unverzahnte Rotation (7-8 kcal/mol), die an der Nachweisgrenze dieser experimentellen Methode liegt. Die Röntgenstrukturanalyse eines molekularen Stirnzahnrads ergab eine Struktur, die mit der berechneten Struktur einer verzahnten Konformation gut übereinstimmte.

Zusammenfassung von Teil Zwei

Die Borromäischen Ringe sind ein topologisches System, in dem drei Ringe in einander verkettet sind, so dass durch den Bruch einer der Ringe die beiden anderen getrennt werden können. Der Link wurde (mindestens) ein Jahrtausend lang als Symbol der Stärke durch Einheit verwendet und hat Mathematiker seit über 130 Jahren fasziniert. Als Chemiker Catenane und Rotaxane durch statistische und gezielte Methoden herzustellen begannen, ist die Synthese eines Borromäischen Links zu einer Art "heiligen Grals" der molekularen Topologie geworden. Seitdem wurden molekulare Borromäische Links durch DNA-Nanotechnologie und Assemblierung synthetisiert, aber eine schrittweise Synthese bleibt unentdeckt. Der entscheidende Schritt im stufenweisen Aufbau eines molekularen Borromäischen Links ist die Bildung eines Ring-im-Ring-Komplexes, welcher zwei Teile beinhaltet, die Bestandteil des abschliessenden, dritten Rings sind. Frühere Versuche, diese verkettete Struktur durch eine Art Einfädeln zu bilden, sind gescheitert.

Zwei neue Strategien wurden entwickelt, um dieses Problem zu überwinden und zu den gewünschten Zwischenprodukten zu gelangen. Die eine Methode beruht darauf eine vorgeformte Kappe einzuführen, die bei der Verbindung mit einem Makrozyklus, als Kappe für den zweiten Ring und als lineare Einheit für den dritten Ring dient. Design und Betrachtung von Modellen zeigten, dass Thioketale gut als Verbindungsstücke

passen würden. Die Synthese einer vorgeformten Kappe basierend auf einem Thioketal wurde durchgeführt. Die zweite Strategie zur Überwindung des Problems des Einfädelns beabsichtigte die Einführung von kleinen hantelförmigen Molekülen in die topologisch gewünschten Positionen durch eine „activated template method“. Bis zu diesem Zeitpunkt war keine der beiden Methoden von Erfolg gekrönt. Dafür wären weitere Versuche nötig. Ein weiterer, hoch-symmetrischer molekularer Borromäischer Link, bei dem alle Verbindungsstücke Thioketale sind, wurde auch in Betracht gezogen. Die Synthese von ersten Bausteinen war erfolgreich.

Table of Contents

SECTION ONE: Development of Molecular Spur Gears

Chapter 1. From Correlated Rotation to Gearing at the Molecular Level 2
1.1. Introduction to Molecular Rotors and Gears 2
1.1.1. Introduction 2
1.1.2. Nomenclature 3
1.1.3. Scope of this Chapter 5
1.2. Interacting Two-Bladed Propellers 5
1.2.1. Introduction 5
1.2.2. Two Two-Bladed Propellers in a Coaxial Arrangement 6
1.2.3. Two Two-Bladed Propellers in a Bent Arrangement 10
1.2.4. Three Two-Bladed Propellers in a Bent Arrangement 12
1.2.5. More than Three Two-Bladed Rotators in Bent Arrangements 18
1.2.6. Two Two-Bladed Rotators in a Collateral Arrangement 18
1.3. Triptycene: A Shape-Persistent, Three-Bladed Molecular Rotator 19
1.3.1. Introduction 19
1.3.2. Triptycene Interacting with Non-Triptycene Rotators 20
1.4. Interacting Triptycene Rotators 25
1.4.1. Two Triptycenes in a Coaxial Arrangement 25
1.4.2. Two Triptycenes in a Bent Arrangement 26
1.4.3. Three Tripytcenes in a Bent Arrangement 32
1.4.4. Two Triptycenes in a Collateral Arrangement 33
1.5. Other Molecular Gear Constructs 34
1.6. Evaluating the Efficiency of Molecular Gears 35
1.7. Goal of this Section 36

Chapter 2. Triptycene-Based Molecular Spur Gears 37
2.1. Summary 37
2.2. Introduction 37
2.3. Conformational Analysis and Molecular Design 38
2.4. Computational Results 43
2.5. Synthesis of Molecular Spur Gears Based on 2,2'-Bibenzimidazole 47
2.5.1. Retrosynthetic analysis 47
2.5.2. Synthesis of Stator Unit 48
2.5.3. Synthesis of Rotator/Axle Components 48
2.5.4. Synthesis of Ethylene-Bridged Spur Gears 50
2.5.5. Synthesis of Spur Gears with Planar Stators 50
2.6. X-ray Structure of a Molecular Spur Gear 51
2.7. Variable-Temperature NMR Studies 52
2.8. Conclusions and Outlook 56

SECTION TWO: Toward the Stepwise Synthesis of a Molecular Borromean Link

Chapter 3. Introduction to Molecular Borromean Links 61
3.1. The Borromean Link 61

3.2. Topology of the Borromean Link 61
3.3. Historical Usage 63
3.4. Chemical Interest 66
3.5. Chemical Synthesis 68
3.6. Borromean Topology in Coordination Frameworks 73
3.7. Microscopic objects with Borromean Topology 73
3.8. Goal of this Section 74

Chapter 4. New Approaches to Metal-Templated Molecular Borromean Links 75
4.1. Summary 75
4.2. Introduction 75
4.3. Strategy One: Introduction of Pre-Templated Cap 79
4.3.1. Introduction 79
4.3.2. Design of Pre-Templated Cap 79
4.3.3. Synthesis of Pre-Templated Cap 85
4.3.4. Synthesis of Templated Ring One 97
4.3.5. Attempts at Forming Templated Ring-in-Ring Complex 101
4.4. Strategy Two: Introduction of Small Threads 108
4.4.1. Introduction 108
4.4.2. Attempt at Forming Templated Ring-in-Ring Complex 110
4.5. Conclusions and Outlook 112

Chapter 5. Thioketals as Templates Towards Molecular Borromean Links 114
5.1. Summary 114
5.2. Introduction 114
5.3. Thioketals as Templates 114
5.3.1. Design of Thioketal-Templated Borromean Link 114
5.3.2. Retrosynthetic Analysis 116
5.3.3. Synthesis of Building Blocks 118
5.3.4. Toward the Synthesis of a Thioketal-Templated Rotaxane 121
5.4. Outlook 124

SECTION THREE: Experimental Section

Chapter 6. Experimental Methods 126
6.1. General Remarks 126
6.1. Experimental Procedures for Section One 127
6.2. *Experimental Procedures for Section Two* 168

References 197

Curriculum Vitae 215

List of Figures

Figure 1.1. Van 't Hoff's description of a carbon atom as a tetrahedron and the resulting single, double, and triple bond motifs, showing rotation about a single bond. 2

Figure 1.2. Components of a rotor: rotator, axle and stator. 4

Figure 1.3. Several types of gear arrangements. 4

Figure 1.4. Range of two-bladed molecular rotators including space-filling models 6

Figure 1.5. Schematic drawing of two-bladed rotators in a coaxial arrangement and the stereochemical consequences of hindered rotation. 7

Figure 1.6. Correlated disrotation and uncorrelated conrotation in intermeshed two-bladed rotators in a bent conformation. 10

Figure 1.7. (top) Cogwheeling circuit Ar^1Ar^2X, where $Ar^1$and Ar^2 are both symmetric but unequal. (Bottom) Cogwheeling circuit of Ar^1Ar^2X, where $Ar^1$and Ar^2 are both desymmetrized and unequal. 11

Figure 1.8. Propeller and plane-propeller proposals for the structure of the crystal violet cation **7**. 13

Figure 1.9. Schematic representation of the four proposed mechanisms through which helicity could be reversed in Ar_3X. 14

Figure 1.10. Residual diastereoisomers of a maximally substituted Ar_3X, showing the eight isomers reachable by two-ring flip processes within each set. 15

Figure 1.11. Residual diastereoisomers of **9**, showing the 16 stereoisomers with (*R*) configuration, arranged in their subsets of isomers that interconvert by the two-ring flip mechanisms. Those with (*S*) configuration are not shown. 17

Figure 1.12. Ring flipping in proximal and collateral two-bladed rotators. 18

Figure 1.13. Drawings of triptycene **13** in different representations, indicating the conventional locant numbering. 19

Figure 1.14. Common three-bladed molecular rotators: methyl group, *t*-butyl group, and triptycene-9-yl group. Of the three, only triptycene has well-defined blades. 20

Figure 1.15. Restricted rotation in compound **16** results in the formation of two enantiomers (left and center) and one meso stereoisomer (right). 21

Figure 1.16. Enantiomerization of derivatives of **17** with peri substituents on one of the triptycene blades. 21

Figure 1.17. Exchange of the (A) and (B) methyl signals could result from geared rotation or isolated rotation of the phenyl ring in compound **26**. 24

Figure 1.18. Cogwheeling circuit of peri-substituted derivatives of **27**. 25

Figure 1.19. (top) Geometrical properties of **30**. (bottom) Molecular structure of **30**, rendered in capped stick (left) and space-filling (right) models. The hydrogen atom that is intermeshed between the benzene rings of the neighboring Tp group is marked in black. 27

Figure 1.20. Schematic view of C_2, C_s, and C_{2v} conformations of triptycene-based gear constructs. 27

Figure 1.21. Meso and enantiomeric phase isomers of Tp_2X, in which one benzene ring contains a labeling group. 28

Figure 1.22. Conformations that would exist with restricted geared rotation, and no gear slippage, in compounds **43b**, **44b**, and **45b**. 34

Figure 2.1. Gear-meshed and gear-clashed conformations of 1,9-dimethyltriptycene. 38

Figure 2.2. Geometrical analysis of two three-bladed rotators, approximated as propellers, triangular prisms, and cylinders, in C_2, C_s, C_{2v}, and C_{2v}* orientations. 39

Figure 2.3. (a) Side-on view of space-filling model of triptycene. (b) top view of space-filling model of triptycene, showing geometric parameters. (c) Space-filling representations of two collateral triptycene groups groups in C_2 (left), C_s (center) and C_{2v} (right) conformations, indicating the minimum axle–axle distances. 41

Figure 4.4. Schematic representation of the phase isomers that could result from adding a substituent to the 4-postion of the triptycene groups in **49**. 43

Figure 2.6. : B97-D/Def2-TZVP calculated C_2, C_s, and C_{2v} structures and energetics of **49a** and **49b** rendered as electrostatic potential maps and HOMOs in each case. 46

Figure 2.8. (top left) X-ray molecular structure of **65a** shown as 50% thermal ellipsoids with hydrogen atoms removed for clarity. (top right and bottom) Overlay of experimental structure of **65a** (green) and calculated C_s structure of **49a** (red). 52

Figure 2.9. Reducing the rate of gear slippage ($k_{slippage}$) would allow for the observation of the *meso* and enantiomeric phase isomers in labeled spur gears if geared rotation is preferred over gear slippage. 53

Figure 2.10. VT-^{1}H-NMR of compound **65b**. 54

Figure 2.11. VT-^{1}H-NMR of compound **65c**. 54

Figure 2.12. VT-^{1}H-NMR of compound **69b**. 55

Figure 2.13. VT-^{1}H-NMR of compound **69b**. 55

Figure 2.14. Isolated rotation of the benzyl groups in **69b** and **69c** results in one conformation reaching another conformation within the same phase isomer subset. 56

Figure 2.15. Chemical shift anisotropy of a proton within the shielding surfaces of 0.1 ppm (yellow), 0.5 ppm (green), 1 ppm (green-blue), 2 ppm (cyan), 5 ppm (blue) and deshielding surface of 0.1 ppm (red). (top) Nitrile group. (center) Benzene ring. (bottom) Extended π-systems benzene (a), naphthalene (b), anthracene (c), tetracene (d), and pentacene (e). 59

Figure 3.1. The Borromean link. 61

Figure 3.2. (a) The trefoil knot. (b) The Hopf link. 62

Figure 3.3. The three links comprising three rings and six crossings. Only the Borromean link has the Brunnian property. 63

Figure 3.4. A six-ring Brunnian link. 63

Figure 3.5. The Borromeo Family crest comprises a variety of symbolic imagery, including the Borromean link in the lower left section. 64

Figure 3.6. (a) Joachim of Fiore's interlocked ring representation of the Holy Trinity. (b) The Holy Trinity represented as a Borromean link, as it was depicted in a 13th century manuscript. 64

Figure 3.7. Borromean topolology is present in the triangles in the Valknut of Norse Mythology. 65

Figure 3.8. The Borromean link was part of the Ballantine Brewery's logo, symbolizing purity, body, and flavor. 65

Figure 3.9. Common representations of the Borromean link: (a) Venn representation, (b) chain representation, (c) orthogonal representation. 67

Figure 3.10. If the rings have directionality, the Borromean link is chiral and exists as two enantiomers. 67

Figure 3.11. The representation of the molecular Borromean link design affects the optimal retrosynthetic strategy. 68

Figure 3.12. Schematic representation of Seeman's DNA-based synthesis of a molecular Borromean link. 69

Figure 3.13. X-ray crystal structure of Stoddart's Borromean link, rendered in capped sticks, with silver balls denoting Zn(II) ions. 70

Figure 4.2. X-ray crystal structure of ring-in-ring complex **76**. 77

Figure 4.3. Retrosynthesis of Borromean link using pre-templated cap strategy. 79

Figure 4.4. Energy levels of various conformations of **86**. 82

Figure 4.5. Products of alkylation and alkyne coupling (not shown) can exist in desired *endo* and undesired *exo* arrangements with minimal energy differences. The product of aryl–aryl cross-coupling is fixed in the desired *endo* conformation. 84

Figure 4.6. ^{1}H–^{1}H-NOESY of compound **112**. 90

Figure 4.7. Benzylic bromination of **113** was monitored by TLC (silica, hexane). On each plate, the left spot is the starting material and the right spot is the reaction mixture. 91

Figure 4.8. GC-MS spectra following benzylic bromination of **113**. 93

Figure 4.9. (top) Reaction scheme to tetrabromide **115**, indicating total amounts of reagents needed. (bottom) no dibromination of the methyl groups was observed, likely because the bromomethyl radical is in a sterically crowded environment when in its preferred conformation, planar to the aromatic ring. 94

Figure 4.10. ESI-MS of Ru(II)-containing products following the reaction shown in Scheme 4.22. 104

Figure 4.11. ESI-MS of products obtained from the reaction shown in Scheme 4.26. 107

Figure 4.12. Comparison of widths of terpyridine–Ru complex and alkyl chain. 108

Figure 4.13. (a) Schematic representation of the activating template strategy for the synthesis of rotaxanes. (b) A metal catalyst is complexed within a macrocycle, then catalyzes the coupling reaction two functionalized pieces, each containing a sterically bulky cap. 109

Figure 4.14. Schematic representation of a molecular Borromean link retrosynthesis using the activated template approach. 110

Figure 5.1. Templated synthesis of a Borromean link requires four connections. 115

Figure 6.1. ORTEP Structure (50% Thermal Ellipsoids) of Compound **65a**. 167

List of Schemes

Scheme 1.1. Feringa's chemically driven molecular motor. 9

Scheme 1.2. Feringa's prototypical light-driven molecular motor. 10

Scheme 1.3. (R) and (S) configurations of maximally substituted of triarylmethane **9**. 16

Scheme 1.4. Kelly's chemically-driven molecular motor that can undergo one unidirectional 120° rotation. 23

Scheme 1.5. Representative conformations of stereoisomers of **36**. 32

Scheme 2.1. Retrosynthetic analysis of molecular spur gears **49a** and **49b**. 47

Scheme 2.2. Synthesis of stator component **52**. 48

Scheme 2.3. Synthesis of rotator/axle components **51a–c**. 49

Scheme 2.4. Mixed regiosomers of methyl-substituted derivatives of **62** were carried to **64c**, which could be separated. 49

Scheme 2.5. Synthesis of ethylene-bridged spur gears **65a**, **65b**, and **65c**. 50

Scheme 2.6. Synthesis of planar stator unit **68** and molecular spur gears **69–c**. 51

Scheme 3.1. Stoddart's original synthesis of a molecular Borromeate by a directed assembly approach. 70

Scheme 3.2. Schmittel's Borromean link-shaped cage complex. 71

Scheme 4.1. Loren's and Klosterman's strategy. A ring-in-ring system is formed and the process of internal threading by metal complexation forms a templated two-ring system en route to a Borromean link. 76

Scheme 4.2. Molecular motifs that allow two linear units to extend roughly perpendicularly to each other. 80

Scheme 4.3. Attempted formation of aryl-fused thioketals of fluorenone. 81

Scheme 4.4. Alkylation, alkyne coupling, and aryl–aryl cross-coupling strategies for the introduction of pre-templated caps to known complexes **87** and **88**. 83

Scheme 4.5. Retrosynthetic analysis of pre-templated cap **89**. 86

Scheme 4.6. Synthesis of dithiol **99** and thioketal **86**. 87

Scheme 4.7. Synthesis of **101** from inexpensive fluorenone **83**. 87

Scheme 4.8. Synthesis of pivaloyl-protected fluorenone **105**. 88

Scheme 4.9. Synthesis of 4-bromo-2,3-dimethylaniline **112**. 89

Scheme 4.10. Sandmeyer reaction to bromoiodoxylene **113**. 90

Scheme 4.11. Benzylic bromination of **113** afforded a mixture of products **114** and **115**, showing partial halogen exchange. 92

Scheme 4.12. Benzylic bromination of **113** in $CHCl_3$. 95

Scheme 4.13. (top) Synthesis of a mixture of thiols **119** and **120** from a mixture of **114** and **115**. (bottom) Synthesis of mixture of thioketals **121** and **122** as a test reaction to determine if halogens proximal to thiol can survive thioketalization conditions. 95

Scheme 1.14. Synthesis of orthogonally protected thioketal construct **123**. 96

Scheme 4.15. Synthesis of TIPS-protected, pre-templated cap **129** containing pinacol boronate esters. 97

Scheme 4.16. Final steps of the synthesis of macrocycle **130**, showing the critical, Eglinton-type macrocyclization step. 98

Scheme 4.17. Synthesis of aryliodopyridine **135** using directed metallation strategy. 99

Scheme 4.18. Loren's and Klosterman's syntheses of terpyridine **136**, employing Stille couplings and a Negishi couplings, respectively. 100

Scheme 4.19. Synthesis of terpyridine **136** from iodide **135** and distannylpyridine **137** using Stille methodology. 100

Scheme 4.20. Synthesis of templated ring one **87.** 101

Scheme 4.21. Attempts at boronate ester–triflate cross-couplings 102

Scheme 4.22. Attempt at alkylboronate–triflate cross-coupling. 103

Scheme 4.23. Attempted coupling of butyl boronate **129** and tetratriflate **88**. 104

Scheme 4.24. Standard preparation of aryl trifluoroboronates from boronic esters with KHF_2. 105

Scheme 4.25. One-pot deprotection and formation of tetrabutylammonium salt **138**. 106

Scheme 4.26. Attempted coupling of arylbis(trifluoroboronate) **138** with tetratriflate **88**. 106

Scheme 4.27. Synthesis of ring-in-ring complex **76**. 111

Scheme 4.28. Synthesis of stoppered alcohol **140**, alkyne **141** and azide **142**. 112

Scheme 5.1. Full desulfurization of tetrathioketal **145** would lead to T_h-symmetric Borromean link **146**. 116

Scheme 5.2. Retrosynthetic analysis of Borromeate **145** to templated one ring compound **149** and pre-templated cap **150**. 117

Scheme 5.3. Retrosynthetic methods for templated macrocycle **149**. 118

Scheme 5.4. Synthesis of pivaloyl-protected cap **156**. 119

Scheme 5.5. Synthesis of orthogonally protected pre-templated cap **160**. 119

Scheme 5.6. Synthesis of pre-templated cap containing triflates **161**. 120

Scheme 5.7. Synthesis of protected quinquephenyl triflate **166**. 121

Scheme 5.8. Schematic representation of a rotaxane **167** that could be generated using the thioketal-templating strategy. 122

Scheme 5.9. Synthesis of 3,6-dibromobenzene-1,2,4,5-tetramethanethol (**172**). 123

Scheme 5.10. Synthesis of dithioketal **175** and attempted Sonogashira cross-coupling. 123

List of Tables

Table 1.1. Classes of Residual Stereoisomers for All Substitution Patterns of Tp_2X under the Full Operation of the Gearing Mode 30

Table 1.2. Barriers to gear slippage in several desymmetrized bevel gears 31

Table 2.1. Correlation between $\Delta\nu$ and coalescence temperature (T_c). 57

Table 6.1. Computational Methods for **49a** (E+ZPE, kcal/mol, and frequencies, cm^{-1}). 162

Table 6.2. Computational Methods for **49b** (E+ZPE, kcal/mol, and frequencies, cm^{-1}). 163

Table 6.3. Crystallographic Data for Compound **65a** 166

SECTION ONE

Development of Molecular Spur Gears

Chapter 1

From Correlated Rotation to Gearing at the Molecular Level

1.1. Introduction to Molecular Rotors and Gears

1.1.1. Introduction

In Jacobus van 't Hoff's controversial and epochal treatise, *La chimie dans l'espace*,[1] he developed the concept of the tetrahedral carbon atom[2,3] and a tetrahedron-based model for describing molecular bonds. According to this simple and astonishingly descriptive model, two tetrahedra may be connected by their points (forming a single bond), their edges (forming a double bond), or their triangular faces (forming a triple bond) (Figure 1.1). A consequence of the point-to-point junction of the single bond is that rotation of the attached groups is allowed, whereas the groups participating in double and triple bonds are rotationally locked. By extending this description to ethane, van 't Hoff discovered perhaps the simplest molecular rotator, the methyl group.

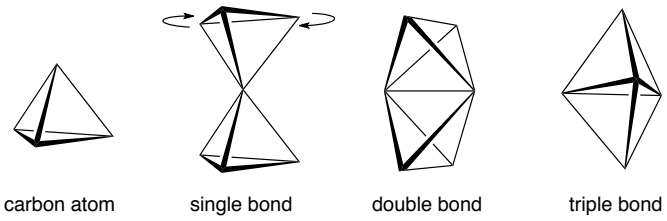

Figure 1.1. *Van 't Hoff's description of a carbon atom as a tetrahedron and the resulting single, double, and triple bond motifs, showing rotation about a single bond.*

That a founding father of stereochemistry first determined rotation at the molecular level is fitting, as any attempt to understand internal dynamics of molecules requires rigorous stereochemical analysis. Without a proper understanding of stereochemistry in hand, discussions of molecular dynamics are destined to be fraught with error.

Breakthroughs in instrumentation over the past century, particularly in X-ray crystallography, have revolutionized our models and improved our understanding of molecular structure. Bond lengths, bond angles, and atomic van der Waals radii combine to provide chemists with an understanding of molecules as objects with hard surfaces as static models. However, molecules may comprise components ranging from extremely rigid to wildly flexible and maneuverable, often rendering static models insufficient to describe molecular behavior. The advent of NMR spectroscopy, variable-temperature NMR methods in particular, has greatly aided in the development of dynamic models, which combine structure and internal mobility to offer a more accurate depiction of molecules.

The dynamic model of molecules evokes the image of a mechanical object[4] and the molecular rotator[5] is a fundamental mechanical component thereof. Remarkably, the laws of classical mechanics can often be successfully applied[6] to the behavior of molecular rotors, which may be tumbling about in a solution,[7] enclosed in a crystalline solid-state,[8] or bound to a surface.[9,10] Modern dynamic models allow for the rational design of molecules comprising multiple rotating pieces that interact, imitating macroscopic mechanical devices such as propellers, gears, switches, or elementary motors.[11]

Advances in synthetic methodology allow chemists to transport molecules from the drawing board to the flask and breakthroughs in stereochemical understanding and analysis permit the elucidation of their dynamic behavior. This chapter will provide a brief overview of molecules that exhibit correlated rotation and gearing of molecular rotators, highlighting their rich stereochemistry.

1.1.2. Nomenclature

Before embarking on a discussion of molecular rotors and gears, a few nomenclatural conventions should be introduced. A *molecular rotor* consists of three basic elements: (1) a *rotator*: the part of the system that rotates (having a smaller moment of inertia); (2) a *stator*: the stationary part of the system (having a larger moment of inertia); and (3) an *axle*: the piece connecting the rotator to the stator (Figure 1.2). The term *rotor* is occasionally used for *rotator*, particularly in the older literature; however, adherence to the proper nomenclature assures the highest degree of clarity in chemical discussion.

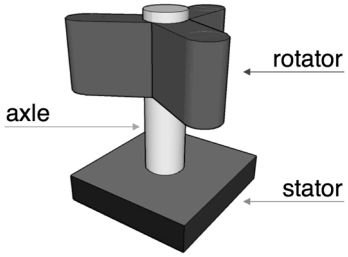

Figure 1.2. *Components of a rotor: rotator, axle and stator.*

Gears are ubiquitous in macroscopic machinery and have been employed in engineering constructs for 5,000 years.[12] They come in many shapes and sizes and virtually every type or arrangement has a name associated with it.[13] Only the types of gears that pertain to the forthcoming chemical discussion will be mentioned here. First, a gear shaft combines two gears whose teeth radiate from the center of a disk and whose axes of rotation lie perpendicular to the plane of the disks at the disks' center. The intermeshing of the gears results in transmittal of rotational force of one gear to the other along a straight line. Next is the bevel gear, which holds the pitch angle of the gears between 0° and 180°. Lastly, the most common type of gear in macroscopic machinery is the spur gear, which holds two gears with teeth along their peripheries in a collateral fashion with parallel axes of rotation.

Figure 1.3. *Several types of gear arrangements.*[14,15]

Finally, a clarification must be made when discussing gearing in a chemical context. Mislow offered a distinction between the *static gear effect*, a common occurrence in chemistry, and the *dynamic gear effect*, which is far rarer. The *static gear effect* refers to the intermeshing of neighboring chemical groups under conditions of significant steric crowding. This effect is exemplified well by hexaalkylbenzenes;

hexaethylbenzene[16] positions its ethyl groups in a zig-zag orientation and hexaisopropylbenzene[17] wedges the isopropyl groups, giving C_{6h} molecular symmetry. In these cases, flipping of one of the alkyl groups results in a reshuffling of the others to regain the desired conformation. The *dynamic gear effect*, on the other hand, is defined as "the special effect on the rate or mechanism of a process that may be attributed to the intermeshing of a chemical rotor with neighboring groups" and coupled molecular rotators that undergo this phenomenon behave analogously to mechanical gears in motion.[18] Molecules exhibiting the dynamic gear effect will be discussed in detail in subsection 1.4.2.

1.1.3. Scope of this Chapter

Rotation of one molecular group in response to motion of another group occurs in any molecule containing two or more interacting molecular rotators, regardless of their size. They exhibit conformational preferences in relation to each other due to van der Waals repulsions or attractions, London dispersion forces, Cuolombic interactions, stereoelectronic effects, etc. Responsive motion of this sort is common in chemistry and a comprehensive account of it is far beyond the scope of this thesis. Instead, this chapter focuses on the conceptual development of molecular gearing by exploring the dynamic behavior of intermeshed two-bladed and three-bladed rotators in various orientations and how the behavior was demonstrated by stereochemical investigation. Systems with more than three rotators or rotators comprising more than three blades have been studied but are generally less understood and fall outside the scope of this chapter. Such constructs will be mentioned in passing with references to additional reading. It is also worth noting that this chapter will only consider solution-phase molecular propellers and gears, though a great deal of interesting work has been done on solid-state and surface-mounted molecular rotors.[19]

1.2. Interacting Two-Bladed Propellers

1.2.1. Introduction

Two-bladed rotators may range from quite small (nitro group) to larger (phenyl group) to extended planar aryl structures (such as the anthracene-9-yl group) (Figure 1.4). Most of the molecules in this section employ phenyl groups, or substituted derivatives thereof, as two-bladed rotators. They are synthetically accessible and exhibit

correlated rotation when forced into appropriately designed, sterically crowded rotator constructs. Not surprisingly, the linear structure of two-bladed propellers renders gearing constructs incorporating them rather inefficient, but the stereochemical investigations that demonstrated their rotational behavior laid much of the groundwork for the conceptual development of molecular gearing and molecular machines.

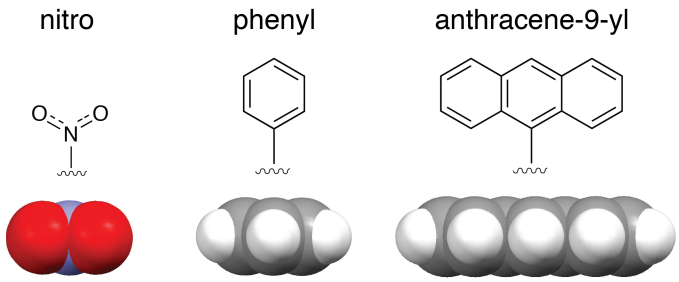

Figure 1.4. *Range of two-bladed molecular rotators including space-filling models.*

1.2.2. Two-Bladed Propellers in a Coaxial Arrangement

1.2.2.1. Atropisomerism

Evoking the image of a gear shaft, molecular rotators may exist in a coaxial arrangement, where their axes of rotation occupy the same line in space. If they are close enough that their hydrodynamic radii overlap, the rotators will intermesh (*i.e.* a static gear effect) and an energy barrier will be associated with the blades slipping over one another. Different substitution patterns induce varying stereochemical consequences (Figure 1.5). Systems comprising propellers that are equal and symmetric (a) will exist as interconverting homomers. The same is true for systems containing two different, yet symmetric, propellers (b) and systems containing one symmetric propeller and one desymmetrized propeller (c). Each of the preceding cases form an achiral species when the propellers are perpendicular to each other, exhibiting D_{2d} (a), C_{2v} (b), or C_s (c) symmetry. If the propellers are equal and desymmetrized (d), the system exists as a set of enantiomers, as the construct has chiral C_2 symmetry in the perpendicular conformation. Interconversion of enantiomers occurs by slippage of the blades over one another, a process in which an achiral transition state is reached. Enantiomers are also present when the system comprises to unequal and desymmetrized propellers, as it exhibits C_1 symmetry in all conformations except the transition state to propeller slippage.

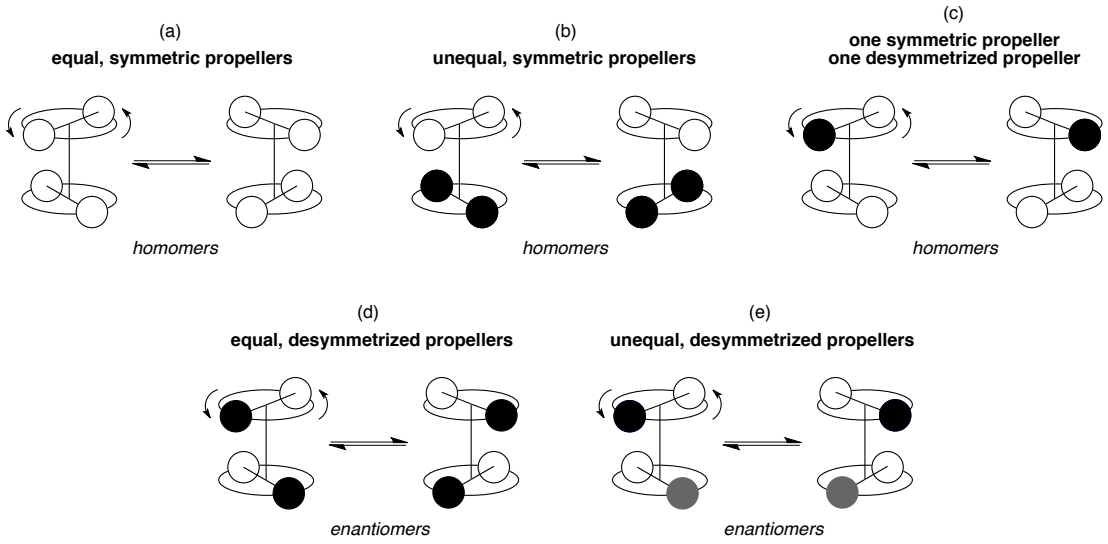

Figure 1.5. *Schematic drawing of two-bladed rotators in a coaxial arrangement and the stereochemical consequences of hindered rotation. This treatment assumes that the propellers are achiral.*

The stereochemical consequences of hindered rotation about a single bond were first observed in 1922 by Christie and Kenner[20] in their resolution of the enantiomers of 6,6'-dinitrobiphenyl-2,2'-dicarboxylic acid (**1**), which has substitution pattern (d) from Figure 1.5. This discovery marked a milestone in chemists' understanding of stereochemistry[21] and the term atropisomerism (borrowed from the Greek *a-*, meaning not, and *-tropos*, meaning rotate) was later proposed by Kuhn[22] and applied to stereoisomers that are formed by restricted rotation. A multitude of atropisomers have since been developed.[23] As the difference between a conformational isomer and a configurational isomer lies in the rate of interconversion, Ōki proposed that atropisomerism requires a half-life of interconversion above 1,000 seconds.

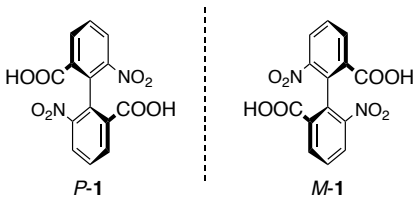

Atropisomerism in coaxial arrangements is not limited to molecules comprising steric crowding about a single bond. The phenomenon has also been observed in sterically crowded diarylacetylenes. In derivatives of bis(2,6-diarylphenyl)acetylene (**2**)

with substitution pattern (d) from Figure 1.5, it was calculated that the compound exists as atropisomers at low temperature, with a barrier to rotation of 7 kcal/mol. The barrier could not be experimentally validated, as it lies at the lower detection limit of variable temperature (VT)-NMR experiments.[24] Derivatives of compound **3**, on the other hand, are much more sterically crowded, resulting in higher energy barriers to rotation. The barriers range from 12 kcal/mol, for the molecule with no substitutents on the phenyl rings to, 18 kcal/mol for the molecule, where the aryl group contains two bulky isopropyl groups at the 3- and 4-positions.[25]

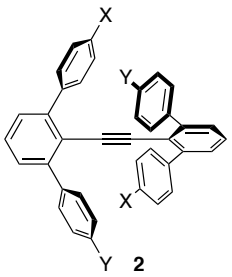

2

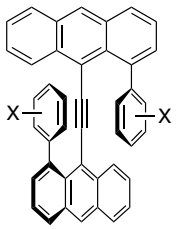

3

1.2.2.2. Application to Molecular Motors

Ben Feringa and coworkers have taken the concept of atropisomerism a step further by creating molecular motors based on biaryl constructs.[26] *Motors* are distinguished from *rotors* by their ability to rotate unidirectionally or at least prefer rotation in one direction over the other. In a prototypical chemically-driven molecular motor system, lactone **4** undergoes a series of chemical reactions that preferentially rotate the substituted phenyl group clockwise (viewed from above) about the naphthalene stator (Scheme 1.1). The critical steps are the reductions of lactones **4** and **5** with enantiomerically pure reducing agents, which afford the resulting biaryls with high stereoselectivity. Selective formation and cleavage of *p*-methoxybenzyl and allyl ethers, and their subsequent esterifications, return the biaryls to lactones, which have significantly reduced barriers to rotation.

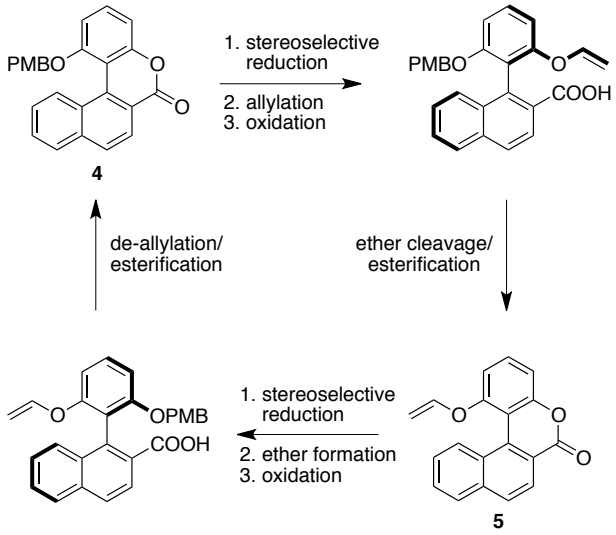

Scheme 1.1. *Feringa's chemically driven molecular motor.*

Feringa's light-driven molecular motors, where two rotators are connected by an alkene, have gained considerable popularity. These motors function by light-induced *cis–trans* isomerization of the double bond, resulting in the formation of a less stable conformation. Subsequent exposure to heat results in a "slipping" of the aryl blades over each other, affording a more stable conformation. Two successive photochemically driven and thermodynamically driven cycles returns the molecule to its original conformation. The first molecules of this type were based on chiral biphenanthrylidines[27] and next-generation constructs are based on more complex heterocycles (Scheme 1.2).[28] Later constructs have been adsorbed on surfaces and behave as surface-bound altitudinal motors.[29] The motors have recently been introduced to a four-wheeled nanoscopic vehicle[30] that moves unidirectionally on a surface, in a highly acclaimed study that received high praise from chemists and the general public.[31] Molecular motor prototypes comprising three-bladed rotators will be discussed in section 1.3.2.

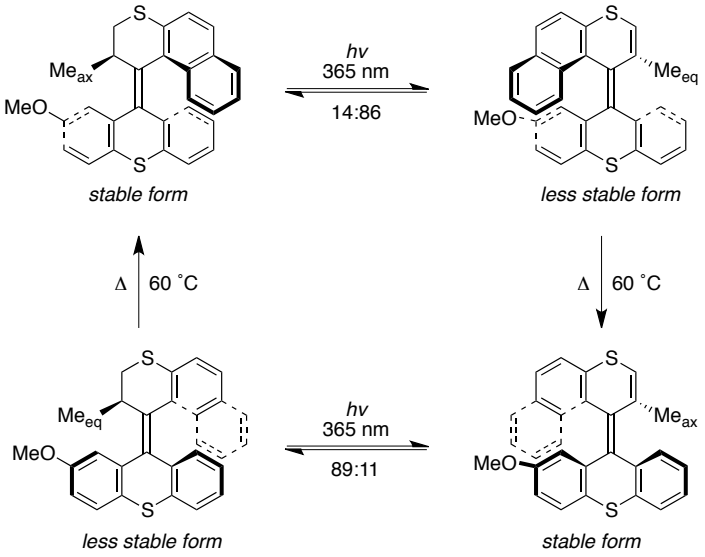

Scheme 1.2. *Feringa's prototypical light-driven molecular motor.*

1.2.3. Two Two-Bladed Propellers in a Bent Arrangement

The molecules described in the previous section show hindered, and sometimes controllable, rotation of molecular groups about one another. In this section, we will first uncover molecules that exhibit a dynamic interaction between rotators such that their rotations are correlated. In a bent arrangement, a central atom or group serves as the stator and sterically crowded, intermeshed rotators may undergo correlated disrotation through a cogwheeling mechanism (Figure 1.6).

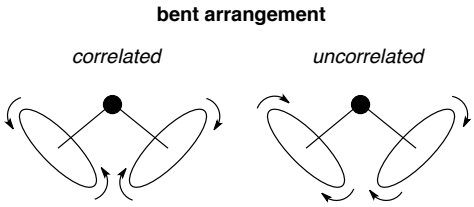

Figure 1.6. *Correlated disrotation and uncorrelated conrotation in intermeshed two-bladed rotators in a bent conformation.*

This effect is exemplified in systems of the type Ar^1Ar^2X, where Ar are sterically crowded, *ortho*-substituted phenyl rings (Figure 1.7). A molecule with two different, yet symmetric, rings will exist as a cogwheeling circuit comprising two enantiomeric, helical conformations and two achiral, perpendicular conformations. Further substitution such that the rings are unequal and differentially substituted on

their *ortho* or *meta* positions generates a larger cogwheeling circuit with four helical and four perpendicular conformations.

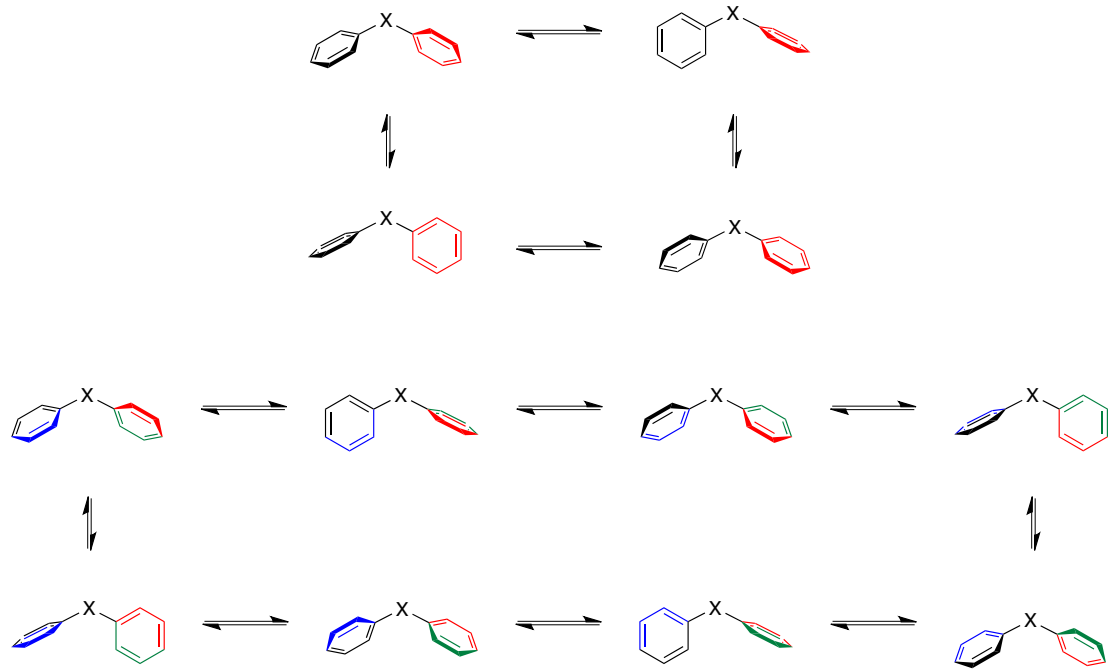

Figure 1.7. *(top) Cogwheeling circuit Ar^1Ar^2X, where Ar^1 and Ar^2 are both symmetric but unequal. (Bottom) Cogwheeling circuit of Ar^1Ar^2X, where Ar^1 and Ar^2 are both desymmetrized and unequal.*

The phenomenon was first described as "concerted rotation" in 1959 by Allen and Moir,[32] who prepared a variety of highly hindered, desymmetrized diphenyl ethers, yet found that the stereoisomers interconvert too quickly to be separated at room temperature. In 1968, Kwart and Alekman[33] reported that the *ortho*-methyl groups in dimesityl carbonium ions undergo rapid exchange in NMR spectra, even at temperatures as low as −60 °C. Combined with computational evidence, the results suggested that the cogwheel effect occurs, as stepwise rotation of the rings would entail highly sterically unfavorable transition states. In 1972, Bergman and Chandler[34] applied variable-temperature NMR experiments to uncover the rotational barriers to substituted diphenyl ethers and found that the barrier to interconversion of enantiomers in (2,6-diisopropylphenyl) (4-nitrophenyl) ether (**6**) is 10.6 kcal/mol if measured from the signals of the isopropyl methyl groups (italicized) and 10.1 kcal/mole if measured from the signals of the *ortho* ring protons (bolded). These values fall within the range of experimental error of the measurement and imply that a concerted cogwheeling

mechanism occurs. If stepwise rotation of one ring about the C(Ar)–O bond, followed by rotation of the other ring, occurred, the process would be expected to be much slower for the isopropyl-substituted ring than for the *ortho*-unsubstituted ring.

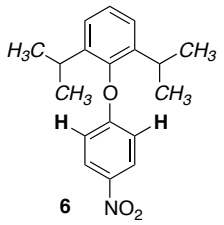

6

Correlated rotation of this type has been observed in a variety of other diphenyl ethers,[35] diphenylsulfides,[36] and diphenylketones,[37] diphenylmethanes,[38] and sterically crowded aromatic amides.[39] Uncovering the rotational behavior of molecules with this construct expanded chemists' understanding of atropisomerism and internal molecular dynamics and played a major role in the conceptual development of molecular gearing.

1.2.4. Three Two-Bladed Rotators in a Bent Arrangement

A model of a molecule comprising three aryl rings attached to a central atom or group evokes the image of a three-bladed propeller, resembling those found in airplanes and motorboats. Though molecules of this type are routinely, and properly, referred to as three-bladed propellers, this discussion will consider them as systems comprising three two-bladed propellers, as the correlated rotational behavior of the aryl rings is what is truly under investigation.

In 1942, G. N. Lewis found spectroscopic evidence for stereoisomers of the crystal violet cation **7**. He observed two conformations that differed in energy by 0.58 kcal/mol and found that 2–3 kcal/mol of energy is required for them to interconvert. He proposed that the D_3 propeller (helical) structure was the lower-energy structure and that the other had a C_2 plane-propeller conformation (Figure 1.8). In the early 1950's Deno argued that the plane-propeller conformation is lower in energy,[40] but the dawn of NMR spectroscopy allowed for structural analysis that definitively demonstrated the existence of the propeller conformation for triaryl carbonium ions.[41]

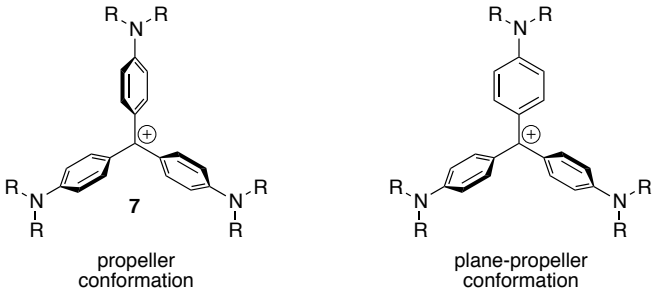

Figure 1.8. *Propeller and plane-propeller proposals for the structure of the crystal violet cation* **7**.

Kurland proposed in 1965 that four distinct ring-flipping mechanisms may operate in the interconversion of helicity: a zero-ring flip, a one-ring flip, a two-ring flip, and a three-ring flip (Figure 1.9). Mislow and coworkers published extensively[42] on the stereochemical consequences of differentially substituted molecules of the type $Ar^1Ar^2Ar^2X$ and one of the first papers[43] on the topic addressed this issue. Dynamic NMR studies of triarylborane **8** showed that the four xylyl methyl singlets coalesce to one singlet at elevated temperature with concomitant coalescence of the two isopropyl methyl doublets to one doublet and that the activation energies for both processes are the same ($\Delta G^{\ddagger}$ = 17.8 kcal/mol). Only stereoisomerization by a mechanisms involving reversal of helicity could explain the coalescence of the isopropyl methyl signals (diasteriotopic to enantiotopic) and only the two-ring flip could account for the coalescence of the four xylyl methyl signals to a singlet.[44] Computational studies of transition state structure provided further validation to the two-ring flip as the dominant mechanism of helicity reversal.[45]

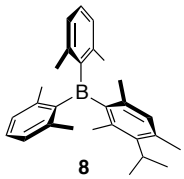

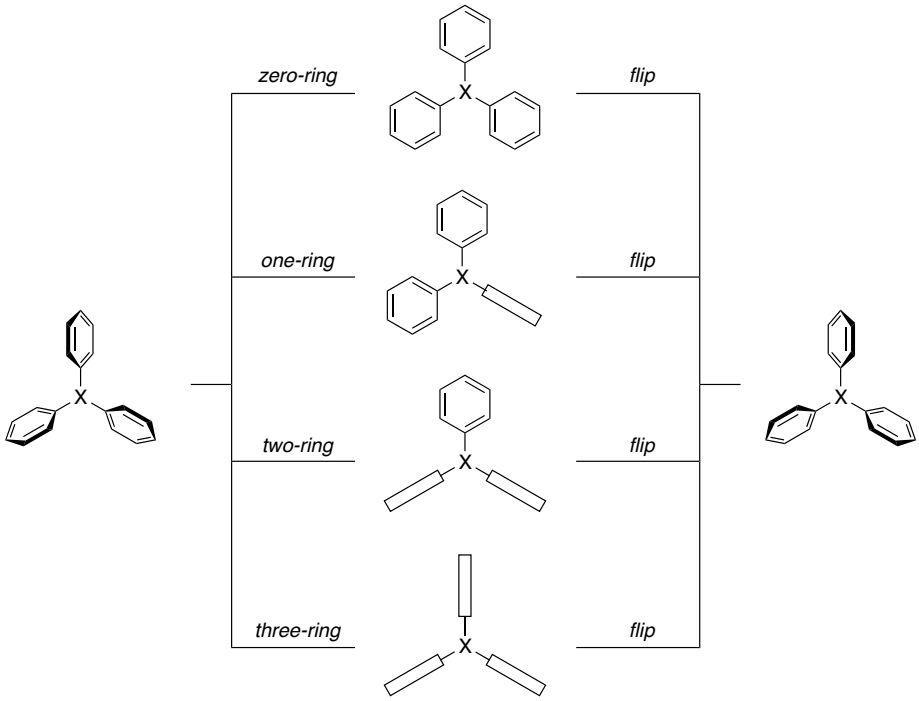

Figure 1.9. *Schematic representation of the four proposed mechanisms through which helicity could be reversed in Ar_3X.*

Correlated rotation through the two-ring flip process entails fascinating stereochemical consequences. Consider a system $Ar^1Ar^2Ar^2X$, in which Ar^{1-3} are all substituted by a different group at their respective *ortho* or *meta*-positions, a condition Mislow called "maximally labeled."[42] If the structure maintains a propeller conformation, there will be 2^4 = 16 conformational isomers. The two-ring flip mechanism partitions the 16 isomers into two sets of eight conformations, which may all interconvert along a pathway best represented by a cube (Figure 1.10). The conformations are well represented by a binary labeling strategy ($n_h n_1 n_2 n_3$), where n_h refers to the helicity (0 for right-handed, 1 for left-handed) and n_{1-3} refer to whether the substituent is projecting toward (0) or away from (1) the viewer. Beginning with (0000), a two-ring flip will result in either (1100), (1010), or (1001), depending on which rings undergo flips. The other set of eight isomers is related by an internal rotation mechanism that induces a change of helicity for each of the eight conformers (a three-ring flip) shown in Figure 1.10 and is substantially higher in energy than the two-ring flip.

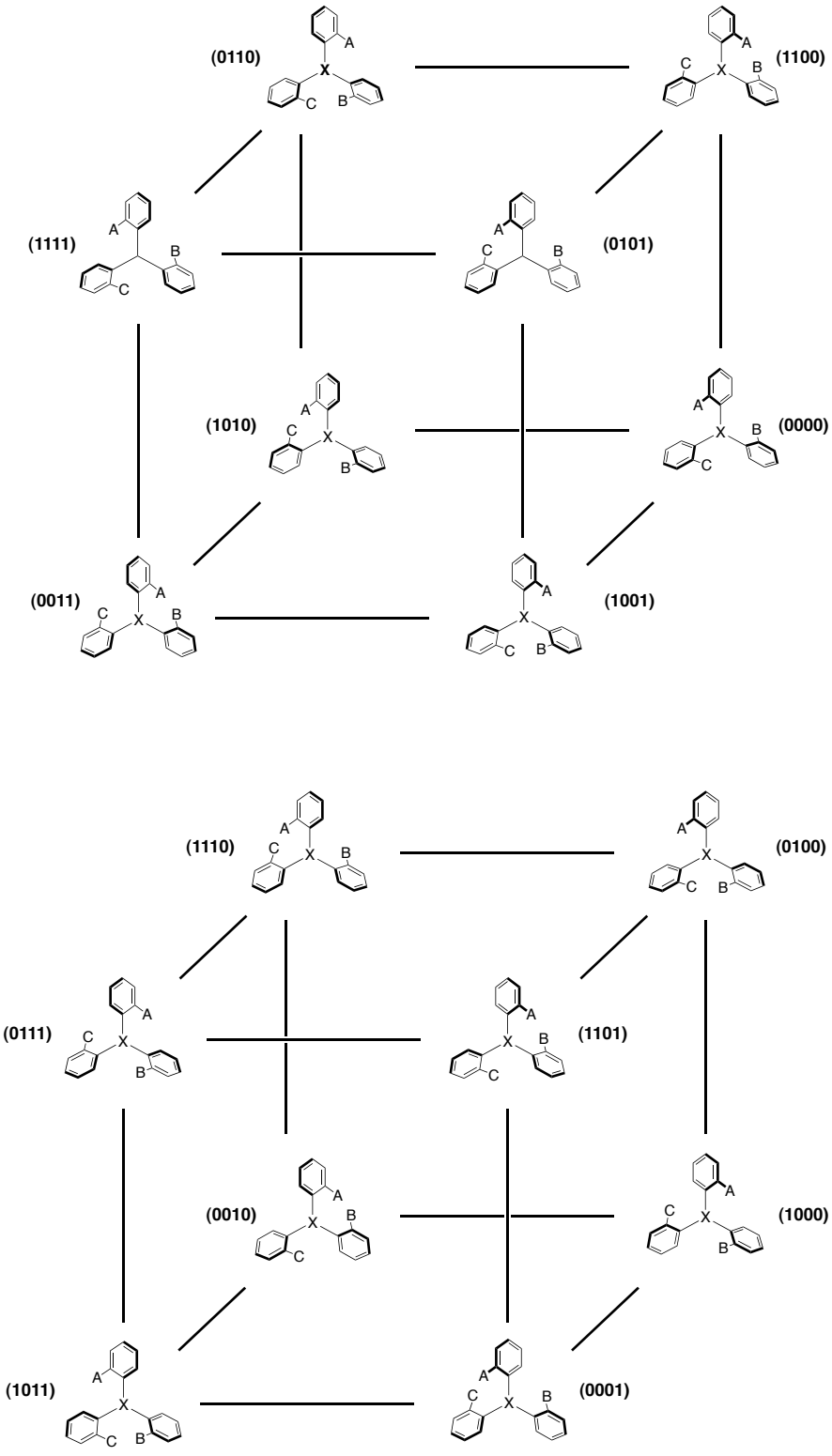

Figure 1.10. *Residual diastereoisomers of a maximally substituted Ar_3X, showing the eight isomers reachable by two-ring flip processes within each set.*

The sets of eight isomers in maximally labeled Ar_3X contain four enantiomeric pairs [compare (0000) and (1111)] and the net stereochemical consequence is that the

compound exists as two achiral diastereomeric forms under the full operation of the two-ring flip. Mislow introduced the term *residual stereoisomerism* to describe this phenomenon, which "results whenever closed subsets of appropriately substituted interconverting isomers are generated from the full set at a particular time scale of observation and under the operation of a given stereoisomerization."[42] The number of residual stereoisomers is found by dividing the number of total isomers by the number of isomers within a subgroup; in the case above, there are 16/8 = 2 residual stereoisomers.

The situation becomes slightly more complex when three aryl groups are connected by a tetrahedral methine center. Mislow predicted [44] and experimentally realized[46] the stereochemical consequences of correlated rotation in triarylmethanes. Substituted dinaphthylphenylmethane **9** contains a stereogenic center on the central carbon atom (Scheme 1.3), yet the compound exists not as a pair of enantiomers, but as two diastereomers (each with an enantiomeric partner) that are separable in reasonable purity by crystallization. Like the maximally substituted Ar_3X compounds shown above, the propellers in **9** (a maximally substituted Ar_3XY system) undergo a series of two-ring flips to generate four subsets of eight isomers [*i.e.* 32 isomers in total: 16 with (*R*) configuration, 16 with (*S*) configuration]. The 16 isomers with (*R*) configuration are shown in Figure 1.11.

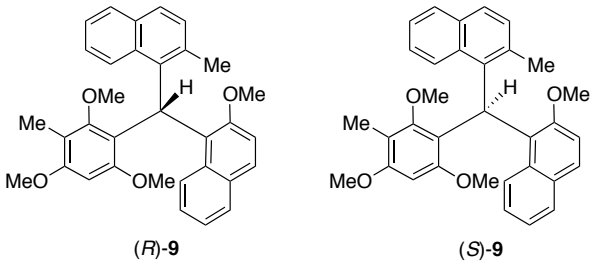

Scheme 1.3. *(R) and (S) configurations of maximally substituted of triarylmethane* ***9****.*

Steically crowded triarylenols may also participate in a two-ring flip processes; however, the dynamic behavior is often more complex and less understood than the systems described above. Much information[47] is available on molecules of this type and they will not be discussed here.

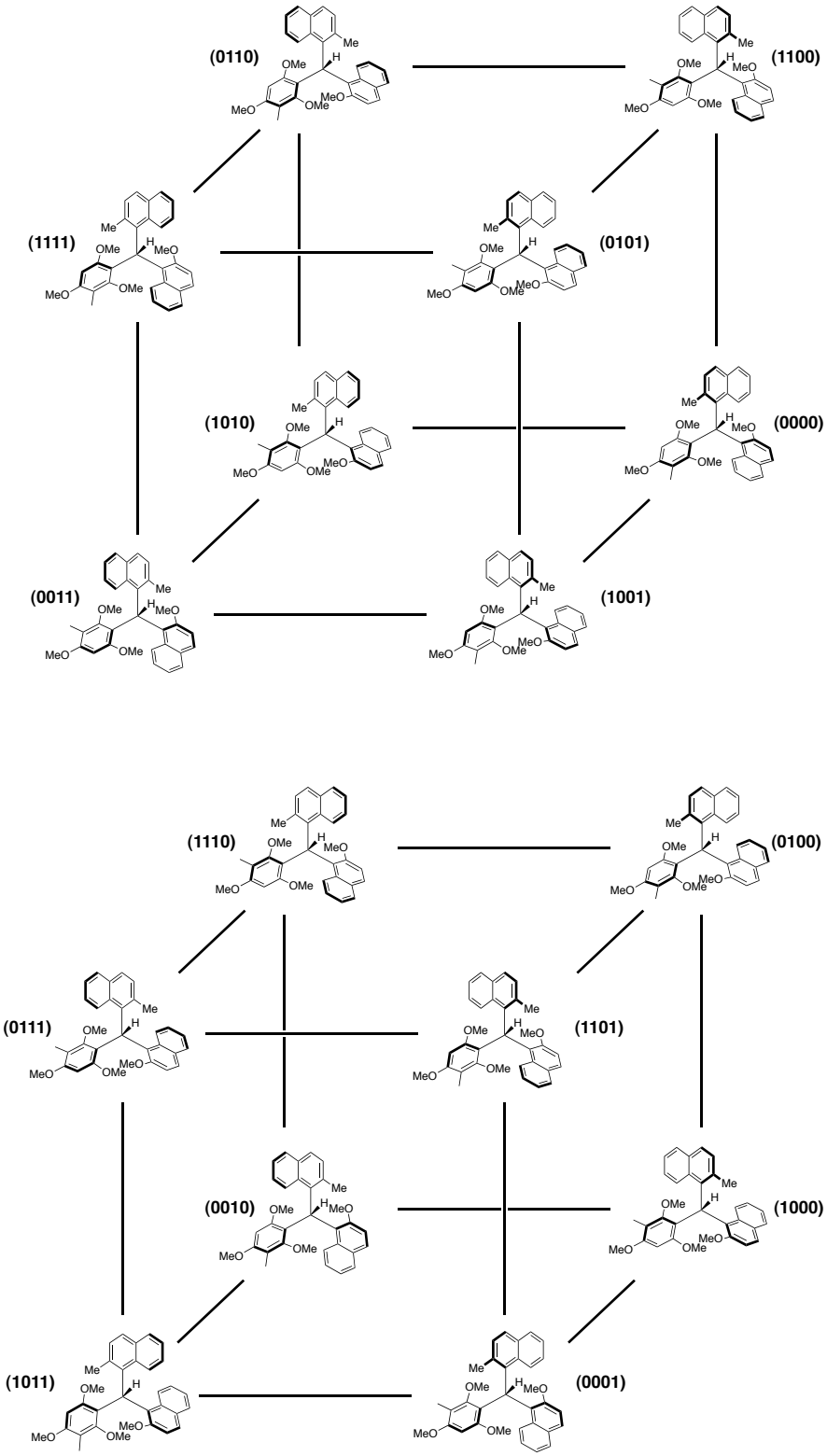

Figure 1.11. *Residual diastereoisomers of* **9***, showing the 16 stereoisomers with (R) configuration, arranged in their subsets of isomers that interconvert by the two-ring flip mechanisms. Those with (S) configuration are not shown.*

1.2.5. More than Three Two-Bladed Rotators in Bent Arrangements

Several examples of correlated rotation in systems with more than three two-bladed rotators have been studied. The conformational nature of tetraphenylmethane has been the topic of much discussion.[48,49,50] Other constructs with interacting aryl groups appear in the form of tetraarylethanes,[51] and tetraarylethenes,[52] as well as systems with aryl groups connected to a ring, *i.e.* pentaarylbenzene,[53] and hexaarylbenzene[54] and tetraarylcyclopentadienone.[55] An interesting computational study indicates that the nitro groups in octanitrocubane may undergo geared rotation.[56]

1.2.6. Two Two-Bladed Rotators in a Collateral Arrangement

So far, we have considered interacting two-bladed propellers in coaxial and bent arrangements. To close this section, systems in which two two-bladed propellers are placed side by side and in parallel (a relationship hereafter referred to as *collateral*) should be addressed. Constructs of this sort show no geared rotation of the propellers, which simply undergo *syn–anti* isomerization (if appropriately substituted) when ample energy is provided to allow for ring flipping (Figure 1.12). The planes of the blades are likely not to be rigidly perpendicular the plane of the stator in the lowest-energy ground-state structure and a correlated back-and-forth rocking of the rotators may occur.

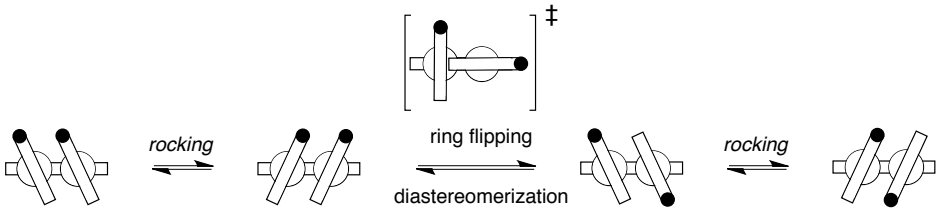

Figure 1.12. *Ring flipping in proximal and collateral two-bladed rotators.*

Careful study of such systems has provided significant insight into the nature of aryl–aryl through-space interactions. A fascinating example is 1,8-diarylnaphthalene, where barriers to rotation of the aryl rings increase monotonically with the Hammett value of a substituent placed at the *para*-position (σ_{para}) of the aryl rotator, suggesting that polar/π effects are the dominant interactions between stacked phenyl groups.[57] Similar studies on 1,8-diarylbiphenylene, which holds the aryl rings at a longer distance

than the naphthalene-based system, show that more effects play major roles in these systems.[58]

Rotators may be held collaterally in cyclic systems. Examples of such constructs are cyclophanes **10**, **11**, and **12**. Phenyl rotation is precluded in **10** by lack of space and phenyl rotation in larger cyclophane **11** is calculated to require >70 kcal/mol.[59] Adding two more methylene groups (as in compound **12**) to the linker significantly decreases the barrier to 18–20 kcal/mol.[59]

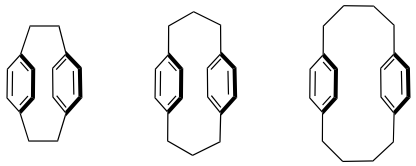

10 **11** **12**

1.3. Triptycene: A Shape-Persistent, Three-Bladed Molecular Rotator

1.3.1. Introduction

Although the static, helical structures of the Ar_3X-type molecules shown in section 1.2.3 clearly evoke the image of macroscopic propellers, the analogy unravels as dynamic processes allow the aryl blades to rotate. By locking the aryl rings in a single orientation, the molecular system that best represents a propeller in both structure and function is triptycene (**13**, Figure 1.13). Due to its shape-persistent structure and synthetic accessibility of derivatives thereof, triptycene has been the most commonly used three-bladed rotator in system in which correlated rotation has been probed.

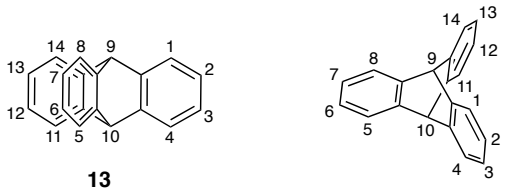

13

Figure 1.13. *Drawings of triptycene* ***13*** *in different representations, indicating the conventional locant numbering.*

Methyl groups and *t*-butyl groups are examples of three-fold symmetric rotators that are smaller than triptycene (Figure 1.14). Early work proposed that smaller three-bladed rotators such as methyl and *t*-butyl groups may intermesh with

each other when crowded together, but this was found not to be the case.[18] Triptycene and derivatives thereof are the only three-bladed rotator frameworks that have shown geared rotation and will dominate the ensuing discussion.

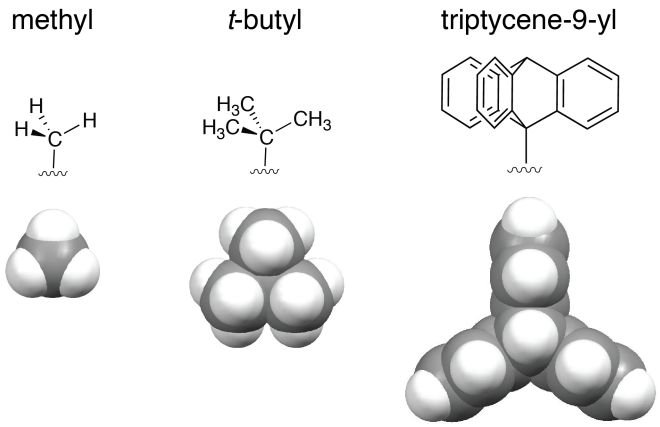

Figure 1.14. *Common three-bladed molecular rotators: methyl group,* t*-butyl group, and triptycene-9-yl group. Of the three, only triptycene has well-defined blades.*

1.3.2. Triptycene Interacting with Other Rotators

1.3.2.1. Coaxial Arrangement

Michinori Ōki pioneered much of the early work on the rotational behavior of molecules comprising triptycene and other rotators at the 9-position. In 1972, it was found that the methyl group in chlorinated 9-methyltriptycene derivative **14** shows a clear AB_2-type splitting ^{1}H-NMR signals below –70 °C, indicating that rotation of the methyl group has an energy barrier of ~14 kcal/mol.[60] This barrier is remarkably high for rotation of a methyl group, significantly higher than the barrier of methyl rotation in another sterically crowded molecule, 2,2-dimethylpropane, which was calculated to be 4.6 kcal/mol[61] and experimentally reported to be 4.3 kcal/mol.[62] Substituting the methyl group with a larger alkyl group increases the barrier to rotation even if the isopropyl groups methyl must only pass over the unsubstituted benzene rings of triptycene. The energy barrier for enantiomerization in compound **15** is 25 kcal/mol.[63]

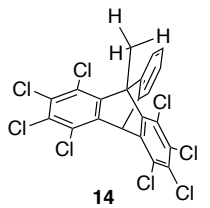

14

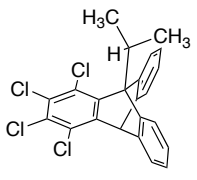

15

Bulky *tert*-alkyl groups have a much higher barrier to rotation about the triptycene moiety, despite no substituents being present in the *peri*-positions of the triptycyl benzene rings.[64] Compound **16** exists as three stereoisomers—a pair of enantiomers and an achiral, *meso* isomer—and the energy barrier to stereoisomerization by rotation is 34 kcal/mol (Figure 1.15).

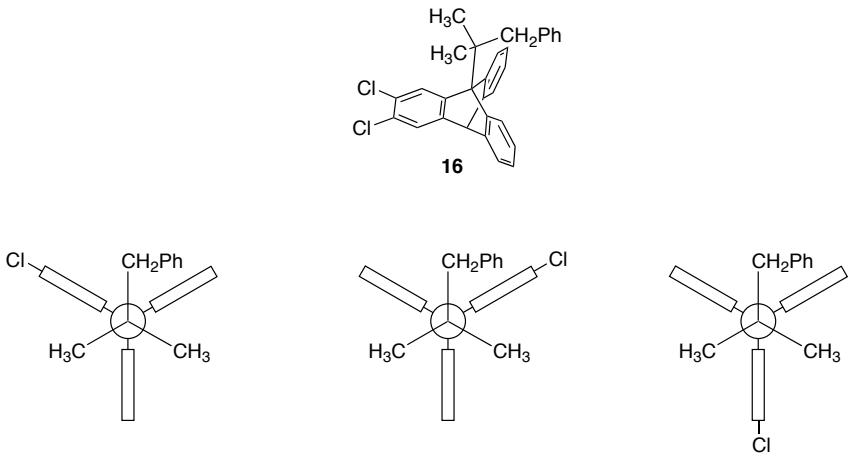

Figure 1.15. *Restricted rotation in compound* ***16*** *results in the formation of two enantiomers (left and center) and one meso stereoisomer (right).*

Ōki took these findings a step farther and applied them to derivatives of 9-aryltriptycene **17**, where the aryl groups contain an *ortho* methyl or methoxy group (Figure 1.16).[65] The activation barriers range from 12.9–14.8 kcal/mol, depending on the substituents, for the interconversion of enantiomers through a C_s transition state. These barriers are notably lower than those for the alkyl-substituted systems shown above, despite the requirement of a highly strained transition state. The low values are accounted for by a high ground state energy that is attributable to a substantial amount of strain due to steric crowding.

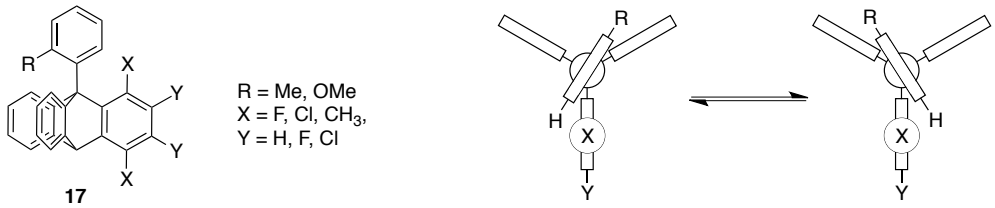

Figure 1.16. *Enantiomerization of derivatives of* ***17*** *with peri substituents on one of the triptycene blades.*

T. Ross Kelly has developed several imaginative molecular machine prototypes in which triptycene interacts with two-bladed rotators in a coaxial arrangement.[66] The first of these molecules were reporteed in 1994,[67] as "molecular brakes" **18** and **19**. In this construct, the triptycene group rotates quickly when the bipyridine unit is not bound to a metal. Upon metal complexation, the bipyridine unit is forced into a *syn* planar conformation, wedging the distal pyridine ring between two blades of the triptycene, blocking rotation. Later he reported helicene-containing compound **20** and several other similar molecules,[68,69] which require ~25 kcal/mol for the triptycene group to rotate.

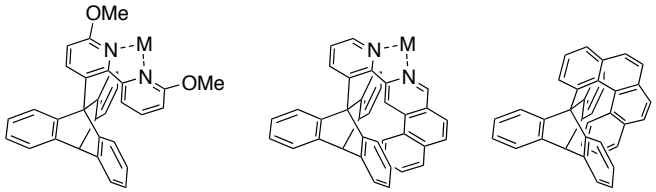

18 **19** **20**

These constructs were reported to be steps toward the development of molecular ratchets. They were later extended toward the development of a chemically driven motor **21**, which can undergo one unidirectional rotation about a single blade of the triptycene moiety (Scheme 1.4).[70,71] Compound **21** is converted to isocyante intermediate **22**, which forms urethane **23**. This tethering of the rotators allows for slippage to be achieved with a lower barrier. Cleavage of the urethane gives **24**, which has undergone unidirectional rotation about one blade of triptycene.

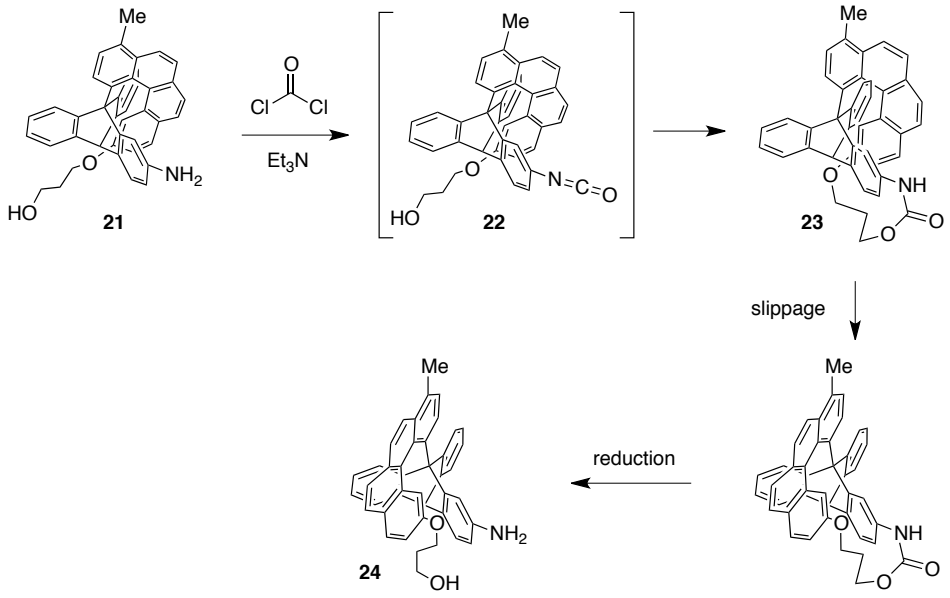

Scheme 1.4. *Kelly's chemically-driven molecular motor that can undergo one unidirectional 120° rotation.*

1.3.2.2. Bent Arrangement

The feasibility of geared rotation between phenyl rings and triptycyl groups in derivatives of 9-benzyltriptycene was a major focus in the field of atropisomerism in the 1970s and 1980s.[23] Benzyl triptycenes were first shown to exhibit restricted rotation about the bridgehead–substituent bond in the mid-1970s,[72] and the barriers to interconversion of the enantiomeric and *meso* stereoisomers of derivatives of **25** were later determined to be ~10 kcal/mol.[73]

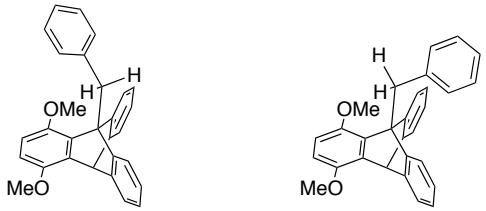

enantiomer of **25** *meso* isomer of **25**

Subsequent studies analyzed derivatives of 9-(3,5-dimethylbenzyl)triptycene (**26**) and attempted to use the methyl groups as NMR probes to determine if correlated rotation of the phenyl group around all of the tripticyl blades (including the sterically bukly, *peri*-substituted benzene rings) or isolated rotation of the phenyl ring is responsible for the interconversion of two achiral *anti peri* (*ap*) conformations (Figure

1.17). Initial studies on a 60 MHz NMR instrument were unclear,[74] but later investigations[75] with a higher field 270 MHz instrument demonstrated that isolated rotation has a lower barrier than geared rotation in these systems. Similar results were observed for derivatives of 9-(3,5-dimethylphenoxy)triptycene.[76]

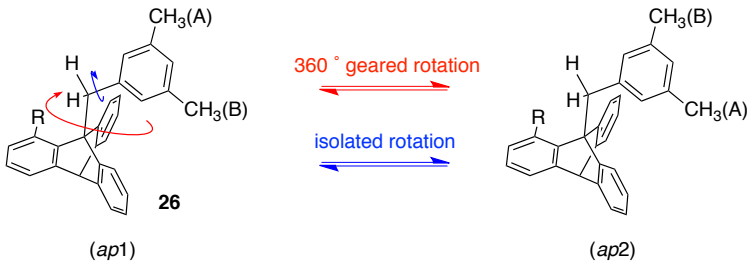

Figure 1.17. *Exchange of the (A) and (B) methyl signals could result from geared rotation or isolated rotation of the phenyl ring in compound* ***26****.*

Increasing the steric bulk of the phenyl group by means of methyl substituents at the 2- and 6-positions[77] highly increases the barrier for isolated phenyl rotation. Derivatives of 9-(2,4,6-trimethylbenzyl)triptycene (**27**) were subjected to dynamic NMR studies,[78] which showed that the 2,6-methyl groups decoalesce upon cooling, giving barriers of interconversion of 12.4 kcal/mol (X = OCH_3), 15.6 kcal/mol (X = CH_3), and 17.5 (X = Br) (Figure 1.18). These values were attributed to the barrier of the enantiomerization process between the *syn clinal* (*sc*) conformations, where the aryl ring must rotate over the *peri*-substituted benzene ring of the triptycene group. The barrier for geared rotation of the aryl group about a *peri* hydrogen was too low to be measured under the same conditions (< 9.7 kcal/mol). Contemporaneous empirical force field studies by Mislow and coworkers[79] indicated that benzyl groups containing methyl groups at the 2- and 6-positions undergo geared rotation about the blades of triptycene as their dominant mode of conformational interconversion.

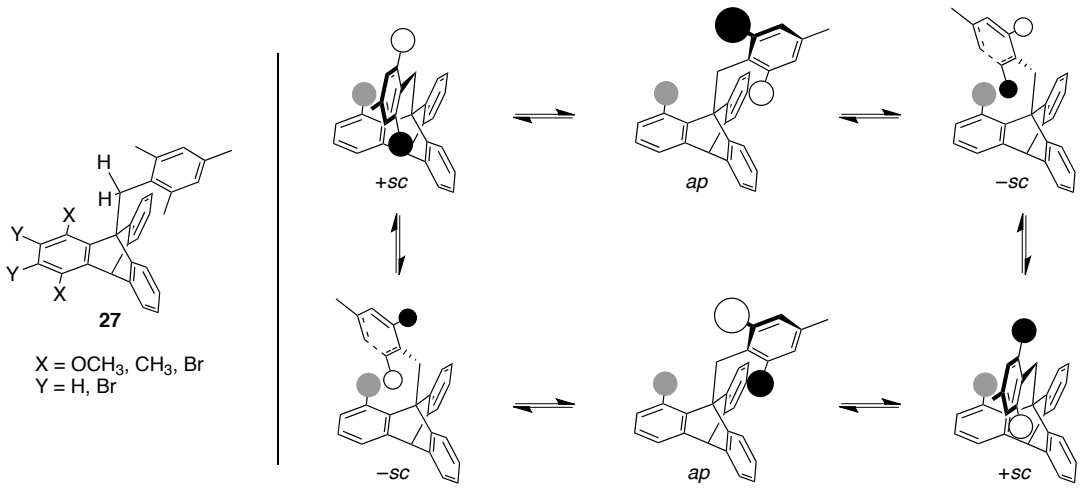

Figure 1.18. *Cogwheeling circuit of peri-substituted derivatives of* ***27****.*

These studies of 9-substituted triptycene derivatives clearly demonstrated that triptycene is a rigid, three-bladed propeller comprising hard blades and open cavities between them. They marked important landmarks in the study of atropisomerism through correlated rotation and inspired great interest in triptycene as a molecular rotator.

1.4. Interacting Triptycene Rotators

1.4.1. Two Triptycenes in a Coaxial Arrangement

When two rotating triptycene moieties are positioned in such a way that their cylindrical gearing profiles overlap, steric interactions will be present and the system will behave as a gear shaft. The rotational barrier about the 9,9' C–C bond in 9,9'-bitriptycyl[80] (**28**) was found to be in excess of 54 kcal/mol.[81] Separating the propellers with an acetylene connector essentially eliminates the barrier to rotation, as the rotational profiles of the triptycenes no longer overlap. By introducing *peri* methyl groups to ditriptycylacetylene, full rotation is again hindered; the barrier to rotation of labeled blades over unlabeled blades in **29** was found to be ~15 kcal/mol. Interestingly, compound **29** was the first published compound in which atropisomerism about a C–C triple bond was observed.[82] Rotational properties of other derivatives of bis(triptycen-9-yl)ethyne have been studied extensively by Toyota, Ōki, and coworkers.[83]

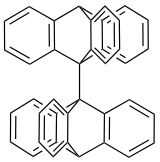

28

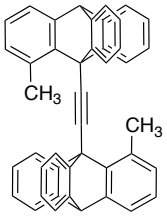

29

The linear relationship between the rotators allows for debate concerning the relationship between the rotators' rotation. One could argue that disrotation is conserved; if observed from a point along the axis, between the two rotators, the rotators rotate in opposite directions. On the other hand, one could argue that rotation of the rotators becomes conrotatory at an interacting angle of 180°, as both rotators appear to rotate in the same direction if such a molecule is observed from a distance.

1.4.2. Two Triptycenes in a Bent Arrangement

Connecting two triptycenes in a bent orientation results in remarkable rotational behavior with fascinating stereochemical consequences.[84] These effects were contemporaneously observed by Mislow in substituted derivatives of ditriptycylmethane (**30**),[85] and by Hiizu Iwamura in ditriptycyl ether (**31**),[86] though they were first predicted by Mislow.[87] The molecules exhibit essentially free rotation of each of the triptycene rings; however, the rotation of the rings is strongly correlated and the system behaves as a nanoscopic bevel gear.

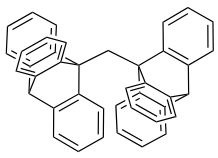

30

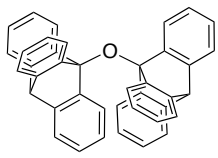

31

The molecular structure of **30**[88] provides insight into its function as a highly efficient molecular gear system (Figure 1.19). The molecule is highly strained, with a bond angle $C(9)_{Tp}$–CH_2–$C(9')_{Tp}$ equal to 129°. If angle vectors are extended to $C(10)_{Tp}$ and $C(10')_{Tp}$, the angle grows even wider, to 138°. The distance from the carbon of the methylene group to the center of the propeller hub (the point at the center of the line connecting C(9) and C(10)) is 2.9 Å.[89] These geometrical constraints force H–C(1) to fit snugly between two benzene rings of the adjacent triptycene moiety.

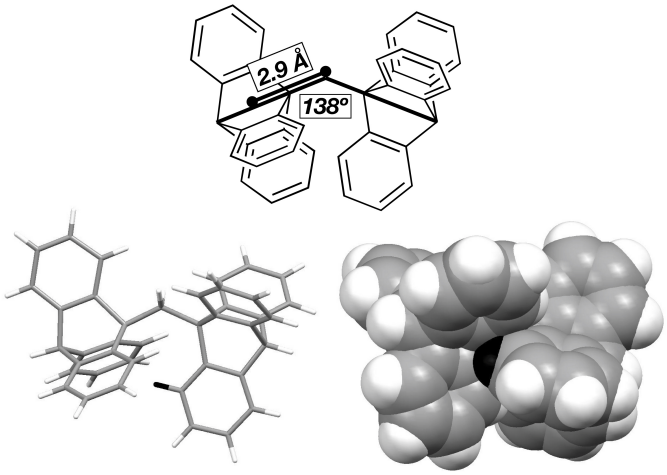

Figure 1.19. (top) Geometrical properties of ***30****. (bottom) Molecular structure of* ***30****, rendered in capped stick (left) and space-filling (right) models. The hydrogen atom that is intermeshed between the benzene rings of the neighboring Tp group is marked in black.*

Further analysis of **30** reveals steric interactions between the benzene rings on each triptycene group that do not allow for gear slippage without significant bending of the blades. Gear slippage requires the bond angle centered at the carbon atom of the methylene group to open even further than in its already strained state. The lowest energy ground state of **30** is of C_2 symmetry. An approximate C_s conformation of **30** corresponds to a transition state of geared rotation, and the transition state to gear slippage is of C_{2v} symmetry[90] (Figure 1.20). The energy difference between the structures of C_2 and C_s symmetry is calculated to be only 0.2 kcal/mol, indicating an extremely low energetic requirement for gearing. In contrast, gear slippage requires significantly more energy, as the C_{2v} structure lies 30 kcal/mol[91] higher in energy than the C_2 conformation.

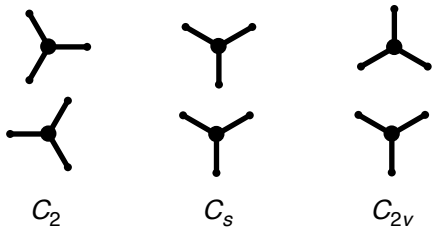

Figure 1.20. *Schematic view of* C_2, C_s, *and* C_{2v} *conformations of triptycene-based gear constructs.*

The process of dynamic gearing gives rise to stereochemical consequences in desymmetrized derivatives of **30** and **31**. Consider a construction **32** in which one of the benzene rings on each triptycene is substituted with one or more labeling groups at the 2-, 3-, or 4-positions, where the substituent will not have a steric repulsion with the neighboring triptycene group during its rotational orbit.

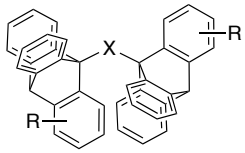

32

Under the process of geared rotation—and the absence of gear slippage—such a compound would exist as a mixture of phase isomers, one achiral isomer and one enantiomeric pair (Figure 1.21). Each subset contains six isomers and interconversion of one subset into another requires gear slippage. The term phase isomerism was introduced in conjunction with molecular gearing to describe residual stereoisomers that are generated as a result of correlated rotation. The concept of residual stereoisomerism was originally introduced in the description of molecular propellers, but has no mechanistic connotations. The molecular propellers described in section 1.2.4 are also correctly called phase isomers.

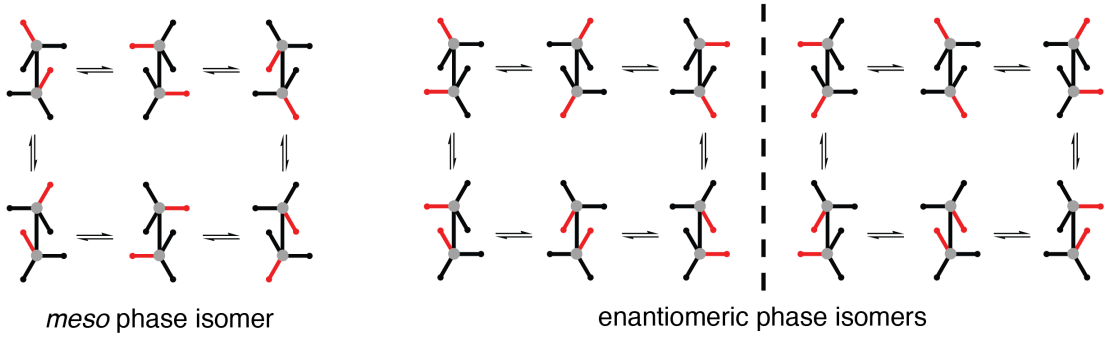

Figure 1.21. *Meso and enantiomeric phase isomers of Tp_2X, in which one benzene ring contains a labeling group.*

Various substitution patterns will lead to different stereochemical consequences and these have been compiled by Mislow (Table 1.1).[92] The substitution patterns that fall into class I result in only one achiral isomer in all cases, whereas those in class II give

only sets of enantiomeric pairs. Both of these classes present the same stereochemical consequences under allowed and disallowed gear slippage, rendering them useless in the determination of dynamic gearing. Classes III and IV offer a distinction between the allowed/disallowed slippage modes and allow for experimental determination of phase isomerism. Patterns in class III provide both *meso* and enantiomeric forms and those in class IV give only enantiomeric forms. Unsubstituted molecules **30** and **31** falls into pattern no. 1 and a molecule with the substitution pattern shown in **32** falls in to pattern no. 9.

Analogs of **30**, **31** and **32** include isostructural derivatives **33**, [93] in which the Triptycene groups are linked by a variety of atoms or groups and a tightly intermeshed vinylene-linked system **34**.[94] A molecular gear that incorporates a clutch function by silane–silicate interconversion **35** has recently been synthesized and studied.[95]

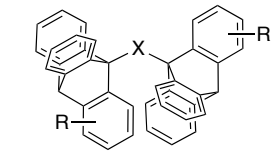

X = S, CHOH, CO, SiH_2, NH

33

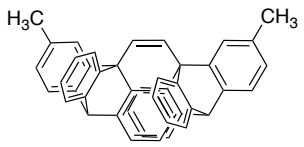

34

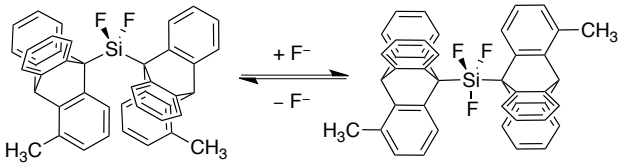

35

Thorough kinetic studies on the process of gear slippage have been performed on several of the bevel gear constructs (Table 1.2).[96] These phase isomers are separable by chromatography and kinetic investigations of their barriers of interconversion between them provides the barrier to gear slippage. The ethers and amine have higher barriers to gear slippage than ditriptycylmethanes. The thioether has roughly the same barrier as the methylene system, while the silane's barrier is significantly lower

Table 1.1. *Classes of Residual Stereoisomers for All Substitution Patterns of Tp_2X under the Full Operation of the Gearing Mode*

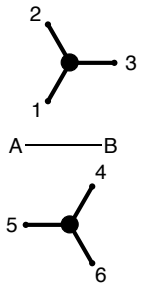

residual isomer or species				
	isomer count[a]			
class	gear slippage disallowed	gear slippage allowed	substitution pattern[b]	pattern no.
I	1/0	1/0	a = b, 1 = 2 = 3 = 4 = 5 = 6	1
	1/0	1/0	a = b, 1 = 2 = 3 ≠ 4 = 5 = 6	2
	1/0	1/0	a = b, 1 = 2 = 3; 4 = 5 ≠ 6	3
	1/0	1/0	a ≠ b, 1 = 2 = 3 = 4 = 5 = 6	4
II	0/1	0/1	a = b, 1 = 2 = 3; 4 ≠ 5 ≠ 6	5
	0/1	0/1	a ≠ b, 1 = 2 = 3 ≠ 4 = 5 = 6	6
	0/1	0/1	a ≠ b, 1 = 2 = 3; 4 = 5 ≠ 6	7
	0/2	0/2	a ≠ b, 1 = 2 = 3; 4 ≠ 5 ≠ 6	8
III	1/1	1/0	a = b, 1 = 2 = 4 = 5 ≠ 3 = 6	9
	1/1	1/0	a = b, 1 = 2 ≠ 3; 4 = 5 ≠ 6	10
	1/1	1/0	a = b, 1 = 4 ≠ 2 = 5 ≠ 3 = 6	11
	1/1	1/0	a ≠ b, 1 = 2 = 4 = 5 ≠ 3 = 6	12
	2/2	2/0	a ≠ b, 1 = 4 ≠ 2 = 5 ≠ 3 = 6	13
IV	0/3	0/1	a = b, 1 = 2 ≠ 3; 4 ≠ 5 ≠ 6	14
	0/3	0/1	a = b, 1 = 4 ≠ 2 = 6 ≠ 3 = 5	15
	0/3	0/1	a ≠ b, 1 = 2 ≠ 3; 4 = 5 ≠ 6	16
	0/3	0/1	a ≠ b, 1 = 4 ≠ 2 = 6 ≠ 3 = 5	17
	0/6	0/2	a = b, 1 ≠ 2 ≠ 3; 4 ≠ 5 ≠ 6	18
	0/6	0/2	a ≠ b, 1 = 2 ≠ 3; 4 ≠ 5 ≠ 6	19
	0/12	0/4	a ≠ b, 1 ≠ 2 ≠ 3; 4 ≠ 5 ≠ 6	20

(a) For each entry (x/y), x = number of meso (achiral) isomers, and y = number of racemic pairs. The isomer count refers to achiral ensembles observed under achiral conditions. (b) A semicolon between sets signifies that the two sets may share some, but not all, of their elements.

Table 1.2. *Barriers to gear slippage in several desymmetrized bevel gears*

substitution pattern[a]			
X	2	3	E_a[c] (kcal/mol)
CH_2	CH_3	CH_3	34[b]
CH_2	Cl	H	32.2 ± 0.1
CH_2	H	Cl	33.1 ± 0.2
O	Cl	H	42.0 ± 0.5
O	H	Cl	43.2 ± 0.3
NH	Cl	H	39.1 ± 0.5
SiH_2	Cl	H	21.1 ± 0.4
S	Cl	H	29.3 ± 0.3

(a) Numbers refer to positions on the labeled triptycene ring (b) $\Delta G^{\ddagger}$ at 145–165 °C. (c) Arrhenius activation energy for the process DL → meso.

The behavior of bis(1,4-dimethyltriptycen-9-yl)methane (**36**)[97] further highlights the rich stereochemistry of the Tp_2X motif (Scheme 1.5). It differs from the previous systems by the presence of methyl groups at the 1-positions of the triptycene groups. Over the course of gearing, the methyl group will eventually be forced to intermesh in the highly overcrowded space between the aryl rings of the neighboring Tp groups. At high temperature (>>200 °C) geared rotation and gear slippage are fast and the compound exists as one achiral species. Upon cooling, the process of gear slippage is frozen out, while gearing continues to occur, leading to two enantiomeric pairs (D and L) and one *meso* isomer as expected from substitution pattern no. 9. Further cooling freezes out the process of gearing also, causing the *meso* isomer to separate into two enantiomeric forms, *d* and *l*. Because the *d* and *l* isomers can interconvert by geared rotation at elevated temperature, they are not phase isomers. Mislow likened this restricted gearing to the motion of screwing a bolt with a monkey wrench using one hand; partial rotation is easy, but full rotation would require an extremely painful contortion of the hand.

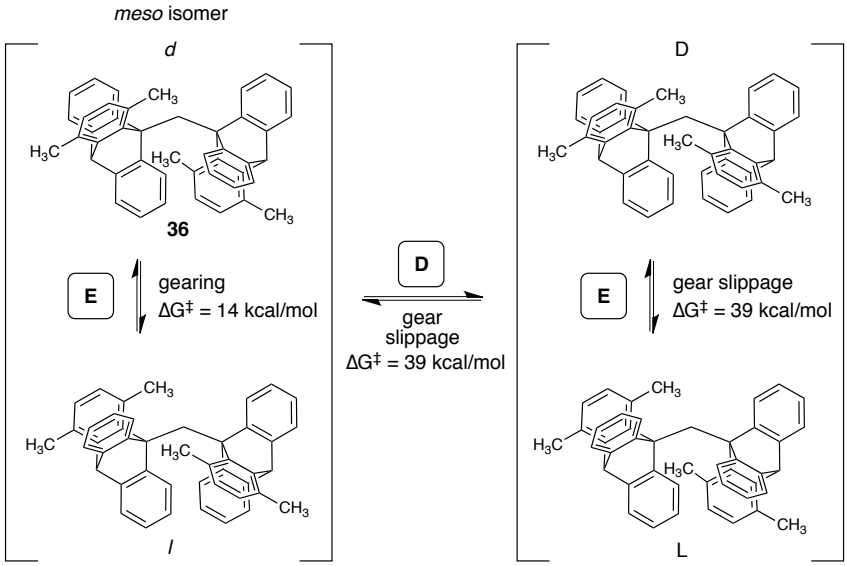

Scheme 1.5. *Representative conformations of stereoisomers of* ***36****. Boxed "E" and "D" refer to enantiomerizations and diastereomerizations, respectively. The process through which the stereoisomers interconvert is shown and their associated energy barriers are provided.*

1.4.3. Three Tripycenes in Bent Arrangement

Molecules with three secured rotator components have been synthesized in linear (**37**)[98] or cyclic [(**38**, **39**)[99] and **40**[100]] arrangements, the former exhibit smooth rotation (E_a < 2 kcal/mol) as a correlated triplet, whereas the parity requirement of disrotatory motion locks the latter in a frustrated state (E_a of rotation = 20 kcal/mol). Each of these arrangements has stereochemical consequences: system **37** is dynamic and exhibits phase isomerism; **38** is static and achiral (C_{3h}) whereas **39** and **40** are static and chiral (C_3).

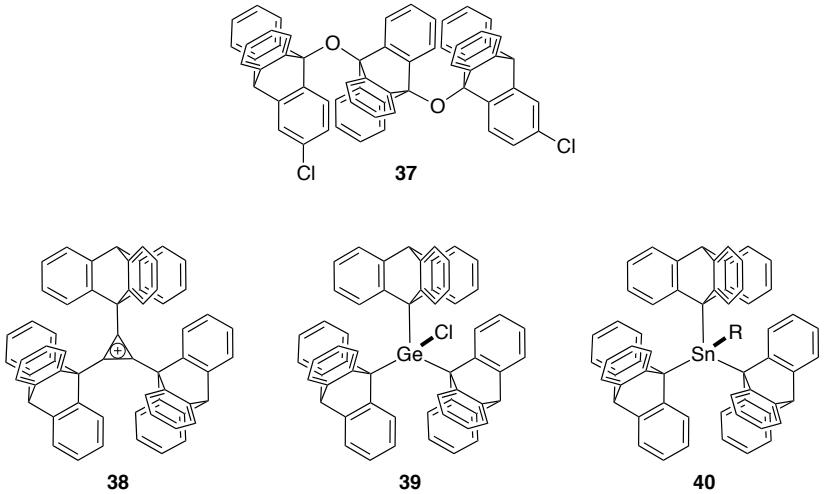

1.4.4. Two Triptycenes in a Collateral Arrangement

Placing two triptycenes in a collateral arrangement evokes the image of a spur gear. In 1989, Mislow and Iwamura envisioned the future development of spur gears as a natural extension to their work on bevel gear constructs.[84] The first systems of this kind appeared in 1999[101] as bis(triptycene)crown ethers **41** and **42** developed by Sachleben, who had previously[102] developed "rope-skipping"[103] triptycenocrown ethers. VT-NMR demonstrated that the triptycene groups undergo fast rotation (on the NMR timescale) above 60 °C and that the rotation is frozen out below –40 °C. Whether or not the rotators undergo correlated, geared rotation is undeterminable, as labeled systems that permit investigations of phase isomers were not synthesized.

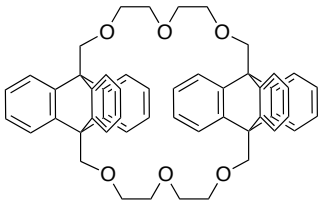

41

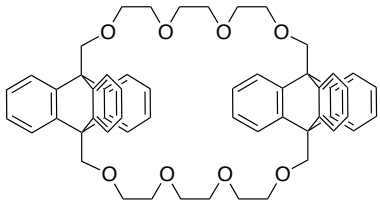

42

Toyota and coworkers recently reported a series of spur gear prototypes **43a**–**45b** with the first thorough stereochemical analysis of such constructs.[104] To assess the rotational behavior of the triptycene groups, DFT calculations were performed on unlabeled **43a** and indicated that the C_s transition state to geared rotation (3.8 kcal/mol) is lower than the C_{2v} transition state to gear slippage (5.5 kcal/mol). Calculations on labeled **44a** were unsuccessful and computational results on the other molecules were not reported.

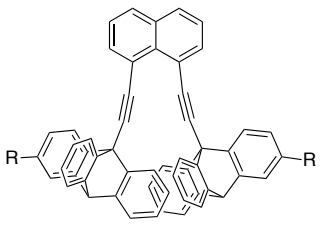

43a R = H
43b R = CH_3

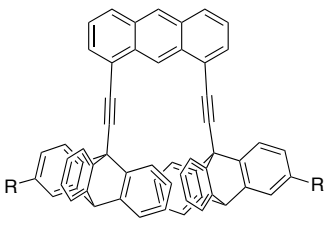

44a R = H
44b R = CH_3

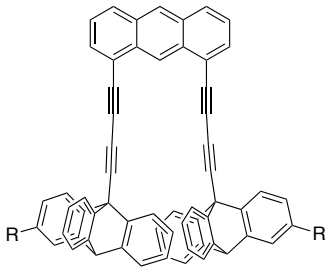

45a R = H
45b R = CH_3

VT-NMR experiments were performed on the labeled compounds in an attempt to establish phase isomerism. Due to the methyl groups at the 3-positions, populations of conformers with inward-facing labeled blades were expected to be negligible and the gearing transition states with an inward-facing labeled blade were ruled out. In the absence of gear slippage, the enantiomeric phase isomers should exist as three interconverting isomers and the *meso* phase isomer should exist as a mixture of enantiomeric conformations (Figure 1.22). However, the VT-NMR experiments failed to show any clear decoalescence, indicating that the barriers to gear slippage in these compounds are likely too low to be measured by this technique.

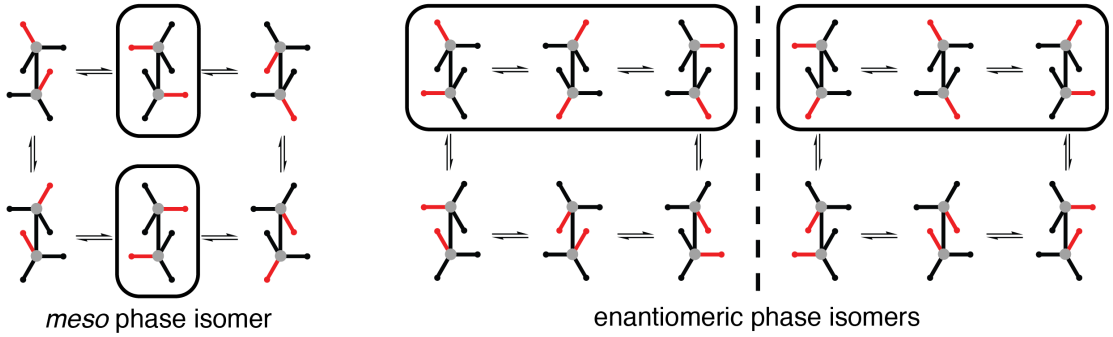

Figure 1.22. *Conformations that would exist with restricted geared rotation, and no gear slippage, in compounds* ***43b****,* ***44b****, and* ***45b****.*

1.5. Other Molecular Gear Constructs

Metallocene molecular gear prototype **46** was developed in 1997 by Richards.[105] In this construct, a four-bladed tetraphenylcyclobutene rotator is intermeshed with a three-bladed triptycene. No experimental evidence for geared rotation is presented, as the 3 × 4 gearing framework precludes the formation of phase isomers; both geared rotation and gear slippage would garner the same set of conformations. Computational studies could have provide insight into the mechanics of the molecule, but were not reported.

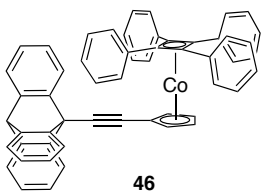

46

Yang and coworkers recently reported the preparation and analysis of pentiptycene-based molecular gears **47**.[106] Unlike the previous examples, which have *n* blades and *n*-fold symmetry, pentiptycene has four blades and two-fold symmetry, complicating the dynamic models of the system. Four-fold geared rotation was found not to be preferred over slippage, as DFT calculations indicated that four-toothed geared rotation requires more energy (5.5 kcal/mol) than uncorrelated slippage (4.7 kcal/mol) or geared rocking motions (2.9 kcal/mol) in unlabeled **47**. However, this detailed and well-performed study serves as the basis for molecular gear constructs with more than three blades.

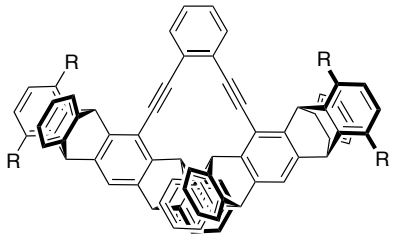

47
R = H, OMe

1.6. Evaluating the Efficiency of Gearing

Given the development of molecular gears and the general interest in molecular machines, it would be useful to have some parameters that characterize gearing efficiency. *Gearing fidelity* (F_{gear}) and *gearing temperature* (T_{gear}) are terms to address this issue.[107] The expression $F_{gear} = k_{geared\ rotation}/k_{gear\ slippage}$ provides a measure of gearing fidelity at a given temperature (298 K, for example) as the average number of geared rotations per gear slip. Gearing temperature is the temperature below which the rate of gear slippage remains slower than a certain value (1 s^{-1} when not otherwise stated) and is expressed as $T_{gear}^{\#}$ where # is the log of the number of slips/second (0 when not otherwise stated).

In molecules **30–35**, the efficiency of gearing is outstanding, giving high values of F_{gear} and T_{gear}; if 2 kcal/mol were the barrier to geared rotation and 35 kcal/mol the barrier to gear slippage, the F_{gear} would be on the order of 10^{23} and the T_{gear} would be 584 K. Because a small difference in $\Delta G^{\neq}_{geared\ rotation}$ and $\Delta G^{\neq}_{gear\ slippage}$ has a significant effect on the rates of the processes, systems whose barriers to geared rotation are only a

few kcal/mol lower in energy than their barriers to gear slippage can still function as efficient gears.

1.7. Goal of this Section

A precise depiction of a molecule as a machine requires that it not only structurally resemble, but also functionally act, as a mechanical component. From this perspective no example of a true molecular spur gear has been demonstrated. The goal of the work presented in the next chapter is the development of molecular spur gears, nanoscopic miniaturizations of the most common type of gear used in machinery.

Chapter 2

Triptycene-Based Molecular Spur Gears*

2.1. Summary

This chapter presents current work on the elucidation of dynamic gearing in molecular spur gears, the most common type of mechanical gear. Molecular design and conformational analysis show that derivatives of 4,4'-bis(triptycene-9-ylethynyl)bibenzimidazole represent suitable constructs to investigate gearing behavior in collateral triptycene groups. To thest this design, DFT calculations (B97-D/Def2-TZVP) were employed and the results suggest that these molecules undergo geared rotation preferentially to gear slippage. Synthesis of derivatives was carried out, providing a series of molecular spur gears, including desymmetrized derivatives, which were subsequently subjected to stereochemical analysis.

2.2. Introduction

Artificial molecular rotors,[5] particularly those with potential applications in the field of molecular devices[108] and machines,[4] represent contemporary chemical miniaturizations of macroscopic engineering constructs. Among the most ubiquitous components in macroscopic machinery for the past two millennia has been the gear,[109] which transforms rotational motion from one axis to another or into translational motion.

At the molecular level, dynamic gearing has been demonstrated in bevel gears comprising intermeshed triptycene groups.[84] Before the work presented in this chapter was published,[110] almost all detailed studies of molecular gear constructs had focused on molecular miniaturizations of bevel gears. Toyota's work on spur gear constructs (pp.

* Large portions of this chapter were reprinted or adapted with permission from reference 110. Copyright © 2012 American Chemical Society.

33–34),[104] which was performed contemporaneously with the work described herein, is the only exception.

This chapter presents the stereochemical analysis, design, calculations, synthesis and dynamic NMR studies of triptycene-based molecular spur gears. Before discussing the details of our study, let us first discuss the conformational analysis necessary to motivate molecular design in this area.

2.3. Conformational Analysis and Molecular Design

Design of molecular gears requires a detailed understanding of conformational analysis and steric shape. Simple valence bond graphs attract one to notions of gearing that are immediately seen as untenable from a space-filling representation. For example, in 1,9-dimethyltriptycene (**48**) (Figure 2.1), the energy minimum ground state was originally assumed[111] to be a gear-meshed C_s conformation in which the methyl groups undergo correlated rotation, but was later calculated[112] to prefer a buttressed, gear-clashed C_s conformation that does not exhibit correlated rotation of the methyl groups. These studies demonstrate that the geometry of a methyl group closely resembles a triangle-based pyramid, its effective steric size is conformation-dependent and cannot be best represented simply by its hydrodynamic radius.[113]

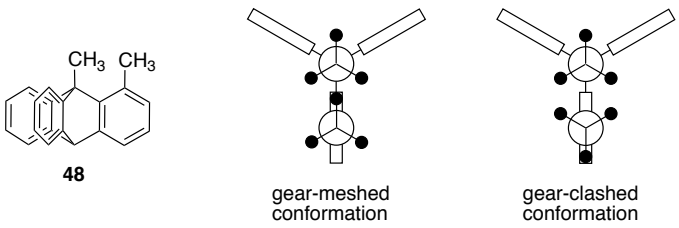

Figure 2.1. *Gear-meshed and gear-clashed conformations of 1,9-dimethyltriptycene. Reprinted with permission from reference 110. Copyright © 2012 American Chemical Society.*

With the caveat in mind that any serious discussion of molecular gearing warrants a rigorous geometric analysis, let us consider a framework that holds two identical three-bladed rotators, with hydrodynamic radii of *r*, in a collateral arrangement. Depending on the nature of the blades, the rotators could be approximated by several models: one extreme could render the rotators as three-toothed propellers of negligible thickness, a moderate estimation could approximate the

components as triangular prisms, and the other extreme case, where the rotators' steric bulk is well approximated by its hydrodynamic radius, may be represented by cylinders (Figure 2.2). Positioning these models in gearing (C_2 and C_s) and gear-clashed (C_{2v} and C_{2v}*) orientations,[114] with respect to the molecular framework, and examining their minimum inter-axle distances establishes their effective steric size.

In any imaginable orientation, the cylinders' minimum inter-axle distance is $2r$. In contrast, minimum axle–axle distances of the propeller or triangular prism approximations depend on their conformations: $0.86r$ (C_2), r (C_s), and r (C_{2v}) for the propeller and $1.15r$ (C_2), $3r/2$ (C_s) and r (C_{2v}) for the triangular prism.

Assuming a hard-surface model, full rotation can only occur in the absence of surface clashing. This condition can be met by increasing the inter-axle distance to a point where one rotator can rotate by 2π without clashing with its static partner, as is the case for the C_s structure in rotators resembling triangle-based pyramids. Alternatively, clashing can be avoided by correlated motion of both rotators (gearing) or by gear slippage.

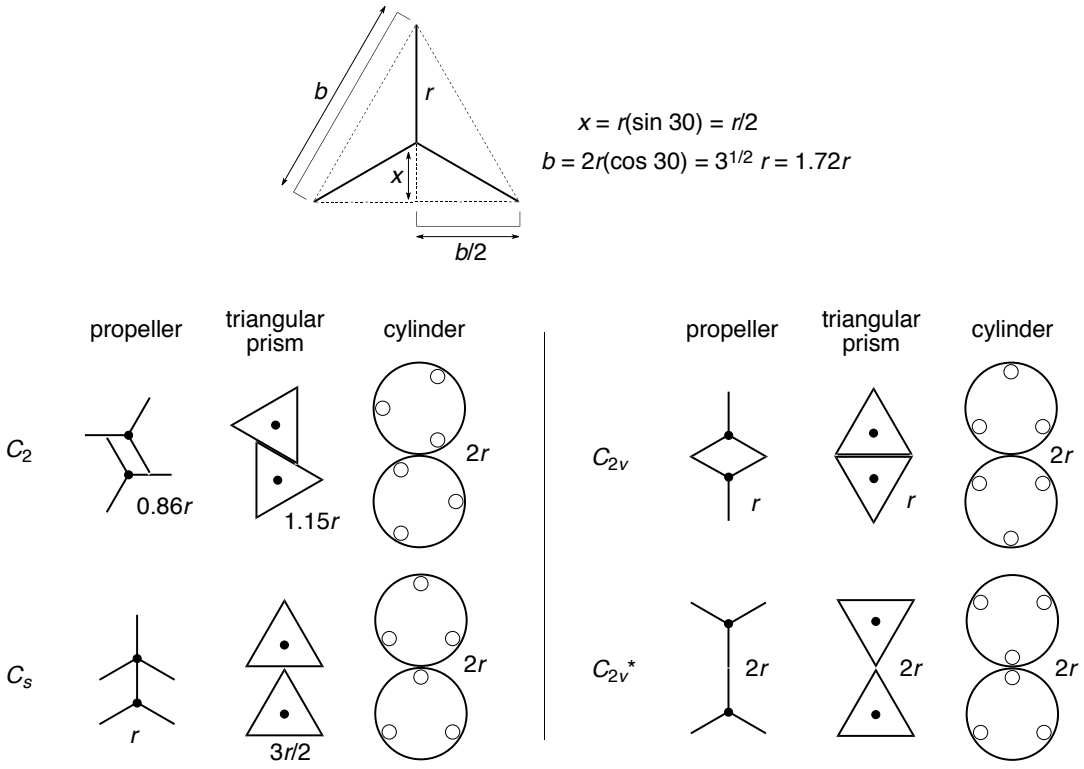

Figure 2.2. *Geometrical analysis of two three-bladed rotators, approximated as propellers, triangular prisms, and cylinders, in C_2, C_s, C_{2v}, and C_{2v}* orientations. The distance from the axle to the blade is r, and the minimum distance between axles is given as a function of r. Adapted with permission from reference 110. Copyright © 2012 American Chemical Society.*

Assuming there is a spring-like tension holding the rotators together, then Hooke's law indicates that the relative inter-axle distance r is a measure of potential energy. From this assumption, the relative potential energy of each conformer can be assessed from its inter-axle distance. In a system with cylinders, all orientations have the same energy and the groups rotate freely and independently of one another. In the case of triangular prisms, the C_{2v} orientation is predicted to be the lowest energy conformation. In the propeller system, the C_2 orientation would suffer the least repulsion due to steric exclusion, whereas C_s and C_{2v} orientations are higher in energy but not distinguished.

Adding a thickness to the blades requires a larger separation for C_s orientations compared to C_{2v} orientations. Thus, the conclusion from the simple mechanical model would then be that C_s orientations would suffer more steric repulsion due to exclusion than C_{2v} orientations at close distances.

A macro-mechanical analysis considers gears to be hard shapes that fit together with shape complementarity defined by steric exclusion.[115] An equivalent molecular model would consider then only steric exclusion when assessing the conformational energy.

In molecular systems, the thickness of the gear blade and the overall shape of the gear might be estimated by the rough van der Waals surface. The length of each blade, measured from the axis of rotation to the edge of the van der Waals radius of H–C(2) and H–C(3) is 5.9 Å. As a consequence of the three-fold axis of rotation, the blades are separated by 120° angles. The rotational profile of triptycene roughly resembles a cylinder, and the largest distance from the circular edge of this cylinder to the intersection of the van der Waals surfaces of the two blades is 3.8 Å.[116] Bringing the triptycene groups in these C_2, C_s, and C_{2v} orientations together as closely as their van der Waals surfaces[117] allow reveals that the minimum axle–axle distances are 7.0 Å, 8.1 Å, and 7.2 Å, respectively (Figure 2.3). Thus, the C_s conformation is required to have a longer axle–axle distance than the C_{2v} conformation by almost 1 Å. In this molecular model, forcing the rotators closer together would increase the energy required for geared rotation more than for gear slippage. Focusing only on van der Waals repulsion by exclusion leaves little hope for this design to result in an effective gear system.

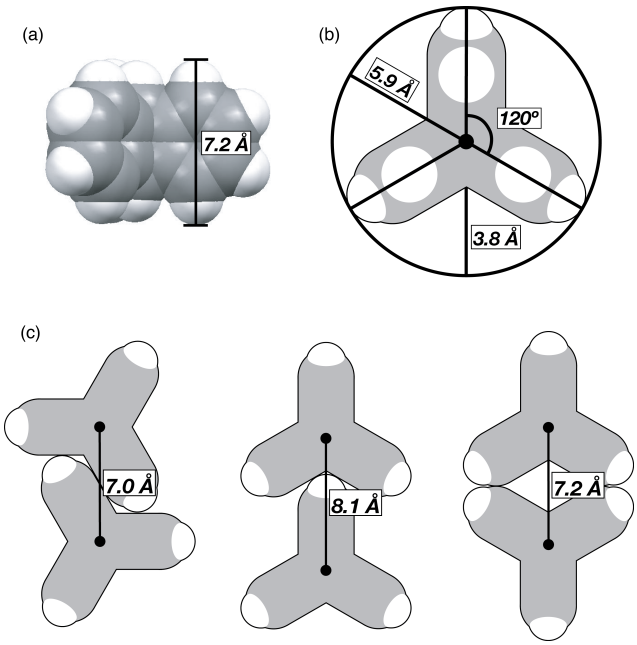

***Figure 2.3**. (a) Side-on view of space-filling model of triptycene. (b) top view of space-filling model of triptycene, showing geometric parameters. (c) Space-filling representations of two collateral triptycene groups groups in C_2 (left), C_s (center) and C_{2v} (right) conformations, indicating the minimum axle–axle distances. Adapted with permission from reference 110. Copyright © 2012 American Chemical Society.*

Fortunately, molecular interactions are more varied than simple hard sphere repulsion. Attractive dispersive terms, along with various electrostatic terms, enrich the analysis and offer the possibility that gearing mechanisms can prevail; for example, van der Waals face-to-face and edge-to-face π–π interactions may stabilize the C_2 and C_s conformations and H–H repulsions or a pocket of vacuum between the triptycene groups may destabilize the C_{2v} conformation. If such were the case, geared rotation could be preferred over gear slippage, albeit unlikely to reach the robust character seen in bevel gears **1–6**. Properly addressing such scenarios exceeds the abilities of simple qualitative models and commitment to full quantum mechanical analysis is thus called for (see section 2.3).

Despite the need for rigorous quantum mechanical computations in order to assign an accurate energy ranking of the conformations, the basic conformational analysis sets rough target dimensions that should allow the triptycene groups to interconvert between C_2 and C_S conformations with minimal strain. The stator must project the two axles in parallel and separate them by an appropriate distance that allows for interaction of the rotators. Our recent work on 1,1'-bridged derivatives of 4,4'-

disubstituted 2,2'-bibenzimidazole (BBI)[118] provides synthetic access to a stator framework that meets these requirements. Substituents at the 4- and 4'-positions extend in parallel at a distance of roughly 8 Å,[119] accommodating a C_s conformation. Acetylene groups extend linearly and provide a sufficient distance between the stator and rotator and their flexibility was expected to allow for a favorable C_2 conformation to be reached with minimal strain. The combination of these rotator, axle, and stator components leads to the generic structure **49**.

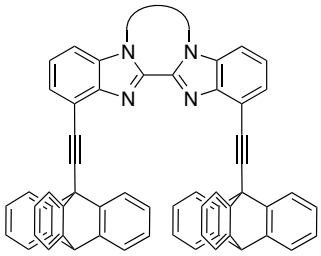

49

The final aspect of the design concerns the location and type of labeling groups that must be added to the rotators to provide desymmetrized derivatives, potentially giving rise to phase isomers. To briefly review from the previous chapter, dynamic gearing of molecular rotators can be established by the observation of phase isomers in desymmetrized derivatives under conditions at which, on the timescale of observation, gear slippage is slow. In three-bladed gears, with one blade labeled, three phase isomers are expected: two enantiomers and one *meso* isomer (Figure 4.4).[120] The phase isomers exist as gearing circuits comprising six energy minimum conformations that, in the absence of gear slippage, may interconvert only through the individual phases of the circuit. Barriers to gear slippage can be calculated by determining the rates at which the phase isomers interconvert.

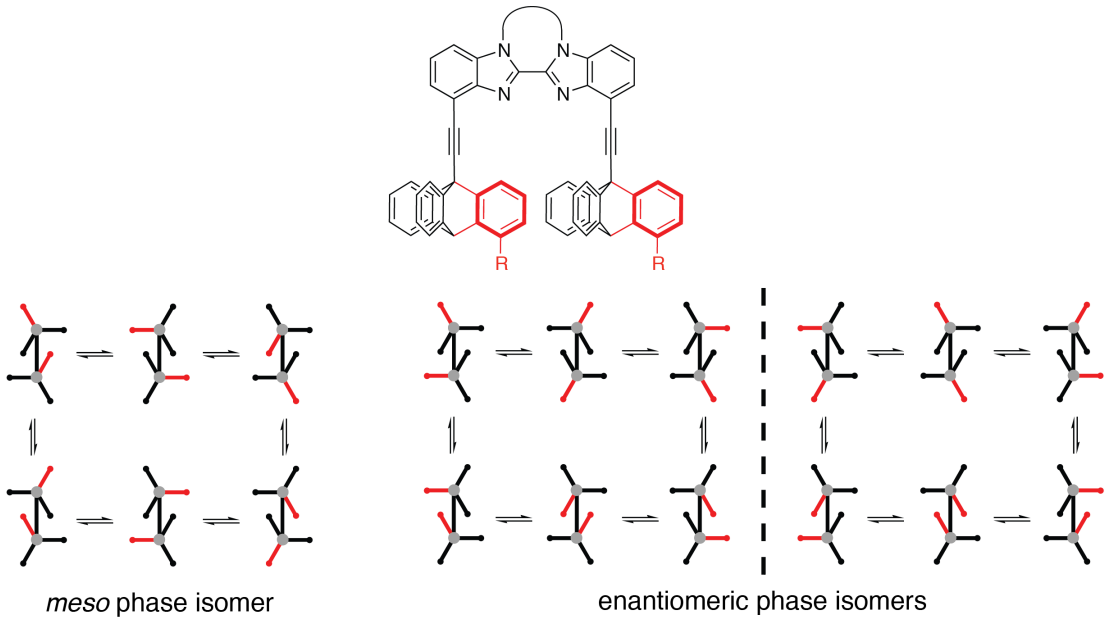

Figure 4.4. *Schematic representation of the phase isomers that could result from adding a substituent to the 4-postion of the triptycene groups in* ***49****. Adapted with permission from reference 110. Copyright © 2012 American Chemical Society.*

Introduction of labeling groups at the 4-positions the triptycene groups avoids steric hindrances between the two triptycene rotators and between the rotators and the stator. In the enantiomeric phase isomers, the labeling groups come in close contact in three of the conformations; in the *meso* phase isomer, they remain distant from one another, a difference that was expected to induce chemical shift differences between the *meso* and enantiomeric phase isomers in NMR spectroscopy. Trifluoromethyl (CF_3) groups were chosen, as they permit ^{19}F-NMR experiments and were expected enhance the chemical shift differences between phase isomers in ^{1}H-NMR spectra. Methyl groups were also chosen, as the behavior of the ^{1}H-NMR signal of this methyl group could indicate the presence of phase isomers at low temperatures.

2.4. Computational Results

Dispersion-enabled DFT, B97-D/Def2-TZVP, was applied to spur gear molecules **49a** and **49b**, which differ in the saturation of the pyrazine ring at the center of the stator.

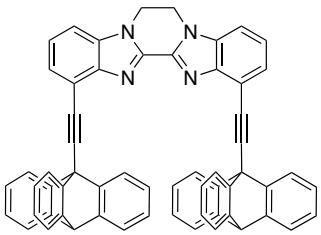

49a

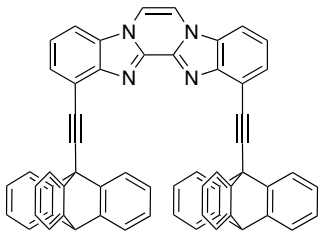

49b

Molecules were fully optimized in C_2, C_s, and C_{2v} conformations and their relative energetics calculated (Figure 4.5). For both **49a** and **49b**, the C_2[121] conformation is the lowest energy ground state minimum. Hessian analysis confirms the C_s conformation as a transition structure for geared rotation and the C_{2v} conformation as a transition state to gear slippage, for **49b**. In **49a**, the C_s and C_{2v} conformations each exhibit two imaginary frequencies, one matching the motion and magnitude of the frequencies in the analogous structures of **49b**, and a much higher mode arising from out-of-plane twisting of the ethylene bridges. This result derives from the central 2,3-dihyropyrazine moiety's preference to adopt a twisted conformation.[122] Planarity of this ring, as required by symmetry in the C_s and C_{2v} conformations, thereby uniformly raises the energies of these conformations to levels that are higher than those of the genuine transition states. Analysis of molecule **49c** indicated that the C_2 conformation is 3.67 kcal/mol lower in energy than the C_{2v} structure.

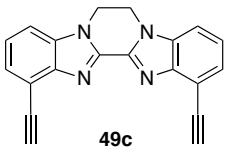

49c

Subtraction of this value from the energies of the C_s and C_{2v} conformations of **49a** provides an estimated value for the energies of the genuine transition state conformations (shown in parentheses in Fig. 4.6). The high consistency between these values and the energies of the respective computed transition state structures of **49b** provides confidence in the accuracy of the calculations.

As expected from Figure 2.3, the distances between the axles of rotation[123] in the triptycene groups increase from C_2 to C_{2v} to C_s in **49a** and **49b**. Distances of 6.84 Å (**49a**) and 6.85 (**49b**) for C_2 conformations and 7.98 (**49a**) and 7.99 (**49b**) for C_s

conformations are ~0.10–0.15 Å shorter than those shown in Figure 2, due to inward bending of the triptycene groups. In the C_2 conformations, face-to-face π–π interactions between the proximal benzene rings and edge-to-face attractions involving the hydrogen atoms connected to the 3-positions of the triptycene groups appear to bring the triptycene groups close together, bending the axles inward. Analysis of the HOMOs shows in-phase orbital interactions between the two triptycene groups.

It is unclear if the C_s structure experiences interactions, though the inward bending of the triptycene groups and their lower energies compared to the C_{2v} structures suggests that a slight attraction may exist. As a consequence of the molecular symmetry, the C_s structures exhibit two nearly degenerate HOMOs, each containing significant density on one of the triptycene groups (one of which is shown for each in Figure 6).

The distances in the C_{2v} structures [7.71 Å (**49a**), 7.74 Å (**49b**)], though shorter than their C_s counterparts, are ~0.5 Å longer than would be required from steric exclusion alone. This widening suggests a destabilizing H–H repulsion between the blades of the triptycene groups, which is further supported by the higher energy of the C_{2v} conformations. The HOMO orbital also shows antibonding interactions between the triptycene groups.

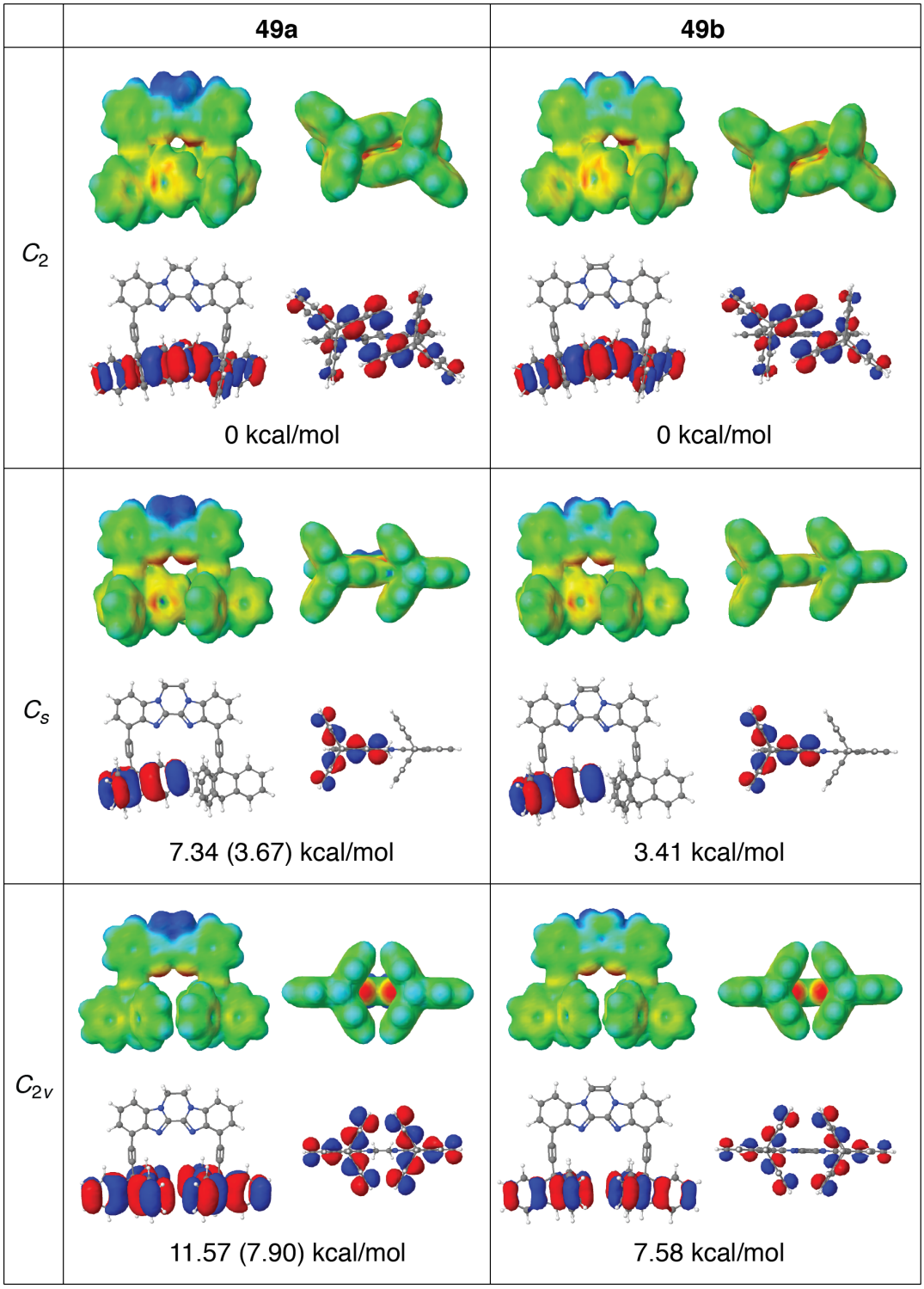

Figure 2.6. *: B97-D/Def2-TZVP calculated C_2, C_s, and C_{2v} structures and energetics of* ***49a*** *and* ***49b*** *rendered as electrostatic potential maps (top, contour level = 0.005) and HOMOs (bottom, contour level = 0.02) in each case. Energies relative to the respective C_2 conformations are given beneath the structures. Values in parentheses indicate the estimated energies for the transition state structures for gearing (C_s) and gear slippage (C_{2v}) in* ***49a****, calculated by subtracting the energetic cost of planarity in the stator/axle unit (see text).Adapted with permission from reference 110. Copyright © 2012 American Chemical Society.*

The computations clearly indicate that gear-meshed conformations C_2 and C_s are favored over the gear-clashed C_{2v} conformation and provide computed (**49b**) and estimated (**49a**) values for $\Delta G^{\ddagger}_{\text{geared rotation}}$ and $\Delta G^{\ddagger}_{\text{gear slippage}}$. From these data, gearing efficency in terms of F_{gear} and T_{gear} can be assessed. The computations thus predict F_{gear} values of 1,300 (**49a**) and 1,100 (**49b**) and T_{gear} values of 138 K (**49a**) and 133 K (**49b**).[124] The results from the calculations support the molecular design and provided motivation for the chemical synthesis and investigation of BBI-based molecular spur gears.

2.5. Synthesis of Molecular Spur Gears Based on 2,2-Bibenzimidazole

2.5.1. Retrosynthetic Analysis

Retrosynthetis of **49a** and **49b** leads to stator component 4,4'-dibromo-BBI (**50**) and rotator/axle component 9-ethynyltriptycene (**51**) (Scheme 2.1). To increase the solubility of the synthetic targets, 4,4'-dibromo-6,6'-di-*tert*-butyl-BBI (**52**) was substituted for **50**. Bibenzimidazole **52** can be disconnected to bromonitroaniline (**53**), which could be prepared from commercially available 4-*tert*-butylaniline (**54**). 9-Ethynyltriptycene, and 4-substituted derivatives thereof, can be disconnected to anthracene-9-carboxaldehyde (**55**) and 3-substituted benzynes (**56**).

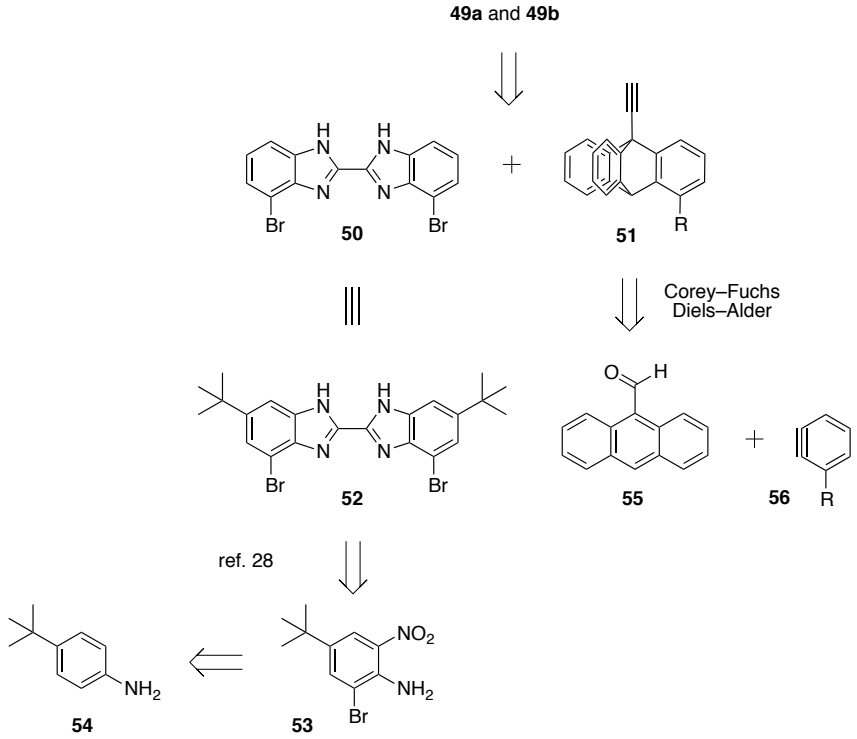

Scheme 2.1. *Retrosynthetic analysis of molecular spur gears* ***49a*** *and* ***49b****.*

2.5.2. Synthesis of Stator Unit

Dibromobibenzimidazole **52** was synthesized in six steps from **54** (Scheme 2.2). Protection of the amino group in **54** with an acetyl group afforded acetanilide **57**, which underwent nitration to generate **58**. Basic hydrolytic deprotection yielded nitroaniline **59** and subsequent bromination yielded **53**.[125] Reduction of the nitro group with $SnCl_2$ afforded bromodiamine **60**. Treatment of **60** with 0.5 molar equiv. of methyl 1,1,1-trichloroacetimidate and a catalytic amount of HCl, followed by basification with K_2CO_3, provided bibenzimidazole **52**.[126]

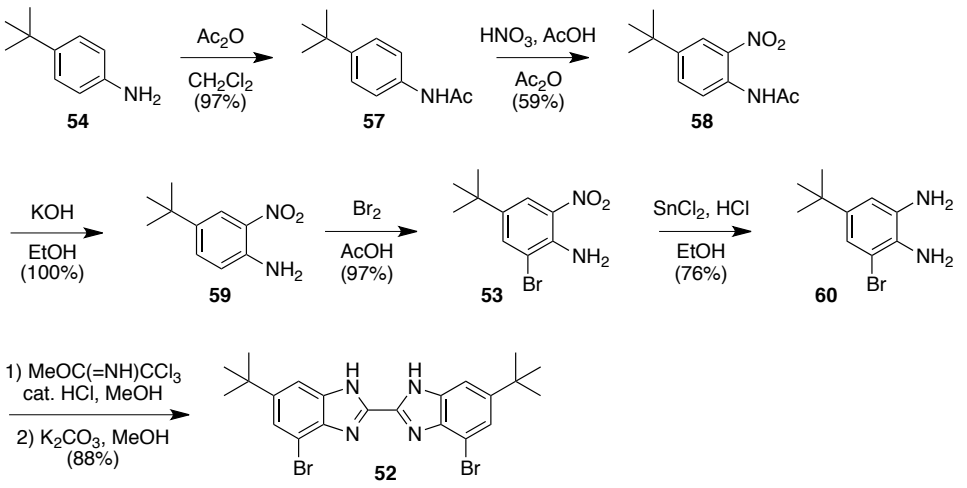

Scheme 2.2. Synthesis of stator component 52.

2.5.3. Synthesis of Rotator/Axle Components

Rotator/axle components 9-ethynyltriptycene **51a** and 4-labeled derivatives **51b–c** were prepared by slightly modifying a published synthesis (Scheme).[127] Aldehyde **55** was converted to cyclic acetal **61**, which was treated with derivatives of benzyne, generated *in situ* from derivatives of anthranilic acid to yield triptycenes **62**. Deprotection gave aldehydes **63**, which could be converted to ethynyltriptycenes **51a–c** by a Corey–Fuchs[128] homologation via dibromoalkenes **64a–c**. An alternate synthesis employing a Sonogashira cross-coupling is known[129] and also provided access to **51a**, but the Corey–Fuchs method was preferable in our hands.

Reaction of **61** with 3-methylbenzyne gave the 1-methyl and 4-methyl derivatives of **62** (Scheme 2.4). These isomers were not separated, but carried on in the synthesis as a mixture until the Wittig step of the Corey–Fuchs methodology, which

selectively reacted with the *anti* isomer and allowed for straightforward purification of **64c** by column chromatography.

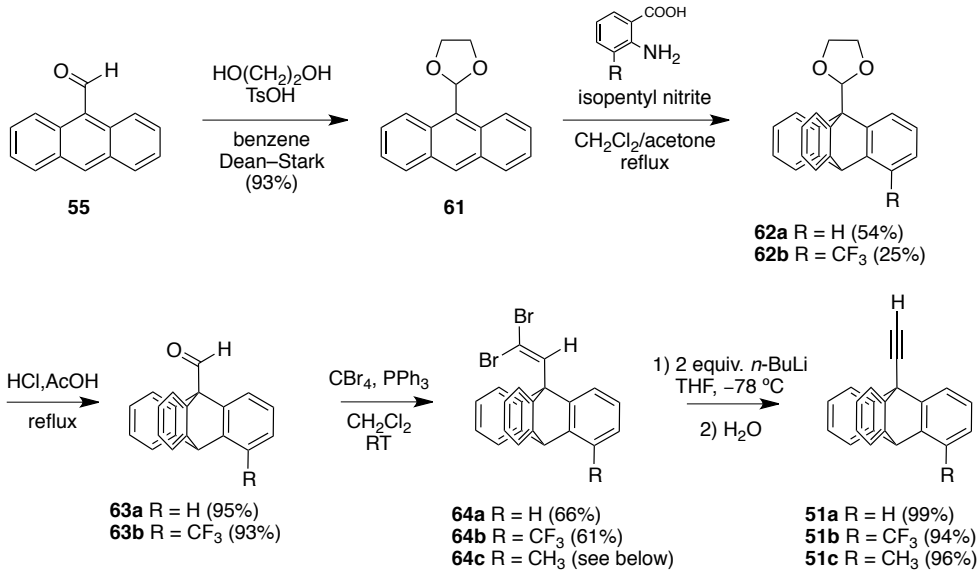

Scheme 2.3. *Synthesis of rotator/axle components* ***51a–c.***

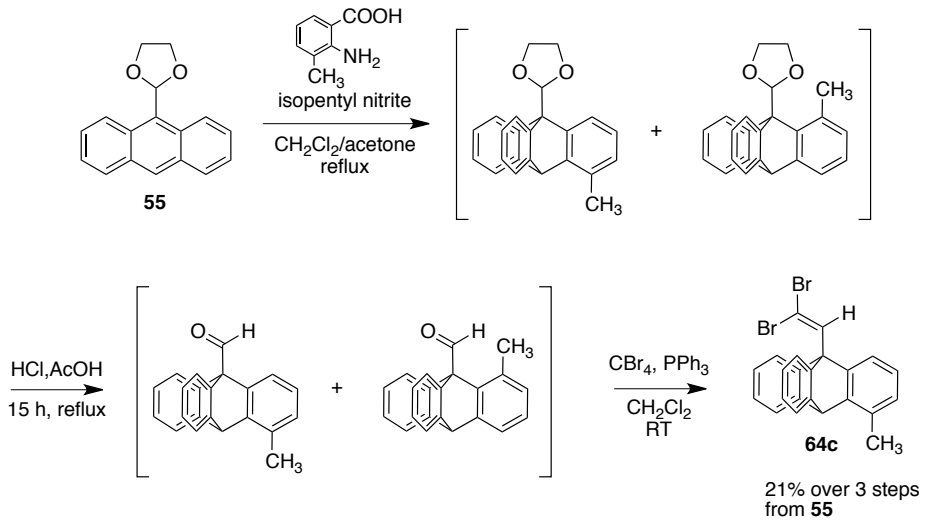

Scheme 2.4. *Mixed regiosomers of methyl-substituted derivatives of* ***62*** *were carried to* ***64c****, which could be separated.*

2.5.4. Synthesis of Ethylene-Bridged Spur Gears

With compounds **51a–c** and **52** in hand, ethylene-bridged molecular spur gears **65a–c** were synthesized (Scheme 2.5). The 1- and 1'-positions of **52** were protected with Boc groups, affording **66**, which was treated with alkynes **51a**, **51b**, or **51c** under standard Sonogashira cross-coupling conditions to yield **67a–c**. Subsequent deprotection, followed by treatment with an excess of 1-bromo-2-chloroethane afforded **65a–c** in yields ranging from 62–64%.

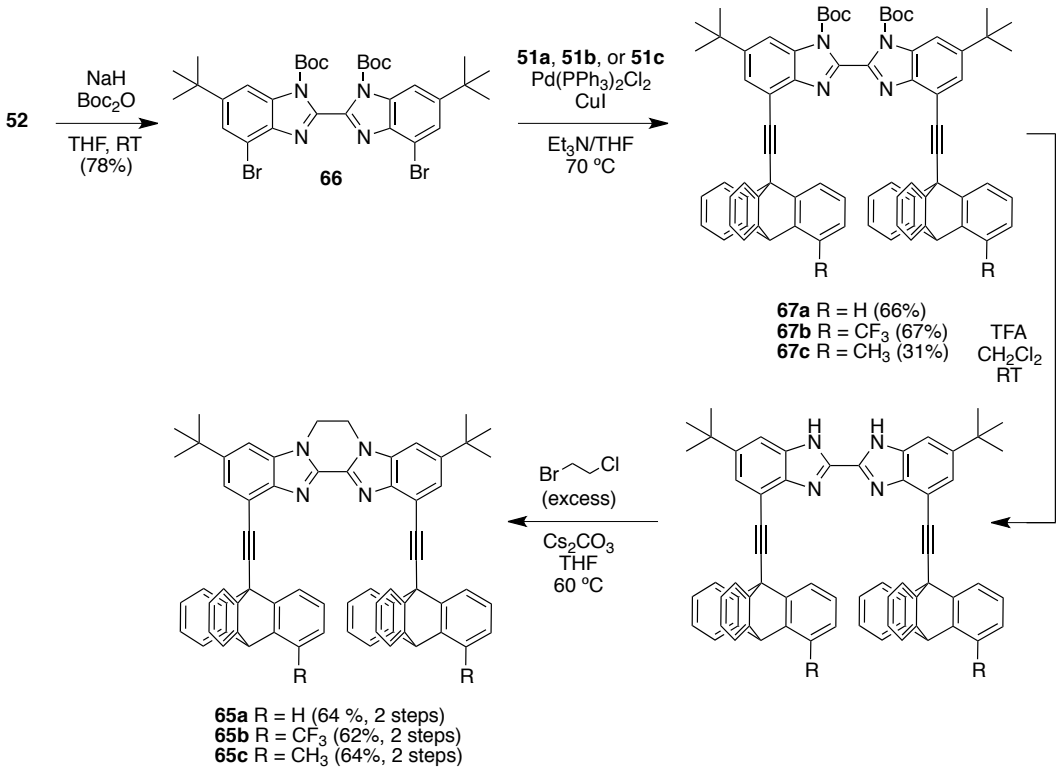

*Scheme 2.5. Synthesis of ethylene-bridged spur gears **65a**, **65b**, and **65c**.*

2.5.5. Synthesis of Spur Gears with Planar Stators

Synthesis of analogs of unsaturated gear **49b** presented a different challenge (Scheme 2.6). Several initial attempts to introduce a vinylene bridge to compound **52** failed, but deprotonation with NaH, followed by treatment with *N*-benzyl-2,3-dibromomaleimide,[130] successfully introduced an unsaturated C–C bond at the desired position, affording heterocycle **68** (Scheme 2.6). The yield of this reaction was routinely ~10%, lower than the reported yield of 36% for the same reaction with unsubstituted BBI.[131] Copper-free cross-coupling reactions[132] with alkynes **51a–c** afforded spur gears

69a–c. Standard Sonogashira conditions using CuI failed, presumably due to complexation of the Cu(I) by **68**.

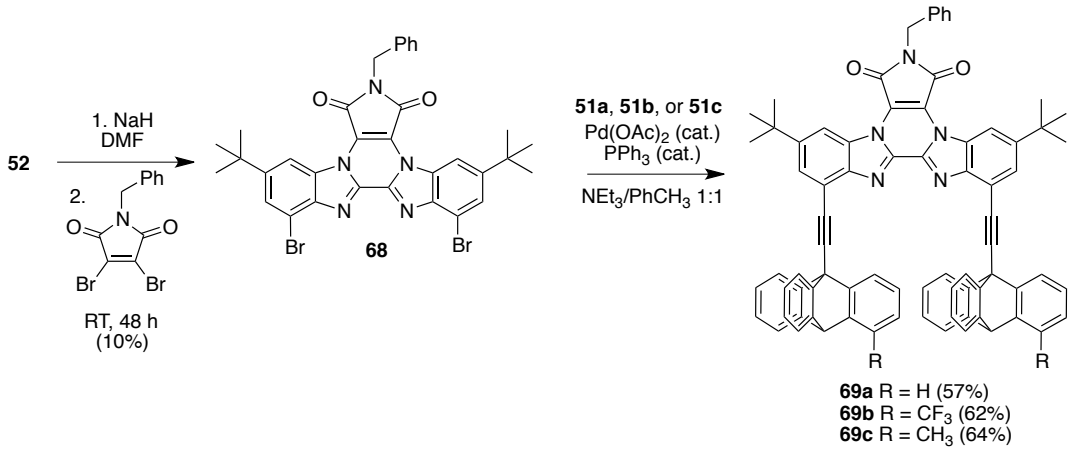

Scheme 2.6. *Synthesis of planar stator unit* ***68*** *and molecular spur gears* ***69–c.***

2.6. X-ray Structure of a Molecular Spur Gear

Single crystals of **65a** were obtained from chlorobenzene and the crystal structure was determined by X-ray crystallography. The asymmetric unit contains one molecule of **65a** and approximately two molecules of chlorobenzene, which are distributed across three partially occupied sites with high disorder. The unit cell contains two molecules of **65a** and the space group is P-1 with the center of inversion located at a point elevated above the plane of the heterocyclic stator component.

The molecular structure, though unsymmetrical, closely resembles the calculated C_s conformation of **49a** (Figure 2.8). The plane of the inward-facing, wedged benzene ring and the planes of the flanking, proximal benzene rings of the neighboring triptycene group intersect at angles of 56.6(2)° and 67.2(2)°. The plane of this wedged benzene ring and the plane of the distal benzene ring on the other triptycene group are close to parallel, intersecting at an angle of 10.4(2)°. The distances between the (9–9') and (10–10') bridgehead atoms of the triptycene groups are 8.420(4) Å and 8.257(4) Å, respectively, longer than those found in the calculated C_s structures **49a** and **49b.**

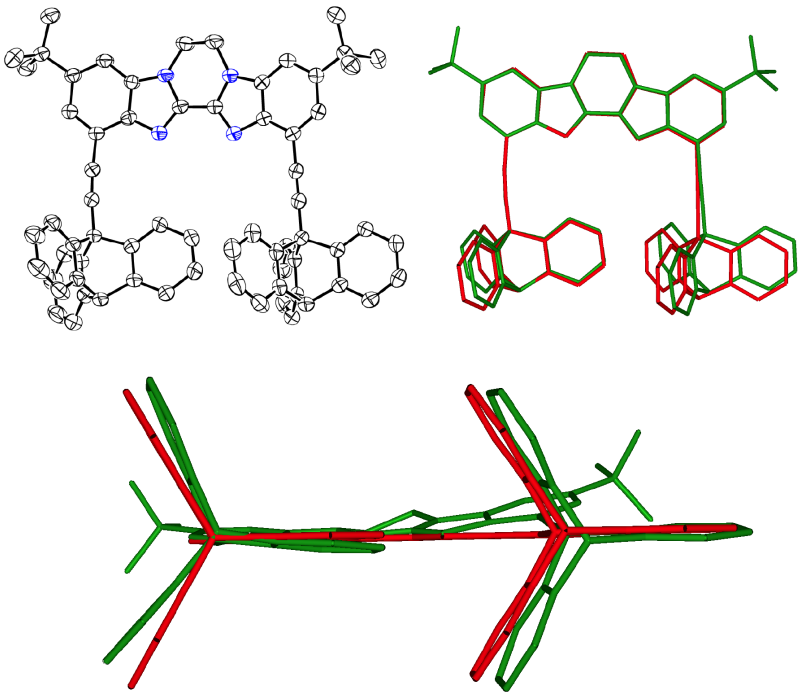

Figure 2.8. *(top left) X-ray molecular structure of* ***65a*** *shown as 50% thermal ellipsoids with hydrogen atoms removed for clarity. (top right and bottom) Overlay of experimental structure of* ***65a*** *(green) and calculated C_s structure of* ***49a*** *(red). Adapted with permission from reference 110. Copyright © 2012 American Chemical Society.*

The molecular structure in the crystal, considered in the context of the calculations, provides further evidence for the preference of the C_s conformation over the C_{2v} conformation. The similarity of the experimental structure to a C_s conformation illustrates that the transition state to geared rotation is a favorable conformation of relatively low energy and provides additional validation to the calculated structures. Deviation from the C_2 conformation, the most stable conformation according to calculations, is attributable to crystal packing forces.

2.7. Variable-Temperature NMR Studies

Although the calculated energy barriers for gear slippage were calculated to be in the range of 7–8 kcal/mol—at the detection limit for VT-NMR studies—compounds **65b**, **65c**, **69b**, and **69c** were probed in an attempt to uncover phase isomerism at low temperature. Determination of coalescence temperatures for the interconversion of *meso* and enantiomeric phase isomers (Figure 2.9) could

experimentally confirm the molecular preference for geared rotation over gear slippage and quantitatively establish the barrier to gear slippage.

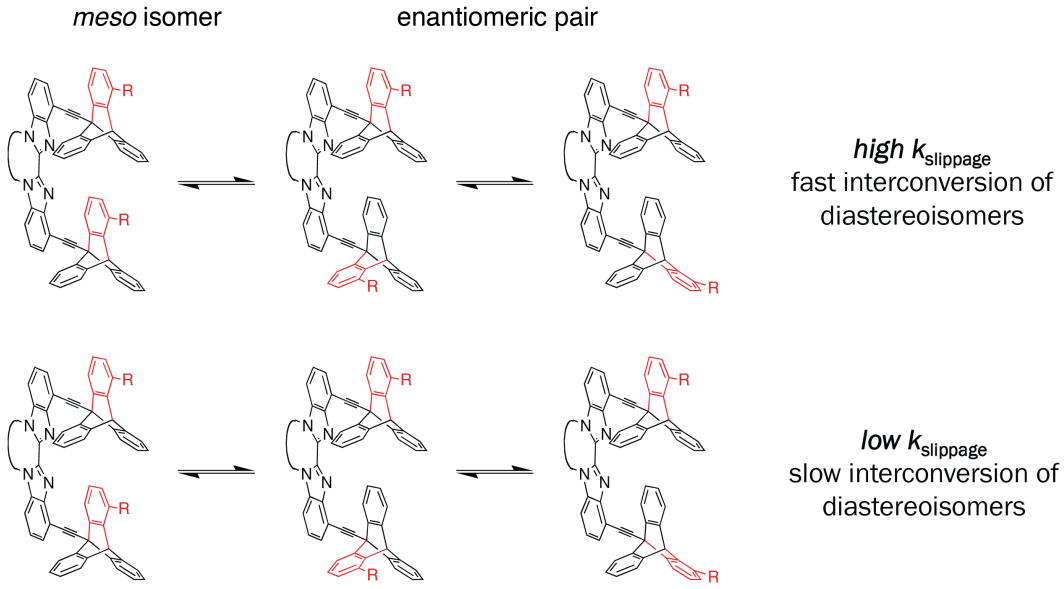

Figure 2.9. *Reducing the rate of gear slippage ($k_{slippage}$) would allow for the observation of the* meso *and enantiomeric phase isomers in labeled spur gears if geared rotation is preferred over gear slippage.*

^{1}H-NMR Samples were measured in the low-freezing solvent $CDCl_2F$[133] at temperatures as low as 150 K (Figures 2.10, 2.11, 2.12, 2.13).[134] The signals of all of the studied molecules significantly broaden upon cooling, but show no clear signs of decoalescence. ^{19}F-NMR spectra of **65b** and **69b** in CD_2Cl_2 were measured at temperatures as low as 180 K and also showed broadening, but no splitting, of the signals. See Chapter 6 for all VT-NMR spectra.

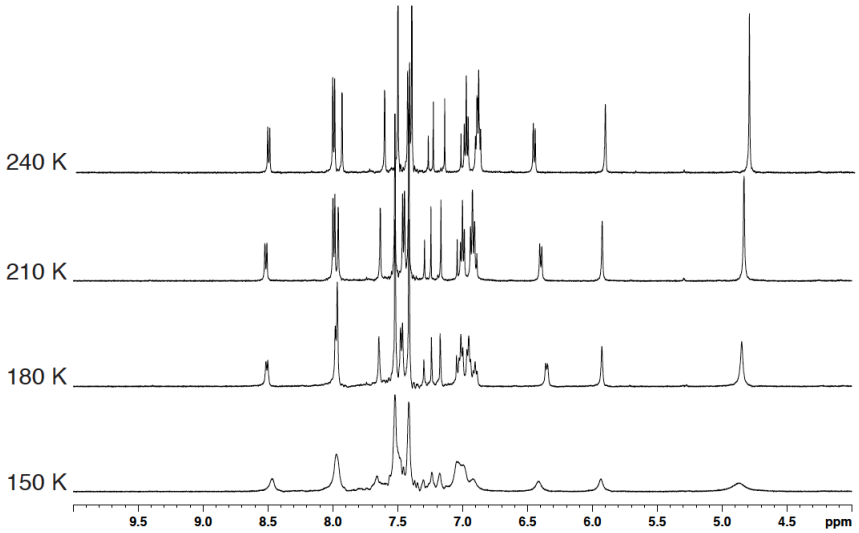

Figure 2.10. VT-^{1}H-NMR of compound ***65b****.*

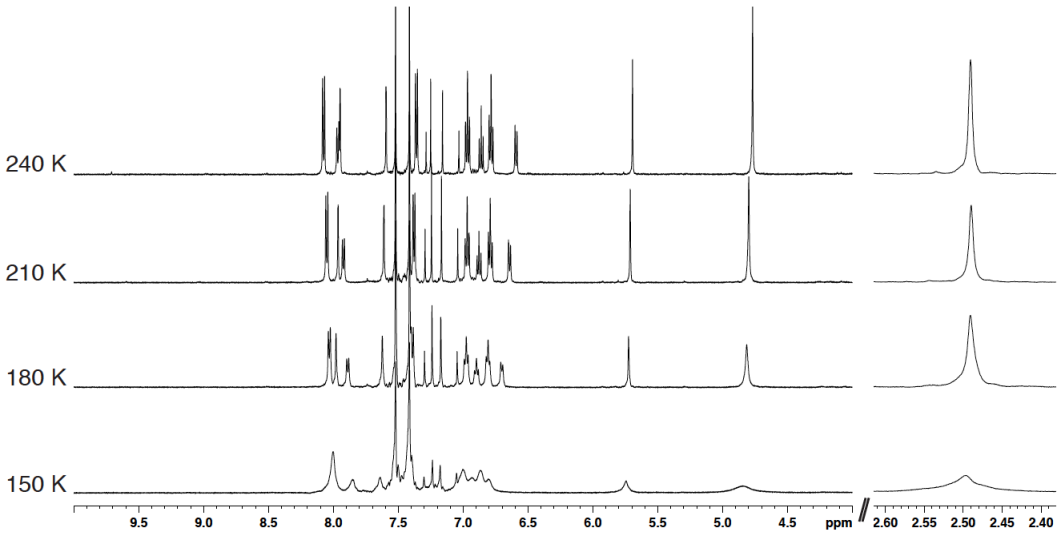

Figure 2.11. VT-^{1}H-NMR of compound ***65c****.*

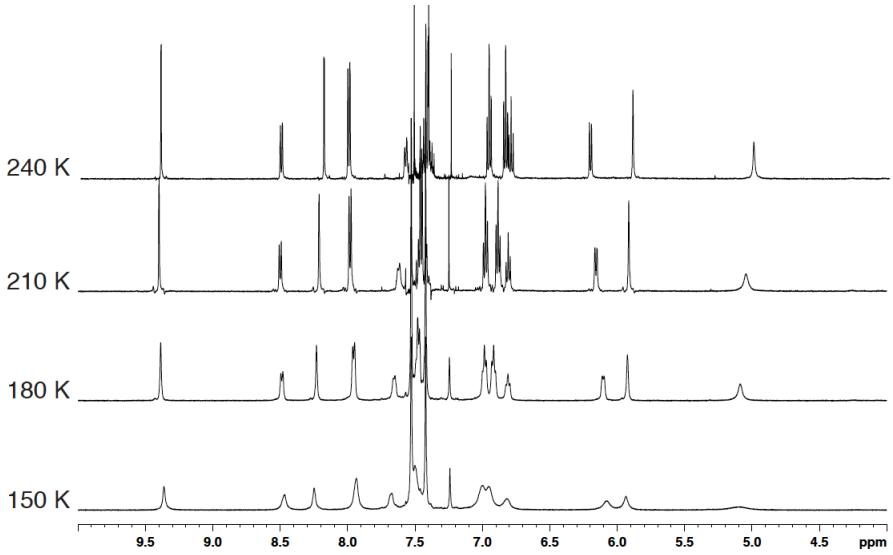

Figure 2.12. *VT-^{1}H-NMR of compound* ***69b****.*

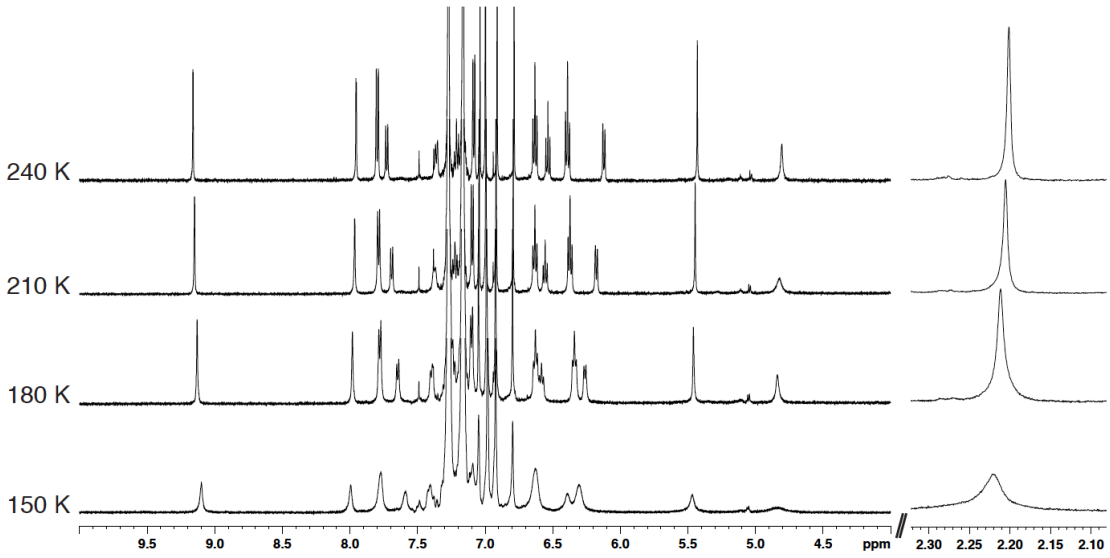

Figure 2.13. *VT-^{1}H-NMR of compound* ***69c****.*

The absence of decoalescence in VT-NMR experiments precludes the determination of the barrier to gear slippage and experimental demonstration that the rotators prefer to undergo geared rotation over gear slippage. Several explanations could account for the absence of observable decoalescence:

1) The chemical shift differences between signals from the enantiomeric and *meso* phase isomers may be so small as to render them unobservable. Considering the

unavoidable peak broadening that results from poorer shimming at low temperature, it is reasonable that decoalescing signals could be undetectable within the broad peaks.

2) The calculated values for the barriers to gear slippage may be higher than reality. If the real barriers to gear slippage lie below 7 kcal/mol, rather than ~7–8 kcal/mol, decoalescence would not be observable even at temperatures as low as 150 K.

Closing this section, it is worth mentioning that the nature of rotation of the benzyl group about the pyrrolodione moiety in **69b–c** would cause no complication in investigations of phase isomers in VT-NMR experiments. If gear slippage is fast compared to rotation of the benzyl group, the stereochemical outcome of two enantiomeric and one *meso* phase isomers does not change (see pattern no. 12 in Table 1.1, page 30).[135] The net stereochemical consequences also do not change if rotation of the benzyl group is faster than gear slippage; a side-to-side flip of the benzyl group may change the nature through which the conformations in a phase isomer interconvert, but interconversion between phase isomers would not occur (Figure 2.14).

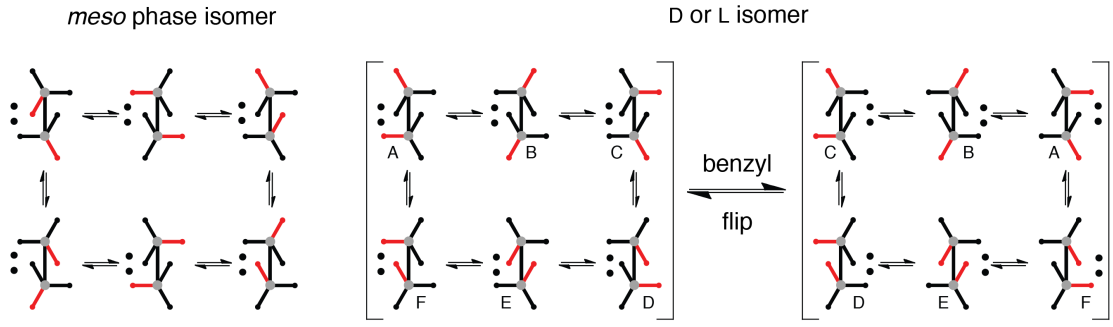

Figure 2.14. *Isolated rotation of the benzyl groups in* ***69b*** *and* ***69c*** *results in one conformation reaching another conformation within the same phase isomer subset.*

2.8. Conclusions and Outlook

Encompassing molecular design, quantum mechanical calculations, chemical synthesis, structural examination, and dynamic stereochemical analysis, this work illustrates the first rigorous investigations into molecular spur gears. Computational results regarding **49a** and **49b**, combined with structural data of **65a**, strongly suggest that the triptycene rotators on these molecules preferentially undergo geared rotation over gear slippage, although VT-NMR studies did not experimentally confirm the presence of phase isomers in **65b–c** and **69b–c**. The syntheses and investigations

reported here form the basis for future work in the field of molecular rotors and machinery.

As technical issues did not allow for conclusive experimental observation of the presence (or absence) of phase isomers, the logical next step is to synthesize systems that would lead to greater chemical dispersion of the NMR signals, increasing the likelihood of observing phase isomers, should they exist. The labeling groups remain distant from each other in the *meso* phase isomer and come close in three of the six energy-minimum conformations in the enantiomeric phase isomers. This difference could be exploited in systems incorporating strongly anisotropic units, including π-systems, which are known to induce significant changes in the chemical shifts of local nuclei. According to the Gutowsky–Holm approximation[136] and the Eyring equation, increasing $\Delta\nu$ between decoalesced signals not only makes observation of decoalesced signals easier to observe, but also increases temperature of coalescence (Table 2.1). By increasing chemical shift dispersion, coalescence occurs at faster exchange rates, therefore T_c will be higher and hence more accessible. Assuming the calculated energies are correct ($\Delta G^{\ddagger}$ = 7.6 kcal/mol for **49b**), then for a T_{gear} of 133 K and a $\Delta\nu$ of 10 Hz, the T_c would be 149 K, at the border of temperatures reachable by NMR.[137] Increasing $\Delta\nu$ to 100 Hz does not change T_{gear}, but would make it possible to observe the effect at T_c of 163 K. Thus, increasing $\Delta\nu$ effectively sets a faster "shutter speed" for coalescence. Such considerations are important in order to assess these systems.

Table 2.1. *Correlation between $\Delta\nu$ and coalescence temperature (T_c).*

$\Delta\nu$ (Hz)	$\Delta\nu$ (ppm, 500 MHz)	T_c (K)	lowest observable $\Delta G^{\ddagger}$ at 150 K (kcal/mol)
1	0.002	162	8.3
10	0.02	175	7.7
20	0.04	180	7.4
50	0.1	187	7.2
100	0.2	192	7.0
250	0.5	199	6.7

Design of next-generation targets incorporates chemical shift anisotropy (CSA) inducers. For example, a construct containing triple bonds as alkynes or nitriles **70** can be envisioned and ^{13}C-labeled derivatives thereof would allow for exploitation the high resolution of ^{13}C-NMR spectroscopy. More advanced targets **71** include gears with differentially labeled triptycene groups, in which one triptycene group contains a CSA inducer and the other triptycene group contains an NMR-active reporter substituent. Potential CSA inducers include alkynes and nitriles, strongly anisotropic aryl or arylethynyl groups, or possibly stable radicals. NMR-active reporter substituents could include the methyl (^{1}H-NMR) and trifluoromethyl (^{19}F-NMR) groups described in this study as well as a variety of ^{13}C-labeled substituents (^{13}C-NMR).

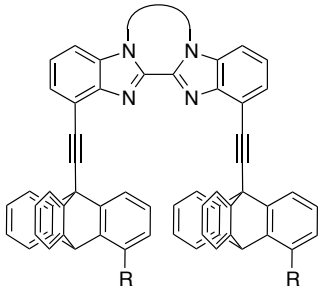

70

R = CCH
R = CN

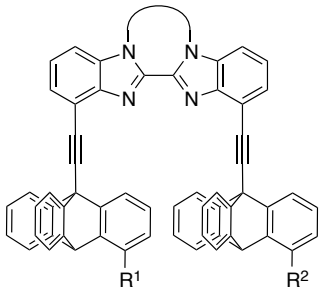

71

R^1 = CSA inducer
R^2 = NMR-active reporter

Computational (*ab initio)* studies by Klod and Kleinpeter[138] have sought to quantify chemical shift dispersion as a function of a proton's location in relation to a group that induces anisotropy (Figure 2.15). Nitriles, for example impart a slight deshielding on protons that lie next to the C–N bond and a stronger shielding effect on protons that lie coaxially to the bond. Chemical shift anisotropy is much stronger in benzene, which induces a 0.5 ppm upfield shift on protons that lie perpendicular to the face of the ring up to 6 Å away. A 0.1 ppm upfield shift is induced up to 9 Å away from the face. Extended annelated systems impart even larger effects; for example, the 0.5 ppm upfield shift surface for anthracene extends to 7 Å from its face.

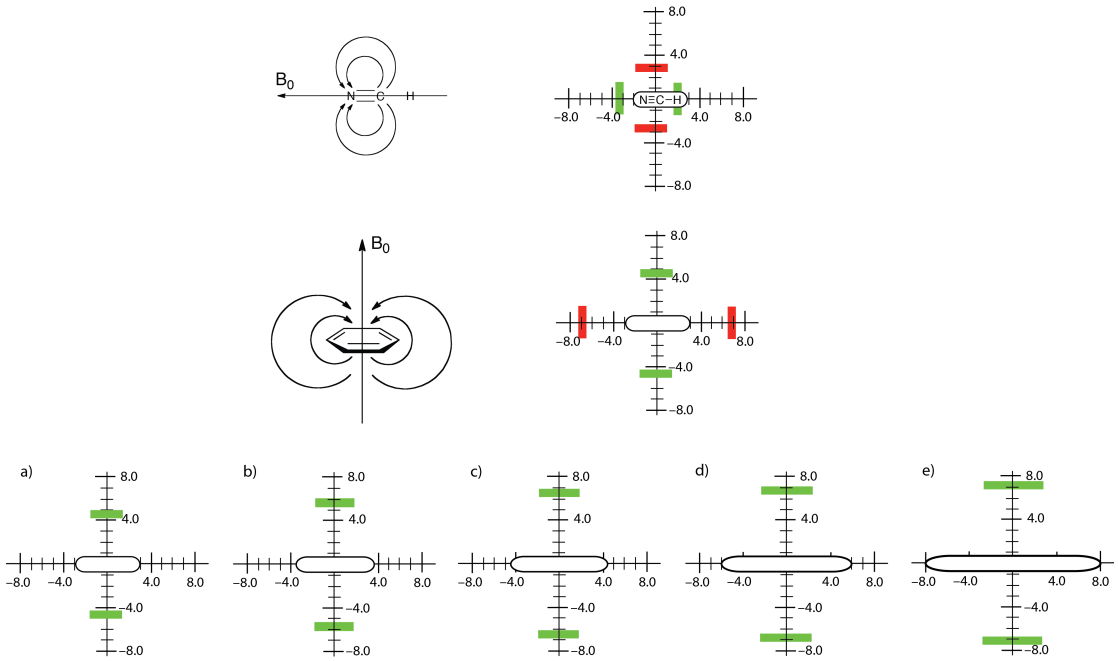

Figure 2.15. *Distances (in Å) from the surface of a group where a proton would experience chemical shift anisotropy. Green mark shows limit of 0.5 ppm shielding effect and red mark shows 0.1 ppm deshielding effect. (top) Nitrile group. (center) Benzene ring. (bottom) π-Systems benzene (a), naphthalene (b), anthracene (c), tetracene (d), and pentacene (e). Values collected from reference 138.*

SECTION TWO

Toward the Stepwise Synthesis of a Molecular Borromean Link

Chapter 3

Introduction to Molecular Borromean Links

3.1. The Borromean Link

At first glance, the Venn representation (Figure 3.1) of the Borromean link may appear to show three intersecting circles arranged in a standard Venn diagram. At second glance, the rings clearly do not intersect, but interlock, and closer inspection reveals that no two rings are interlocked but the special arrangement of all three rings holds the link together. Breakage of any one ring allows the other two to separate.

Figure 3.1. The Borromean link.

3.2. Topology of the Borromean Link

Peter Guthrie Tait, the legendary mathematician, first described in 1876 that the Borromean link is formed by three "unknotted" rings and that no two rings are interlocked.[139] The connectivity of the rings was mathematically proven in 1993,[140] two years after a proof demonstrating that Borromean links may not be composed of rigid circles[141] was published.

In the jargon of mathematical topology, a link is considered trivial (or an unknot) when it can be reduced to a single ring with no crossings by twisting and pulling but not by breaking and reattaching a string. A single, circular piece of string is a trivial link, though it may possess any of an infinite number of twists and contortions.

On the other hand, a non-trivial knot or link may not be transformed into (a) trivial link(s) without breaking the string.

Knots and links are characterized their minimal diagrams, the graphical representation in which the lowest number of crossings is shown. Topologically distinguishable links are described by Rolfsen's notation,[142] K_n^i, where K is the number of crossings in the minimal diagram, i is the number of components (omitted when i = 1), and n is an indexing number that generally increases with the complexity of the system. Complexity is somewhat subjective and it is not always obvious which knots and links should have which indexing number, so it is advisable to refer to a knot atlas when characterizing a non-trivial knot or link.[142] In this notation, a single trivial link is described by 0_1; there are no crossings, there is only one component, and the index number is 1. The simplest one-component, non-trivial link is the famous trefoil knot (Figure 3.2a), which is described by 3_1, as the minimal diagram has three crossings. Two otherwise trivial links may be interlocked as a chain. The simplest link of this type is the Hopf link, characterized by 2_1^2 (Figure 3.2b).

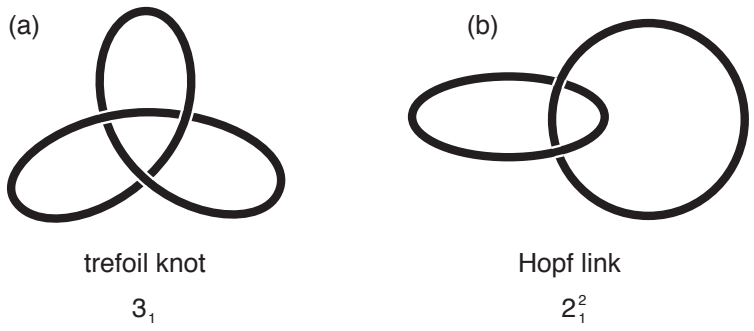

Figure 3.2. *(a) The trefoil knot. (b) The Hopf link.*

The simplest links with three components have six crossings and three links of this type exist (6_1^3, 6_2^3, and 6_3^3, Figure 3.3). The 6_2^3 link is the Borromean link and is the only example in the series not having two interlocking rings. Links exclusively composed of trivial sublinks that may separate upon breakage of one unit are called *Brunnian links*, in reference to topologist Hermann Brunn. The Borromean link is, thus, the simplest of an infinite number of Brunnian links. An example of a higher-order, six-ring Brunnian system is shown below (Figure 3.4).

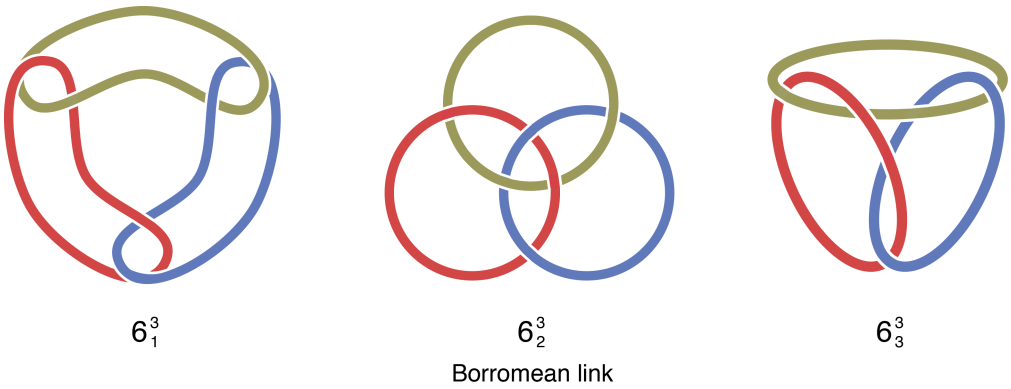

Figure 3.3. *The three links comprising three rings and six crossings. Only the Borromean link has the Brunnian property.*

Figure 3.4. *A six-ring Brunnian link. If any one ring is broken, the other five rings are free to separate.* [*]

3.3. Historical Usage

Iconographic images of the Borromean link have been employed to represent the uniting of three entities into a singular unit that requires participation of all its members to exist or function properly; in other words, strength-in-unity.[143] Its name derives from the aristocratic Milanese Borromeo family, who placed the symbol in their crest in the fifteenth century to represent the inseparable union—forged by intermarriage—between them and the Sforza and Visconti families (Figure 3.5). The

[*] Figure taken from http://www.knotplot.com/brunnian/ (February 20, 2012).

rings are displayed on a number of buildings, sculptures, and pottery in and around Milan, particularly in areas where the family once dominated.

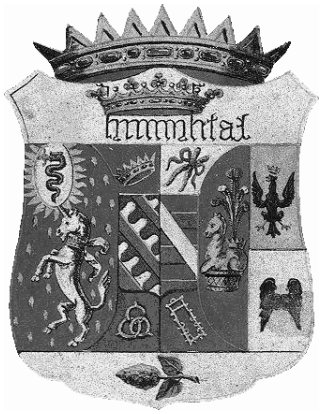

***Figure 3.5. The** Borromeo Family crest comprises a variety of symbolic imagery, including the Borromean link in the lower left section.*

In Christian iconography, the inseparable and eternal union joining God the Father, God the Son, and God the Holy Spirit as the Holy Trinity has been represented by three rings. The rings are sometimes not interlocked, as in the famous *Scutum Fidei*, or interlocked in a non-Borromean arrangement, as in Joachim of Fiore's depiction (Figure 3.6a), which is topologically identical to the 6_1^3 link. The oldest known representations of the Holy Trinity as a Borromean link (Figure 3.6.b) appeared in a thirteenth-century manuscript held at the Municipal Library of Chartres, which was sadly destroyed by war-related fire in 1944.[143] Fortunately, historians transcribed the figure of the Trinity into a work on Christian iconography[144] prior to the manuscript's destruction.

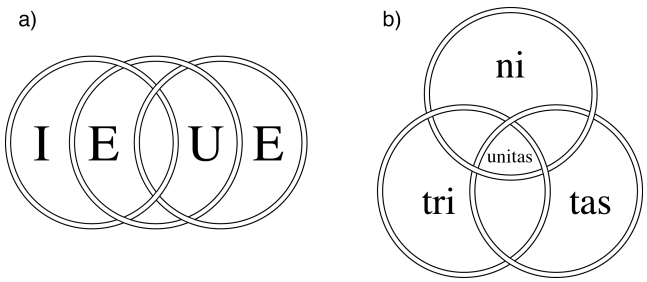

***Figure 3.6.** (a) Joachim of Fiore's interlocked ring representation of the Holy Trinity. (b) The Holy Trinity represented as a Borromean link, as it was depicted in a 13th century manuscript.*

The Borromean Link appears in several other historical contexts. The *Valknut*, consisting of three triangles exhibiting Borromean topology, appears on various objects throughout northern Europe (Figure 3.7) and once served as an important symbol in Germanic mythology.[145]

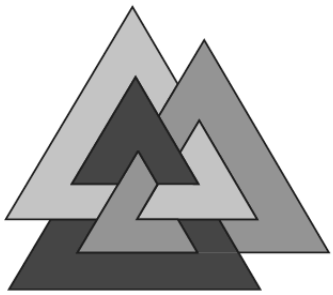

Figure 3.7. *Borromean topolology is present in the triangles in the Valknut of Norse Mythology.*

Before attaining the name "Borromean," the link was referred to as Ballantine rings or a brewer's trademark, particularly in the United States, in reference to America's Ballantine Brewery's famous use of the symbolism (Figure 3.8). First used in 1879, the symbol, representing purity, body, and flavor, was designed by the company's founder, Peter Ballantine, and was purportedly inspired by the wet rings left on the table while he enjoyed a glass of the cold beverage.[146]

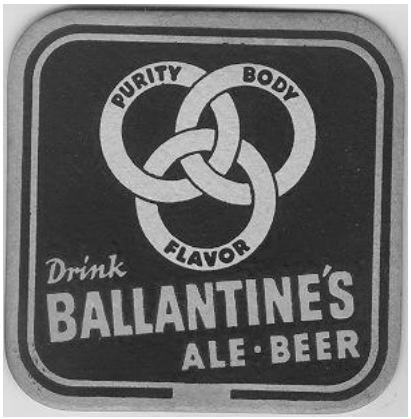

Figure 3.8. *The Borromean link was part of the Ballantine Brewery's logo, symbolizing purity, body, and flavor.*

3.4. Chemical Interest

In 1961, Wasserman—who had published the first catenane synthesis a year earlier[147]—and Frisch introduced the concept of chemical topology in a seminal work that discussed a number of interlocked rings and knots and expounded the statistical probabilities of forming such topological arrangements with molecular systems.[148] Here, the Borromean link first appears in the chemical literature, though the authors referred to it as a "brewer's trademark." Expected to require at least 30 carbon atoms per ring to form as a set of cyclic hydrocarbons, it was predicted to be less likely to form than (3)-catenane under statistical methods. Frisch and Wasserman were privy to a seminal manuscript written by van Gulick, which described how molecular Borromean links (as well as other links and knots, including the trefoil knot) could be generated by a braiding approach.[149] Interestingly, van Gulick's original manuscript was summarily rejected by the editors at *Tetrahedron* in 1960 for not being chemistry and was not resubmitted. It finally resurfaced—after prodding by topological chemists—more than 30 years after the original submission.[150] Tauber first employed the epithet "Borromean" to describe the topological system in 1963;[151] perhaps because the first use of the name in a mathematical context appeared in 1962.[152]

Borromean links may adopt a variety of forms with varying symmetries (Figure 3.9).[153] First, if all rings are equal, its Venn representation (a) exhibits chiral D_3 symmetry. It can be then transformed into achiral forms. The chain representation (b) has D_{2d} symmetry and its orthogonal representation (c) is a highly symmetric T_h conformation. Permutation of the orthogonal representation such that the planes of the ellipses are no longer perpendicular to each other—but each of the dihedral angles change equally—results in an achiral S_6 form. Because the link can be represented as achiral forms, it is said to be topologically achiral, or amphicheiral.[154] Amphiceirality* in links is rather rare; only three of the 91 two-component links with nine or fewer crossings (2_1^2, 6_2^2, 8_8^2) and only three of the 35 three-component links with nine or fewer crossings (6_2^3, 8_4^3, 8_6^3) are topologically achiral.

* *Amphicheirality* is a term coined by the mathematical topology community and its use of a seemingly unusual spelling of *chiral* appears to derive from Lord Kelvin's original spelling, *cheiral*. See ref. 156.

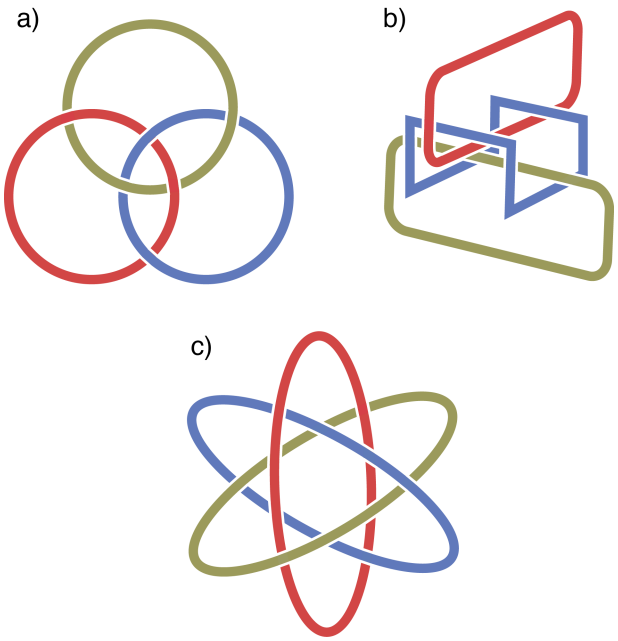

Figure 3.9. *Common representations of the Borromean link: (a) Venn representation, (b) chain representation, (c) orthogonal representation.*

Introducing directionality to the rings in a Borromean link results in stereochemical consequences. Tauber showed that directionality in Borromean rings leads to a set of enantiomers (Figure 3.10).

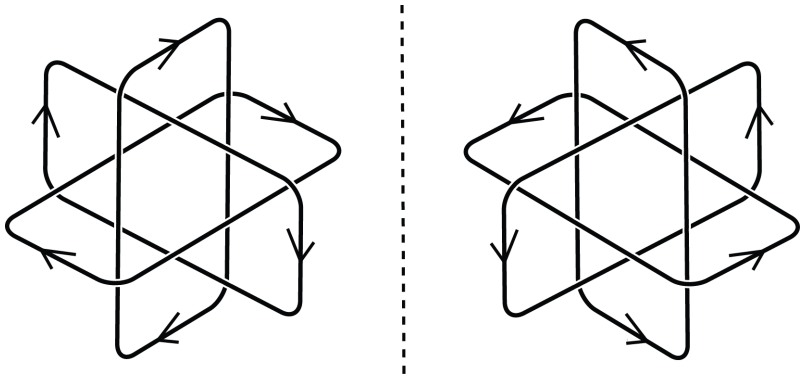

Figure 3.10. *If the rings have directionality, the Borromean link is chiral and exists as two enantiomers.*

As designed syntheses of molecular catenanes, rotaxanes, and other mechanically bonded species became more commonplace,[155] significant interest focused on the realization of a molecular Borromean link, which was seen as a sort of Holy Grail of topological chemistry.[156] In 1993, Walba predicted its future synthesis by a stepwise

approach.[157] Though the following 20 years have offered the first examples of molecular Borromean links (*vide infra*), a strictly stepwise synthesis has yet to be demonstrated, though many other rings and knots have been produced.[158]

3.5. Chemical Synthesis

Depending on its representation, the retrosynthetic analysis of the Borromean link may vary (Figure 3.11).[159] In its Venn representation (a), the link may be disconnected to a hexa-templated intermediate that is derived from a D_3 tri-templated structure containing three linear units. This approach entails a host of stereochemical challenges has not yet been attempted in classical organic chemical methodology, though a DNA-based Borromean link, the first molecular Borromean link, was synthesized in this manner (*vide infra*). A chain-represented Borromean link (b) may be retrosynthetically disconnected to a D_{2d} system with four templates that could derive from a C_{2v} di-templated system. In its orthogonal representation, the system could be disconnected to a ring-in-ring complex, requiring two templating sites, which could be derived from a single macrocycle.

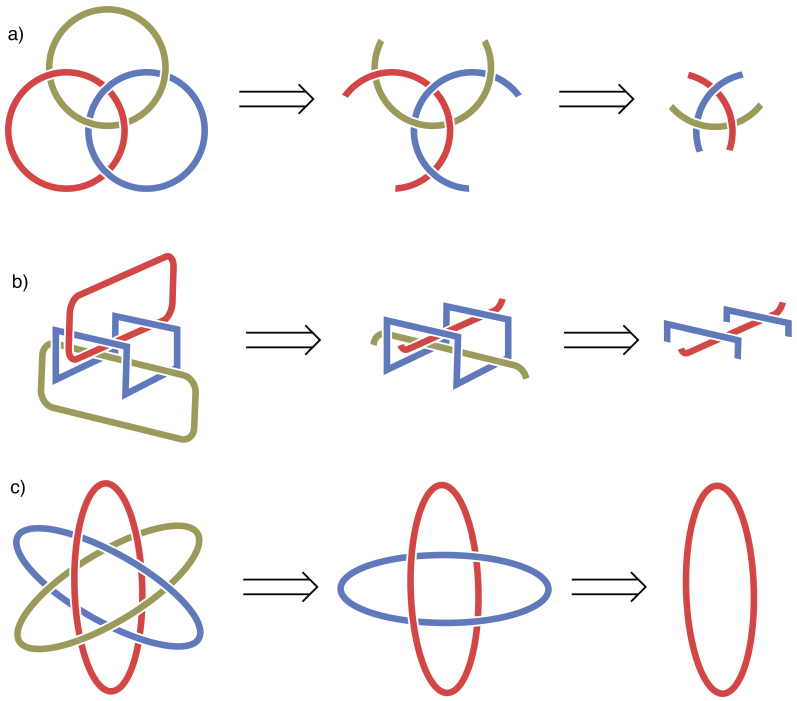

Figure 3.11. *The representation of the molecular Borromean link design affects the optimal retrosynthetic strategy.*

Seeman and co-workers synthesized the first molecular Borromean link[160] in 1997 by exploiting his DNA nanotechnology[161] approach (Figure 3.12), which had hitherto been employed to generate highly intricate structures, including a cubic [6]catenane[162] and truncated octahedral [14]catenane.[163] It is not obvious that the molecule has Borromean topology at first glance, because it is highly deformed. Consider the Venn representation of the Borromean ring and twist the parts of the rings present at each of the crossings so that three crossings arise (Polar representation). This object can then be deformed to a 3D structure that is structurally analogous to Seeman's DNA construct, which can was formed by ligation of two building blocks comprising three appropriately shaped and ligated DNA oligomers. Seeman cleverly engineered specific restriction sites into the DNA strands; enzymatic cleavage of the site resulted in two non-linked DNA macrocycles and a linear strand, demonstrating that the construct is indeed a Borromean link.

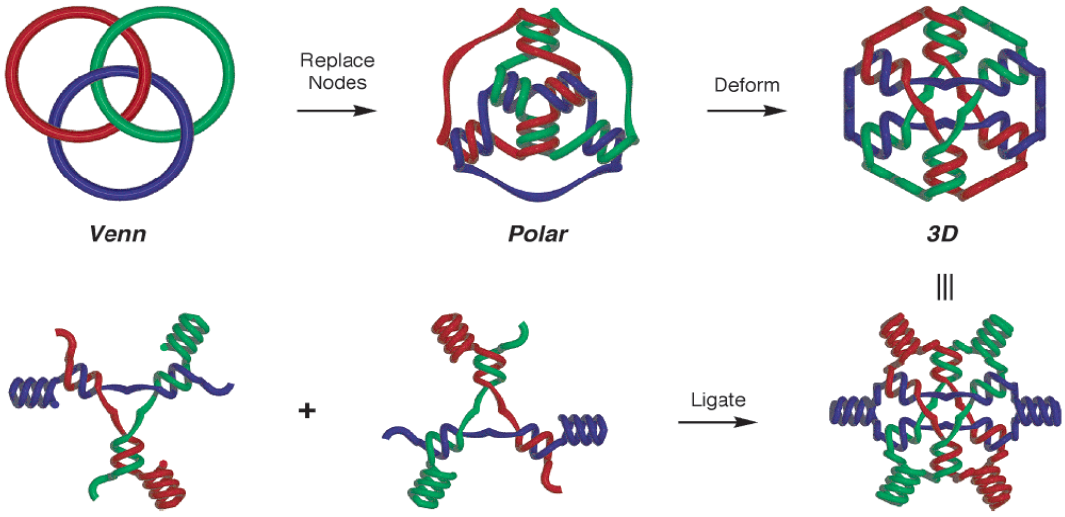

Figure 3.12. *Schematic representation of Seeman's DNA-based synthesis of a molecular Borromean link. Reprinted with permission from reference 164. Copyright © 2005 American Chemical Society.*

Seeman's landmark achievement was followed by Stoddart's elegant directed assembly[164] of a molecular Borromeate in 2004.[165] The method relies upon two dynamic processes, reversible imine formation[166] and metal complexation (Scheme 3.1).[167] Pyridine-2,6-dicarboxaldehyde (**73**), bipyridine diamine (**74**), and Zn(II) were combined and the resulting thermodynamic minimum energy structure is an orthogonal Borromean link construct with time-averaged[168] T_h symmetry, whose

structure was confirmed by X-ray crystallography (Figure 3.13). The methodology is robust, allowing for the generation of several derivatives,[169] including chiral examples,[170] and permitting its use in undergraduate teaching laboratories.[171] Stoddart has also reported MS and ^{1}H-NMR evidence for de-metallated, true Borromean links.[172] These were formed by reducing the imines with $NaBH_4$, precluding hydrolysis of the imines, and extracting the Zn(II) ions with EDTA, though the authors were unable to purify the product.

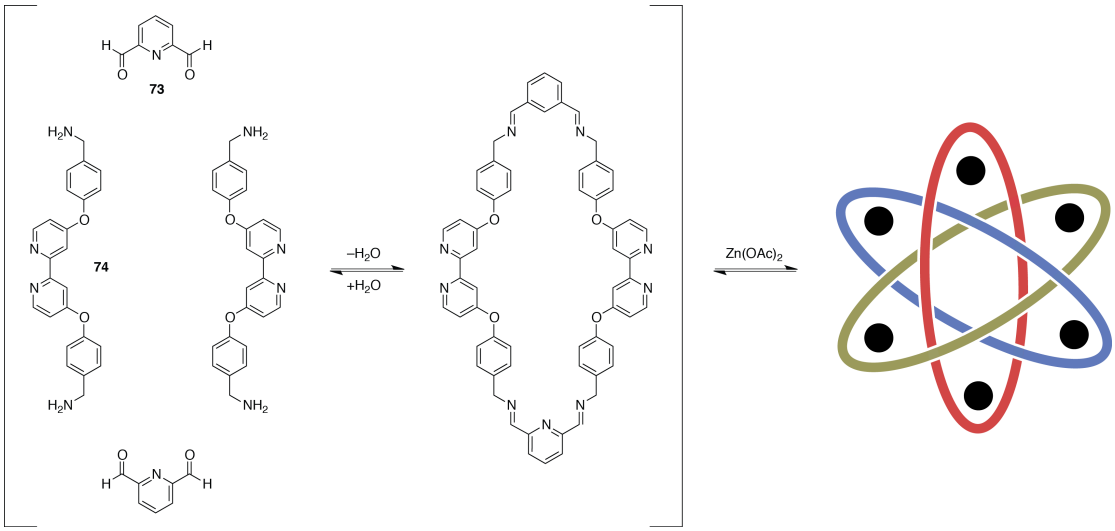

Scheme 3.1. *Stoddart's original synthesis of a molecular Borromeate by a directed assembly approach.*

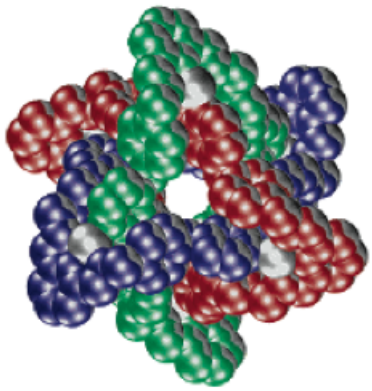

Figure 3.13. *X-ray crystal structure of Stoddart's Borromean link, rendered as space-filling model, with silver balls denoting Zn(II) ions. Counterions and hydrogen atoms removed for clarity. Reprinted with permission from reference 164. Copyright © 2005 American Chemical Society.*

Using a dynamic complexation with Cu(I), Schmittel and coworkers made a variety of supramolecular structures, including one with Borromean topology.[173] By combining bis(pyridinylaryl)phenanthroline **75** and $[Cu(MeCN)_4]PF_6$ in a 1:1 ratio, a hexanuclear cage with Borromean topology was produced (Scheme 3.2). Unlike Stoddart's systems, this construct does not have a template connecting the rings. Instead, the Cu(I) metal ions serve as parts of the *endo* ring rods as they pass under the *exo* caps of the other rings.

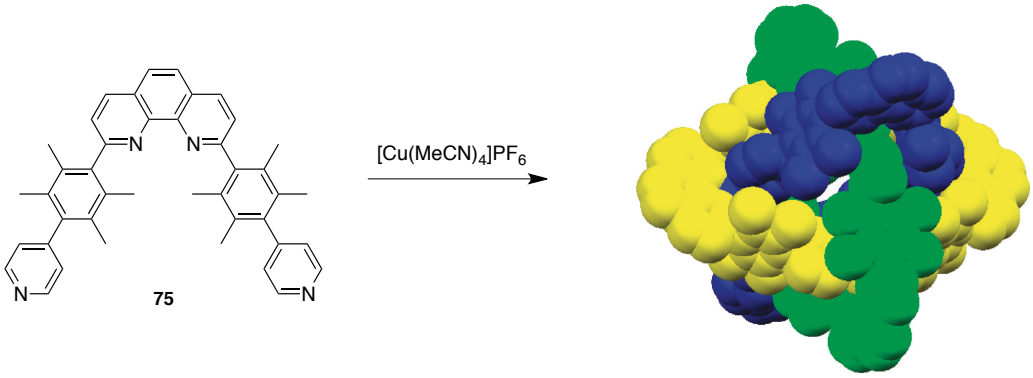

Scheme 3.2. *Schmittel's Borromean link-shaped cage complex. Adapted with permission from reference 173. Copyright © 2009 American Chemical Society.*

Though several strategies for generating molecular Borromeates by supramolecular assembly are known, interest in a stepwise synthesis has not waned. The stepwise approach is certainly more challenging than a supramolecular approach and, by addressing and overcoming these challenges, chemists can learn a great deal about how to generate interlocked molecules that are more complex than simple catenanes and rotaxanes. The major source of motivation, however, may simply be the chemist's desire to create molecules with aesthetic appeal and the Borromean link is inarguably one of the most pleasing topological structures. Its stepwise construction has proven to be highly challenging, yet it is not so intricate as to place it out of reach.

In 2003, Siegel reported the synthesis of ring-in-ring molecule **76**, which is templated by two Ru(II)–terpyridine complexes.[174,175] The molecule was designed to have two bipyridine units as the outer caps of the internal ring with the expectation that they could be used to form metal complexes within the loop with another, linear ligand, which would serve as part of the final ring. Macrocyclization of the final ring on the outside of ring one would form a molecular Borromeate. Disappointingly, complexation with the bipyridines was never observed, despite numerous attempts.

Later, analogs that replaced the bipyridine cap with a longer unit or terpyridine groups were generated, but these were found to also not generate any complexes.[176] Molecules of this type as building blocks to a molecular Borromean link will be discussed further in Chapter 4.

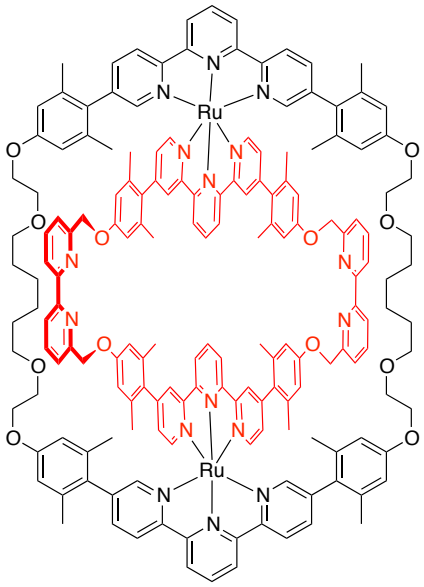

76

Stoddart also attempted a stepwise synthesis using a much simpler system employing donor–acceptor π-interactions with paraquat derivatives.[177,178] Ring-in-ring complex **77** employs crown ethers as the loop of the inside ring. Threading of this ring was attempted with a linear dialkyl ammonium linker, which could have provided a route to a Borromean ring. However, threaded complexation of the ammonium cation by the crown ether failed. Stoddart and coworkers have gone on to prepare several other donor–acceptor-based ring-in-ring complexes, though they have not yet succeeded in forming a molecular Borromean link.[179]

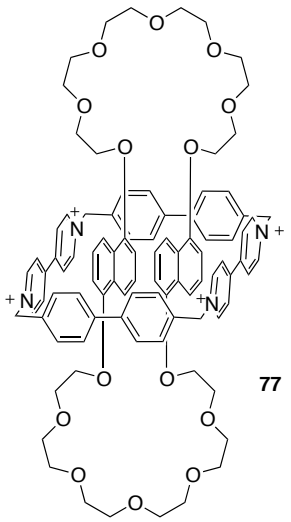

77

3.6. Borromean Topology in Coordination Frameworks

Coordination polymers are crystalline solid-state structures consisting of a supramolecular matrix and may have interlocked or interwoven topologies. Coordination polymers with Borromean topology were originally discovered by Ciani and coworkers.[180] Solid-state structures of two isomorphous, polymeric Ag(I) complexes, $[Ag_2(H_2L)_3](NO_3)_2$ and $[Ag_2(H_2L)_3](ClO_4)_2$, where H_2L = *N*,*N*'-bis(salicylidine)-1,4-diaminobutane, were originally misinterpreted by other researchers,[181] but Ciani showed that Borromean topology is present in the solid state. Since their discovery, solid networks with Borromean topology have been observed in several cases,[182] though their occurrence is rather rare.

3.7. Microscopic Objects with Borromean Topology

Though they do not employ chemical methods in the classical sense using molecular design and synthesis, it is worth mentioning a few examples of Borromean link formation on the microscopic level. Whitesides and coworkers forged a variety of interlocked structures, including the Borromean link, by a clever microfabrication strategy that prints patterns onto a continuous metal film and welding along two cylinders with appropriately spaces notches and channels on their surfaces.[183] The metallic structure is ~2 millimeters in length. Muševič and coworkers have recently developed a strategy to generate interlocked structures in chiral nematic liquid crystals

and one of these structures was found to have Borromean topology on the sub 30 μm scale.[184]

3.8. Goal of this Section

The unique and remarkable topology of the Borromean link continues to captivate mathematicians and chemists and interest in higher-order, mechanically bonded structures is as great as it has ever been.[167] These factors motivated a new campaign toward the stepwise synthesis of a molecular Borromean link, a research project that had laid dormant in the Siegel group for four years. In the following chapters, new work toward the synthesis of a molecular Borromean link will be presented and discussed.

Chapter 4

New Approaches to Metal-Templated Molecular Borromean Links

4.1. Summary

Two new strategies have been employed in the attempted synthesis of a molecular Borromean link. The first of these involved the introduction of a pre-templated cap to a known templated macrocycle. If successful, this step would create a ring-in-ring complex that is already templated with linear rods that can eventually connect to form the third ring of a Borromean link. A combination of design, modeling, and synthesis has led to the generation of thioketal-templated pre-templated cap constructs with the proper geometic requirements to form Borromean link precursors. However, attempts to couple this unit to the templated macrocycle have not yet been successful. The second strategy, which is still in its early stages, attempted to form a templated ring-in-ring complex by an activated template approach, and has also has been unsuccessful so far, though the strategy has great potential in the eventual stepwise synthesis of a molecular Borromean link.

4.2. Introduction

Previous members of the Siegel research group, most notably Jon Loren[174,175] and Jeremy Klosterman,[176] have prepared a number of ring-in-ring complexes toward the synthesis of a molecular Borromean link. Their procedure employs an initial ring (hereafter referred to as *ring one*) comprising two terpyridine moieties, which is treated with a metal complex containing another extended terpyridine unit (Figure 4.1). This templated system is carried forward to generate a second ring (hereafter referred to as *ring two*) that contains a ligand, either bipyridine (bpy) or terpyridine (terpyridine) on its outer loop. To achieve the proper topology, the final ring (hereafter referred to as *ring three*) must pass through thes loops and continue around the outside of the

aliphatic chain of ring one. This arrangement could be reached by forming a complex between the ligand-containing caps of ring two and a new metal–ligand unit that serves as a precursor to ring three. Completion of the Borromean link could finally be accomplished by macrocyclization to form ring three.

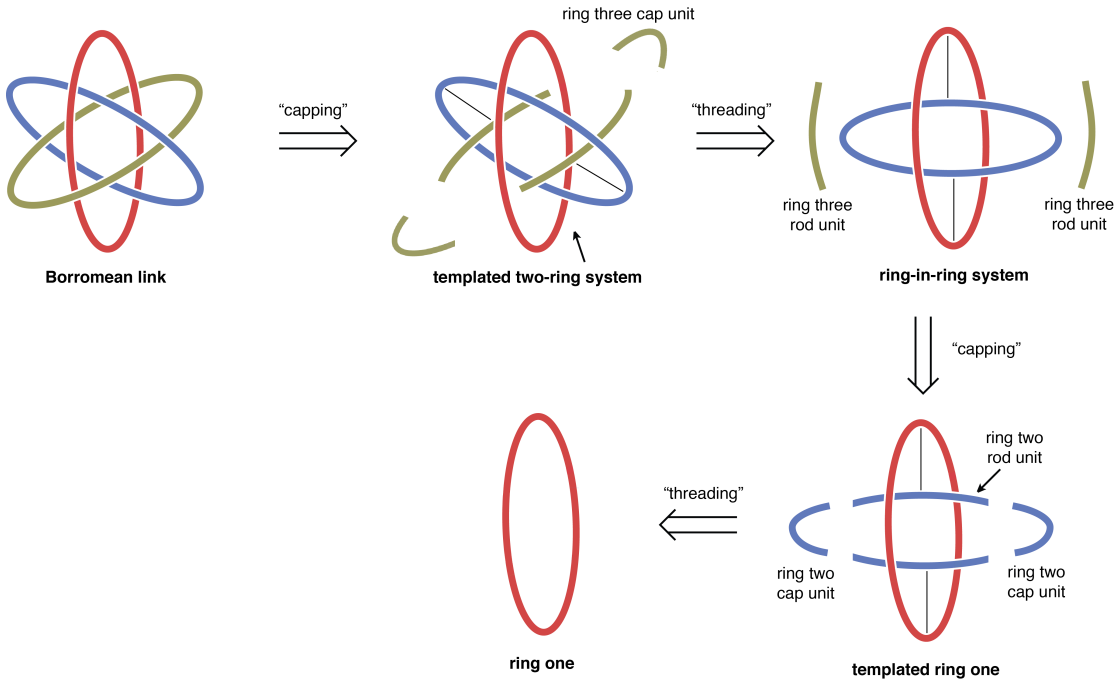

Scheme 4.1. *Loren's and Klosterman's strategy. A ring-in-ring system is formed and the process of internal threading by metal complexation forms a templated two-ring system en route to a Borromean link.*

Loren's original ring-in-ring complex **76** comprised bipyridines on the outer loops of ring two, with the intention of generating internal metal complexes to serve as linkers for eventual generation ring three. All attempts to thread linear bipyridine-containing rods in the form of Cu(I) complexes failed, and ring three could not be introduced. It was postulated from analysis of the X-ray crystal structure (Figure 4.2), which shows the bipyridines in their preferred *transoid* conformations[185] and exhibits considerable compression of ring one, than an undesired, spring-like tension may develop in the molecule if the bipyridine moieties adopt a complexation-capable *cisoid* conformation. Loren attempted to overcome this issue by introducing extended phenanthroline motifs to the loop of ring two, generating **78**. However, this compound also failed to undergo threading toward the formation of ring three.

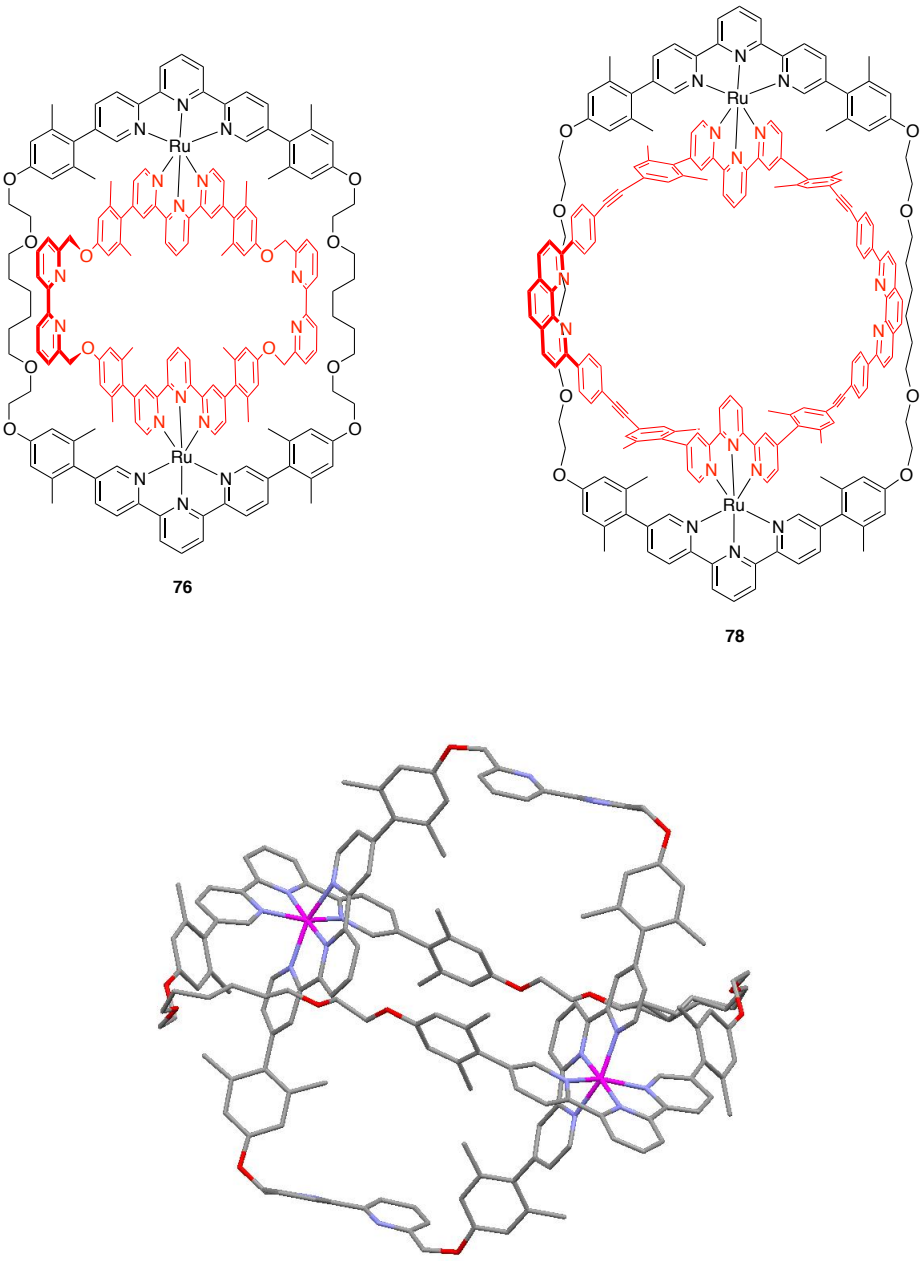

Figure 4.2. *X-ray crystal structure of ring-in-ring complex* **76**. *Hydrogen atoms and counterions removed for clarity.*

Klosterman later expounded three hypotheses concerning the necessary conditions for threading to occur in molecules of this type: (1) switching to a tridentate ligand would allow more stable, octahedral complexes (*e.g.* Ru(II) complexes) to be formed, (2) rigidity of the loop of ring two is essential, and (3) the tridentate ligand should extend from ring one in such a way that it prevents its compression and that it creates a loop that is as large as possible. He synthesized terpyridine-containing compound **79** and attempted to thread terpyridine-based units, but was unable to form

a threaded species. Using an alternate method, treatment of **79** with $RuCl_3$ afforded complex **80**, but treatment with ligands still failed to form a threaded product. Low-quality crystals of **79** were grown and subjected to synchrotron X-ray diffraction and the molecular structure revealed that the distance between the Ru(II) ions in **79** and **76** are very similar (15.7 Å and 16.5 Å, respectively). Next-generation complexes **81** and **82** extended ring two by the addition of acetylene groups, but threading attempts with these complexes also failed.

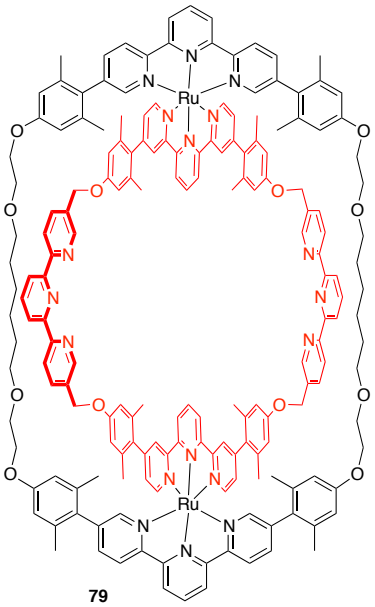

79

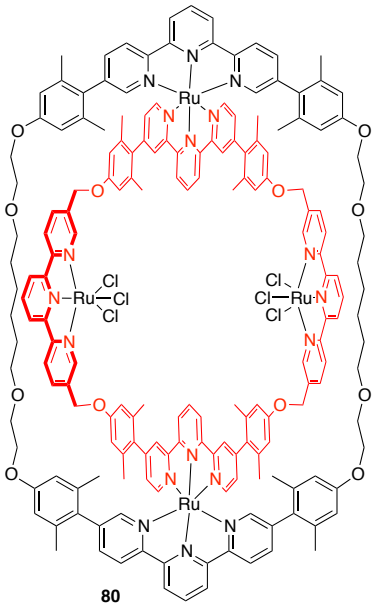

80

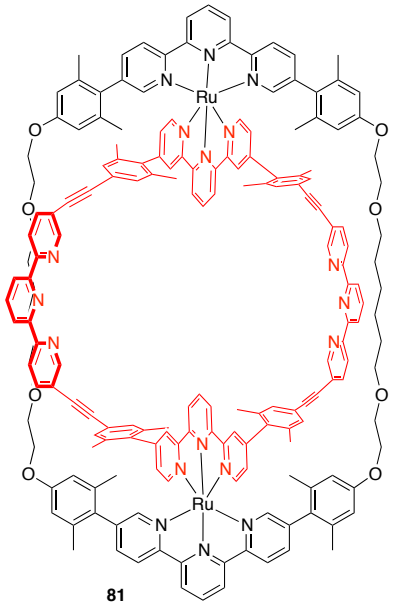

81

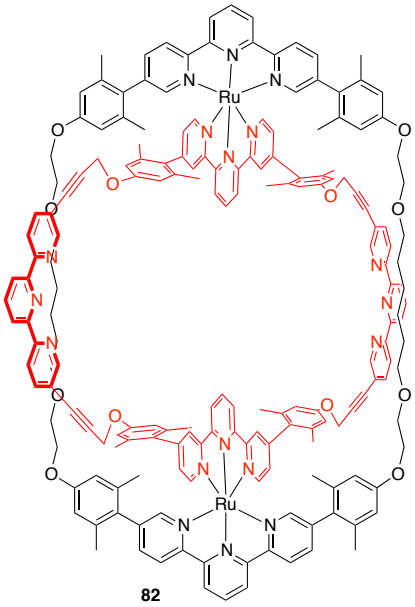

82

In this chapter, attempts at overcoming this problem, while still using a Ru(II)-templated ring-in-ring, are described. First, in section 4.3, a strategy employing a pre-

templated cap will be discussed. Next, in section 4.4, an attempt to overcome the problem by employing an active metal templating strategy will be shown.

4.3. Strategy One: Introduction of Pre-Templated Cap

4.3.1. Introduction

The problem of threading may be overcome by taking templated ring one and affixing a pre-threaded cap, which contains both the cap that completes the formation of ring two and a rod unit that serves as part of ring three. The retrosynthesis of a molecular Borromean link would then only need two successive de-capping disconnections to arrive at templated ring one (Figure 4.3). Klosterman attempted to form templated two-ring systems by this approach using heteroleptic complexes as pre-templated caps; however, he was unsuccessful. The present attempt sought to engineer novel pre-templated caps that have an ideal structural framework to allow them to fit well onto the templated one-ring compound.

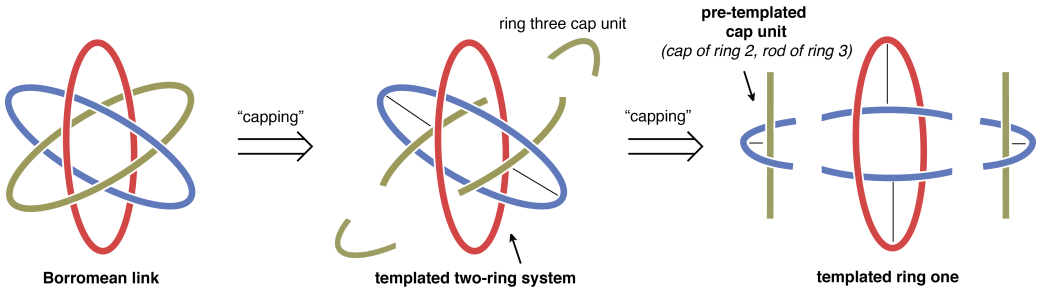

Figure 4.3. Retrosynthesis of Borromean link using pre-templated cap strategy.

4.3.2. Design of Pre-Templated Cap

Several design principles must be addressed to develop an appropriate pre-templated cap construct. The piece must contain two distinct units that are held roughly perpendicularly. One of these units will serve as the cap of ring two and must have a crescent shape with functionalized arms extending in the same direction. The other unit will be part of ring three and must be held between these arms, as the design requires ring three to exist inside ring two. Several chemical constructs meet these needs, including properly substituted octahedral and tetrahedral metal complexes, *ortho*-substituted biaryls, biarylacetylenes, phenylcarbazoles, and spiroketal-type constructs (X = O, S, Se, NH) of fluorene (Scheme 4.2).

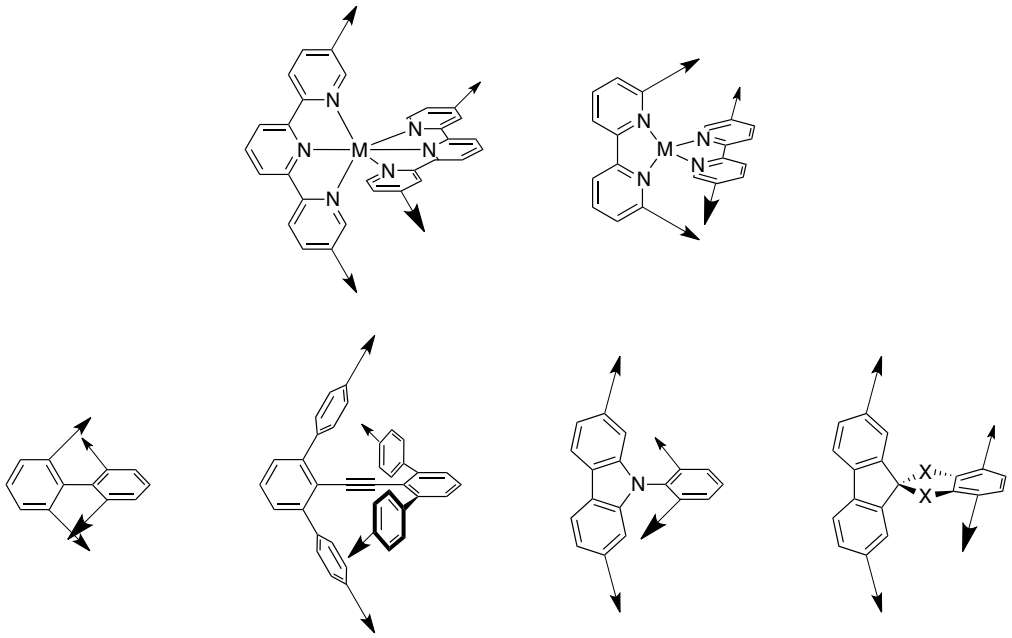

Scheme 4.2. *Molecular motifs that allow two linear units to extend roughly perpendicularly to each other.*

Ideally, the link connecting the two units of the pre-templated cap should be removable, allowing for disconnection of the templated system into individual, interlocked rings in the Borromean link construct. Of the above examples, only the alkyne, spiroketal, and metal complex—depending on the nature of the complex—can be cleaved by conventional and selective means. The spiroketal generated from fluoren-9-one **83** and catechol **84** appeared to have the desired structural characteristics for this construct. However, this ketal has never been prepared, and is highly unfavorable, as conjugation[186] and steric crowding both disfavor ketal formation.[187] Nonetheless, several attempts to generate this compound were performed and resulted in no observable ketal formation (Scheme 4.3). A ketalization attempt with fluoren-9-one and benzene-1,2-dimethanol also afforded no ketal product.

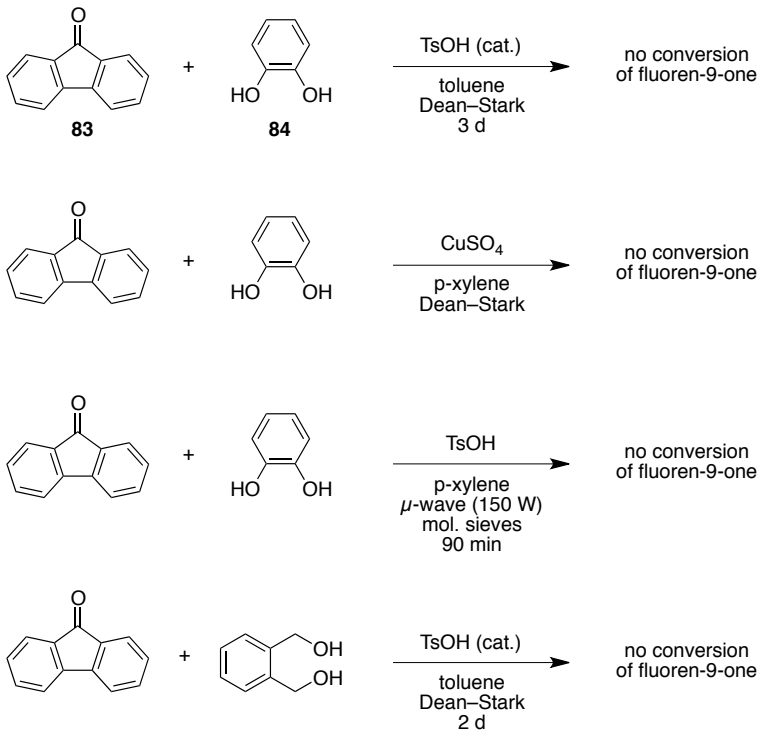

Scheme 4.3. *Attempted formation of aryl-fused thioketals of fluorenone.*

With ketals appearing not to be viable options in this approach, attention turned to thioketals, the dithio analogs of ketals.[188] Thioketals are generally prepared by a straightforward reaction with carbonyl groups and thiols in the presence of an acid (Brønsted or Lewis) catalyst and are much more stable under acidic conditions than their analogous ketals.[189] Thioketal **85** is unknown but the comparable compound **86** has been generated from fluoren-9-one and benzene-1,2-dimethanethiol with either $AlCl_3$[190] or silica gel/$FeCl_3$[191] as catalyst. This motif highly attractive because, in addition to offering the desired perpendicular geometry of substituents, thioketals can often be selectively removed by oxidation or, much more interestingly, de-sulfurization by hydrogenation with Raney-nickel.

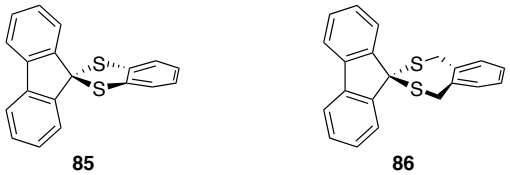

Thioketal **86** contains a seven-membered dithiepine ring that does not exist in a planar conformation. PM3 calculations on **86** indicate C_s chair, a C_2 twist, a C_s boat,

and C_1 biplanar conformations all have energies within 6 kcal/mol of each other (Figure 4.4).[192] The lowest-energy chair conformation holds the two units connected to the thioketal perpendicularly, allowing for the proper geometrical requirements to be met in pre-templated cap constructs based on thioketals of this type.

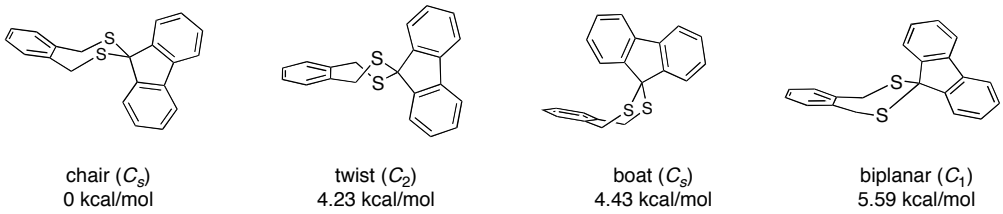

Figure 4.4. *Energy levels of various conformations of* ***86****.*

With a templating motif in mind, the next issues to be dealt with are the methods by which the pre-templated caps should be installed and how these would affect the nature of the resulting products. Loren's templated ring one is rather flexible, owing to the aliphatic chains in the ring, and can accommodate pre-templated caps of several sizes. One could envision pre-templated caps being attached to the system via alkylation, alkyne–aryl coupling, or aryl–aryl cross coupling with known **87** or **88** (Scheme 4.3).

CPK models indicated that the products resulting from alkylation or alkyne couplings may easily rotate from the desired *endo* arrangement to the undesired *exo* conformation if R (in Scheme 4.4) is hydrogen (Figure 4.5). Larger, extended R groups in this system would not allow rotation to occur, but would result in the formation of mixtures of *endo* and *exo* products. On the other hand, analysis of CPK models showed that the product of aryl–aryl cross-couplings would strongly favor the desired *endo* arrangement; the *exo* conformation could not be built without highly distorting the system and breaking bonds.

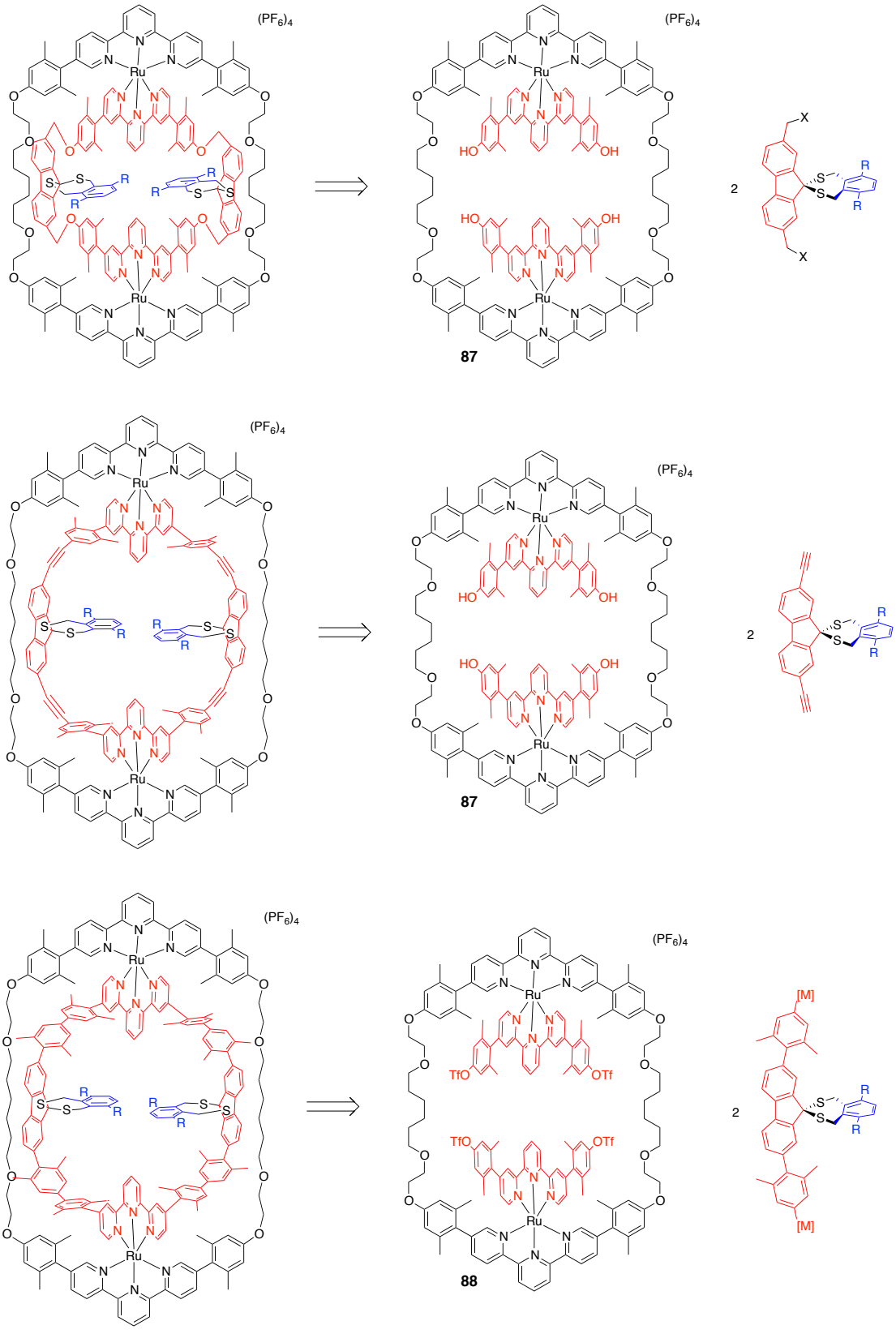

Scheme 4.4. Alkylation, alkyne coupling, and aryl–aryl cross-coupling strategies for the introduction of pre-templated caps to known complexes 87 and 88.

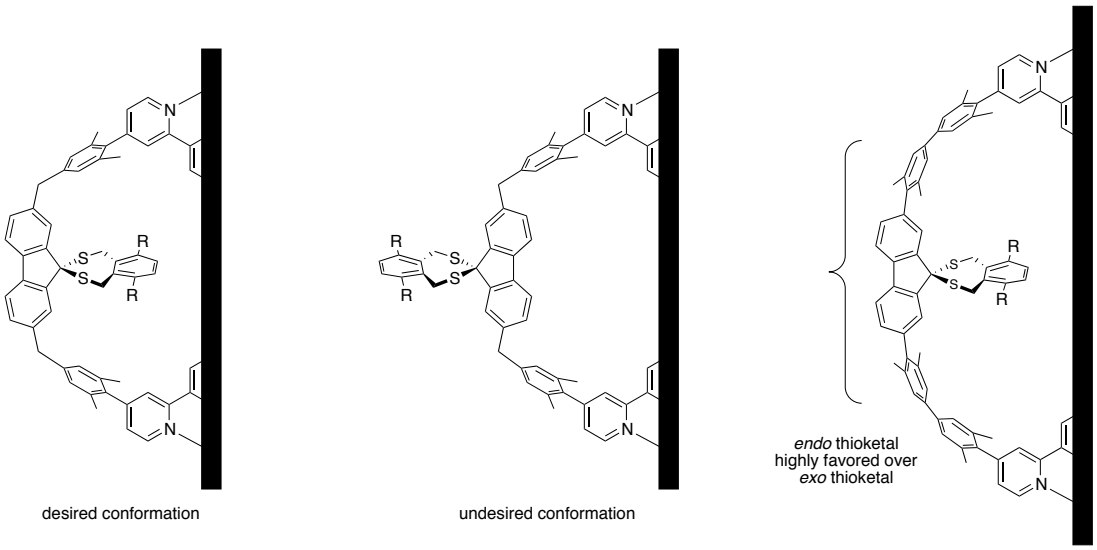

Figure 4.5. *Products of alkylation and alkyne coupling (not shown) can exist in desired* endo *and undesired* exo *arrangements with minimal energy differences. The product of aryl–aryl cross-coupling is fixed in the desired* endo *conformation.*

As aryl–aryl cross-couplings appear to offer the best method to install the pre-templated cap—and because templated ring one tetratriflate **88** is known—it followed that the cap unit in the system should be functionalized such that it may be metallated on its ends. An obvious method for meeting this functional requirement is the introduction of boron-based species by transformation of aryl triflates, which could derive from alcohols that are protected during the earlier stages of the synthesis. The internal rod unit of the pre-templated cap system should be long enough to extend out of the cavity of a templated two-ring system, and should be functionalized to allow for alkylation. Protected hydroxyphenyl units should serve this purpose well. The combination of these design principles leads to target construct **89**.

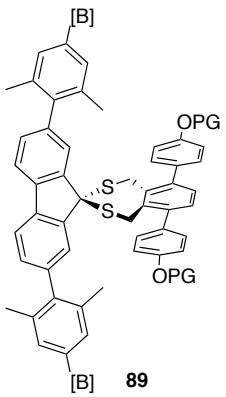

89

4.3.3. Synthesis of Pre-Templated Cap

4.3.3.1. Retrosynthetic Analysis

The first step in the retrosynthesis (Scheme 4.5) is the functional group interconversion of boron-containing groups at the ends of the cap unit to ditriflate **90**. Traditional boronation through an aryl metalate (*e.g.* aryllithium) intermediate would be an unfavorable strategy for the final step of the synthesis, but Miyaura ($C(sp^2)$–B) boronylations are frequently performed with aryl triflates, often affording boronic esters in high yield. The triflates are then simply disconnected to alcohols, which are retrosynthetically protected with protective groups (PG2) orthogonal to those on the rod unit (PG1) in **91**. The orthogonally protected intermediate is disconnected to difunctionalized thioketal **92**, where PG2 can survive transition metal-catalyzed cross-coupling conditions and PG1 can survive conditions required to form the aryl metalate. Thioketal **92** is then disconnected into two intermediates, the protected, substituted fluorenone **93** and the functionalized dithiol **94**. Substituted fluorenone is disconnected to 2,7-dibromofluorene (**95)** and aryl metalate **96**. Dithiol **94** is finally converted to the corresponding dibromide **97**, which is further disconnected to functionalized *o*-xylene **98** by a retro-benzylic bromination

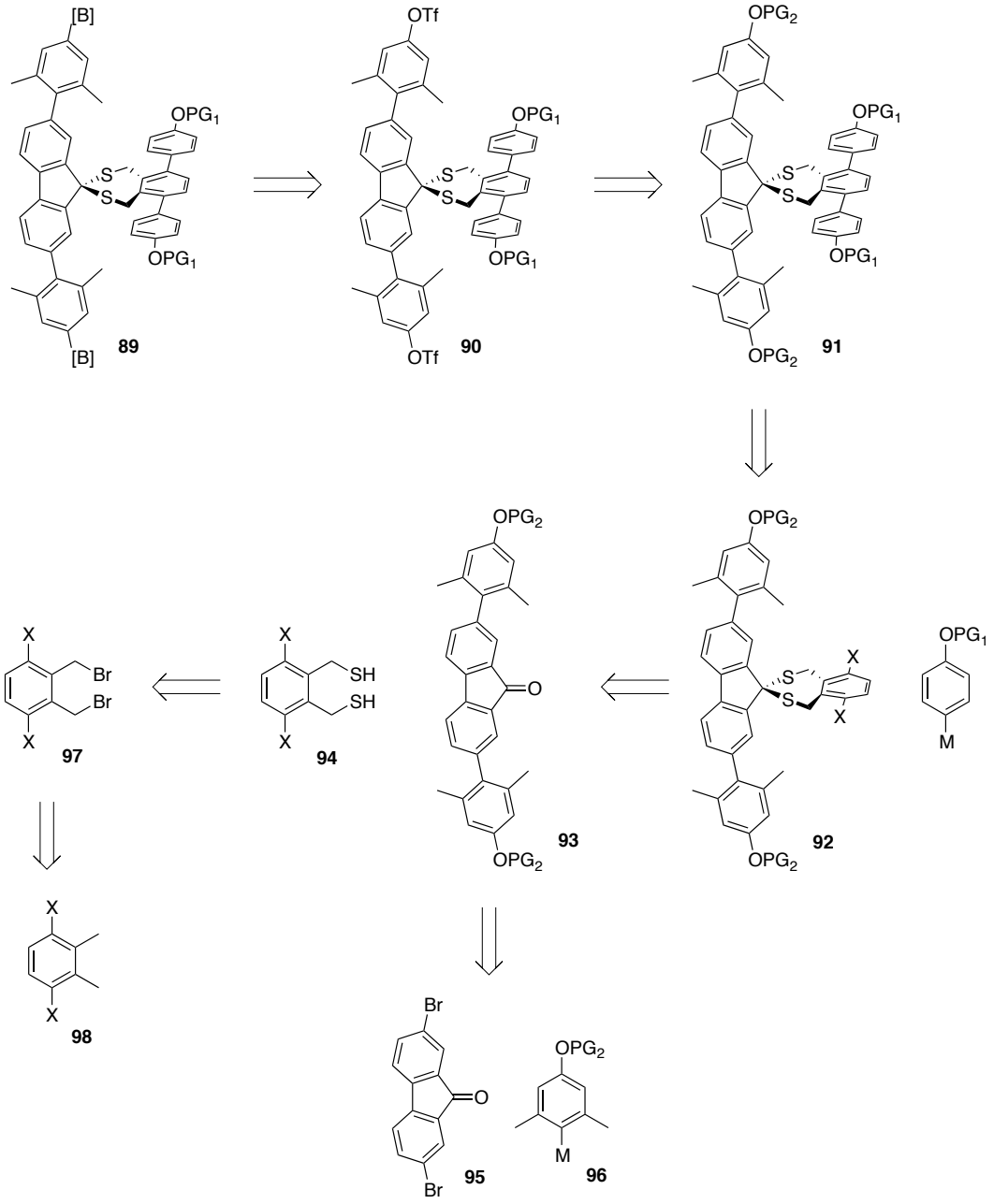

Scheme 4.5. *Retrosynthetic analysis of pre-templated cap* ***89****.*

4.3.3.3. Initial Studies

In order to test the feasibility of using this molecular construct and synthetic strategy, a few initial experiments were preformed before beginning the synthesis. The thioketalization reaction to afford **86** was attempted (Scheme 4.6). Benzene-1,2-dimethanethiol (**99**) was prepared from 1,2-bis(bromomethyl)benzene (**100**) by treatment with thiourea and subsequent hydrolysis of the imidothiocarbamate

intermediate. The reaction of **99** and fluoren-9-one **83** with 0.5 equiv. $AlCl_3$ afforded thioketal **86** in 75% yield.

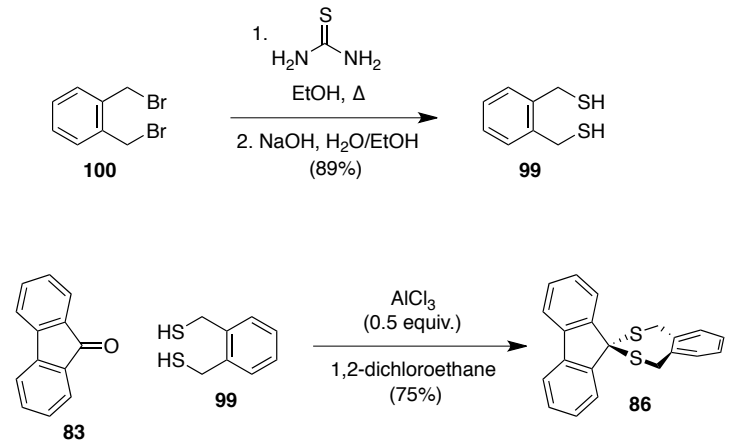

Scheme 4.6. *Synthesis of dithiol* ***99*** *and thioketal* ***86****.*

4.3.3.4. Synthesis of Functionalized Fluorenone

The synthetic design employs dibromofluorenone **101** as a starting point. This compound is commercially available, but too expensive to prudently serve as a starting material for a multi-step synthesis. Following a recently published procedure,[193] inexpensive fluorenone **83** was dibrominated, affording multi-gram quanitities of **101** (Scheme 4.7).

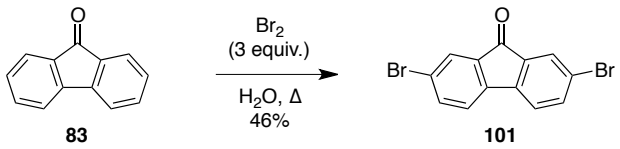

Scheme 4.7. *Synthesis of* ***101*** *from inexpensive fluorenone* ***83****.*

With dibromofluorenone **101** in hand, the synthesis of protected, substituted fluorenone **102** was carried out (Scheme 4.8). A search of literature on protective groups did not reveal any protective groups that could be expected to survive harsh lithiation and Lewis acidic condition and be readily and selectively cleaved at a later stage in the synthesis. For this reason, a protective group exchange needed to be included. A Negishi cross-coupling of **101** with 4-methoxy-2,6-dimethylphenylzinc chloride (**102**) afforded bis(methoxyaryl)-substituted fluorenone **103**. The methoxy-

substituted zincate was chosen because it is readily prepared from 4-bromo-3,5-dimethylanisole, which is easily and inexpensively prepared in multi-gram quantities by regioselective bromination[194] of 3,5-dimethylanisole. De-methylation of aryl methyl ethers to aryl alcohols requires rather harsh conditions and was performed at this stage by suspending compound **103** in molten pyridine hydrochloride at 185 °C. The resulting diol **104** was subsequently converted to pivaloyl [–OC(O)C$(CH_3)_3$] diester **105** with pivaloyl chloride in the presence of triethylamine and catalytic DMAP. Pivaloyl groups are known to survive the highly Lewis acidic conditions required in the thioketalization, but undergo alkyl addition in the presence of alkyllithium reagents, precluding their presence in the aryl zincate in the first step, but allowing for deprotection at a later step (*vide infra*).

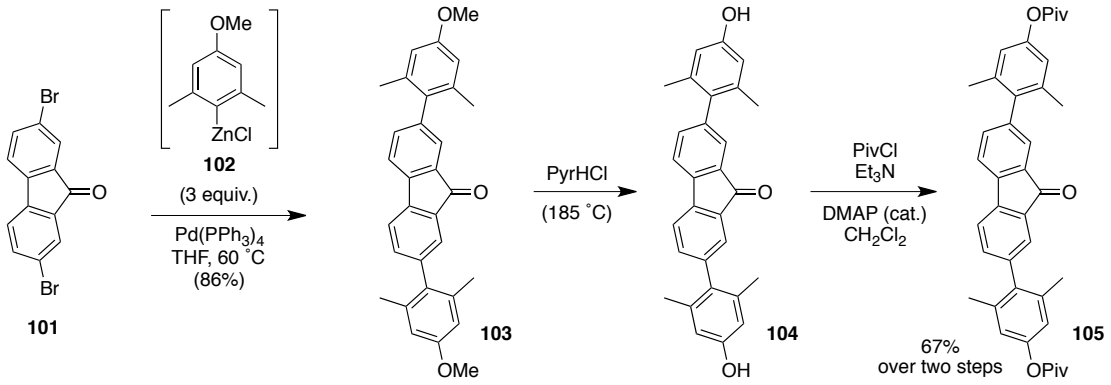

Scheme 4.8. *Synthesis of pivaloyl-protected fluorenone* ***105****.*

4.3.3.5. Synthesis of 1,4-Dihalo-2,3-dimethanethiol

The retrosynthesis of the pre-templated cap calls for a 3,6-difunctionalized 1,2-xylene **98** to serve as a starting point to develop functionalized dithiol **94**. The functionalization must undergo oxidative addition in a cross-coupling reaction later in the synthesis and dihalo derivatives would be the most obvious selections for this reactivity. Dibromoxylene **106** and dichloroxylene **107** are commercially available but cost an unreasonable price for such an early step in the synthesis. Dimethylhydroquinone **108** could also be protected for bromination and thioketalization and triflated later in the synthesis to undergo cross-coupling, but this compound is also expensive.

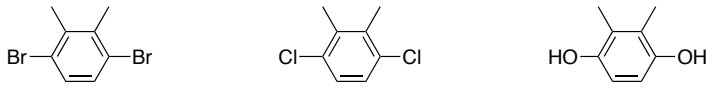

106 **107** **108**

To overcome the financial issue, an efficient synthesis of 1,4-dihalo-2,3-dimethyl starting from 2,3-dimethylaniline **109** was undertaken (Scheme 4.9). Treatment of **109** with 1 equivalent of bromine at 0 °C resulted in the immediate formation of a mixture of *ortho*- and *para*-brominated products. Treating **109** with acetic anhydride afforded acetanilide **110**, whose acetyl functionality served to concomitantly reduce the π-donation of the amine and sterically block the *ortho*-position toward electrophilic substitution. Bromination afforded **111** and subsequent acidic hydrolysis provided bromoaniline **112**.

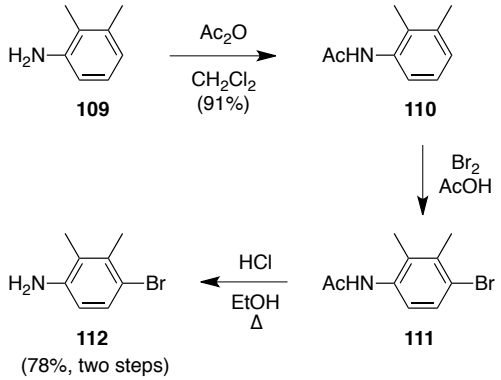

Scheme 4.9. *Synthesis of 4-bromo-2,3-dimethylaniline* ***112****.*

Though NMR and MS spectra matched those reported in the literature,[195] a ^{1}H–^{1}H-NOESY experiment was performed to ensure that product **112** had the desired regiochemistry (Figure 4.6). The NOESY spectrum showed clear cross peaks between the signals from the amine [H(a)] and one of the methyl groups [H(b)] and between the amine and one of the aromatic protons [H(e)]. Both the aromatic protons [H(d)–H(e)]—and the methyl protons [H(b)–H(c)]—exhibit cross peaks, but H(d) and H(c) couple with no other protons, indicating that the bromine atom must be located at the desired 4-position.

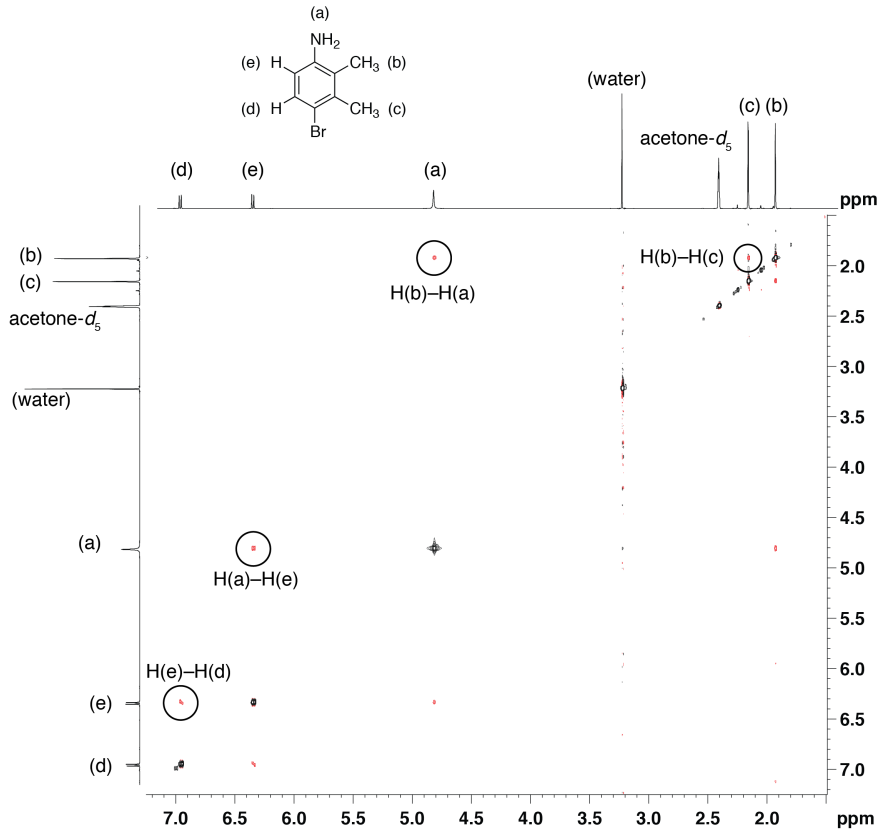

Figure 4.6. ^{1}H–^{1}H-NOESY *of compound* ***112****.*

The conversion of bromoaniline **112** into a dibromide by a Sandmeyer reaction is known,[196] but iodination to 1-bromo-4-iodo-2,3-dimethylbenzene (**113**) provided better results in our hands (Scheme 4.10). Formation of the diazonium ion *in situ*, followed by quenching with NaI afforded compound **113** in 91% yield.[197] Compound **113** was expected to be usable in the synthesis, as both halogens can undergo oxidative addition in a cross-coupling reaction; additionally, the iodine's ability to undergo oxidative addition faster than the bromine may provide a route to differentially coupled building blocks if they are desired

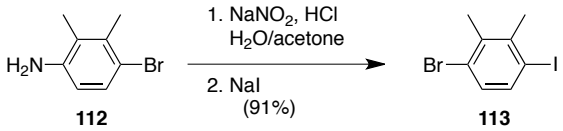

Scheme 4.10. *Sandmeyer reaction to bromoiodoxylene* ***113****.*

Compound **113** was subjected to standard benzylic bromination conditions—*N*-bromosuccinnamide (NBS) and catalytic benzoyl peroxide (BPO) in $CDCl_4$—and the reaction was monitored by TLC (Figure 4.7). After 15 minutes, the formation of a product was observed and two products were visible after one hour, implying that the first spot was the monobrominated species and the second spot the desired dibrominated compound. After 17 h, both products were still observed, with the second spot being slightly larger. An additional portion of NBS and BPO was added and the reaction was heated for an additional three hours, after which the intermediate spot almost disappeared. One final portion of NBS and BPO, followed by four more hours of stirring, resulted in only the second spot being observed.

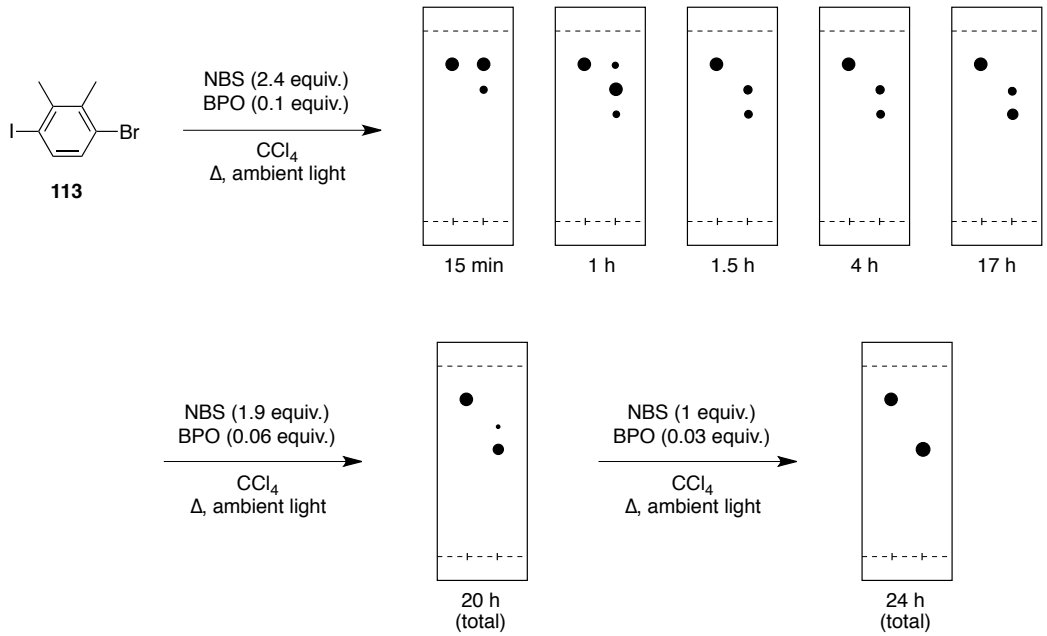

Figure 4.7. *Benzylic bromination of* ***113*** *was monitored by TLC (silica, hexane). On each plate, the left spot is the starting material and the right spot is the reaction mixture.*

The product was purified by column chromatography and its ^{1}H-NMR spectrum revealed that a mixture of products, 1-bromo-2,3-bis(bromomethyl)-4-iodobenzene (**114**) and 1,4-dibromo-2,3-bis(bromomethyl)benzene (**115**) had been obtained (Scheme 4.11). The products were easily distinguished by their molecular symmetry and integration of their signals showed 63% of **114** and 37% of **115**. The total conversion was high, affording a 94% total yield of the mixture. This type of

halide exchange has been reported in the benzylic bromination of 1,4-diodo-2,5-dimethylbenzene.[198]

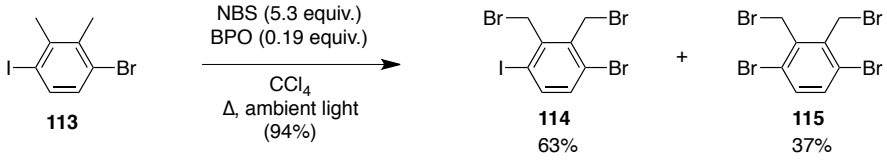

Scheme 4.11. *Benzylic bromination of* ***113*** *afforded a mixture of products* ***114*** *and* ***115****, showing partial halogen exchange.*

To investigate this reaction further, the reaction was performed again and monitored by GCMS (Figure 4.8). The goal of this study was to observe the reaction intermediates and to investigate how much of the reagents are needed to push the reaction fully to the halogen-exchanged product **115**. The reaction with **113** was initiated with 3.0 equiv. NBS and 0.1 equiv. BPO. After one hour of heating (spectrum a), starting material **113** was the major component in the reaction (9.02 min) and the two mono-benzylic brominated intermediates **116** and **117** were present (11.3 min). After three hours (spectrum b), the peak from **113** had almost disappeared and intermediates **116** and **117** exhibited the largest peaks. Two other peaks appeared , one belonging to compound **114** (13.01 min) and one attributable to de-iodinated species **118** (10.36 min). An additional 2.0 equiv. of NBS and 0.067 equiv. BPO were added at this point. After 90 minutes (spectrum c, 4.5 hours total), halogen-exchanged product **115** (12.12 min) emerged and the peaks from intermediates **116** and **117** decreased. The spectrum taken after an additional 90 minutes (spectrum d, 6 hours total) showed **114** as the major peak, with **115**, **116**, **117**, and **118** giving smaller peaks. An additional batch of 1.0 equiv. NBS and 0.033 equiv. BPO was added and, 2 hours after the addition (spectrum e, 8 hours total), the products **114** and **115** gave the largest peaks and intermediates **116** and **117** gave very small peaks. After 2 more hours (spectrum f, 10 hours total), only a small amount of **118** was detected and the peak from **115** had grown in comparison to **114**. The reaction was then subjected to multiple additions of NBS and BPO over several days to increase the amount of **115** in relation to **114**. It was found that an additional 11 equiv. NBS and 0.43 BPO needed to be added to obtain compound **114** with only a very small amount of **115**. (spectrum g).

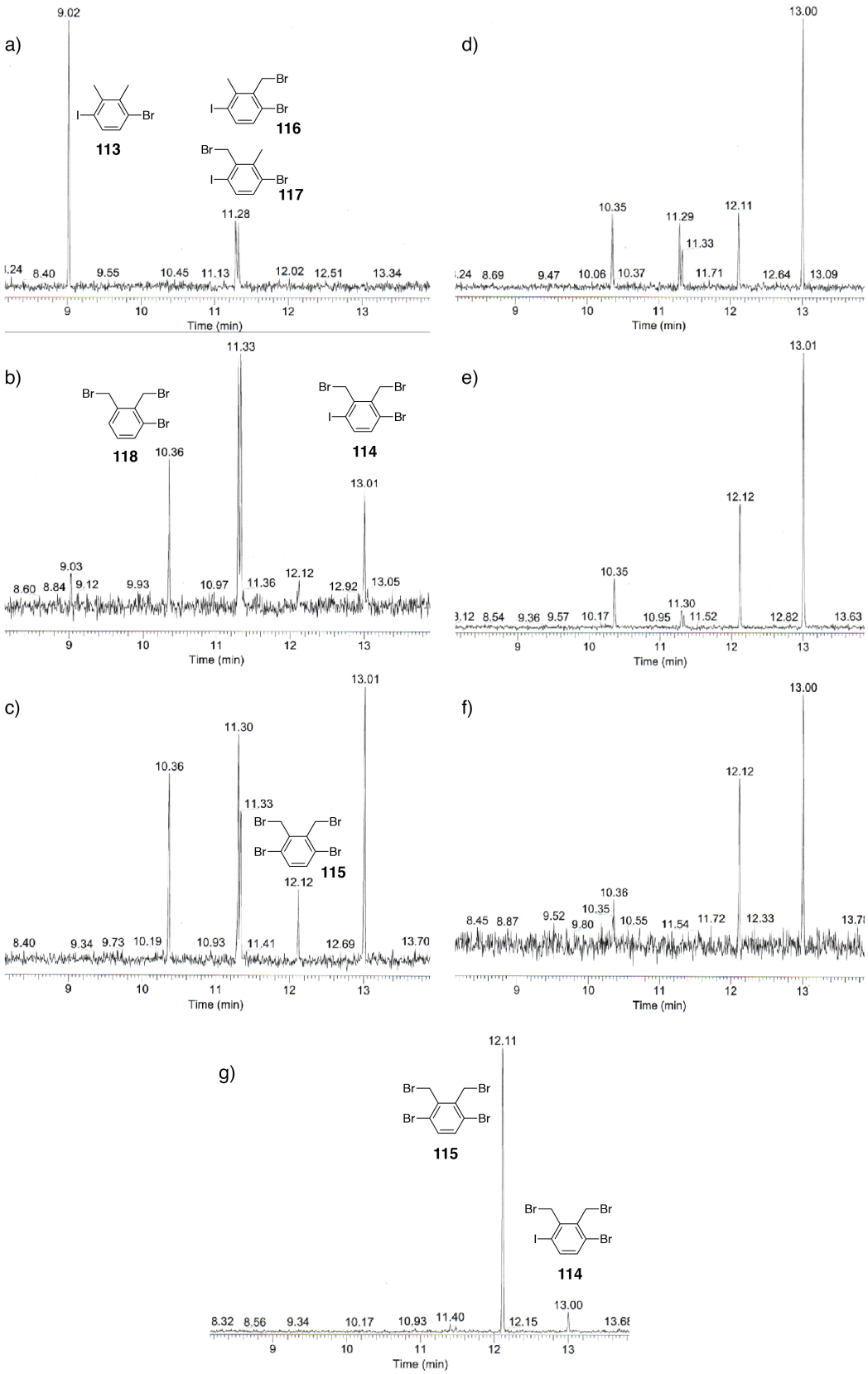

Figure 4.8. GC-MS spectra following benzylic bromination of ***113****. See text for details.*

In total, the reaction from **113** to **115** required 17 equiv. of NBS and 0.63 equiv. of BPO and 95 hours of stirring at reflux (Figure 4.9), rendering the transformation rather inefficient. If compound **115** were desired instead of **114**, bromination at the Sandmeyer step from **112** would likely provide the compound in a more economical fashion. Interestingly, despite the large excess of NBS that was added to the reaction, no dibromation of the methyl groups was observed. A feasible explanation for this result is that formation the bromomethyl radical of **114** or **115** is unfavorable. Steric clashing between the bromine atom and its neighbors (the bromomethyl group or the halide group) likely precludes the adoption of the desired coplanar conformation that maximizes delocalization of the radical with the benzene ring.

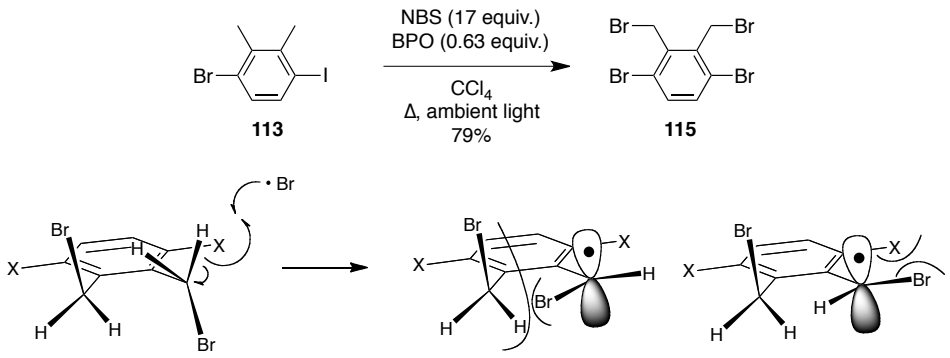

Figure 4.9. *(top) Reaction scheme to tetrabromide **115**, indicating total amounts of reagents needed. (bottom) no dibromination of the methyl groups was observed, likely because the bromomethyl radical is in a sterically crowded environment when in its preferred conformation, planar to the aromatic ring.*

As CCl_4 is expensive and hazardous,[199] and because the benzylic bromination comes at the beginning of a multi-step synthesis, the reaction was attempted in the more agreeable solvent $CHCl_3$. The reactions are performed at reflux and the boiling point of $CHCl_3$ (62 °C), is lower than that of CCl_4 (77 °C), reducing the rate of the reaction. The reaction requires multiple additions of reagents, totaling 15 equiv. of NBS and 0.3 equiv. of BPO, and the reaction requires more than two days for both methyl groups to be brominated (Scheme 4.12). This methodology has been applied to the multi-gram synthesis of a mixture of **114** (52%) and **115** (48%) with 87% total conversion.

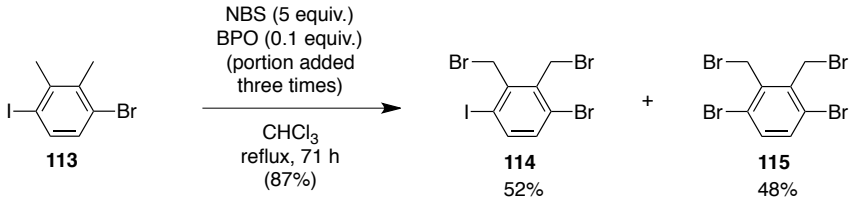

Scheme 4.12. *Benzylic bromination of* ***113*** *in* $CHCl_3$.

The mixture of products was then carried on without separation in the thiolization step, yielding a mixture of dithiols **119** and **120** in 96% yield (Scheme 4.13). To ensure that this dithiol could undergo the thioketalization reaction, it was treated with fluorenone **83** and $AlCl_3$, affording a mixture of thioketals **121** and **122** in 79% total yield. It is important to note that overlapping of ^{1}H-NMR signals in the thiols and thioketals makes it difficult to assess the genuine ratio of **121** and **122**, but for reaction setup and yield calculation, the ratio of the bromomethyl species was maintained.

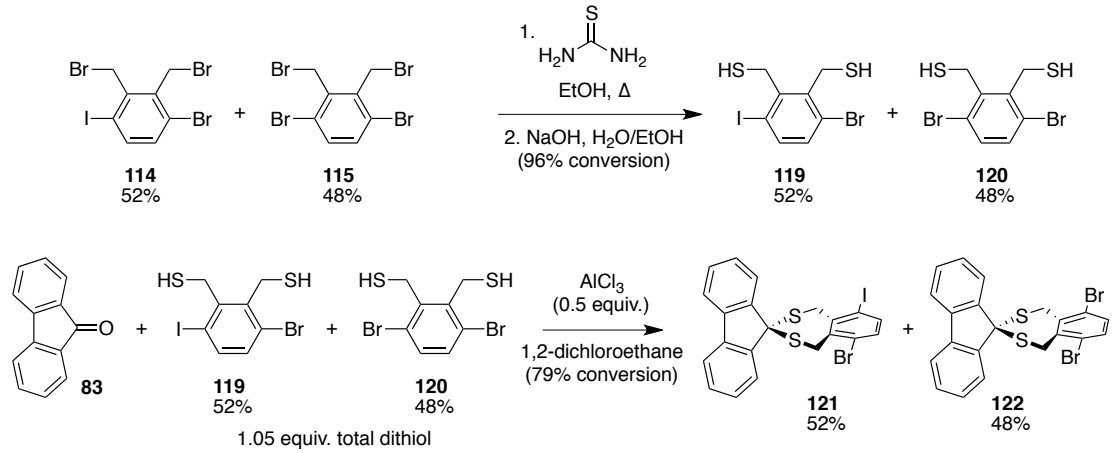

Scheme 4.13. *(top) Synthesis of a mixture of thiols* ***119*** *and* ***120*** *from a mixture of* ***114*** *and* ***115****. (bottom) Synthesis of mixture of thioketals* ***121*** *and* ***122*** *as a test reaction to determine if halogens proximal to thiol can survive thioketalization conditions.*

4.3.3.6. Synthesis of Pre-Threaded Cap Unit

With fluorenone derivative **105** thioketal mixture **119** and **120** in hand, the synthesis of orthogonally protected thioketal **123** was carried out (Scheme 4.14). First, the thioketalization reaction proceeded in moderate yield, providing a mixture of products **124** and **125**, which were not separated and used directly in the following step.

Negishi cross-coupling methodology with *in situ* formation of TIPS-protected aryl zincate **126** afforded orthogonally protected thioketal **123** in reasonable yield.

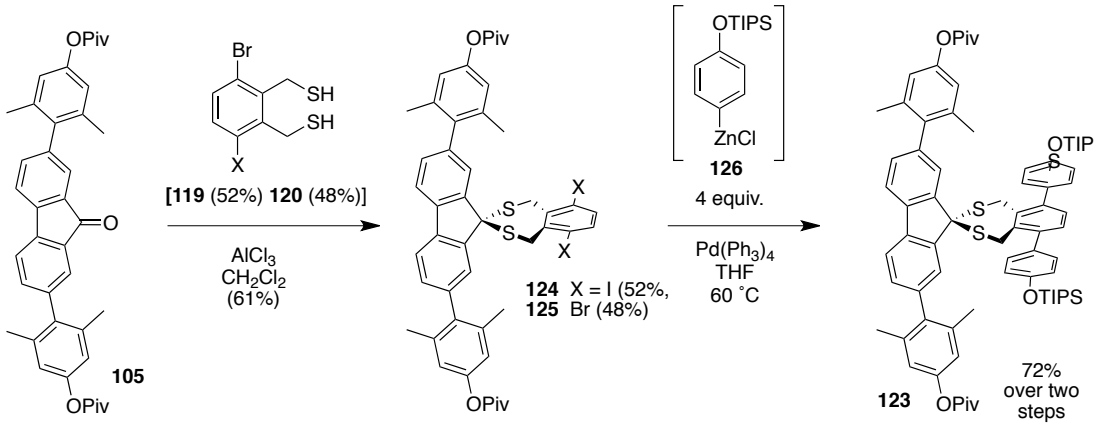

Scheme 1.14. *Synthesis of orthogonally protected thioketal construct* ***123****.*

Orthogonally protected compound **123** marked a starting point to prepare the desired pre-templated cap containing boronate species on the ends of the cap (Scheme 4.15). High-yielding selective deprotection of the pivaloyl group was accomplished by treatment of **123** with MeLi, followed by aqueous workup, affording diol **127**, which was subsequently triflated to yield ditriflate **128**. Boronic esters were introduced to the desired position via a Miyaura borylation, affording **129**.

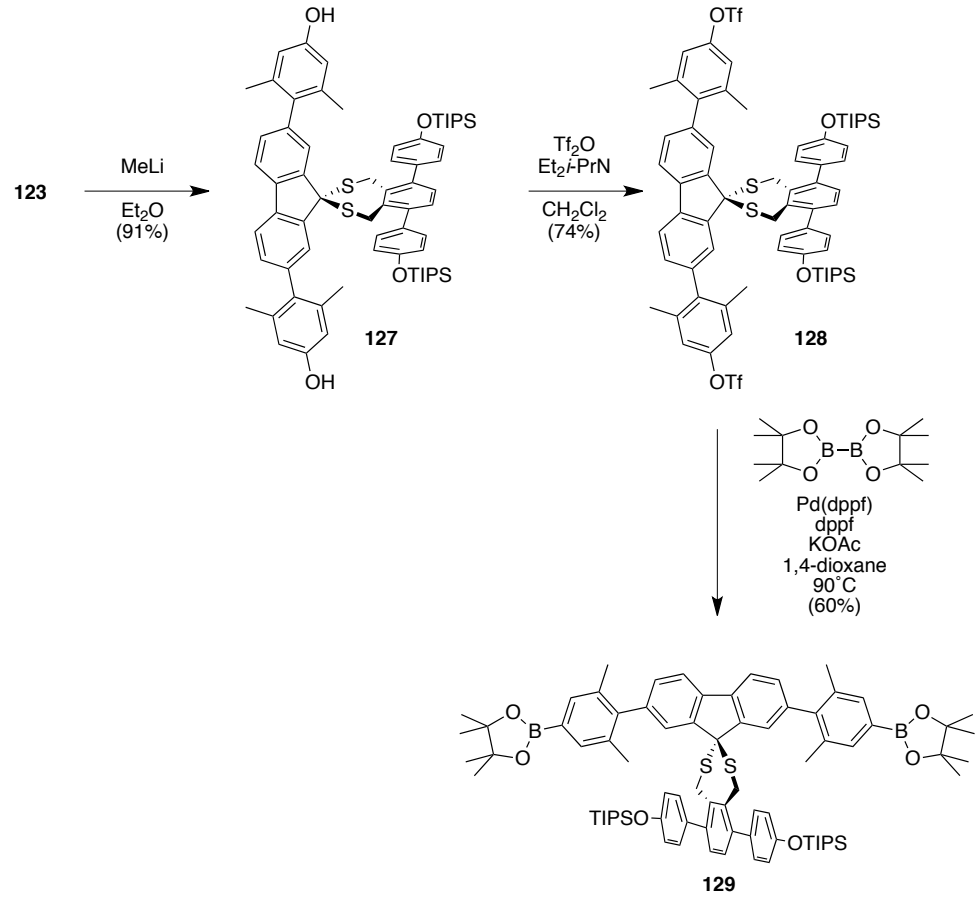

Scheme 4.15. *Synthesis of TIPS-protected, pre-templated cap* ***129*** *containing pinacol boronate esters.*

4.3.4. Synthesis of Templated Ring One

With compound **129** in hand, completion of the basic structure of the pre-templated cap unit was achieved. Next, it was necessary to reproduce the synthesis of Ru(II)-templated ring one **87**, and the tetratriflated derivative **88**, to test if the pre-templated cap strategy would be successful in generating a templated two-ring system.

Macrocycle **130** was synthesized according to the procedures described by Loren and Klosterman (Scheme 4.16.). A series of Negishi couplings with differentially substituted pyridine-based building blocks begins a synthesis that eventually ends with synthetic intermediate bis(alkynylaryl)terpyridine **131**. Next comes the critical step in the synthesis, where a high-yielding macrocyclization is accomplished by an Eglinton-type alkyne coupling using a pre-templation method. First, 0.5 equiv. of Cu(II) is added, forming a D_{2d}-symmetric 2:1 (ligand:metal) complex with two units of **131**. After complexation takes place, excess Cu(II) is added and the reaction is heated for 2 days, inducing copper-mediated coupling of the proximal alkynes, affording a D_2-

symmetric, "figure eight" complex **132**. Finally, the Cu(II) are extracted from the complex with a cyanide wash, affording tetraalkyne macrocycle **133**. Hydrogenation of **133** affords desired macrocyle **130.**

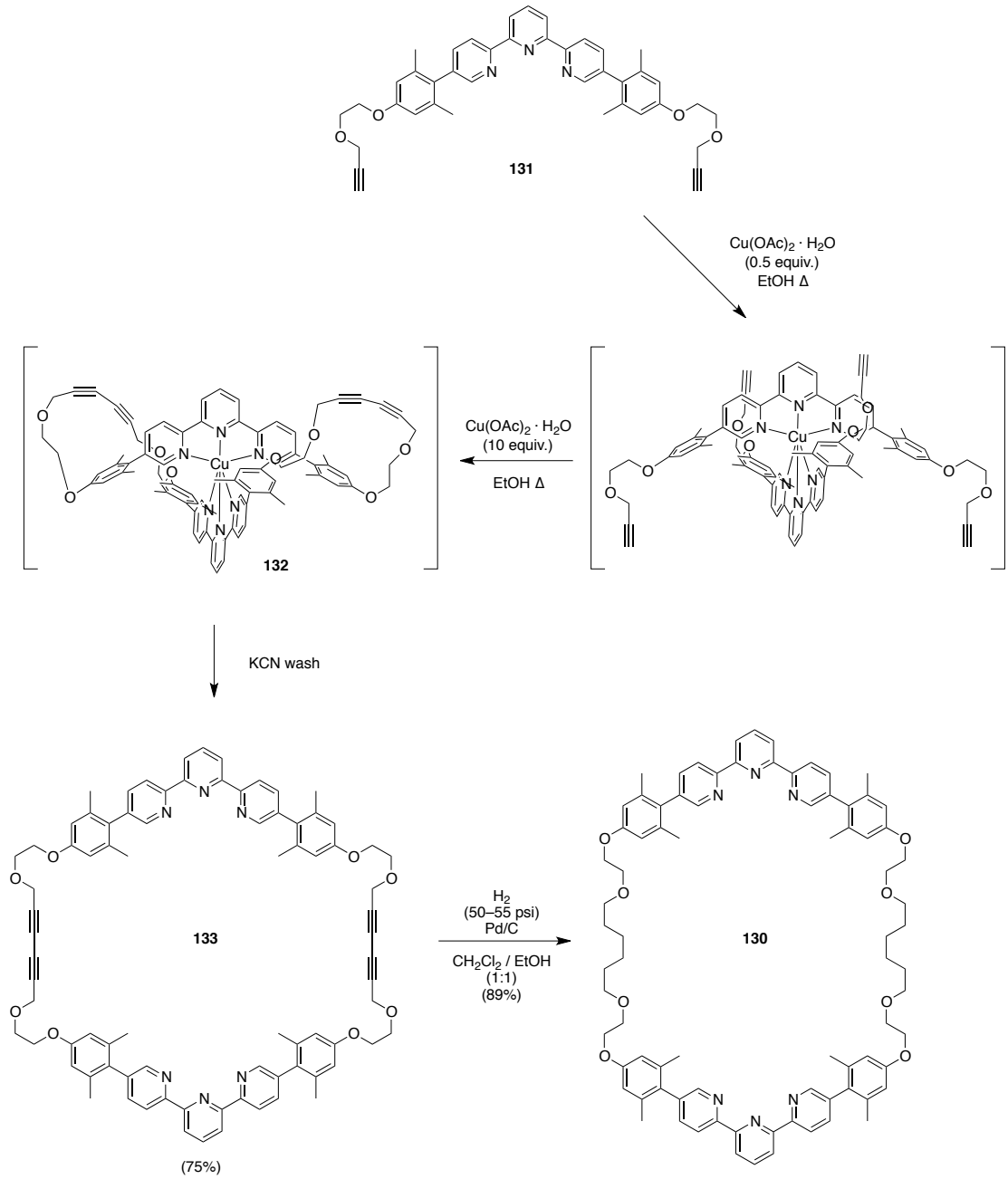

Scheme 4.16. *Final steps of the synthesis of macrocycle* ***130****, showing the critical, Eglinton-type macrocyclization step.*

Templation of ring one is accomplished by the formation of metal complex (ruthenium will be used exclusively in this work) at the terpyridine units of ring one

with the terpyridine units of a rod piece. This piece is introduced as a trichloro ruthenium complex **134**.

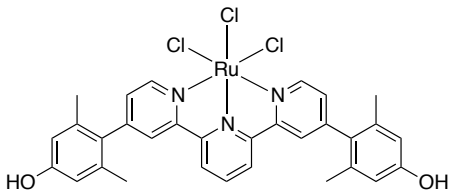

134

Loren and Klosterman both used aryliodopyridine **135** as a starting point in the synthesis of **134**. Using the directed *ortho*-metalation strategy developed by Klosterman, compound **135** was synthesized in moderate yield. (Scheme 4.17).

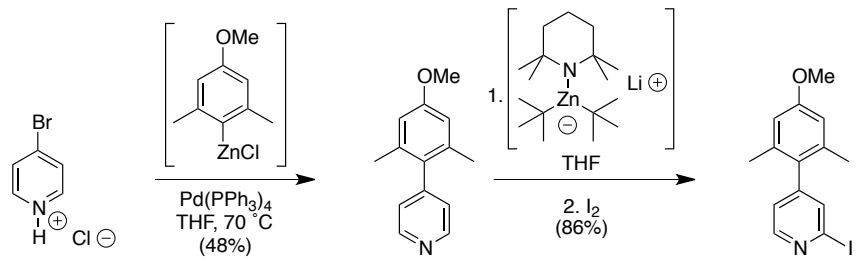

135

Scheme 4.17. *Synthesis of aryliodopyridine **135** using directed metallation strategy.*

The critical step in the synthesis of **135** is the next step, where 4,4"-diarylterpyridine **136** is formed by a cross-coupling strategy (Scheme 4.18). Loren converts **135** into a trimethylstannane, which undergoes Stille coupling to afford **136**. The yield is unfavorable at only 36%. Klosterman later reported a strategy using Negishi couplings, which afforded **136** in 72% yield.

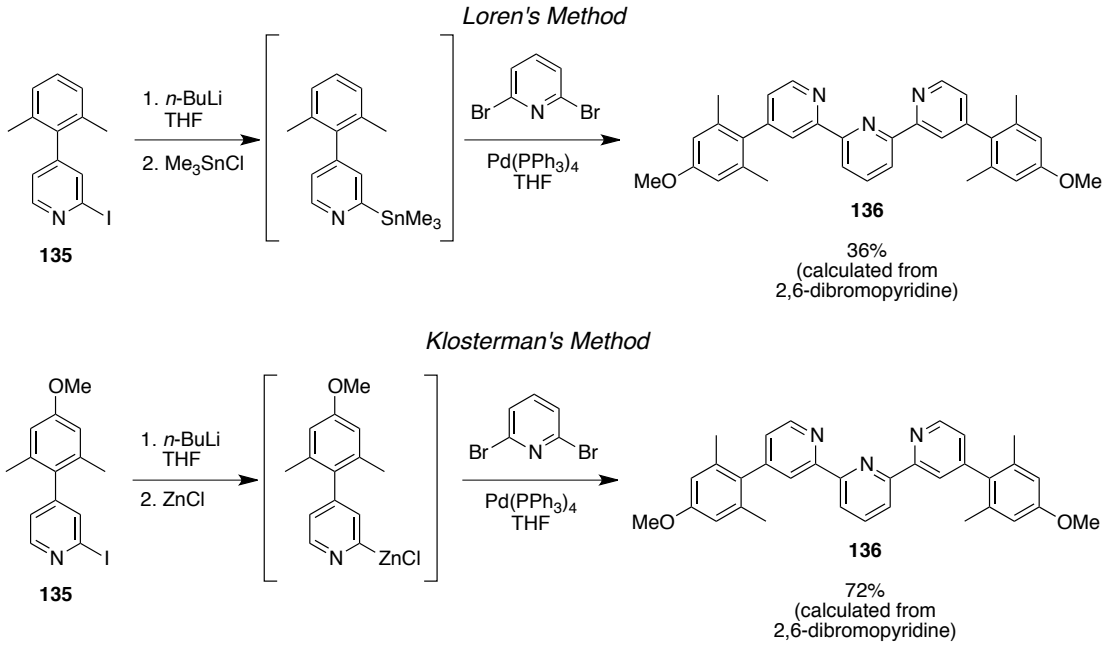

Scheme 4.18. *Loren's and Klosterman's syntheses of terpyridine* ***136****, employing Stille couplings and a Negishi couplings, respectively.*

Both of the above methods were attempted, and the yields were significantly lower than those reported above. The major product in each case was the bipyridine generated by homocoupling of the metallate, which still occurred even with solvent that had been deoxygenated by multiple cycles of degassing by the freeze-pump-thaw method. A direct Stille coupling of **135** with 2,6-bis(trimethylstannyl)pyridine **137**[200] was attempted and afforded terpyridine **136** in low yield, but gave reproducible results (Scheme 4.19).

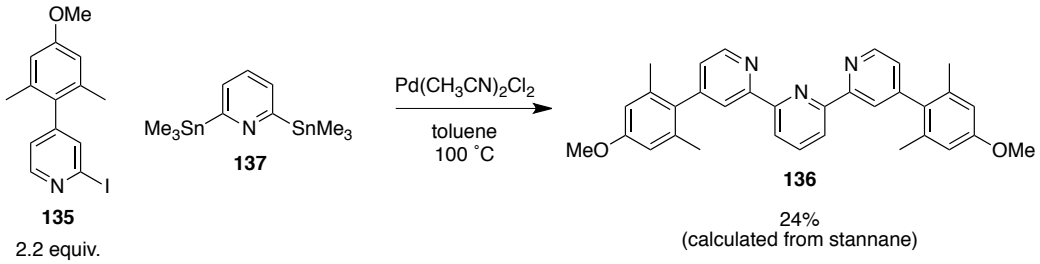

Scheme 4.19. *Synthesis of terpyridine* ***136*** *from iodide* ***135*** *and distannylpyridine* ***137*** *using Stille methodology.*

Compound **136** was de-methylated in molten pyridine hydrochloride, affording diol **138**. Treatment with $RuCl_3$ in hot EtOH yielded complex **134** (Scheme 4.20).

Treating macrocycle **130** with complex **134**, followed by workup and purification afforded templated ring one complex **87** as a $(PF_6)_4$ salt. A portion of this product was carried on to the tetratriflate according to the procedure by Loren.[175]

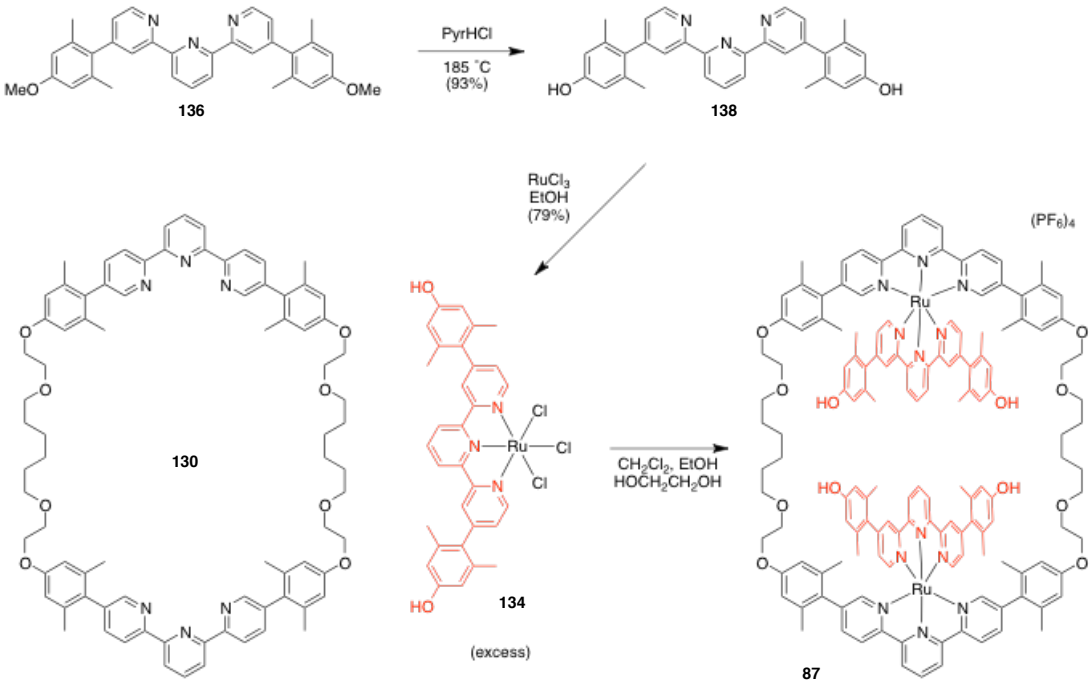

Scheme 4.20. Synthesis of templated ring one 87.

4.3.5. Attempts at Forming Templated Ring-in-Ring Complex

Suzuki–Miyaura cross-couplings[201] between aryl triflates and aryl boronate esters are known to be less efficient than the reactions with their boronic acid counterparts.[202] There are examples in the literature in which Ar–B(pin) and Ar'–OTf undergo cross coupling and the vast majority of these comprise strong π-donating groups (hydroxide or alkoxide, R_2N–) on the aryl boronic ester[203] or electron-withdrawing groups on the aryl triflate,[204] or both.[205] Exceptions exist,[206] though they often afford cross-coupled products with low to moderate yields.

To test the effectiveness of diboronic ester **128** in cross coupling reactions with triflates, Suzuki–Miyaura reactions with test triflate **138** were performed (Scheme 4.21). Standard conditions with K_2CO_3 as base and $Pd(PPh_3)_4$ as catalyst afforded no observable cross-coupled product and resulted in deprotection of the TIPS groups after 2 days of stirring and heating. Using a suspension of K_3PO_4 in DMF,[202a] neither cross-

coupling nor deprotection was observed after 2 days. Coupling also failed under conditions employing the contemporarily popular PEPPSI-*i*-Pr[207] catalyst.

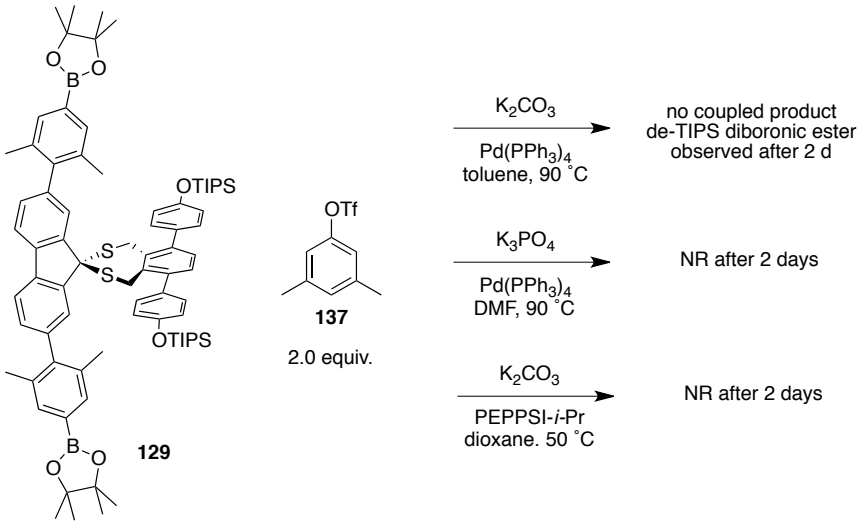

Scheme 4.21. *Attempts at boronate ester–triflate cross-couplings.*

Boronates are known to undergo cross-coupling with aryl triflates more efficiently. Lithium arylbutylborates, formed by treating an arylboronic ester with butyllithium, have been shown to perform well as nucleophilic partners in Suzuki–Miyaura-type reactions, even with relatively inactive mesyl sulfonic acids.[208] Initial butylation, followed by treatment with 2.0 equiv. of triflate **137** and coupling conditions afforded a mixture of dicoupled product and monocoupled product, and educt, with ^{1}H-NMR integrations indicating that the dicoupled product was formed in approximately 50% yield (Scheme 4.22). Since only 2.0 molar equiv. of **137** was used, the result showed that this technique might offer a useful method for coupling diboronate ester **129** and tetratriflate **88**.

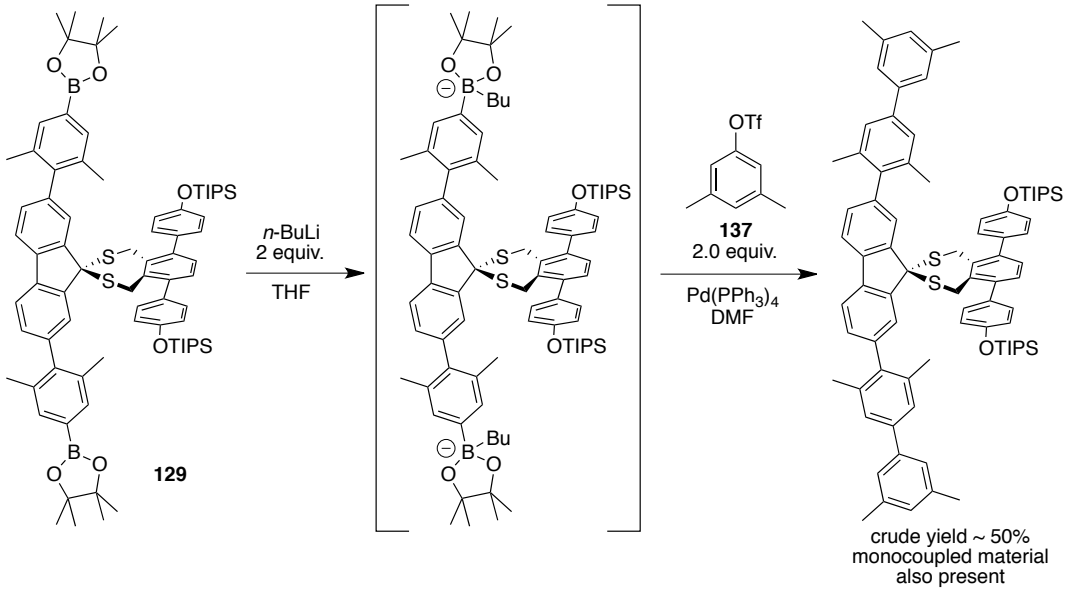

Scheme 4.22. *Attempt at alkylboronate–triflate cross-coupling.*

An excess (10 equiv.) of boronic ester was treated with butyllithium and treated with tetratriflate **88** (Scheme 4.23). The conditions shown above were used and the reaction continued for 2 days. After workup and chromatography, the red, Ru(II)-containing material was collected and subjected to ESI-MS analysis (Figure 4.10). The spectrum displayed a number of peaks and the largest of these were attributable to the educt and hydrolyzed, de-triflated derivatives thereof. The range m/z = 600–750 shows four peaks, attributable to the tetra-alcohol, the mono-triflate, the di-triflate forms, and the tetra-triflates as tetracations. The range m/z = 850–1050 exhibits four peaks from the same species as trications, each containing one PF_6^- counterion. Not surprisingly, ^{1}H-NMR spectra of the mixture of products were highly complicated and did not offer much additional insight.

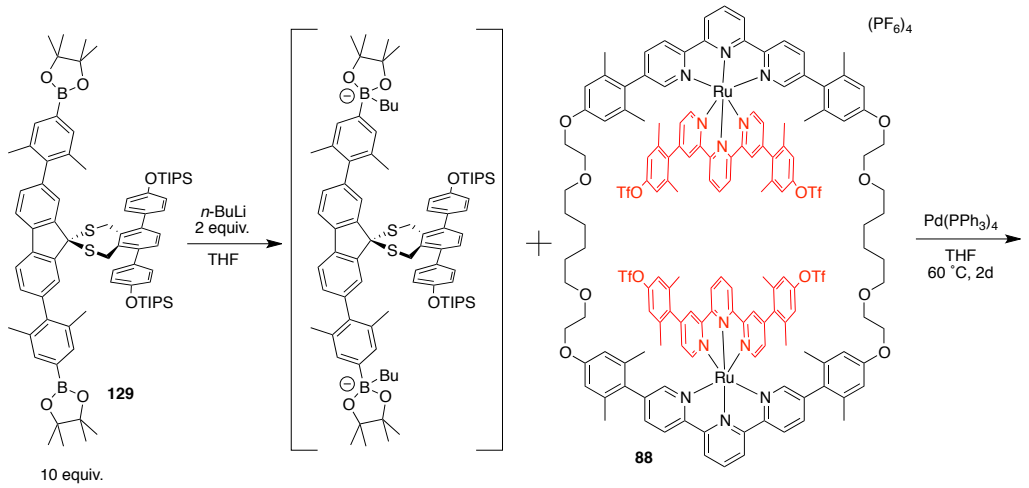

Scheme 4.23. Attempted coupling of butyl boronate **129** *and tetratriflate 88.*

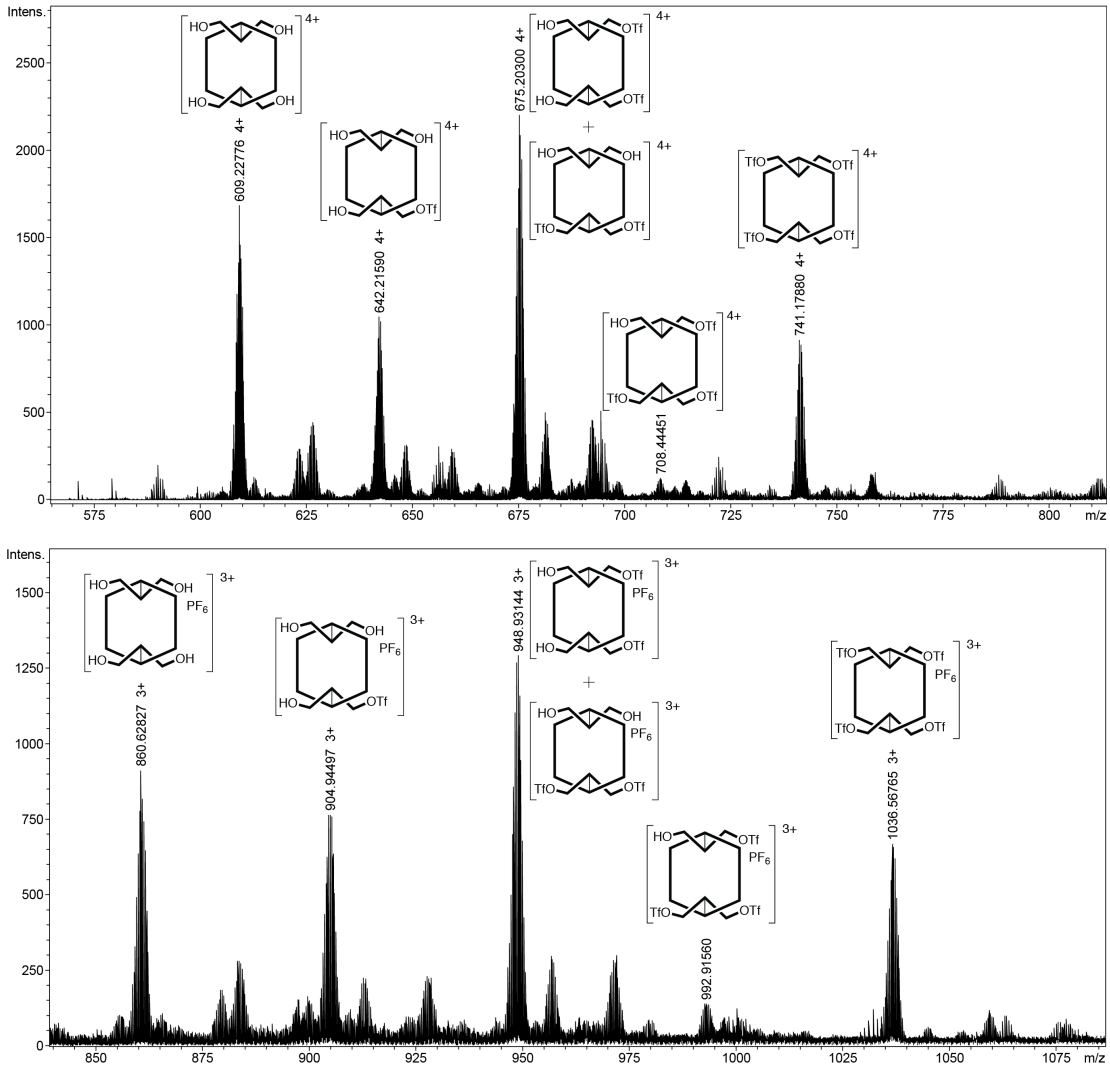

Figure 4.10. ESI-MS of Ru(II)-containing products following the reaction shown in Scheme 4.23. Only educt **88** *and de-triflated derivatives thereof could be identified. (top) range: m/z = 550–850, (bottom) range: m/z = 840–1085.*

The failure of this reaction to yield any observable cross-coupled products led us to consider other boron-containing groups that could be synthetically accessible from compound **129**. Aryl trifluoroboronates have gained increasing prominence in organic synthesis over the past several years as a robust partner in cross-coupling.[209] The reactivity of aryl trifluoroboronates was originally discovered by Genet in the late 1990s,[210] but its utility in cross-couplings has been extensively developed by Molander[211] over the past decade. Mechanistic studies[212] indicate that their reactivity derives from an ability to slowly release[213] aryl boronic acids, toward the generation active aryl trihydroxyboronate intermediates, in the course of the reaction. This option was especially attractive as aryl trifluoroboronates are highly useful in couplings with aryl triflates.[214]

Preparation of aryl trifluoroboronates from from aryl (pincol)boronates is accomplished by treatment with KHF_2[215] in a highly chemoselective reaction that is benign toward variety of functional groups (Scheme 4.24).[216] Not surprisingly, silyl protecting groups do not survive the reaction, as the fluoride ions present in the mixture induce deprotection, which may be advantageously used in a one-pot deprotection/trifluoroboronation step.[217]

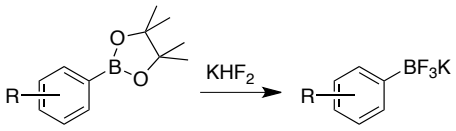

Scheme 4.24. *Standard preparation of aryl trifluoroboronates from boronic esters with* KHF_2.

Initial attempts to form the dipotassium bis(trifluoroboronate) of **129** resulted in the formation of a precipitate that was insoluble in common solvents, including acetone, acetonitrile, chloroform, dichloromethane, THF, methanol, ethanol, and water. Certain aryl trifluoroboronates are sparingly soluble in organic solvents and their solubility can be enhanced by exchanging the counterion K^+ with a bulky organic cation, such as tetra-*n*-butylammonium (TBA).[218] Synthesis of TBA_2 bis(trifluoroboronate) **138** was accomplished by a tandem deprotection/trifluorination reaction (Scheme 4.25). Compound **129** was first treated with TBAF to deprotect the TIPS groups, before the trifluorination step with KHF_2, affording product **138**. The reaction

generates an equimolar amount of pinacol, which can be removed by an azeotropic distillation with methanol/water, cleverly devised by Aggarwal, et al.[219]

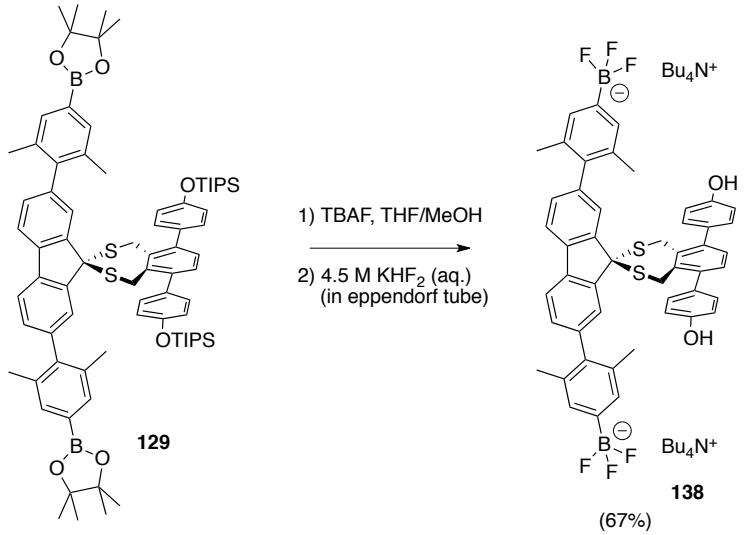

Scheme 4.25. *One-pot deprotection and formation of tetrabutylammonium salt* ***138****.*

With bis(trifluoroboronate) **138** in hand, the cross-coupling reaction with tetratriflate **88** was attempted (Scheme 4.26). Methods developed by Molander,[214] using $Pd(OAc)_2$ as catalyst, tricyclohexylphosphine as ligand, and Cs_2CO_3 as base, were applied. Reactions with these conditions are known to be rather slow, requiring > 20 hours in some cases, so this reaction was heated and stirred for 8 days, during which LC-MS of the reaction mixture showed no evidence of cross-coupled products.

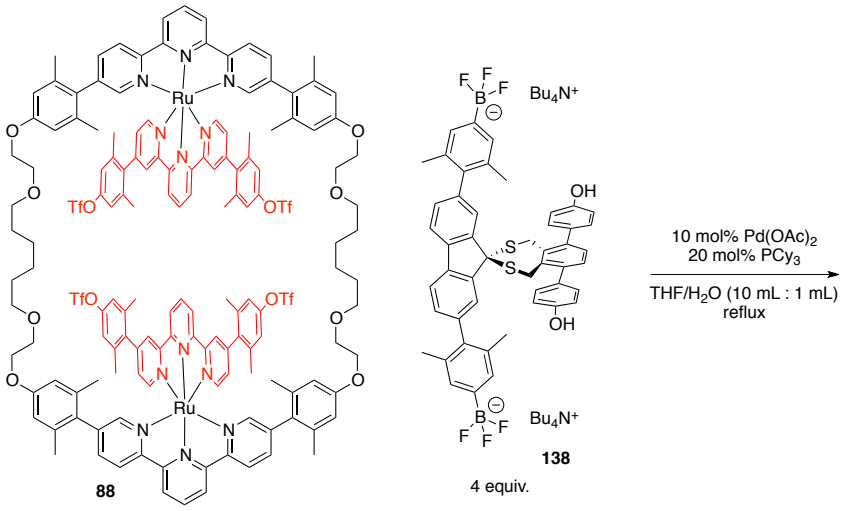

Scheme 4.26. *Attempted coupling of arylbis(trifluoroboronate)* ***138*** *with tetratriflate* ***88****.*

After workup and column chromatography to collect the red, Ru(II)-containing products, ESI-MS was performed, showing several peaks that were not attributable to cross-coupled products (Figure 4.11). The major peak at m/z = 1037 corresponds to the tetratriflate {[**88**(PF6)]}$^{3+}$ and the peak at 993 corresponds to the same framework with an alcohol replacing one of the triflates. The peak at 774.7 appears as a monocation and was not assigned. ^{1}H-NMR spectra showed primarily **88** and peaks arising from de-triflated derivatives thereof.

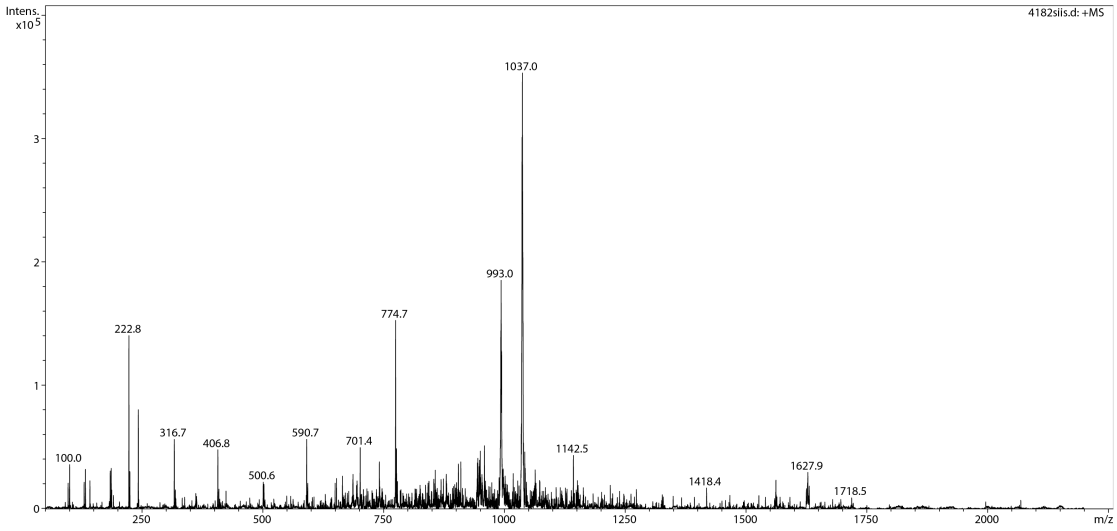

Figure 4.11. *ESI-MS of products obtained from the reaction shown in Scheme 4.26.*

The reasons for the failure of these cross-coupling strategies are unclear. Concerns about whether the pre-templated cap is appropriately spaced to fit properly onto the system are secondary, as no evidence of even a mono-coupled species was observed. The reactions were run in small scale, in highly dilute conditions, and for extended periods of time, which may have favored several of the known side reaction pathways that are known to occur during Suzuki–Miyaura couplings, including homocoupling or oxidation of the nucleophile, and protodeboronation.[220] It would be worth compiling a large amount of **129** that would allow for optimization studies. For example, the standard reaction with boronic acids has not yet been attempted and the wealth of knowledge concerning the Suzuki reaction offers volumes of reaction conditions that may afford a templated ring-in-ring compound en route to a molecular Borromean link.

4.4. Strategy Two: Introduction of Small Threads

4.4.1. Introduction

The failure of threading attempts by Loren and Klosterman has been attributed to steric crowding and unfavorable conformational distortion in ring-in-ring molecule **76**. Ligand–metal complexes are rather bulky threads; for example, a terpyridine–Ru complex measures 8.8 Å from H–C(4') to Ru (Figure 4.12). The effective thickness is even longer considering that these species are introduced as trichloro complexes. The impetus behind the strategy shown in this section is that the thermodynamic preference against threading may be alleviated by simply introducing a smaller thread. The width of an alkyl chain, for example, measures roughly 3.7 Å and would likely fit easily through the loop of ring two if one were able to place it there.

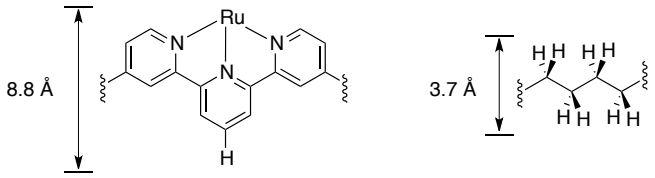

Figure 4.12. *Comparison of widths of terpyridine–Ru complex and alkyl chain.*

The passing an aliphatic chain through the loop of ring two in a reaction flask is highly unlikely due to statistical and entropic effects. The groups of Leigh and Goldup have overcome this limitation by developing clever active templating strategies[221] for generating rotaxanes with macrocycles that are much smaller than those reachable by classic templating strategies such as metal complexation, hydrogen bonding, etc, which the authors call "passive" templates. In their strategy, an active metal is complexed within the macrocycle and subsequently catalyzes a coupling reaction to generate the dumbbell-shaped molecule within the macrocycle (Figure 4.13). This approach was first applied to rotaxane synthesis by a Cu(I)-catalyzed 1,3-dipolar cycloaddition of a terminal alkyne and terminal azide within a macrocycle.[222] Since its discovery, the reaction has been applied to a variety of macrocycles,[223] and different types of coupling reactions, including Cu(I)-[224] or Pd(II)-[225] catalyzed alkyne–alkyne homocouplings, Heck reactions,[226] and Michael additions.[227]

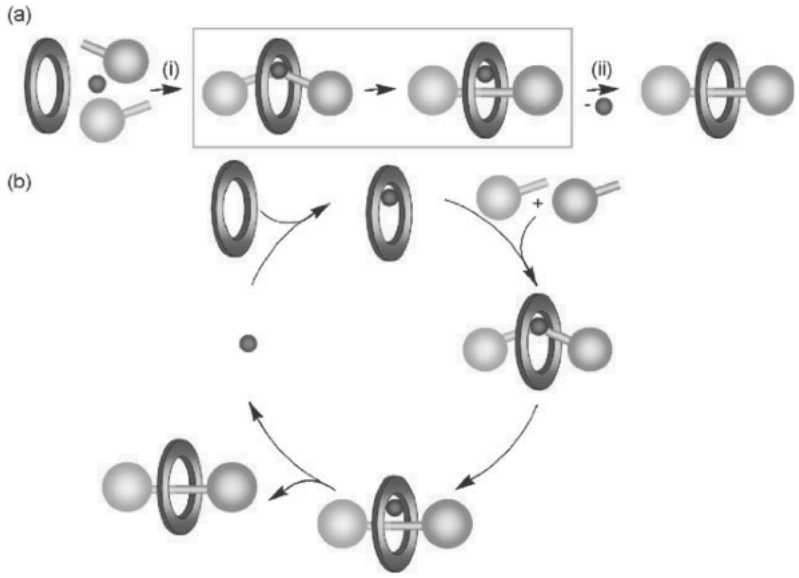

Figure 4.13. *(a) Schematic representation of the activating template strategy for the synthesis of rotaxanes. (b) A metal catalyst is complexed within a macrocycle, then catalyzes the coupling reaction two functionalized pieces, each containing a sterically bulky cap. Removal of the catalyst results in the formation of a rotaxane. Reprinted with permission from reference 222. Copyright © 2007 American Chemical Society.*

Applying this strategy to the directed synthesis of a molecular Borromean link, a ring-in-ring complex comprising ligands on the outer loop of ring two may undergo metal complex to afford an activated ring-in-ring system (Figure 4.14). The metal catalysts in this construct may then catalyze internal coupling reactions, affording a threaded two-ring system. At this point Borromean topology would virtually be reached and all that is needed are two capping reactions that transform the two dumbbell-shaped molecules to a macrocycle.

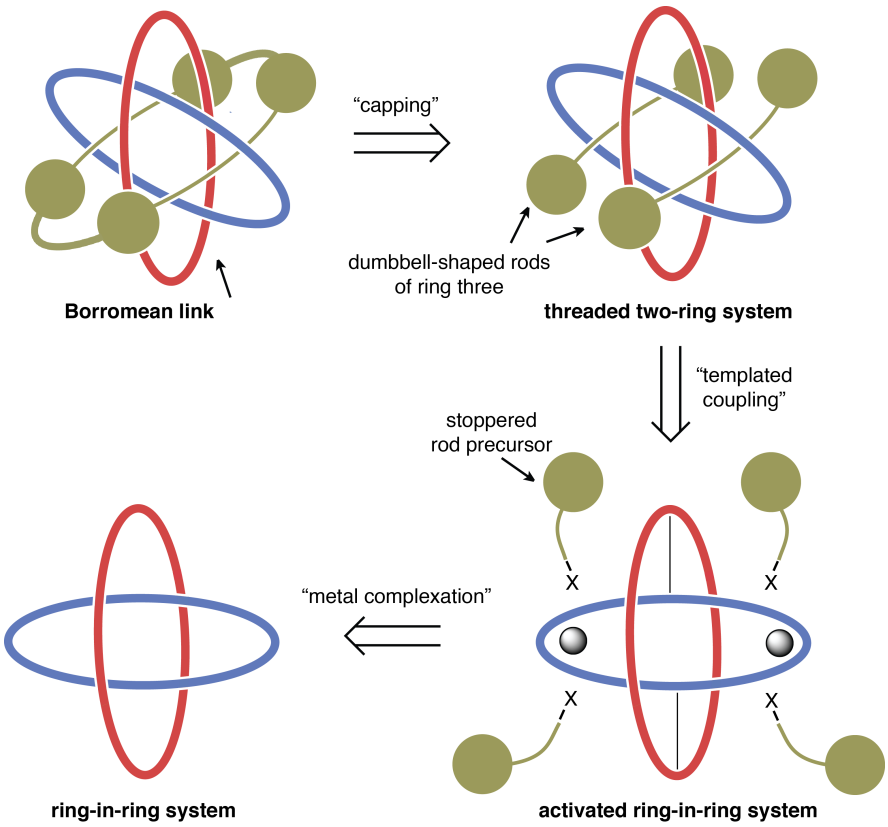

Figure 4.14. Schematic representation of a molecular Borromean link retrosynthesis using the activated template approach.

4.4.2. Attempt at Forming Templated Ring-in-Ring Complex

Of the many types of reactions that have been exploited in the activated template approach, it was necessary to evaluate which reaction offers the best strategy to a Borromean link synthesis. Recently, it was shown that Cu(I)-mediated rotaxane formation by a 1,3-dipolar cycloaddition is highly dependent on the size of the macrocycle.[228] Small macrocycles produced rotaxanes very efficiently by this method and the ligand structure is similar to the cap of ring two in ring-in-ring complex **76**, indicating that this reaction may be useful for the synthesis of threaded derivatives.

Ring-in-ring complex **76** was synthesized by modifying a procedure developed by Loren (Scheme 4.27).[229] Treating templated ring one **87** with 6,6'-bis(bromomethyl)-2,2'-bipyridine (**139**) under basic conditions afforded **76**. Dibromide **139** was prepared according to literature procedures.[230]

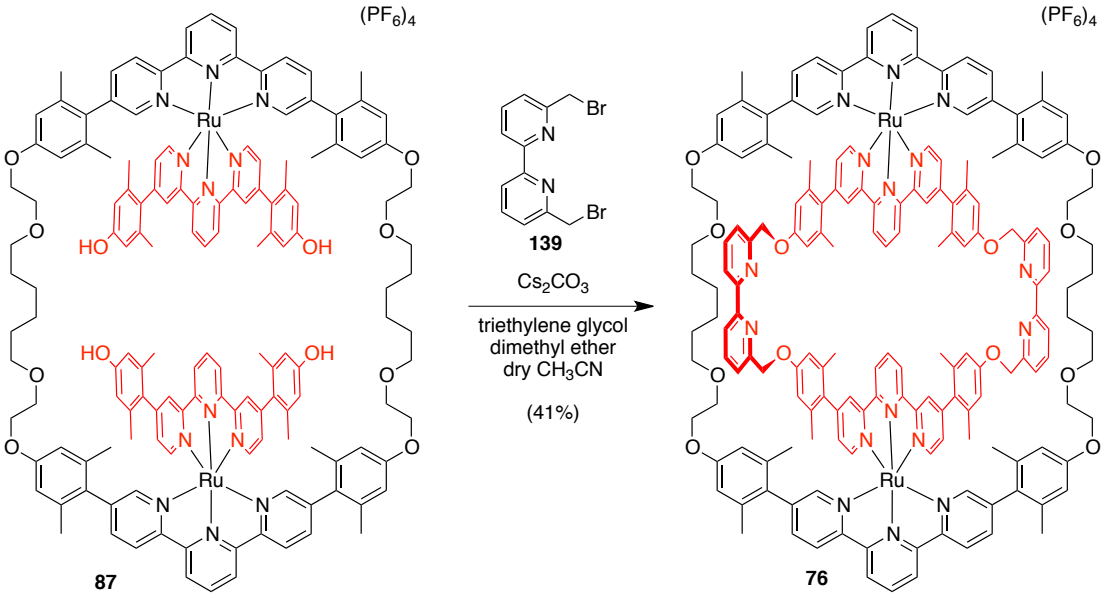

Scheme 4.27. Synthesis of ring-in-ring complex 76.

Next, the stoppered units that serve as the dumbbell-shaped molecule in the eventual rotaxane were synthesized. Stoppered phenol **140** serves as an intermediate in the synthesis of stoppered alkyne **141** and stoppered azide **142**. Treatment of diethyl carbonate with 4-*t*-butylphenyllithium, prepared *in situ* from 1-bromo-4-*t*-butylbenzene, resulting in the formation of triarylmethanol **143** (Scheme 4.28).[231] Dissolving **143** with molten phenol and adding a catalytic amound of H_2SO_4 afforded phenol **140** in good yield.[232] Phenol **140** was then carried forward to alkyne **141** by reaction with alkynyltosylate **144**. Azide **142** was prepared according to literature procedures[233] from **140** by first alkylating with 1,3-dibromopropane, then treating with NaN_3.

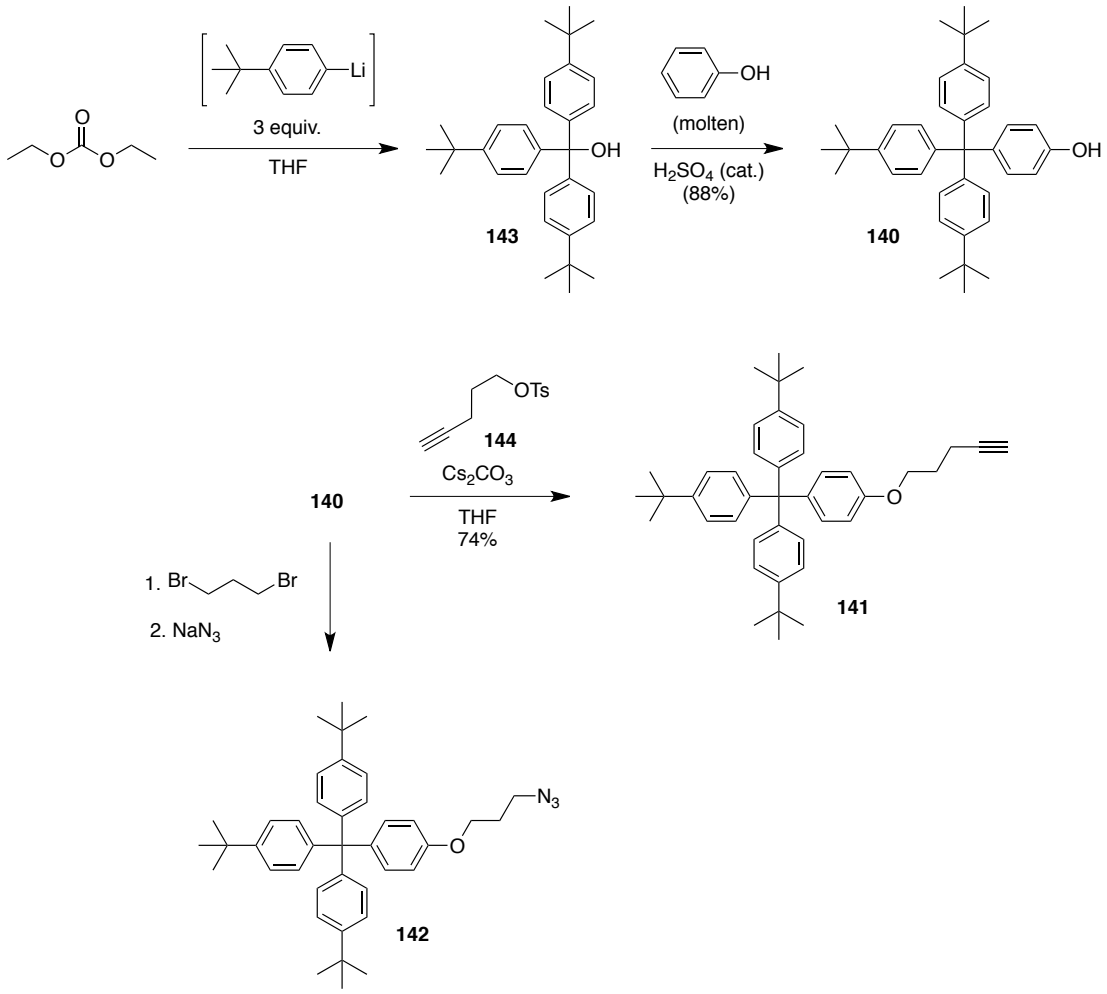

*Scheme 4.28. Synthesis of stoppered alcohol **140**, alkyne **141** and azide **142**.*

With ring-in-ring complex **76**, alkyne **141**, and azide **142** in hand, an activated template-driven threading reaction was attempted. The reaction was run according to Goldup's experimental procedure,[228] but after five days of reaction time, the ring-in-ring complex was still the dominant peak by LCMS and no threaded compounds were observed.

4.4. Conclusions and Outlook

Both of the strategies described in this chapter have so far failed to overcome the problem of threading in ring-in-ring complexes, though there is much more work to be done. In each of the synthetic strategies, a critical step is required at a stage in which minimal material is present. Future work should initially focus on generating a stockpile of precursors from which creativity can flow.

An interesting outcome of the pre-templated cap approach was the development of thioketals based on fluorenone, which hold a cap and a rod roughly perpendicular to each other. This previously unexplored molecular motif may find application as a novel covalent templating framework, an idea that will be discussed in the following chapter.

The activated template approach has great potential for the formation of a templated ring-in-ring complex. Only preliminary results have been obtained so far and these initial attempts failed to afford the desired complex. The wide range of reactivity that has been demonstrated by the Leigh and Goldup groups in their syntheses of small rotaxanes by this approach offers many new possibilities and a significant amount of future work should focus on this strategy.

Another strategy that has been undertaken in the Siegel group by a MSc student, Helen Seifert, has attempted to use longer, linear internal complexes in the templated ring one structure. The rationale behind this approach is that longer, linear rods may greatly widen the loop through which the threading reaction must occur. This approach has yet to yield a ring-in-ring system, but has great potential toward the development of novel ring-in-ring systems toward the development of Borromean links.

Chapter 5

Thioketals as Templates Towards Molecular Borromean Links

5.1. Summary

The thioketal syntheses described in the previous chapter motivated the design of a molecular Borromean link synthesis in which the only templates are thioketals. The envisioned final product of this synthesis is a Borromean link with T_h symmetriy comprised entirely of extended aromatic hydrocarbon macrocycles. Synthesis of preliminary building blocks toward this construct was accomplished.

5.2. Introduction

Metal-templating techniques[167] pioneered by Sauvage and donor-acceptor strategies[234] developed by Stoddart have dominated modern development of mechanically bonded knots and links. This chapter will present current work that aimed at employing novel templating techniques toward the synthesis of molecular Borromean link. The first of these designs took the thioketal-templating strategy shown in the previous chapter and sought to develop a synthesis of a Borromean ring exclusively using thioketals as templates. Though this strategy is novel—to my knowledge, thioketals have never been employed as templates in catenane or rotaxane synthesis—it is highly reminiscent of older ketal-based syntheses of catenanes and rotaxanes developed by Gottfried Schill.[235]

5.3. Thioketals as Templates

5.3.1. Design of a Thioketal-Templated Borromean Link

The work discussed in the previous chapter shows that thioketals of derivatives of benzene-1,2-dimethanethiol and fluoren-9-one are synthetically accessible and serve as appropriately oriented templated cap units. Work on this structural motif led to the

design of a molecular Borromean link that could be generated by using thioketals as the sole templating agents. A schematic diagram shows that four junctions would be required to accomplish this feat (Figure 5.1).

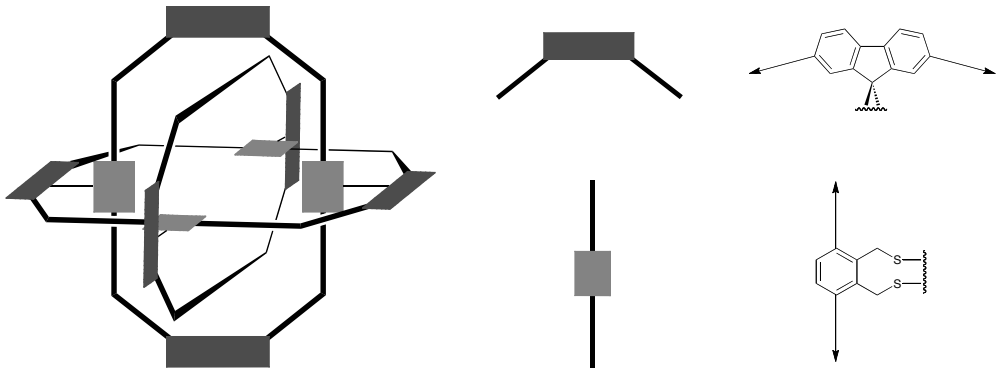

Figure 5.1. *Templated synthesis of a Borromean link requires four connections.*

In order to achieve real Borromean links, the templates must be removed at the final step of the synthesis. Thioketals could serve as excellent templates, as they are covalently bonded linkers that are inert to many reaction conditions and can be cleaved selectively. Due to their demonstrated utility as protecting groups[236] and *Umpolung*-inducing motifs[237] for carbonyl functionalities, hydrolysis of thioketals to carbonyls has been well studied and is well understood.[238] Another possibility for removal the thioketal templates is Raney-nickel-induced desulfurization.[239] This route is highly attractive and could lead to Borromean links that composed solely of hydrocarbon macrocycles.

With a templating scheme in place, the next issues requiring attention were the size and nature of the macrocycles participating in the link. It is desirable to generate links with high symmetry, where all of the individual macrocycles are equivalent. Examination of CPK models indicated that Borromean ring precursor **145** could accomodate three macrocycles without inducing significant strain (Scheme 5.1). If compound **145**, which has D_{2h} symmetry, could undergo a full de-sulfurization reaction, T_h-symmetric (time-averaged) Borromean link **146** could be generated.

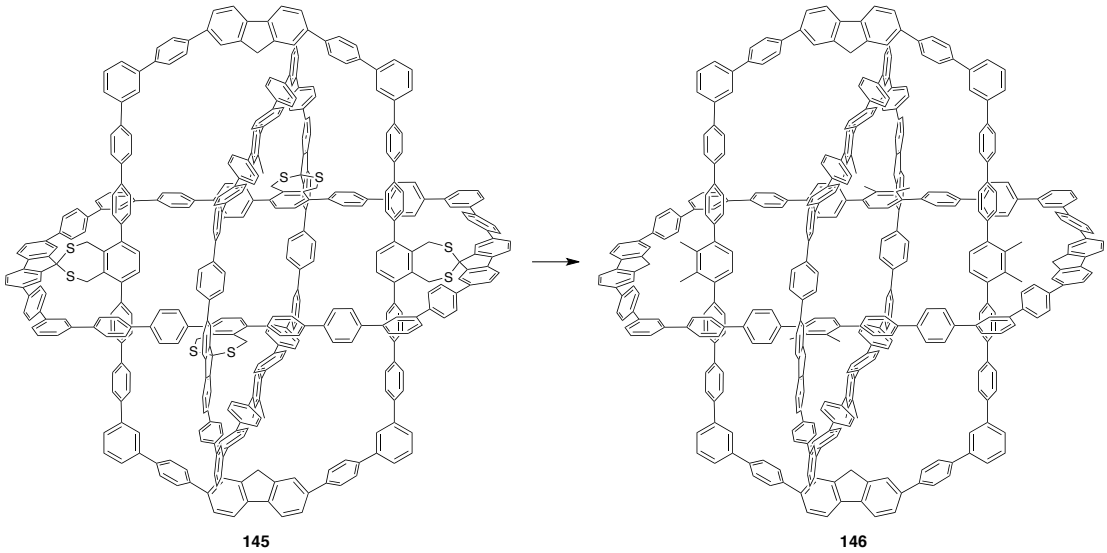

Scheme 5.1. *Full desulfurization of tetrathioketal* ***145*** *would lead to* T_h*-symmetric Borromean link* ***146****.*

Synthesis of polyaromatic structure **145** is likely to be limited by sparing solubility of precursors. This potential problem could be overcome by introducing solubilizing groups, which could easily be placed on the 4,4-biphenyl linkers connecting the benzothiepane units to the 2,7-bis(biphenyl)fluorene caps. Initial work focused on preparing precursors to compound **145** and did not attempt to introduce solubilizing features, as reactivity was considered to be more important than solubility at the onset of the project.

5.3.2. Retrosynthetic Analysis

Borromeate **145** can be disconnected by retro-cross-couplings to afford a templated two-ring compound **147** and a fluorene-based cap **148** (Scheme 5.2). Construct **147** can then be disconnected by the same retro-reactivity to give templated one-ring compound **149** and pre-templated cap **150**. Pre-templated cap **150** was expected to be easily synthetically accessible by using the methodologies developed for forming thioketals that were discussed in Chapter 4, section 4.2.3. Retro-Suzuki couplings of triflates were viewed as the most promising cross-coupling in the retrosynthesis, given the easy generation of triflates from alchohols, which can be appropriately protected in other steps of the synthesis.

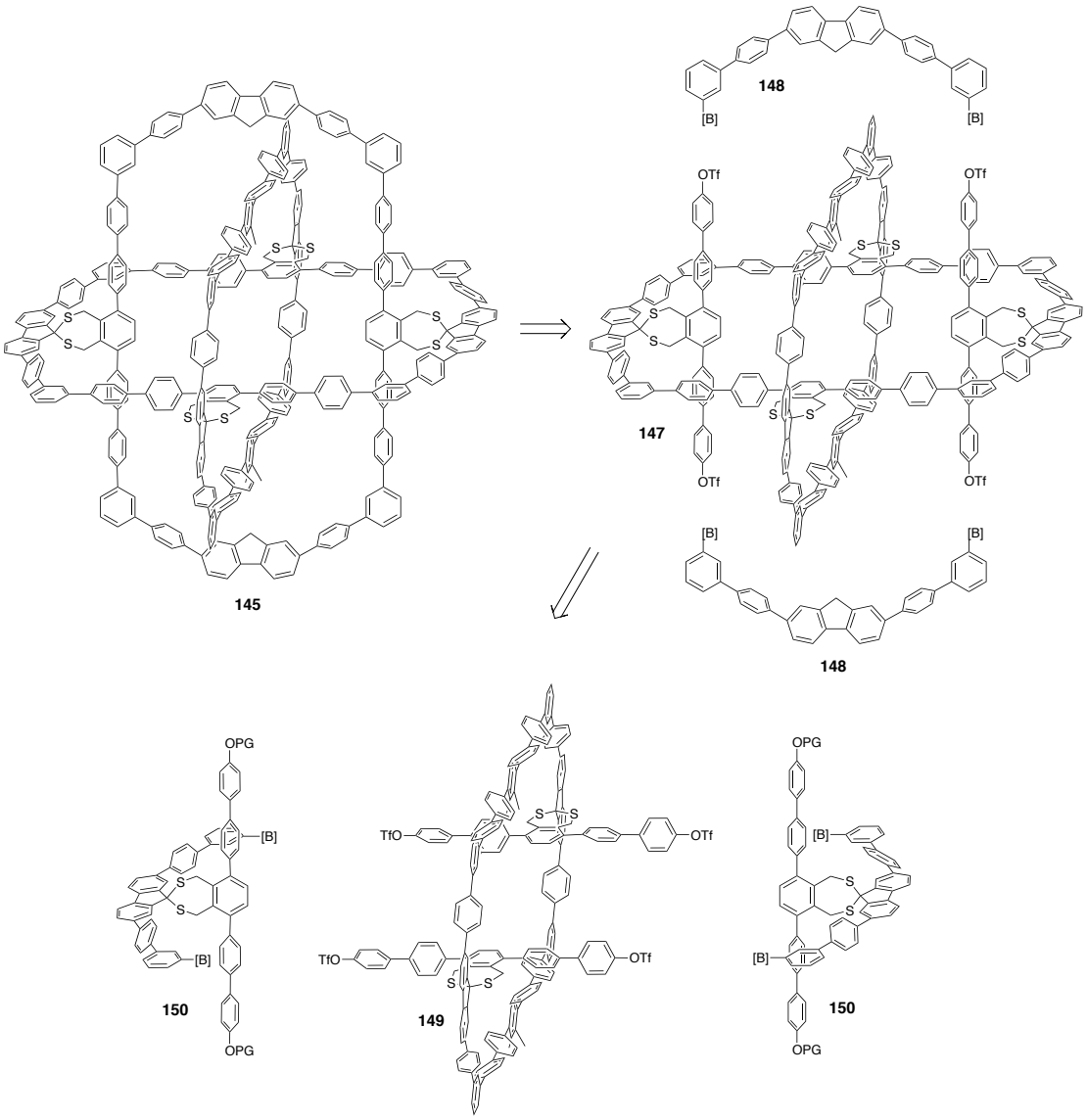

Scheme 5.2. *Retrosynthetic analysis of Borromeate **145** to templated one ring compound **149** and pre-templated cap **150**.*

Next, the retrosynthesis of templated macrocycle **149** must be considered (Scheme 5.3). Method A disconnects **149** to a quinquephenyl ditriflate **151** and pre-templated cap **150**. This method would require two rods and two caps to form macrocycle **149**. Method B disconnects **149** to pre-templated cap **150** and an extended pre-templated cap **152**, which can be disconnected to protected triflate **153** and **150**. Though Method B requires more steps, it was seen as the best option for initial synthetic studies

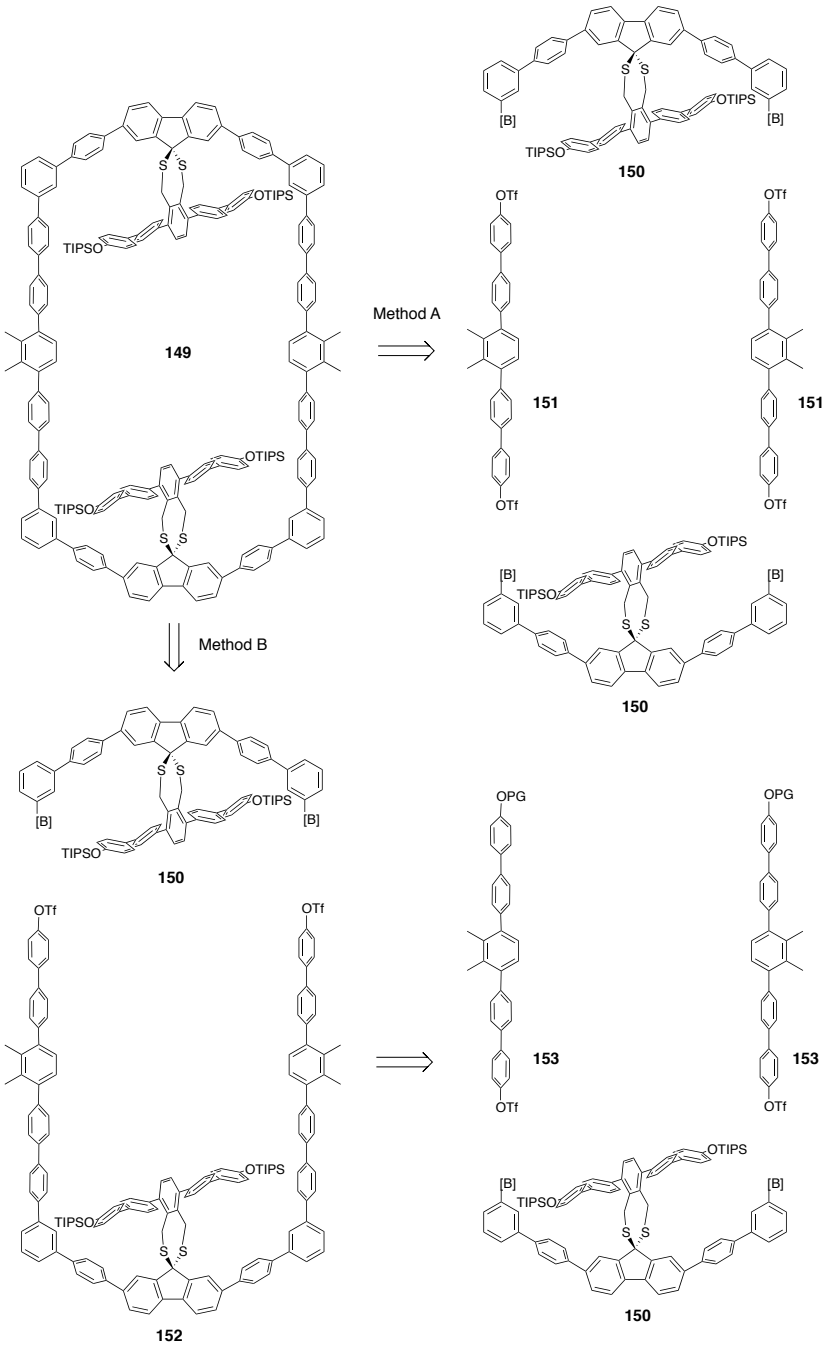

Scheme 5.3. *Retrosynthetic methods for templated macrocycle* ***149****.*

5.3.3. Synthesis of Building Blocks

As it is used at two critical points in the retrosynthesis, initial focus was placed on the synthesis of pre-templated cap **150** (Scheme 5.4), which could be made by a similar synthesis that was employed to generate **129** (p. 98). First, dibromofluorene **100** was treated with TIPS-protected biphenylzincate **154**, prepared *in situ* from the corresponding bromide,[240] under Negishi coupling conditions to afford protected

bis(biphenyl)fluorenone **155**. Initial studies showed that the deprotected diol is too insoluble to react with pivalyol anhydride. Since the bis(tetrabutylammonium) dialkoxide salt is soluble in CH_2Cl_2, a one-pot protecting group exchange was developed, which yielded pivaloyl-protected **156** in good yield.

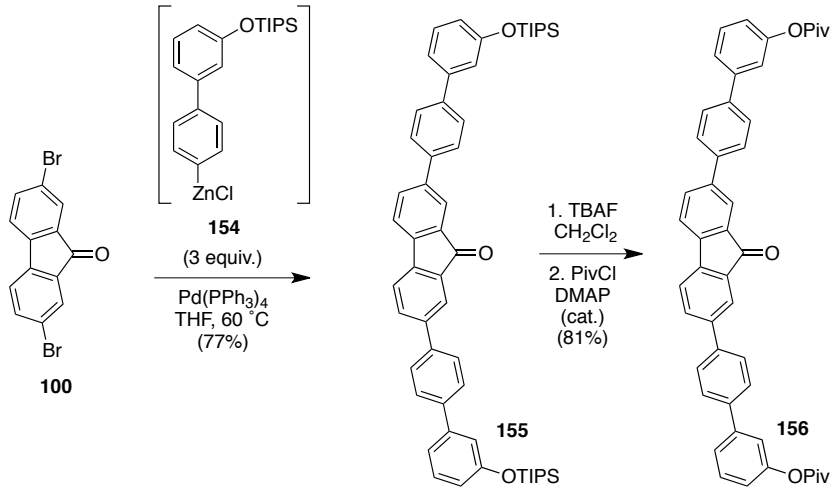

Scheme 5.4. *Synthesis of pivaloyl-protected cap* ***156****.*

Compound **156** was then subjected to thioketalization with a mixture of thiols **119** and **120**, to afford a mixture of compounds **157** and **158** (Scheme 5.5), which were not separated and used as a mixture in the following step. Negishi cross-coupling with biphenylzincate **159**, prepared from the corresponding bromide, afforded orthogonally protected pretemplated cap **160**.

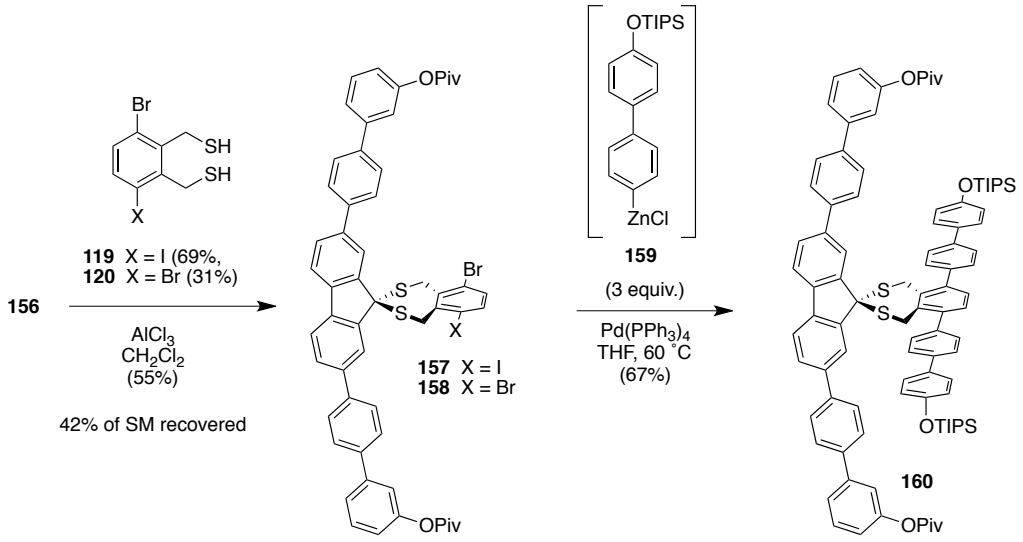

Scheme 5.5. *Synthesis of orthogonally protected pre-templated cap* ***160****.*

Compound **160** was then carried to pre-templated cap triflate **161** (Scheme 5.6). A high-yielding, selective deprotection of the pivaloyl group was accomplished by treating **160** with 4 equiv. of MeLi in ether, affording diol **162**, which was triflated to afford compound **161** in good yield.

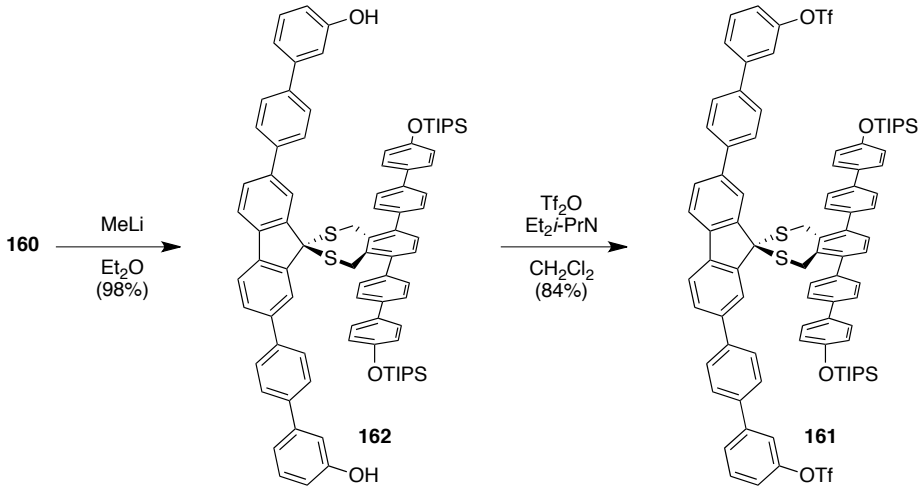

Scheme 5.6. *Synthesis of pre-templated cap containing triflates* ***161****.*

With pre-templated cap **161** in hand, attention turned to the synthesis of protected quinquephenyl triflate **153**. Negishi cross-coupling of **113** with zincate **159** at room temperature selectively coupled at the iodide to afford terphenyl **163** (Scheme 5.7). Deprotection of the TIPS groups and subsequent re-protection with a pivaloyl group gave compound **164** in good yield. Compound **164** was subjected to another Negishi cross-coupling with zincate **159**, at elevated temperature, to afford orthogonally protected quinquephenyl **165**. An initial attempt to transform the TIPS-protected alcohol unto a triflate in a one-pot reaction was performed. TBAF was added to **165** in THF and, after complete deprotection, triflic anhydride was added to the reaction mixture. Trace amounts of triflic acid catalyzed polymerization of THF and triflate **166** was obtained in only 11% yield, while the deprotected alcohol was recovered in 68% crude yield. Due to time restraints, this reaction was not optimized, though it would likely proceed smoothly in CH_2Cl_2.

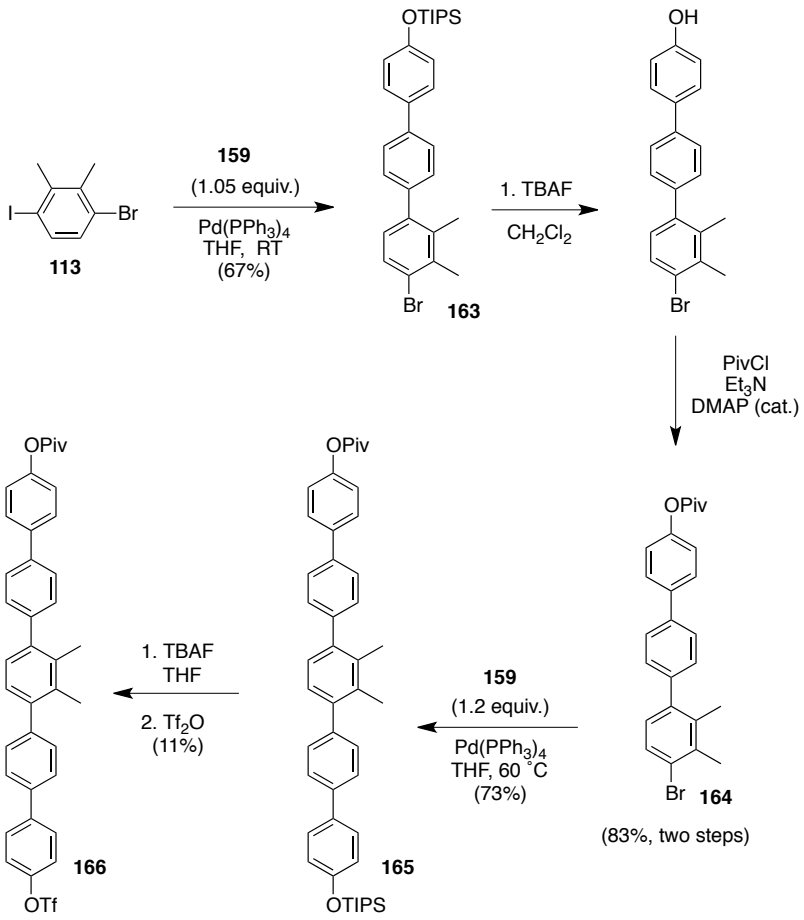

Scheme 5.7. Synthesis of protected quinquephenyl triflate ***166****.*

Unfortunately, the project only reached this point and no borylations of triflates or subsequent macrocyclizations were attempted. However, the syntheses of these building block serve as starting points for the generation of interlinked structures, including the Borromean link, using the thioketal templating motif.

5.3.4. Toward the Synthesis of a Thioketal-Templated Rotaxane

With well-established methods to obtain thioketals of fluorene in hand, attention shifted to the exploratin of smaller mechanically bonded systems using this template. As an initial test of the system, the synthesis of rotaxane **167** from dithioketal **168** was designed (Scheme 5.8). Dithioketal **168** can be retrosynthetically disconnected to tetra-protected alcohol **169**, which can be further disconnected by a retro cross-coupling to a difunctionalized construct **170**. Using the thioketalization strategies that have already been developed in this thesis, compound **170** could be disconnected to fluorenone **171** and difunctionalized tetrathiol **172**.

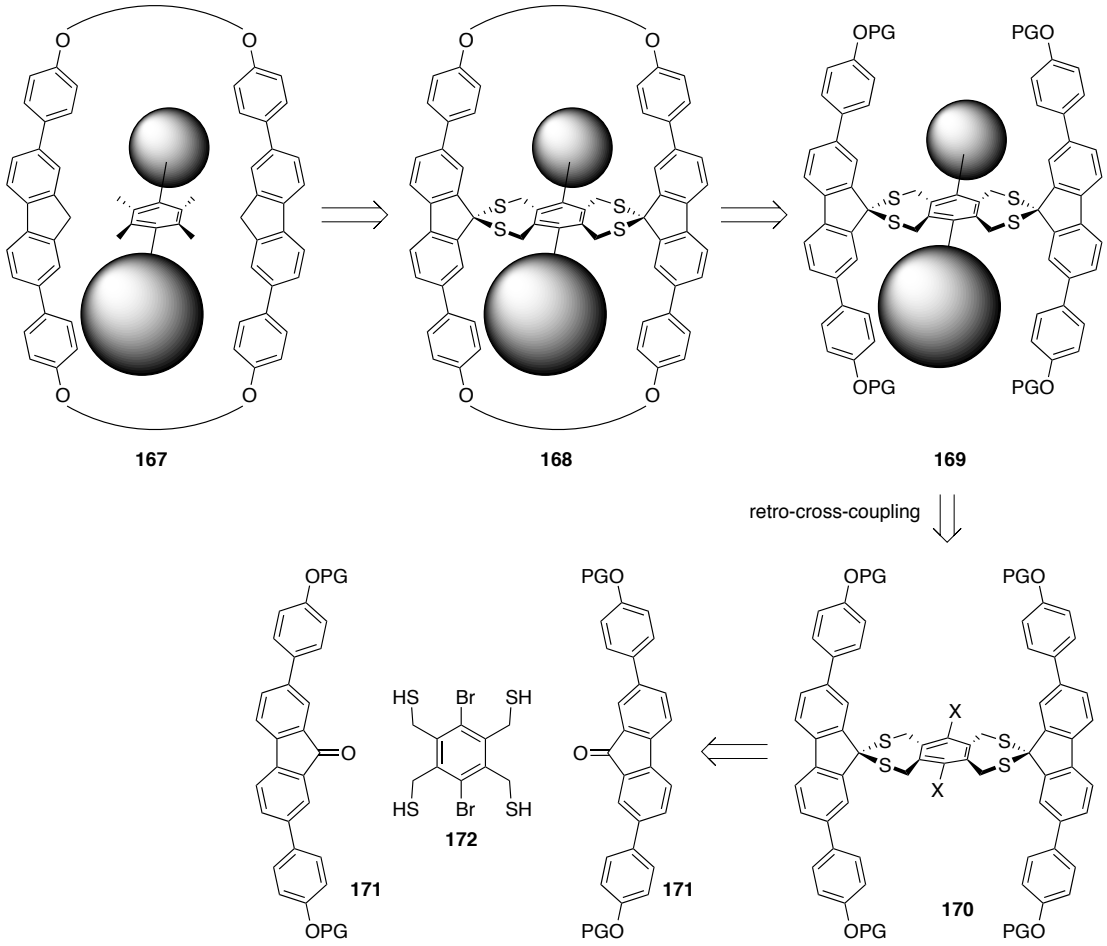

Scheme 5.8. *Schematic representation of a rotaxane* ***167*** *that could be generated using the thioketal-templating strategy.*

Synthesis of tetrathiol **172** was accomplished in three steps from durene (Scheme 5.9). First, durene was brominated using an iodine-catalyzed bromination method developed by Miller,[241] affording dibromodurene **173** Next, light-induced benzylic bromination was accomplished by treatment of **173** with bromine in CCl_4 and visible light, according to the procedure reported by Hopf,[242] yielding **174** Finally, compound **174** was subjected to standard thiolation, affording a mixture of partially thiolated species, out of which tetrathiol **172** could be obtained by recrystallization in 37% yield.

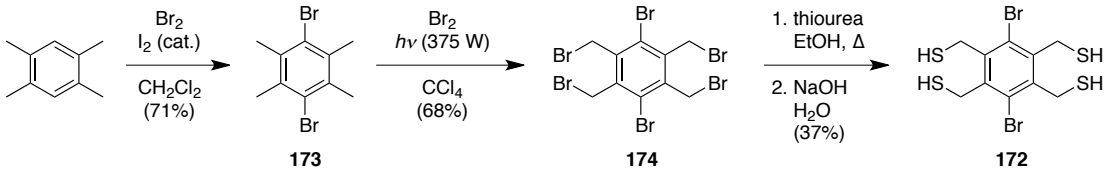

Scheme 5.9. *Synthesis of 3,6-dibromobenzene-1,2,4,5-tetramethanethol (**172**).*

Next, tetrathiol **172** was subjected to thioketalization conditions with two equivalents of protected fluorenone **105**. The thioketalization reaction was successful, affording compound **175**, Though the yield is rather low (Scheme 5.10). In order to install sterically bulky groups to serve as caps on the eventual dumbbell-shaped part of the rotaxane, a Sonogashira coupling with bulky alkyne **161** was attempted. After three days of stirring and heating, no conversion of **175** was observed. The failure of the Sonogashira reaction was likely due to the steric crowding of the alkyl bromides, severely reducing the rate of oxidative addition of this site. Optimization studies with palladium catalysts comprising smaller phosphine ligands may provide a solution to this issue.

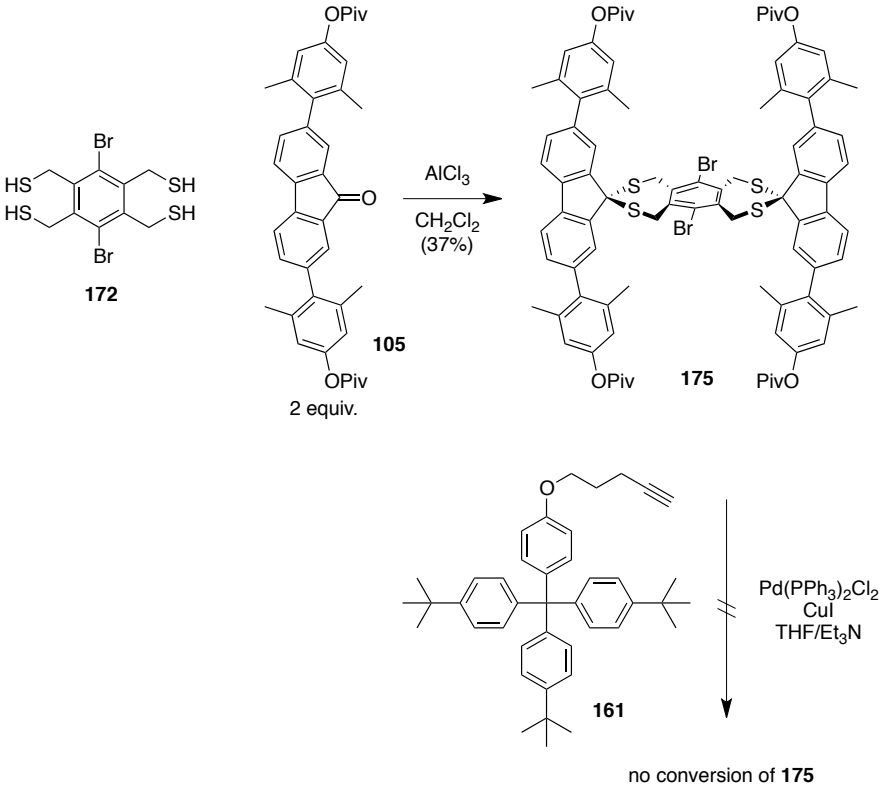

Scheme 5.10. *Synthesis of dithioketal **175** and attempted Sonogashira cross-coupling.*

5.4. Outlook

Fifteen years have past since Seeman's DNA nanotechnology approach yielded the first molecular Borromean link and eight years have past since Stoddart's elegant directed assembly of another. As several top research groups have continued to forge campaigns toward a stepwise synthesis of Borromean links, it is perhaps surprising that a successful example has not yet been reported. Siegel and Stoddart have both generated ring-in-ring complexes toward the eventual synthesis of molecular Borromean links, but positioning a part of the third ring in the proper location to form a templated two-ring system has failed so far in all cases, despite numerous, well thought out attempts.

There may be a multitude of reactions that will need to be run and wide variety of products that will need to be prepared to accomplish this goal. Perhaps a templated synthesis resembling those described in this synthesis, or another clever solution that has not been dreamed up yet, will provide true molecular Borromean links. The beauty and elegance of aesthetically pleasing topological objects, combined with the formidable, yet inspring, challenges in their syntheses, will continue to motivate chemists to assemble a variety of novel, interlocked knots and links well into the foreseeable future

SECTION THREE

Experimental Section

Chapter 6

Experimental Methods

6.1. General Remarks

Unless otherwise noted, all reactions were performed under nitrogen. Anhydrous THF and toluene was supplied from an Mbraun solvent purification system. $PdCl_2(PPh_3)_2$ was prepared according to the reported protocol.[243] Unless otherwise noted, commercially available reagents and solvents were used as received without further purification.

Analytical thin-layer chromatography was performed with Macherey–Nagel POLYGRAM SIL N-HR/UV_{254} or ALOX N/UV_{254}. Flash silica gel column chromatography was performed with Merck silica gel 60 (particle size 0.040–0.063 mm). Flash alumina column chromatography was performed with deactivated (5% water) Fluka alumina (particle size 0.05–0.15 mm, pH 7.0±0.5). Melting points were recorded on a Büchi B-540 melting point apparatus. For characterization purposes, proton nuclear magnetic resonance (^{1}H-NMR) spectra were all recorded on Bruker instruments (AV-300 and ARX-300 at 300 MHz, AV2-400 at 400 MHz, and AV-500 at 500 MHz). Variable-temperature ^{1}H-NMR experiments were performed on a Bruker DRX-500 Ultrashield spectrometer, equipped with a Bruker BVTE 3900 temperature insulation system, at 500 MHz. Chemical shifts are reported in ppm relative to $CHCl_3$ (7.26) and DMSO-d_6 (2.50). Multiplicity is indicated by one or more of the following: s (singlet); d (doublet); t (triplet); dd (doublet of doublets); td (triplet of doublets); m (multiplet); br (broad). Carbon-13 nuclear magnetic resonance (^{13}C-NMR) spectra were recorded on Bruker instruments (ARX-300 at 75 MHz, AV2-400 at 100 MHz, and AV-500 at 125 MHz). Chemical shifts are reported relative to $CDCl_3$ (δ 77.2) or DMSO-d_6 (δ 39.5). Fluorine-19 nuclear magnetic resonance (^{19}F-NMR) spectra were recorded on Bruker instruments (AV-300 at 282 MHz, AV2-400 at 376 MHz). Chemical shifts are repored in ppm relative to CCl_3F (δ 0) as either an internal standard or an external standard in $CDCl_3$. Infrared spectra

reported as KBr pellets were recorded on a Perkin Elmer Spectrum One (PE); measurements reported as "neat" were recorded on a Jasco FT/IR-4100.

6.2. Experimental Procedures for Section One

6.2.1. Synthetic Procedures

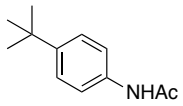

4-*tert*-Butylacetanilide (**57**): To a solution of 4-*tert*-butylaniline (**54**) (40.00 g, 0.268 mol) in dichloromethane (400 mL) was slowly added acetic anhydride (28 mL, 0.30 mol) at 0° C. The reaction mixture was stirred for 30 min under air, during which colorless plates of product formed. The reaction mixture was concentrated and hexane was added. The precipitate was filitered and washed with hexane, giving **57** as colorless plates (49.90 g, 97%).

Rf 0.34 (alumina, CH_2Cl_2);

mp 173.1–173.3 °C;

^{1}H NMR (400 MHz, $CDCl_3$, δ) 7.41 (d, 2H, ^3J = 8.8 Hz), 7.33 (d, 2H, ^3J = 8.8 Hz), 2.16 (s, 3H), 1.30 (s, 9H);

^{13}C NMR (100 MHz, $CDCl_3$, δ) 168.8, 147.4, 135.5, 125.9, 120.1, 34.5, 31.5, 24.6;

IR (KBr) 3290*s*, 3253*s*, 3187*s*, 3121*s*, 3060*m*, 2961*s*, 2904*m*, 2865*m*, 2802*w*, 1902*w*, 1689*s*, 1667*s*, 1610*s*, 1548*s*, 1517*s*, 1464*m*, 1402*s*, 1377*s*, 1361*m*, 1324*s*, 1305*m*, 1268*s*, 1202*w*, 1188*m*, 1113*w*, 1038*w*, 1019*m*, 1010*m*, 970*m*, 943*w*, 837*s*, 828*m*, 760*s*, 733*m*, 708*w*, 603*m*, 554*s*, 517*w* cm^{-1};

LRMS (ESI) m/z = 214.0 ($M+Na^+$).

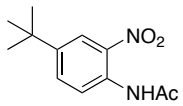

4-*tert*-Butyl-2-nitroacetanilide (**58**): To a stirring mixture of acetic acid (190 mL, 3.3 mol) and acetic anhydride (160 mL, 1.7 mol) at 0° C was added nitric acid (99.5% reagent grade, 63 g, 41 mL, 1.1 mol). After 5 min, compound **57** (20.04 g, 0.105 mol) was added to this mixture in portions. The reaction mixture was stirred at 0° C under air for 30 min. Water was slowly added to quench the reaction, which was kept in an ice bath, until the addition of water no longer turned the reaction mixture dark. *Caution!* Addition of water causes the mixture to heat significantly. In portions, the quenched reaction mixture was then subjected to further additions of water, which caused a yellow precipitate to form. The precipitate was washed with water and dried *in vacuo* and recrystallized in EtOH to give **58** as yellow crystals (17.88 g, 72%).

Rf 0.76 (alumina, CH_2Cl_2);

mp 107.6–107.9 °C;

^{1}H NMR (400 MHz, $CDCl_3$, δ) 10.20 (br s, 1H), 8.64 (d, 1H, ^3J = 8.8 Hz), 8.18 (d, 1H, ^4J = 2.4 Hz), 7.68 (dd, 1H, ^3J = 8.8 Hz, ^4J = 2.4 Hz), 2.28 (s, 3H), 1.34 (s, 9H);

^{13}C NMR (125 MHz, $CDCl_3$, δ) 169.2, 147.1, 136.4, 133.6, 132.5, 122.3, 122.2, 34.8, 31.2, 25.7;

IR (KBr) 3343*s*, 3112*w*, 3066*w*, 2966*s*, 2908*m*, 2872*m*, 1980*w*, 1794*w*, 1705*s*, 1624*m*, 1583*s*, 1543*s*, 1518*s*, 1454*s*, 1397*s*, 1364*s*, 1340*s*, 1283*s*, 1266*s*, 1230*m*, 1204*w*, 1161*m*, 1119*w*, 1079*m*, 1035*w*, 997*w*, 899*m*, 856*m*, 828*w*, 759*m*, 738*w*, 691*m*, 579*m*, 543*w*, 521*w*, 426*w* cm^{-1};

LRMS (EI) m/z = 236.1 (14.0%, $[M]^+$), 221.1 (7.2%, $[M–CH_3]^+$), 194.1 (25.4%, $[M–COCH_3]^+$), 179.1 (100%, $[M–C(CH_3)_3]^+$), 133.1 (13.4%, $[M–(NO_2+NHAc)]^+$), 43.0 (9.2%, $[COCH_3]^+$).

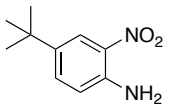

4-*tert*-Butyl-2-nitroaniline (**58**): To a solution of **58** (13.90 g, 59 mmol) in EtOH (20 mL), at reflux, were slowly added KOH pellets (3.60 g, 65 mmol). The reaction

mixture was stirred at reflux for 15 min under air then poured into 150 mL of a stirring mixture of ice and water. The resulting precipitate was filtered, washed with water, and dried *in vacuo* to yield **20** as an orange solid (11.4 g, 100%).

Rf 0.72 (alumina, CH_2Cl_2); mp 106.5–106.7 °C;

^{1}H NMR (400 MHz, $CDCl_3$, δ) 7.43 (dd, 1H, ^3J = 8.8, ^4J = 2.4 Hz), 6.77 (d, 1H, ^3J = 8.8 Hz), 5.97 (br s, 2H), 1.28 (s, 9H);

^{13}C NMR (100 MHz, $CDCl_3$, δ) 142.8, 140.5, 134.0, 132.0, 121.9, 118.8, 34.2, 31.2;

IR (KBr) 3475*s*, 3355*s*, 3181*m*, 2958*s*, 2866*m*, 1772*w*, 1637*s*, 1595*s*, 1562*s*, 1512*s*, 1458*s*, 1404*s*, 1366*s*, 1341*s*, 1290*s*, 1239*s*, 1203*s*, 1179*s*, 1118*s*, 1089*s*, 916*m*, 887*m*, 824*s*, 769*m*, 723*m*, 659*m*, 574*m*, 458*m* cm^{-1};

HRMS (ESI) Calcd for $C_{10}H_{14}N_2O_2$ (M) 194.1055, found 194.1056.

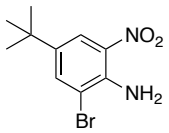

2-Bromo-4-*tert*-butyl-6-nitroaniline (**53**): To a solution of **59** (11.51 g, 59 mmol) in acetic acid (90 mL) was slowly added bromine (3.2 mL, 9.9 g, 62 mmol) at room temperature. The mixture was stirred for 30 min at room temperature under air then poured into a stirring mixture of ice and water. The orange precipitate was then filtered and dried *in vacuo* to yield **53** as an orange solid (15.81 g, 98%).

Rf 0.72 (alumina, CH_2Cl_2);

mp 73.2–73.5 °C;

^{1}H NMR (400 MHz, $CDCl_3$, δ) 8.11 (d, 1H, ^4J = 2.4 Hz), 7.74 (d, 1H, ^4J = 2.4 Hz), 6.47 (br s, 2H), 1.29 (s, 9H);

^{13}C NMR (100 MHz, $CDCl_3$, δ) 140.30, 140.27, 137.1, 132.6, 122.2, 112.2, 34.4, 31.2;

IR (KBr) 3479*s*, 3369*s*, 3076*w*, 2967*s*, 2948*s*, 2905*m*, 2866*m*, 1838*w*, 1808*w*, 1620*s*, 1576*s*, 1538*s*, 1521*s*, 1506*s*, 1457*s*, 1443*m*, 1396*m*, 1362*m*, 1344*s*, 1324*m*, 1248*s*, 1138*s*, 1091*s*, 1022*m*, 917*m*, 892*m*, 847*m*, 822*m*, 764*m*, 732*m*, 721*m*, 622*m*, 517*w*, 461*w*, 421*w* cm^{-1};

HRMS (ESI) Calcd for $C_{10}H_{13}Br_1N_2O_2$ (M) 272.0160, found 272.0160.

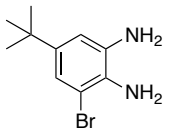

3-Bromo-5-*tert*-butylbenzene-1,2-diamine (**60**): To a solution of **53** (10.55 g, 39 mmol) in ethanol (50 mL) and concentrated HCl (12 mL) was added anhydrous $SnCl_2$ (36.67 g, 193 mmol). The reaction stirred under nitrogen at 60 °C for 16 h. Water was added to the reaction mixture and this mixture was poured into a stirring, aqueous solution of NaOH (3 mol/L), resulting in the formation of a white precipitate. Saturated, aqueous $NaHCO_3$ solution was added until the pH of the solution reached ~ 8. CH_2Cl_2 was added and the mixture was stirred for an additional 5 min. The fine, white precipitate was removed by filtration through celite in a large Büchner funnel. The precipitate was repeatedly washed with CH_2Cl_2. The combined filtrate was separated and the aqueous phase was extracted with CH_2Cl_2. The combined organic phases were washed with brine, dried under Na_2SO_4, and concentrated to give **60** as a white solid. (9.00 g, 96%). *Note:* the product is unstable in air and decomposes to a brown solid over days (decomposition occurs much faster in solution). If product is impure, alumina column chromatography (hexane/EtOAc = 9/1 → 5/5) affords pure product.

Rf 0.11 (alumina, CH_2Cl_2);

mp 95.8–96.8 °C;

^{1}H NMR (400 MHz, $CDCl_3$, δ) 6.98 (d, 1H, ^4J = 2.0 Hz), 6.68 (d, 1H, ^4J = 2.0 Hz), 3.69 (br s, 2H), 3.47 (br s, 2H), 1.25 (s, 9H);

^{13}C NMR (100 MHz, $CDCl_3$, δ) 144.1, 135.3, 130.8, 120.5, 113.3, 111.5, 34.3, 31.6;

IR (KBr) cm^{-1}; 3422*s*, 3372*s*, 3325*s*, 3234*s*, 2961*s*, 2904*s*, 2867*s*, 1743*w*, 1623*s*, 1567*s*, 1498*s*, 1446*m*, 1419*s*, 1390*m*, 1360*s*, 1296*s*, 1238*s*, 1204*m*, 1127*w*, 1100*m*, 1066*m*, 1021*m*, 955*m*, 873*s*, 840*s*, 771*s*, 706*s*, 649*s*, 526*m*, 427*w*;

HRMS (ESI) Calcd for $C_{10}H_{15}Br_1N_2$ ($M+H^+$) 243.0497, found 243.0492.

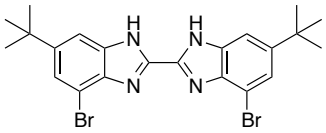

4,4'-Dibromo-6,6'-di-*tert*-butyl-2,2'-bibenzimidazole (**52**): To a solution of **60** (2.78 g, 11.4 mmol) in MeOH (50 mL) was added methyl 2,2,2-trichloroacetimidate (0.71 mL, 1.0 g, 5.7 mmol), followed by concd. HCl (0.05 mL) at 0 °C under N_2, and the obtained mixture was stirred at room temperature. To this mixture were added three portions of K_2CO_3 (393 mg, 2.8 mmol; 786 mg, 5.6 mmol; 786 mg, 5.6 mmol) at intervals of 3 h, 3 h and 15 h. The reaction mixture was stirred another 24 h after the final addition, and water and Et_2O were then added. The resulting precipitate was collected, washed with water and Et_2O, and dried *in vacuo* to give **52** as a white solid (2.53 g, 88%).

Rf 0.15 (streaks) (silica, CH_2Cl_2);

mp >330 °C;

^{1}H NMR (400 MHz, DMSO-d_6, δ) 7.54 (d, 1H, ^4J = 1.4 Hz), 7.51 (d, 1H, ^4J = 1.4 Hz), 1.36 (s, 18H);

^{13}C NMR (100 MHz, DMSO-d_6, δ) 148.4, 143.6, 140.0, 135.6, 123.5, 111.8, 107.7, 34.7, 31.3;

IR (KBr) 3081*s*, 2963*s*, 2868*s*, 1722*w*, 1625*m*, 1567*s*, 1466*m*, 1435*m*, 1388*s*, 1329*s*, 1298*m*, 1267*m*, 1236*m*, 1202*m*, 1097*w*, 1025*w*, 979*m*, 949*m*, 858*s*, 836*w*, 759*m*, 656*m*, 628*m*, 513*m*, 441*w* cm^{-1};

HRMS (ESI) Calcd for $C_{22}H_{24}Br_2N_4Na$ ($M+Na^+$) 525.0265, found 525.0261.

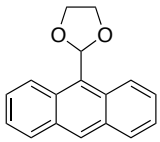

2-(Antracene-9-yl)-1,3-dioxolane (**61**): To a solution of anthracene-9-carboxaldehyde (**55**) (10.04 g, 48.5 mmol) in benzene (50 mL) was added ethylene glycol (5.4 mL, 6.0 g, 97 mmol) and *p*-toluenesulfonic acid (20 mg). A Dean–Stark trap was attached to the round-bottom flask containing the reaction mixture, which was then stirred at reflux for 48 h. The reaction mixture was cooled to RT and water was added. The resulting precipitate was filtered, washed with water and dried *in vacuo* to afford **61** as a yellow solid (11.30 g, 93%).

Rf 0.29 (silica, 5:5 CH_2Cl_2–hexane);

mp 97.9–99.0 °C;

^{1}H NMR (400 MHz, $CDCl_3$, δ) 8.30 (d, 2H, ^3J = 9.2 Hz), 8.27 (s, 1H), 7.76 (d, 2H, ^3J = 8.4 Hz), 7.32–7.19 (m, 4H), 4.40–4.21 (m, 4H), 4.06–4.00 (m, 4H);

^{13}C NMR (100 MHz, $CDCl_3$, δ) 131.6, 131.0, 130.5, 129.2, 126.3, 124.9, 124.4, 101.8, 65.4;

IR (neat) 3052*w*, 2952*w*, 2886*m*, 1671*w*, 1624*w*, 1527*w*, 1445*w*, 1308*w*, 1257*w*, 1189*w*, 1161*w*, 1108*s*, 1032*s*, 963*s*, 894*m*, 730*s*, 617*m*, 547*w* cm^{-1};

LRMS (EI) m/z = 206 (100%, $[M–C_2H_2O]^+$), 178 (99.6%, $[M–C_3H_4O_2]^+$), 151 (20%), 88 (22%, $[C_7H_4]^+$), 76 (17%, $[C_6H_4]^+$).

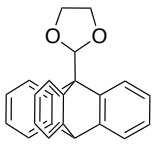

2-(Triptycene-9-yl)-1,3-dioxolane (**62a**): A dilute solution of **61** (5.02 g, 20 mmol) in CH_2Cl_2 (500 mL) heated to reflux while stirring. Separate solutions of anthranilic acid (9.05 g, 66 mmol) in acetone (40 mL) and *iso*-pentyl nitrite (8.0 mL, 7.0 g, 60 mmol) in CH_2Cl_2 (40 mL) were each added simultaneously and at the same rate over 6 h by a

double syringe pump. Following the addition of reagents, the reaction mixture was allowed to stir at reflux for an additional 16 h. The solvent was then removed *in vacuo* and the residue was subjected to column chromatography (silica, 9:1→ 5:5 hexane–CH_2Cl_2). Removal of CH_2Cl_2 from the column fractions containing the product (rotory evaporator, 40 °C, 600–400 mbar) yielded fine, colorless crystals of **62a** (3.55 g, 54%).

Rf 0.31 (silica, 5:5 CH_2Cl_2–hexane);

mp 287.1–287.4 °C;

(*Note*: NMR spectra are complicated by slow rotation of the dioxolane ring around the Triptycene group at 300 K)

^{1}H NMR (400 MHz, $CDCl_3$, δ) 7.67 (d, 2H, ^2J = 6.8 Hz), 7.58–7.56 (m, 1H), 7.38–3.36 (m, 3H), 7.04–6.97 (m, 6H), 5.35 (s, 1H), 4.52–4.46 (m, 2H), 4.41–4.34 (m, 2H);

^{13}C NMR (100 MHz, $CDCl_3$, δ) 146.70, 146.67, 144.4, 141.8, 125.4, 125.12, 125.09, 124.9, 124.8, 123.7, 123.51, 123.48, 104.4, 65.2, 56.4, 54.8;

IR (neat) 3062*w*, 3036*w*, 2894*w*, 1457*m*, 1397*w*, 1264*w*, 1140*m*, 1108*s*, 1043*m*, 1002*m*, 945*m*, 911*m*, 764*m*, 740*s*, 703*m*, 683*w*, 639*s*, 618*s*, 596*w*, 480*m* cm^{-1};

LRMS (EI) m/z = 326 (95%, $[M]^+$), 265 (46%, $[M–C_2H_3O_2]^+$), 253 (100%, $[M–C_3H_5O_2]^+$), 126 (20%), 73 (74%, $[C_3H_5O_2]^+$).

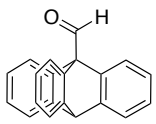

Triptycene-9-carboxaldehyde (**63a**): To a stirring mixture of **62a** (3.10 g, 9.5 mmol) in glacial acetic acid (150 mL) was added concd. HCl (20 mL). The mixture was stirred at reflux for 18 h, and then allowed to cool to RT and poured into water. The resulting precipitate was filtered, washed with water, and dried *in vacuo* to afford **63a** as a white solid (2.54 g, 95%).

Rf 0.43 (silica, 5:5 CH_2Cl_2–hexane);

mp 243.0–243.8 °C;

^{1}H NMR (400 MHz, $CDCl_3$, δ) 11.22 (s, 1H) 7.63–7.61 (m, 3H), 7.44–7.42 (m, 3H), 7.08–7.04 (m, 6H), 5.40 (s, 1H);

^{13}C NMR (100 MHz, $CDCl_3$, δ) 201.2, 146.0, 142.8, 126.0, 125.4, 124.2, 122.6, 61.0, 54.4;

IR (neat) 3069*w*, 3020*w*, 2958*w*, 2834*w*, 1730*s*, 1453*s*, 1131*w*, 749*s*, 626*m*, 612*m*, 479*m* cm^{-1};

LRMS (EI) m/z = 282 (75%, $[M]^+$), 253 (100%, $[M–CHO]^+$), 126 (28%).

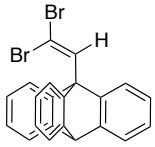

9-(2,2-Dibromoethen-1-yl)triptycene (**64a**) : To a solution of tetrabromomethane (5.46 g, 16 mmol) in CH_2Cl_2 (10 mL) was slowly added triphenylphosphine (8.57 g, 33 mmol) at 0 °C. The reaction mixture was allowed to stir for 15 min and then a solution of **63a** (2.32 g, 8.2 mmol) in CH_2Cl_2 (30 mL) was then added. The ice bath was removed and the reaction mixture was allowed to stir at RT for 18 h. The reaction was quenched with water and the phases were separated. The aqueous phase was extracted with CH_2Cl_2 and the combined organic phases were washed with sat. NaCl solution, dried over Na_2SO_4, and concentrated. The resulting residue was purified by column chromatography (silica, 9:1 hexane–CH_2Cl_2) to afford **64a** as a white solid (2.36 g, 66%).

Rf 0.65 (silica, 5:5 CH_2Cl_2–hexane);

mp 215.6–216.2 °C;

^{1}H NMR (400 MHz, $CDCl_3$, δ) 8.10 (s, 1H) 7.47–7.45 (m, 3H), 7.42–7.40 (m, 3H), 7.04–7.02 (m, 6H), 5.38 (s, 1H);

^{13}C NMR (100 MHz, $CDCl_3$, δ) 145.5, 142.4, 132.4, 125.7, 124.9, 124.8, 124.2, 96.5, 58.4, 54.4;

IR (neat) 3069*w*, 3015*w*, 2958*w*, 1607*w*, 1573*w*, 1457*m*, 1263*w*, 929*w*, 865*w*, 788*s*, 767*m*, 737*s*, 704*m*, 635*m*, 612*m*, 592*m*, 556*w*, 494*m*, 477*w* cm^{-1};

LRMS (EI) m/z = 440 (9%, $[M(^{81}Br_2)]^+$), 438 (17% $[M(^{81}Br^{79}Br)]^+$), 436 (9%, $[M(^{79}Br_2)]^+$), 278 (100%, $[M–(Br_2)]^+$, 252 (12%, $[M–C_2H_2Br_2]^+$, 138 (30%).

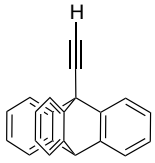

9-Ethynyltriptycene (**51a**): To a solution of **64a** (0.99 g, 2.3 mmol) in THF (5 mL), cooled to -78 ºC, was slowly added *n*-BuLi (1.6 mol/L in hexane, 2.9 mL, 4.6 mmol). The reaction mixture was warmed to RT and stirred for 90 min. Water was then added and the phases were separated. The aqueous phase was extracted with CH_2Cl_2 and the combined organic phases were washed with sat. NaCl solution, dried over Na_2SO_4, and concentrated, **51a** as colorless crystals (624 mg, 99%).

Rf 0.64 (silica, 5:5 CH_2Cl_2–hexane);

mp 239.2–240.5 °C;

1H NMR (500 MHz, $CDCl_3$, d) 7.75 (dd, 3H, 3J = 7.0 Hz, ^{4}J = 1.5 Hz), 7.39 (dd, 3H, 3J = 7.0 Hz, 4J = 1.5 Hz), 7.05 (quint. d, 6H, 3J = 7.0 Hz, ^{4}J = 1.5 Hz), 5.42 (s, 1H), 3.28;

13C NMR (100 MHz, $CDCl_3$, d) 144.5, 144.1, 125.9, 125.4, 123.6, 122.5, 80.7, 78.6, 53.4, 53.1;

IR (neat) 3298*w*, 3288*w*, 3069*w*, 2963*w*, 1454*s*, 1291*w*, 1265*w*, 1184*w*, 1025*w*, 859*w*, 743*s*, 700*w*, 641*s*, 607*m*, 481*m*, 442w cm^{-1};

LRMS (EI) m/z = 278 (100%, $[M]^+$), 138 (37%).

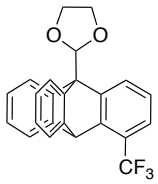

2-[4-(Trifluoromethyl)triptycene-9-yl]-1,3-dioxolane (**62b**): A dilute solution of **61** (1.14 g, 4.4 mmol) in CH_2Cl_2 (100 mL) was stirred and heated to reflux. A solution of 3-(trifluoromethyl)anthranilic acid (3.00 g, 66 mmol) in acetone (20 mL) and a solution of *iso*-pentyl nitrite (1.8 mL, 1.6 g, 13 mmol) in CH_2Cl_2 (20 mL) were each added simultaneously over 5 h by a double syringe pump. Following the addition of reagents, the reaction mixture was allowed to stir at reflux for an additional 16 h. The solvent was then removed *in vacuo* and the residue was subjected to column chromatography (silica, 9:1→ 8:2 hexane–CH_2Cl_2. Crystallization from a mixture of hexane–CH_2Cl_2 afforded **62b** as colorless crystals (565 mg, 32%).

Rf 0.37 (silica, 5:5 CH_2Cl_2–hexane);

mp 219.7–220.1 °C;

(*Note*: NMR spectra are complicated by slow rotation of the dioxolane ring around the Triptycene group)

^{1}H NMR (400 MHz, $CDCl_3$, δ) 7.85 (d, 0.67H, ^3J = 8.0 Hz), 7.76 (d, 0.33H ^3J = 7.8 Hz), 7.69–7.67 (m, 1.33H) 7.59–7.56 (m, 0.67H), 7.43–7.40 (m, 2H), 7.28 (d, 1H, ^3J = 7.9 Hz), 7.12–7.00 (m, 5H), 6.36 (s, 0.33H), 6.34 (s, 0.67H), 5.85 (br s, 1H), 4.54–4.50 (m, 2H), 4.40–4.35 (m, 2H)

^{13}C NMR (100 MHz, $CDCl_3$, δ) 146.4, 145.32, 145.12, 145.07, 145.05, 144.4, 143.83, 143.78, 141.3, 128.23, 126.9, 125.8, 125.54, 125.53, 125.49, 125.30, 124.93 (q, $J_{C,F}$ = 32 Hz), 124.87, 124.8, 124.64 (q, $J_{C,F}$ = 272 Hz), 124.54 (q, $J_{C,F}$ = 272 Hz), 124.54, 124.2, 124.1, 123.48, 123.46, 123.3, 123.2, 121.8 (q, $J_{C,F}$ = 5.0 Hz), 121.6 (q, $J_{C,F}$ = 5.0 Hz), 103.9, 65.16, 65.14, 65.07, 56.2, 56.0, 51.0, 50.9 ;

^{19}F NMR (282 MHz, $CDCl_3$, δ) –59.47 (s, 1F), –59.54 (s, 2F);

IR (neat) 3067*w*, 2958*w*, 2893*w*, 2765*w*, 1600*w*, 1460*w*, 1437*w* 1404*w*, 1323*m*, 1300*w*, 1265*w*, 1153*m*, 1108*s*, 1092*s*, 1073*m*, 1046*m*, 1002*m*, 940*m*, 921*w*, 802*m*, 761*m*, 735*s*, 704*m*, 680*m*, 656*w*, 638*m*, 621*m*, 582*w*, 500*w*, 487*m*, 454*w* cm^{-1};

MS (EI, m/z) 394.0 (84, $[M]^+$), 350.0 (13), 333.0 (22), 321.0 (49), 252.0 (43), 126.0 (13), 73.0 (100), 45.0 (11);

HRMS (EI) Calcd for $C_{24}H_{17}F_3O_2$ (M) 394.1181, found 394.1178.

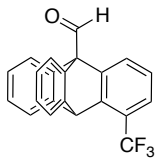

4-(Trifluoromethyl)triptycene-9-carboxaldehyde (**63b**): To a stirring mixture of **62b** (402 mg, 1.0 mmol) in glacial acetic acid (20 mL) was added concd. HCl (2.5 mL). The mixture was stirred at reflux for 15 h, then allowed to cool to RT and poured into water. The resulting precipitate was filtered, washed with water, and dried *in vacuo* to afford **63b** as a white solid (333 mg, 93%).

Rf 0.47 (silica, 5:5 CH_2Cl_2–hexane);

mp 174.7–175.2 °C;

^{1}H NMR (500 MHz, $CDCl_3$, δ) 11.22 (s, 1H), 7.88 (d, 1H, ^3J = 7.7 Hz), 7.62–7.60 (m, 2H), 7.50–7.48 (m, 2H), 7.34 (d, 7.9 Hz), 7.15–7.07 (m, 5H), 5.90 (s, 1H);

^{13}C NMR (125 MHz, $CDCl_3$, δ) 200.4, 145.0, 144.5, 142.5, 126.5, 126.1, 125.9, 125.8 (q, $J_{C,F}$ = 31.0 Hz) 125.3, 124.8, 124.5 (q, $J_{C,F}$ = 272 Hz) 122.6, 122.4 (q, $J_{C,F}$ = 5.0 Hz), 60.8, 50.9 (d, J = 1.9 Hz);

19F NMR (282 MHz, $CDCl_3$, δ) –60.00;

IR (neat) 3071*w*, 2848*w*, 2744*w*, 1732*m*, 1600*w*, 1458*m*, 1436*m*, 1324*s*, 1295*m*, 1266*w*, 1156*s*, 1116*s*, 1093*s*, 1060*m*, 803*w*, 741*m*, 683*w*, 631*m*, 619*m*, 483*m* cm^{-1};

MS (EI, m/z) 350.0 (72, $[M]^+$), 333.0 (16), 321.0 (76), 301 (14), 281 (33), 252 (100), 250 (24), 126.0 (28), 113 (13);

HRMS (EI) Calcd for $C_{22}H_{13}F_3O_2$ (M) 350.0918, found 350.0914.

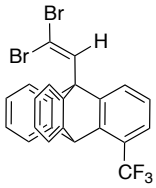

9-(2,2-Dibromoethen-1-yl)-4-(trifluoromethyl)triptycene (**64b**): To a solution of tetrabromomethane (569 mg, 1.71 mmol) in CH_2Cl_2 (4 mL) was slowly added triphenylphosphine (898 mg, 3.43 mmol) at 0 °C. The reaction mixture was allowed to stir for 15 min and a solution of **63b** (274 mg, 0.86 mmol) in CH_2Cl_2 (3 mL) was then added. The ice bath was removed and the reaction mixture was allowed to stir at RT for 17 h. The reaction was quenched with water and the phases were separated. The aqueous phase was extracted with CH_2Cl_2 and the combined organic phases were washed with sat. NaCl solution, dried over Na_2SO_4, and concentrated. The resulting residue was purified by column chromatography (silica, 9:1 hexane–CH_2Cl_2) to afford **64b** as a white solid (240 mg, 61%).

Rf 0.66 (silica, 5:5 CH_2Cl_2–hexane);

mp 184.7–185.4 °C;

^{1}H NMR (500 MHz, $CDCl_3$, δ) 8.12 (s, 1H), 7.65 (d, 1H, ^2J = 7.7 Hz), 7.49–7.46 (m, 4H), 7.34 (d, 1H ^3J = 7.9 Hz), 7.13 (t, 1H, ^3J = 7.8 Hz), 7.09–7.06 (m, 4H), 5.90 (br s);

^{13}C NMR (100 MHz, $CDCl_3$, δ) 144.2 (br), 142.4 (br), 131.9, 127.1 (br), 126.1, 125.7 (q, $J_{C,F}$ = 30 Hz), 125.3, 124.7, 124.6 (q, $J_{C,F}$ = 272 Hz) 124.5, 123.5 (br), 122.5 (q, $J_{C,F}$ = 5.0 Hz) 97.3, 58.4, 50.7;

^{19}F NMR (282 Hz, $CDCl_3$, δ) –59.72;

IR (neat) 3070*w*, 2921*w*, 1597*w*, 1458*m*, 1434*m*, 1318*s*, 1264*w*, 1155*s*, 1116*s*, 1090*s*, 936*w*, 849*w*, 822*m*, 804*m*, 778*s*, 763*m*, 706*w*, 685*w*, 627*w*, 617*m*, 492*m* cm^{-1};

MS (EI) 507.8 (15, $[M\{2\times^{81}Br\}]^+$) 505.8 (31, $[M\{^{79}Br,^{81}Br\}]^+$), 426.9 (29, $[M-^{79}Br]^+$), 424.9 (28, $[M-^{81}Br]^+$), 346.0 (100, $[M-Br_2]^+$), 277.0 (58), 262.5 (13), 152.5 (11), 138.0 (36);

HRMS (EI) Calcd for $C_{23}H_{13}Br_2F_3$ (M) 503.9336, found 503.9333.

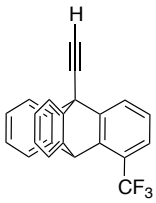

9-Ethynyl-4-(trifluoromethyl)triptycene (**51b**): To a solution of **64b** (202 mg, 0.40 mmol) in THF (1 mL), cooled to –78 °C, was slowly added *n*-butyllithium (1.6 mol/L in hexane, 0.50 mL, 0.79 mmol). The reaction mixture was warmed to RT and stirred for 20 min. Water was then added and the phases were separated. The aqueous phase was extracted with CH_2Cl_2 and the combined organic phases were washed with sat. NaCl solution, dried over Na_2SO_4, and concentrated, affording **51b** as colorless crystals (130 mg, 94%).

Rf 0.66 (silica, 5:5 CH_2Cl_2–hexane);

mp 171–173 °C;

^{1}H NMR (400 MHz, $CDCl_3$, δ) 7.94 (d, 1H ^3J = 7.6 Hz), 7.77–7.75 (m, 2H), 7.44–7.43 (m, 2H), 7.33 (d, 1H, ^3J = 7.8 Hz), 7.17–7.04 (m, 5H), 5.90 (d, 1H, $J_{H,F}$ = 1.5 Hz), 3.32 (s, 1H);

^{13}C NMR (100 MHz, $CDCl_3$, δ) 146.4, 143.7, 143.4 (d, $J_{C,F}$ = 1.9 Hz), 143.1, 126.4, 126.0, 125.9, 125.6 (q, $J_{C,F}$ = 31 Hz), 125.2, 124.6 (q, $J_{C,F}$ = 272 Hz), 124.2, 122.6, 122.5 (q, $J_{C,F}$ = 5.0), 81.3, 78.1, 53.2, 50.0 (d, $J_{C,F}$ = 1.9 Hz);

^{19}F NMR (282 Hz, $CDCl_3$, δ) –59.76;

IR (neat) 3300*m*, 3070*w*, 3018*w*, 1609*w*, 1457*m*, 1433*m*, 1317*s*, 1292*m*, 1265*w*, 1186*m*, 1154*s*, 1136*m*, 1111*s*, 1089*s*, 1068*m*, 1049*w*, 1026*w*, 928*w*, 803*m*, 762*m*, 745*s*, 733*w*, 702*w*, 685*m*, 653*s*, 627*m*, 488*m*; cm^{-1};

MS (EI) 346.0 (100, $[M]^+$), 277 (58), 138 (25);

HRMS (EI) Calcd for $C_{23}H_{13}F_3$ (M) 346.0969, found 346.0966.

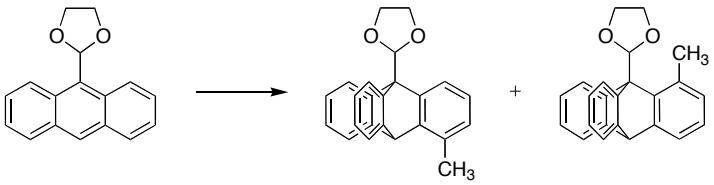

2-(4-methyltriptycene-9-yl)-1,3-dioxolane and 2-(1-methyltriptycene-9-yl)-1,3-dioxolane: A dilute solution of **61** (5.00 g, 20 mmol) in CH_2Cl_2 (250 mL) was stirred and heated to reflux. A solution of 3-methylanthranilic acid (9.97 g, 66 mmol) in acetone (40 mL) and a solution of *iso*-pentyl nitrite (8.0 mL, 7.0 g, 60 mmol) in CH_2Cl_2 (40 mL) were added simultaneously over 4 h with a double syringe pump. Following the addition of reagents, the reaction mixture was allowed to stir at reflux for an additional 14 h. The reaction mixture was washed with sat. $NaHCO_3$, washed with sat. NaCl, dried over $NaSO_4$ and concentrated *in vacuo*. The residue was subjected to column chromatography (silica, 9:1→ 7:3 hexane–CH_2Cl_2. Crystallization from a mixture of hexane–CH_2Cl_2 afforded a mixture of 2-(4-methyltriptycene-9-yl)-1,3-dioxolane and 2-(1-methyltriptycene-9-yl)-1,3-dioxolane as colorless crystals (total yield: 4.45 g, 67%), which were not separated and used directly in the next step.

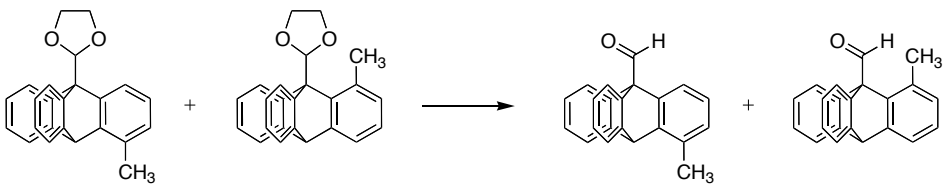

4-Methyltriptycene-9-carboxaldehyde and 1-methyltriptycene-9-carboxaldehyde: To a stirring mixture of 2-(4-methyltriptycene-9-yl)-1,3-dioxolane and 2-(1-

methyltriptycene-9-yl)-1,3-dioxolane (4.45 g, 13 mmol) in glacial acetic acid (150 mL) was added concd. HCl (30 mL). The mixture was stirred at reflux for 15 h, then allowed to cool to RT and poured into water. The resulting precipitate was filtered, washed with water, and dried *in vacuo* to afford a mixture of 4-methyltriptycene-9-carboxaldehyde and 1-methyltriptycene-9-carboxaldehyde as a white solid (3.67 g, 95% yield of mixture of isomers) that was used directly in the next step.

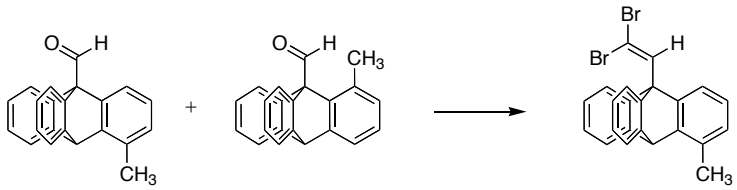

9-(2,2-Dibromoethen-1-yl)-4-methyltriptycene (**64c**) : To a solution of tetrabromomethane (7.85 g, 23.6 mmol) in CH_2Cl_2 (30 mL) was slowly added triphenylphosphine (12.39 g, 47.3 mmol) at 0 °C. The reaction mixture was allowed to stir for 15 min and a solution of 4-methyltriptycene-9-carboxaldehyde and 1-methyltriptycene-9-carboxaldehyde (3.50 g, 11.8 mmol) in CH_2Cl_2 (30 mL) was then added. The ice bath was removed and the reaction mixture was allowed to stir at RT for 6 h. The reaction was quenched with water and the phases were separated. The aqueous phase was extracted with CH_2Cl_2 and the combined organic phases were washed with sat. NaCl, dried over Na_2SO_4, and concentrated. The resulting residue was purified by column chromatography (silica, 9:1 hexane–CH_2Cl_2) to afford64**5c** as a white solid (1.80 g, 21% yield over three steps from compound **61**.

Rf 0.68 (silica, 5:5 CH_2Cl_2–hexane);

mp 196.8–197.5 °C;

^{1}H NMR (400 MHz, $CDCl_3$, δ) 8.10 (s, 1H), 7.47–7.45 (m, 2H), 7.42–7.40 (m, 2H), 7.32 (d, 1H, ^3J = 7.4 Hz), 7.06–7.02 (m, 4H), 6.92 (t, 1H, ^3J = 7.5 Hz), 6.88 (d, 1H ^3J = 7.1 Hz), 5.64 (s, 1H), 2.53 (s, 3H);

^{13}C NMR (100 MHz, $CDCl_3$, δ) 145.2 (br), 143.6 (br), 142.7 (br), 132.7, 132.2, 127.3, 125.6, 124.8, 124.3, 124.2, 123.3, 121.2, 96.4, 58.6, 50.4, 18.9;

IR (neat) 3066*w*, 2979*w*, 2921*w*, 2854*w*, 1602*m*, 1456*m*, 1418*w*, 1263*m*, 1187*w*, 1032*w*, 931*w*, 847*w*, 791*s*, 779*s*, 733*s*, 701*m*, 656*w*, 642*m*, 620*m*, 607*w*, 593*m*, 559*w*, 550*m*, 534*w*, 486*w*, 437*w* cm^{-1};

MS (EI) 453.9 (12, $[M\{2\times^{81}Br\}]^+$), 451.9 (25, $[M\{^{79}Br,^{81}Br\}]^+$), 449.9 (12, $[M\{2\times^{79}Br\}]^+$), 373.0 (27, $[M-^{79}Br]^+$), 371.0 (27, $[M-^{81}Br]^+$), 292.1 (100, $[M-(HBr+Br)]^+$), 277.0 (58, $[M-(Br_2+CH_3)]^+$), 138 (17)

HRMS (EI) Calcd for $C_{23}H_{16}Br_2$ (M) 449.9619, found 449.9619.

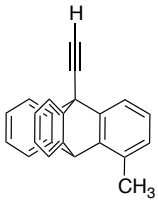

9-Ethynyl-4-methyltriptycene (**51c**): To a solution of **64c** (170 mg, 0.38 mmol) in THF (2 mL), cooled to –78 °C, was slowly added *n*-butyllithium (1.6 mol/L in hexane, 0.48 mL, 0.75 mmol). The reaction mixture was warmed to RT and stirred for 1 h min. Water was then added and the phases were separated. The aqueous phase was extracted with CH_2Cl_2 and the combined organic phases were washed with sat. NaCl, dried over Na_2SO_4, and concentrated, affording **51a** as colorless crystals (106 mg, 96%).

Rf 0.68 (silica, 5:5 CH_2Cl_2–hexane);

mp 197.0–197.8°C;

^{1}H NMR (400 MHz, $CDCl_3$, δ) 7.79 (d, 2H, ^3J = 6.6 Hz), 7.66 (d, 1H, ^3J = 7.3 Hz), 7.24 (d, 2H, ^3J = 6.4 Hz), 7.12–7.05 (m, 4H), 7.00–6.96 (m, 1H), 6.92–6.91 (m, 1H), 5.69 (s, 1H), 3.30 (s, 1H), 2.56 (s, 3H);

^{13}C NMR (100 MHz, $CDCl_3$, δ) 144.4, 144.3, 144.0, 142.6, 131.8, 127.5, 125.8, 125.4, 125.0, 123.6, 122.6, 120.4, 80.6, 78.9, 53.3, 49.6, 18.7;

IR (neat) 3283*w*, 3065*w*, 2979*w*, 2923*w*, 2854*w*, 1587*w*, 1455*m*, 1418*w*, 1379*w*, 1293*w*, 1264*w*, 1184*w*, 1026*w*, 783*w*, 743*s*, 698*w*, 656*m*, 647*m*, 607*w*, 550*w*, 486*w*, 440*w*.

MS (EI) 292.1 (100, $[M]^+$), 277 (98, $[M-CH_3]$), 138 (32);

HRMS (ESI) Calcd for $C_{23}H_{16}$ (M) 292.1252, found 292.1250.

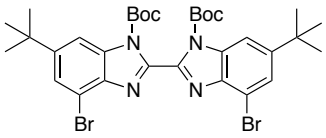

1,1'-bis(*tert*-butoxycarbonyl)-4,4'-dibromo-6,6'-di-*tert*-butyl-2,2'-bibenzimidazole (**66**): To a solution of **52** (0.97 g, 2.0 mmol) in THF (5 mL), NaH (259 mg, 55–65% in oil, 5.9–7.0 mmol) was added portionwise at 0 °C, and the resulting mixture was stirred for 15 min at room temperature. $(Boc)_2O$ (1.33 g, 5.9 mmol) in THF (5 mL) was added at 0 °C and the reaction mixture was stirred for 22 h at room temperature. The reaction mixture was concentrated *in vacuo*, water was added, and the mixture was extracted with Et_2O. The combined extracts were washed with water and sat. NaCl solution, dried over Na_2SO_4, and concentrated *in vacuo*. The resulting solid was recrystallized from CH_2Cl_2/hexane to give **66** as colorless crystals (1.05 g, 78%).

Rf 0.42 (silica, 5:5 CH_2Cl_2–hexane); mp >300 °C;

^{1}H NMR (300 MHz, $CDCl_3$, δ) 8.06 (d, 1H, ^4J = 1.6 Hz), 7.65 (d, 1H, ^4J = 1.6 Hz), 1.41 (s, 18H), 1.36 (s, 18H);

^{13}C NMR (100 MHz, $CDCl_3$, δ) 151.4, 147.6, 144.0, 139.4, 133.1, 126.1, 113.7, 110.9, 86.2, 35.6, 31.7, 27.8;

IR (KBr) 2958*s*, 2870*m*, 1746*s*, 1610*m*, 1572*w*, 1495*m*, 1478*s*, 1348*s*, 1289*s*, 1252*m*, 1233*m*, 1202*s*, 1149*s*, 1132*s*, 1108*s*, 1015*w*, 959*m*, 888*w*, 867*m*, 838*m*, 768*m*, 756*m*, 712*w*, 691*w*, 659*w*, 619*w*, 519*w*, 500*w*, 472*w* cm^{-1};

HRMS (ESI) Calcd for $C_{32}H_{40}Br_2N_4O_4Na$ ($M+Na^+$) 725.1314, found 725.1317.

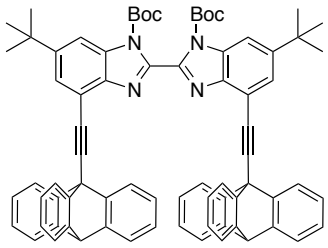

1,1'-bis(*tert*-butoxycarbonyl)-4,4'-bis(triptycen-9-ylethynyl)-6,6'-di-*tert*-butyl-2,2'-bibenzimidazole (**67a**): To a nitrogen-flushed solid mixture of **66** (402 mg, 571 μmol), **51a** (396 mg, 1.42 mmol), CuI (24 mg, 130 μmol), and $Pd(PPh_3)_2Cl_2$ (42 mg, 60 μmol) were added degassed, dry THF (10 mL) and degassed triethylamine (10 mL). The reaction mixture was stirred and heated to 70 °C. After 8 h, the solvents were removed from the reaction mixture and the remaining black solid was subjected to column chromatography (alumina, hexane/CH_2Cl_2 = 9:1 –> 8:2), giving **67a** as a white solid (413 mg, 66%).

Rf 0.65 (alumina, CH_2Cl_2/hexane 5:5);

mp >300 °C;

^{1}H NMR (300 MHz, $CDCl_3$, δ) 8.24 (d, 2H, ^4J = 1.8 Hz), 8.01–7.98 (m, 6H), 7.91 (d, 2H, ^4J = 1.8 Hz), 7.33–7.30 (m, 6H), 7.00–6.91 (m, 12H), 5.37 (s, 1H), 1.52 (s, 18H), 1.43 (s, 18H);

^{13}C NMR (125 MHz, $CDCl_3$, δ) 149.8, 148.1, 144.7, 144.5, 142.3, 133.2, 126.6, 125.6, 125.4, 123.3, 115.2, 112.7, 89.4, 88.7, 85.8, 54.2, 53.5, 35.6, 32.00, 28.0;

IR (KBr) 3066*m*, 2964*s*, 2869*w*, 1753*s*, 1660*m*, 1479*m*, 1457*s*, 1402*s*, 1370*s*, 1358*s*, 1338*s*, 1303*s*, 1290*s*, 1249*s*, 1202*m*, 1159*s*, 1139*s*, 1122*s*, 1077*w*, 1057*m*, 1025*m*, 979*w*, 872*m*, 842*m*, 829*m*, 749*s*, 661*w*, 641*s*, 608*m*, 570*w*, 482*m*; cm^{-1};

HRMS (ESI) Calcd for $C_{76}H_{66}N_4O_4Na$ ($M+Na^+$) 1121.4982, found 1121.4987.

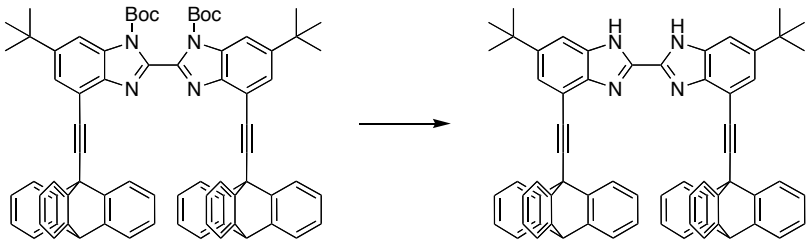

4,4'-bis(triptycen-9-ylethynyl)-6,6'-di-*tert*-butyl-2,2'-bibenzimidazole: To a solution of **28a** (413 mg, 0.38 mmol) in CH_2Cl_2 (4 mL) under air was added trifluoroacetic acid (0.45 mL). The reaction mixture was stirred at room temperature for 3 h, after which water, sat. $NaHCO_3$ solution, and additional CH_2Cl_2 were added. The layers were separated and the aqueous phase was extracted with CH_2Cl_2. The combined organic phases were washed with saturated NaCl solution and dried over Na_2SO_4, and concentrated, affording crude 4,4'-bis(triptycen-9-ylethynyl)-6,6'-di-*tert*-butyl-2,2'-bibenzimidazole as a white solid (280 mg), which was used directly in the next step.

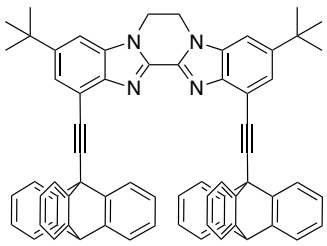

6,7-Dihydro-1,12-bis(triptycen-9-ylethynyl)-3,10-di-*tert*-butylbenzimidazo [2',1':3,4][1,4]diazino[1,2-*a*]benzimidazole (**65a**): Crude 4,4'-bis(triptycen-9-ylethynyl)-6,6'-di-*tert*-butyl-2,2'-bibenzimidazole (50. mg, 56 μmol) was dissolved in THF (5 mL). To this solution were added Cs_2CO_3 (54. mg, 170 μmol) and a large excess of 1-bromo-2-chloroethane (1 mL). The reaction mixture was stirred for 17 h at 60 °C. An aqueous solution of 25% NH_4OH was added to the mixture, which was then stirred for 15 min. Water and CH_2Cl_2 were added and the layers were separated. The aqueous phase was extracted with CH_2Cl_2 and the combined organic phases were washed with sat. NaCl, dried under Na_2SO_4 and concentrated *in vacuo*. The resulting residue was recrystallized, which, following removal of solvent from the crystals, afforded **65a** as a white solid (40 mg, 64% over two steps from **67a**).

Rf 0.65 (alumina, CH_2Cl_2/hexane 5:5);

mp >300 °C;

^{1}H NMR (300 MHz, $CDCl_3$, δ) 8.07 (d, 6H, ^3J = 7.5 Hz), 7.89 (d, 2H, ^4J = 1.8 Hz), 7.52 (d, 2H, ^4J = 1.8 Hz), 7.30 (d, 6H, 7.2 Hz), 6.94 (td, 6H, ^3J = 7.5 Hz, ^4J = 1.2 Hz), 6.73 (td, 6H, ^3J = 7.5 Hz, ^4J = 1.1 Hz), 5.37 (s, 2H), 4.78 (s, 4H), 1.54 (s, 18H);

^{13}C NMR (125 MHz, $CDCl_3$, δ) 148.1, 144.7, 144.5, 143.8, 142.2, 134.5, 126.1, 125.6, 125.5, 123.3, 123.2, 115.6, 106.5, 89.7, 88.8, 54.3, 53.6, 41.0, 35.5, 32.0;

IR (KBr) 3067*m*, 3017*m*, 2957*s*, 2867*m*, 1906*w*, 1797*w*, 1609*m*, 1456*s*, 1420*m*, 1380*m*, 1363*m*, 1338*s*, 1325*s*, 1301*m*, 1290*m*, 1250*m*, 1201*w*, 1174*w*, 1152*m*, 1081*w*, 1025*m*, 914*w*, 867*w*, 845*m*, 747*s*, 699*w*, 660*m*, 641*s*, 607*m*, 563*m*, 523*w*, 481*m*, cm^{-1};

HRMS (ESI) Calcd for $C_{68}H_{52}N_4Na$ (M+Na^+) 947.4090, found 947.4099.

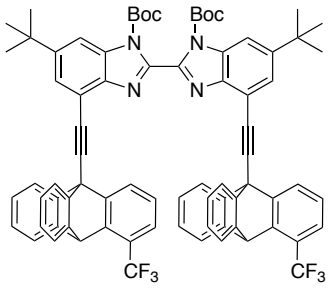

1,1'-bis(*tert*-butoxycarbonyl)-4,4'-bis[4-(trifluoromethyl)triptycen-9-ylethynyl]-6,6'-di-*tert*-butyl-2,2'-bibenzimidazole (**67b**): To a nitrogen-flushed solid mixture of **66** (81 mg, 12 μmol), **51b** (100 mg, 290 μmol), CuI (4.6 mg, 23 μmol), and $Pd(PPh_3)_2Cl_2$ (8.9 mg, 12 μmol) were added degassed, dry THF (2 mL) and degassed triethylamine (2 mL). The reaction mixture was stirred and heated to 70 °C. After 4 h, the solvents were removed from the reaction mixture and the remaining black solid was subjected to column chromatography (alumina, hexane/CH_2Cl_2 = 9:1 –> 8:2), giving **67b** as a white solid (95 mg, 67%).

Rf 0.74 (alumina, CH_2Cl_2/hexane 5:5);

mp >300 °C; ^{1}H NMR (400 MHz, $CDCl_3$, δ) 8.32–8.28 (m, 4H), 8.04 (d, 4H, ^{3}J = 7.1 Hz), 7.96 (s, 2H), 7.40 (d, 4H, 7.0 Hz), 7.90–6.94 (m, 12 H), 5.87 (s, 2H), 1.56 (s, 18H), 1.50 (s, 18H);

^{1}H NMR (400 MHz, $CDCl_3$, δ) 8.32–8.29 (m, 4H), 8.04 (d, 4H, ^{4}J = 7.1 Hz), 7.96 (s, 2H), 7.40 (d, 4H, ^{4}J = 7.0 Hz), 7.09–6.95 (m, 12 H), 5.87 (s, 2H), 1.56 (s, 18H), 1.50 (s, 18H);

^{13}C NMR (100 MHz, $CDCl_3$, δ) 149.9, 148.1, 146.8, 144.8, 144.3, 143.17, 143.13, 142.4, 133.1, 126.9, 126.5, 126.1, 125.8, 125.3, 124.8 (q, $J_{C,F}$ = 31 Hz), 124.6 (q, $J_{C,F}$ = 272 Hz), 123.9, 123.3, 122.2 (q, $J_{C,F}$ = 5.0 Hz), 114.9, 112.9, 89.8, 88.2, 86.0, 54.2, 50.0, 35.7, 32.0, 28.0;

^{19}F NMR (376 MHz, $CDCl_3$, δ) –59.75;

IR (neat) 2965*w*, 1751*m*, 1603*w*, 1480*w*, 1458*w*, 1434*w*, 1404*m*, 1356*m*, 1327*m*, 1301*s*, 1250*m*, 1143*s*, 1119*s*, 1090*m*, 1068*w*, 872*w*, 843*w*, 804*w*, 763*m*, 745*m*, 704*w*, 685*w*, 653*m*, 628*w*, 489*w* cm^{-1};

HRMS (ESI) Calcd for $C_{78}H_{64}N_4O_4$ (M+H$^+$) 1235.4910, found 1235.4903.

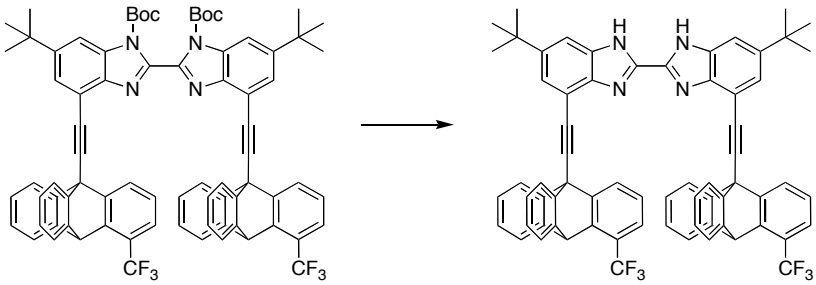

4,4'-bis[4-(trifluoromethyl)triptycen-9-ylethynyl]-6,6'-di-*tert*-butyl-2,2'-bibenzimidazole: To a solution of **28b** (40 mg, 32 μmol) in CH_2Cl_2 (1 mL) under air was added trifluoroacetic acid (0.05 mL). The reaction mixture was stirred at room temperature for 3 h, after which water; saturated, aqueous $NaHCO_3$; and hexane were added. The layers were separated and the aqueous phase was extracted with CH_2Cl_2. The combined organic phases were washed with saturated NaCl and dried under Na_2SO_4, and concentrated, affording crude 4,4'-bis[4-(trifluoromethyl)triptycen-9-

ylethynyl]-6,6'-di-*tert*-butyl-2,2'-bibenzimidazole as a white solid (33 mg), which was used directly in the next step.

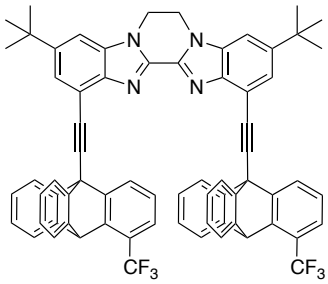

6,7-Dihydro-1,12-bis[4-(trifluoromethyl)triptycen-9-ylethynyl]-3,10-di-*tert*-butylbenzimidazo[2',1':3,4][1,4]diazino[1,2-*a*]benzimidazole (**65b**): Crude 4,4'-bis(triptycen-9-ylethynyl)-6,6'-di-*tert*-butyl-2,2'-bibenzimidazole (33 mg, 32 μmol) was dissolved in THF (5 mL). To this solution were added Cs_2CO_3 (31 mg, 96 μmol) and a large excess of 1-bromo-2-chloroethane (0.5 mL). The reaction mixture was stirred for 18 h at 60 °C. An aqueous solution of 25% NH_4OH was added to the mixture, which was then stirred for 15 min. Water and CH_2Cl_2 were added and the layers were separated. The aqueous phase was extracted with CH_2Cl_2 and the combined organic phases were washed with sat. NaCl, dried under Na_2SO_4 and concentrated *in vacuo*. The resulting residue was crystallized from chlorobenzene, affording **65b** as a white solid (21 mg, 62% over two steps from **67b**).

Rf 0.52 (silica, 5:5 CH_2Cl_2–hexane);

mp >300 °C;

^{1}H NMR (500 MHz, $CDCl_3$, δ) 8.53 (d, 2H, ^3J = 7.6 Hz), 8.01 (d, 4H, ^3J = 7.4 Hz), 7.86 (d, 2H, ^4J = 1.6 Hz), 7.53 (d, 2H, ^4J = 1.7 Hz), 7.38 (d, 4H, ^3J = 6.7 Hz), 6.96 (td, 4H, ^3J = 7.5 Hz, ^4J = 1.2 Hz), 6.89–6.81 (m, 6H), 6.42 (d, 2H, ^3J = 7.1 Hz), 5.86 (s, 2H), 1.54 (s, 18H);

^{13}C NMR (125 MHz, $CDCl_3$, δ) 148.4, 146.7, 144.4, 144.3, 143.3, 142.9, 142.4, 134.5, 127.1, 126.0, 125.8, 125.6, 124.7 (q, $J_{C,F}$ = 31 Hz), 124.6 (q, $J_{C,F}$ = 272 Hz), 123.9, 123.1, 121.91 (br s), 115.3, 106.7, 90.0, 88.5, 54.3, 50.1, 41.1, 35.6, 32.0, 29;

^{19}F NMR (376 MHz, $CDCl_3$, δ) –59.70;

IR (neat) 2957*m*, 2918*m*, 2849*m*, 1608*w*, 1458*m*, 1434*w*, 1324*m*, 1296*m*, 1181*w*, 1152*m*, 1137*m*, 1119*s*, 1098*m*, 1089*m*, 1069*m*, 1024*w*, 968*w*, 845*w*, 802*m*, 745*s*, 701*w*, 685*w*, 652*m*, 563*w*, 490*w* cm^{-1};

HRMS (ESI) Calcd for $C_{70}H_{51}F_6N_4O_4$ ($M+H^+$) 1061.4017, found 1061.4016.

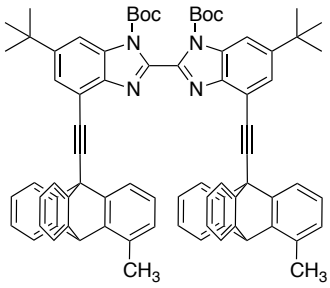

1,1'-Bis(*tert*-butoxycarbonyl)-4,4'-bis(4-methyltriptycen-9-ylethynyl)-6,6'-di-*tert*-butyl-2,2'-bibenzimidazole (**67c**): To a nitrogen-flushed solid mixture of **66** (57 mg, 81 μmol), **51c** (59 mg, 202 μmol), CuI (3.0 mg, 16 μmol), and $Pd(PPh_3)_2Cl_2$ (5.6 mg, 8.1 μmol) were added degassed, dry THF (2 mL) and degassed triethylamine (2 mL). The reaction mixture was stirred and heated to 70 °C. After 14 h, the solvents were removed from the reaction mixture and the remaining black solid was subjected to column chromatography (alumina, hexane/CH_2Cl_2 = 9:1 –> 8:2), affording **67c** as a white solid (28 mg, 31%).

Rf 0.80 (alumina, CH_2Cl_2/hexane 5:5);

mp 285–286 °C;

^{1}H NMR (500 MHz, $CDCl_3$, δ) 8.25 (d, 2H, ^4J = 1.7 Hz), 8.01 (d, 4H, ^3J = 7.1 Hz), 7.93 (d, 2H, ^4J = 1.7 Hz), 7.86 (d, 2H, ^3J = 7.4 Hz), 7.32 (d, 4H, ^3J = 7.5 Hz), 6.98 (td, 4H, ^3J = 7.5 Hz, ^4J = 1.1 Hz), 6.93 (td, 4H, ^3J = 7.1 Hz, ^4J = 1.1 Hz), 6.88 (t, 2H, ^3J = 7.5 Hz), 6.78 (d, 2H, ^3J = 7.5 Hz), 5.62 (s, 2H), 2.49 (s, 6H), 1.53 (s, 18H), 1.43 (s, 18);

^{13}C NMR (125 MHz, $CDCl_3$, δ) 149.8, 148.1, 145.0, 144.61, 144.59, 144.4, 142.7, 142.3, 133.2, 131.4, 127.3, 126.7, 125.54, 125.46, 125.0, 123.34, 123.29, 121.2, 115.3, 112.6, 89.3, 89.0, 85.8, 54.4, 49.7, 35.6, 32.0, 28.0, 18.7;

IR (neat) 2957*s*, 2924*s*, 2869*m*, 1752*m*, 1605*w*, 1458*s*, 1403*m*, 1370*m*, 1358*m*, 1327*m*, 1304*s*, 1249*m*, 1140*s*, 1119*s*, 1026*w*, 975*w*, 873*w*, 844*w*, 760*s*, 745*s*, 654*w*, 645*w* cm^{-1};

HRMS (ESI) Calcd for $C_{78}H_{71}N_4O_4$ ($M+H^+$) 1127.5469, found 1127.5459.

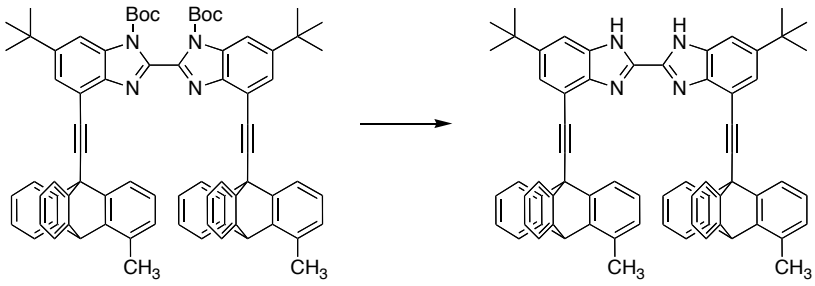

4,4'-Bis(4-methyltriptycen-9-ylethynyl)-6,6'-di-*tert*-butyl-2,2'-bibenzimidazole: To a solution of 28c (19 mg, 17 μmol) in CH_2Cl_2 (2 mL) under air was added trifluoroacetic acid (0.2 mL). The reaction mixture was stirred at room temperature for 3 h, after which water; saturated, aqueous $NaHCO_3$; and hexane were added. The layers were separated and the aqueous phase was extracted with CH_2Cl_2. The combined organic phases were washed with saturated NaCl and dried under Na_2SO_4, and concentrated, affording crude 4,4'-bis(4-methyltriptycen-9-ylethynyl)-6,6'-di-*tert*-butyl-2,2'-bibenzimidazole as a white solid (14 mg), which was used directly in the next step.

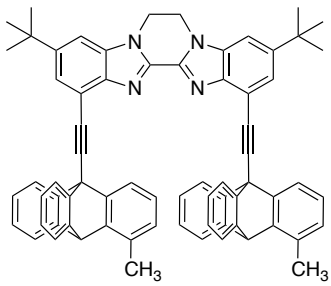

6,7-Dihydro-1,12-bis[4-(trifluoromethyl)triptycen-9-ylethynyl]-3,10-di-*tert*-butylbenzimidazo[2',1':3,4][1,4]diazino[1,2-*a*]benzimidazole (**65c**): Crude 4,4'-bis(4-

methyltriptycen-9-ylethynyl)-6,6'-di-*tert*-butyl-2,2'-bibenzimidazole (14 mg, 15 μmol) was dissolved in THF (2 mL). To this solution were added Cs_2CO_3 (15 mg, 45 μmol) and a large excess of 1-bromo-2-chloroethane (0.2 mL). The reaction mixture was stirred for 24 h at 60 °C. An aqueous solution of 25% NH_4OH was added to the mixture, which was then stirred for 15 min. Water and CH_2Cl_2 were added and the layers were separated. The aqueous phase was extracted with CH_2Cl_2 and the combined organic phases were washed with sat. NaCl, dried under Na_2SO_4 and concentrated *in vacuo*. The resulting residue was purified by successive alumina (8:2 hexane–CH_2Cl_2) and silica (4:6 hexane hexane–CH_2Cl_2) column chromatography, affording **65c** as a white solid (10 mg, 64% over two steps from **67c**).

Rf 0.29 (alumina, CH_2Cl_2/hexane 5:5);

mp >300 °C;

^{1}H NMR (500 MHz, $CDCl_3$, δ) 8.08 (d, 4H, ^3J = 7.4 Hz), 7.97 (d, 2H, ^3J = 7.5 Hz), 7.84 (d, 2H, ^4J = 1.6 Hz), 7.49 (d, 2H, ^4J = 1.6 Hz), 7.30 (d, 4H, ^3J = 7.2 Hz), 6.94 (t, 4H, ^3J = 7.2 Hz), 6.83 (t, 2H, ^3J = 7.5 Hz), 6.73 (t, 4H ^3J =7.0 Hz), 6.51 (d, 2H, ^3J = 7.5 Hz), 5.62 (s, 2H), 4.76 (s, 4H), 2.47 (s, 6H), 1.53 (s, 18H);

^{13}C NMR (125 MHz, $CDCl_3$, δ) 148.1, 145.1, 144.6, 144.3, 143.8, 142.6, 142.2, 134.5, 131.2, 127.2, 126.1, 125.6, 125.4, 125.1, 123.3, 123.2, 121.2, 115.6

106.4, 89.6, 89.1, 54.5, 49.7, 41.0, 35.5, 32.0, 18.7;

IR (neat) 3065*w*, 2959*w*, 2927*w*, 2866*w*, 1671*w*, 1608*w*, 1456*m*, 1420*m*, 1381*w*, 1363*w*, 1337*m*, 1327*m*, 1258*w*, 1153*w*, 845*w*, 783*w*, 746*s*, 655*w*, 645*m* cm^{-1};

HRMS (ESI) Calcd for $C_{70}H_{57}N_4$ ($M+H^+$) 935.4577, found 935.4577.

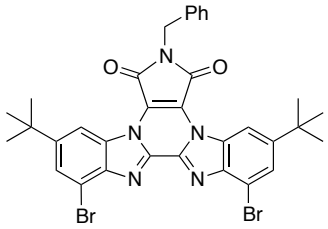

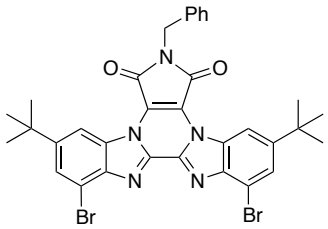

7-Benzyl-1,13-dibromo-3,11-di-*tert*-butyl-6*H*-benzamidazo[2',1':3,4]pyrrolo [3',4':5,6]-pyrazino[1,2-*a*]benzimidazole-6,8(7*H*)-dione (**68**): To a solution of **52** (400 mg, 0.79 mmol) in DMF (8 mL) was added NaH (76 mg of a 55–65% mixture, ~ 1.8 mmol). After stirring 1h, 2,3-dibromo-*N*-(phenylmethyl)maleimide[244] (411 mg, 1.2 mmol) was added. The reaction was stirred for 24 h at RT and an additional 24 h at 100 °C. The reaction mixture was cooled and 10% NH_4Cl solution was added. The precipitate was collected and purified by column chromatography (alumina, 8:2 hexane–CH_2Cl_2) to afford **68** as a yellow solid (139 mg, 26%).

Rf 0.18 (alumina, CH_2Cl_2/hexane 5:5);

mp >300 °C;

^{1}H NMR (500 MHz, $CDCl_3$, δ) 9.16 (d, 2H, ^4J = 1.5 Hz), 7.83 (d, 2H, ^4J =1.5 Hz), 7.54–7.51 (m, 2H), 7.42–7.31 (m, 4H), 5.02 (s, 2H), 1.50 (s, 18H);

^{13}C NMR (100 MHz, $CDCl_3$, δ) 161.8, 151.2, 141.4, 139.1, 135.5, 130.6, 129.2, 128.8, 128.6, 128.5, 120.4, 114.3, 111.7, 42.5, 36.0, 31.9;

IR (neat) 2958*m*, 2926*m*, 2859*s*, 1724*s*, 1666*w*, 1611*w*, 1588*w*, 1454*m*, 1392*s*, 1332*s*, 1297*m*, 1270*m*, 1187*w*, 1070*w*, 870*w*, 730*m*, 699*m*, 655*m*, 511*w*, 420*w* cm^{-1};

HRMS (ESI) Calcd for $C_{33}H_{30}Br_2N_5O_2$ ($M+H^+$) 686.0761, found 686.0760.

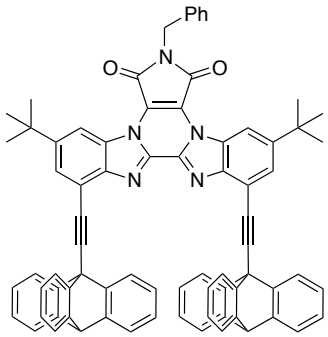

7-Benzyl-3,11-di-*tert*-butyl-1,13-bis(triptycen-9-ylethynyl)-6*H*-benzamidazo [2',1':3,4]pyrrolo[3',4':5,6]pyrazino[1,2-*a*]benzimidazole-6,8(7*H*)-dione (**69a**): A solid mixture of **68** (16 mg, 23 μmol), **51a** (16 mg, 58 μmol), $Pd(OAc)_2$ (1 mg), triphenylphosphine (2 mg) was flushed with nitrogen. Deoxygenated Et_3N (2 mL) and dry, deoxygenated toluene (2 mL) were added to the mixture, which was then stirred and heated to 100 °C for 15 h. The precipitate (NH_4Br) was filtered and the filtrate was taken up in CH_2Cl_2 and this solution was washed with sat. NH_4Cl, then sat. NaCl, dried over Na_2SO_4, then concentrated. The resulting residue was subjected to preparative thin-layer chromatography (5:5 hexane–CH_2Cl_2, two runs) to afford **69a** (13 mg, 52%).

Rf 0.70 (alumina, CH_2Cl_2/hexane 5:5);

mp >300 °C;

^{1}H NMR (300 MHz, $CDCl_3$, δ) 9.34 (d, 2H, ^4J = 1.4 Hz), 8.14 (d, 2H, ^4J = 1.5 Hz), 8.06 (d, 6H, ^3J = 7.4 Hz), 7.59 (d, 2H, ^3J = 7.1 Hz), 7.47–7.38 (m, 3H), 7.26 (d, peak covered by $CHCl_3$ peak, ^3J = 6.5 Hz), 6.87 (t, 6H, ^3J = 7.4 Hz), 6.60 (t, 6H, ^3J = 7.4 Hz), 5.36 (s, 2H), 5.05 (s, 2H), 1.62 (s, 18H);

^{13}C NMR (125 MHz, $CDCl_3$, δ) 162.1, 149.8, 144.5, 144.4, 144.2, 139.8, 135.6, 130.6, 129.2, 129.0, 128.9, 128.6, 125.6, 125.5, 123.2, 123.1, 120.2, 115.8, 113.2, 89.6, 89.1, 54.2, 53.5, 42.5, 36.0, 32.0;

IR (neat) 2959*w*, 2916*w*, 2852*w*, 1721*m*, 1601*w*, 1456*s*, 1393*m*, 1334*m*, 1315*m*, 1291*w*, 1252*w*, 1025*w*, 908*m*, 877*w*, 815*w*, 751*s*, 732*s*, 700*w*, 658*w*, 641*m*, 607*w* cm^{-1};

HRMS (ESI) Calcd. for $C_{77}H_{56}N_5O_2$ ($M+H^+$) 1082.4428, found 1082.4420.

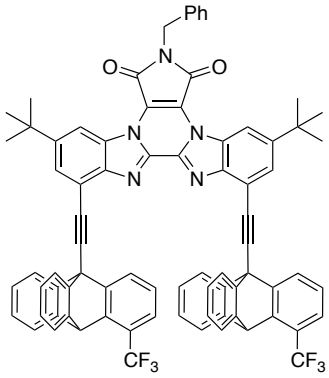

7-Benzyl-3,11-di-*tert*-butyl-1,13-bis(4-[trifluoromethyl]triptycen-9-ylethynyl)-6*H*-benz-amidazo[2',1':3,4]pyrrolo[3',4':5,6]pyrazino[1,2-*a*]benzimidazole-6,8(7*H*)-dione (**69b**): A solid mixture of **68** (52 mg, 73 μmol), **51b** (63 mg, 180 μmol), $Pd(OAc)_2$ (2 mg), triphenylphosphine (4 mg) was flushed with nitrogen. Deoxygenated Et_3N (3 mL) and dry, deoxygenated toluene (3 mL) were added to the mixture, which was then stirred and heated to 100 °C for 12 h. The precipitate (NH_4Br) was filtered and the filtrate was taken up in CH_2Cl_2 and this solution was washed with sat. NH_4Cl, then sat. NaCl, dried over Na_2SO_4, then concentrated. The resulting residue was subjected to column chromatography (alumina, 8:2 → 5:5 hexane–CH_2Cl_2) to afford **69b** (57 mg, 62%).

Rf 0.70 (alumina, CH_2Cl_2/hexane 5:5);

mp >300 °C;

^{1}H NMR (500 MHz, $CDCl_3$, δ) 9.33 (d, 2H, ^4J = 1.6 Hz), 8.50 (d, 2H, ^3J = 7.5 Hz), 8.13 (d, 2H, ^4J = 1.6 Hz), 8.01 (d, 4H ^3J = 7.5 Hz), 7.56 (d, 2H, ^3J = 7.5 Hz), 7.44 (d, 2H, ^3J = 7.5 Hz), 7.39–7.36 (m, 5H), 6.94 (t, 4H, ^3J = 7.5 Hz), 6.80–6.76 (m, 6H), 6.24 (d, 2H, ^3J = 7.8 Hz), 5.85 (s, 2H), 5.00 (s, 2H), 1.63 (s, 18H);

^{13}C NMR (125 MHz, $CDCl_3$, δ) 162.1, 150.0, 146.4, 144.5, 144.2, 143.2, 142.8, 139.8, 135.6, 130.5, 129.2, 129.0, 128.7, 128.4, 126.9, 126.0, 125.8, 125.6, 125.5, 124.6 (q, J_{C-F} = 31 Hz), 124.5 (q, J_{C-F} = 272 Hz), 123.9, 123.0, 121.9 (br s), 120.2, 115.4, 113.4, 89.4, 89.2, 54.1, 50.0, 42.5, 36.0, 32.0;

^{19}F NMR (376 MHz, $CDCl_3$, δ) –59.72;

IR (neat) 3067*w*, 2957*m*, 2924*m*, 2854*w*, 1781*w*, 1724*s*, 1666*w*, 1601*w*, 1456*s*, 1394*m*, 1328*s*, 1309*s*, 1155*m*, 1119*m*, 1089*w*, 877*w*, 744*s*, 698*w*, 657*w* cm^{-1};

HRMS (ESI) Calcd for $C_{79}H_{54}F_6N_5O_2$ ($M+H^+$) 1218.4176, found 1218.4171.

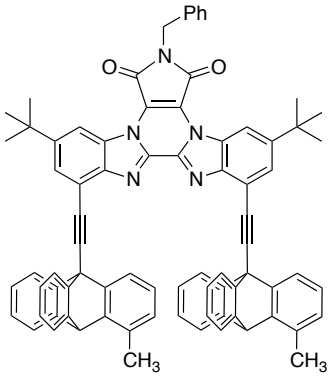

7-Benzyl-3,11-di-*tert*-butyl-1,13-bis(4-[trifluoromethyl]triptycen-9-ylethynyl)-6*H*-benzamidazo[2',1':3,4]py-rrolo[3',4':5,6]pyrazino[1,2-*a*]benzimidazole-6,8(7*H*)-dione (**69c**): A solid mixture of **68** (50 mg, 73 μmol), 12c (53 mg, 180 μmol), $Pd(OAc)_2$ (2 mg), triphenylphosphine (4 mg) was flushed with nitrogen. Deoxygenated Et_3N (3 mL) and dry, deoxygenated toluene (3 mL) were added to the mixture, which was then stirred and heated to 100 °C for 18 h. The precipitate (NH_4Br) was filtered and the filtrate was taken up in CH_2Cl_2 and this solution was washed with sat. NH_4Cl, then sat. NaCl, dried over Na_2SO_4, then concentrated. The resulting residue was subjected to column chromatography (alumina, 8:2 → 5:5 hexane–CH_2Cl_2) to afford **69c** (52 mg, 64%).

Rf 0.67 (alumina, CH_2Cl_2/hexane 5:5);

mp >300 °C;

^{1}H NMR (400 MHz, $CDCl_3$, δ) 9.32 (d, 2H, ^4J = 1.7 Hz), 8.13 (d, 2H, ^4J = 1.7 Hz), 8.04 (d, 4H, ^3J = 6.9 Hz), 7.98 (d, 2H ^3J = 7.4 Hz), 7.59 (d, 2H, ^3J = 7.2 Hz), 7.47–7.43 (m, 2H), 7.39–7.36 (m, 1H), 7.26 (d, 4H, ^3J = 6.6 Hz), 6.86 (td, 4H, ^3J = 7.5 Hz, ^4J = 1.2 Hz), 6.75 (t, 2H, ^3J = 7.5 Hz), 6.61 (td, 4H, ^3J = 7.5 Hz, ^4J = 1.2 Hz), 6.31 (d, 2H, ^3J = 7.5 Hz), 5.59 (s, 2H) 5.04 (s, 2H), 2.42 (s, 6H), 1.63 (s, 18H);

^{13}C NMR (125 MHz, $CDCl_3$, δ) 162.2, 149.7, 144.8, 144.3, 144.25–144.24 (two signals), 142.4, 139.8, 135.6, 131.1, 130.6, 129.2, 129.0, 128.8, 128.6, 127.1, 125.6,

125.4, 125.2, 123.2, 123.1, 121.1, 120.2, 115.9, 113.1, 90.0, 88.9, 54.5, 49.7, 42.4, 36.0, 32.0, 18.7;

IR (neat) 2963*s*, 2916*s*, 2864*s*, 1721*s*, 1663*s*, 1601*m*, 1456*s*, 1393*m*, 1334*m*, 1312*m*, 1250*w*, 1182*w*, 1026*w*, 907*m*, 876*w*, 731*s*, 701*w*, 657*w*, 645*w* cm^{-1};

HRMS (ESI) Calcd for $C_{79}H_{60}N_5O_2$ ($M+H^+$) 1110.4742, found 1110.4744.

6.1.2 Variable Temperature NMR ^{1}H-NMR Spectra

Variable Temperature ^{1}H-NMR Spectra of **65b**.

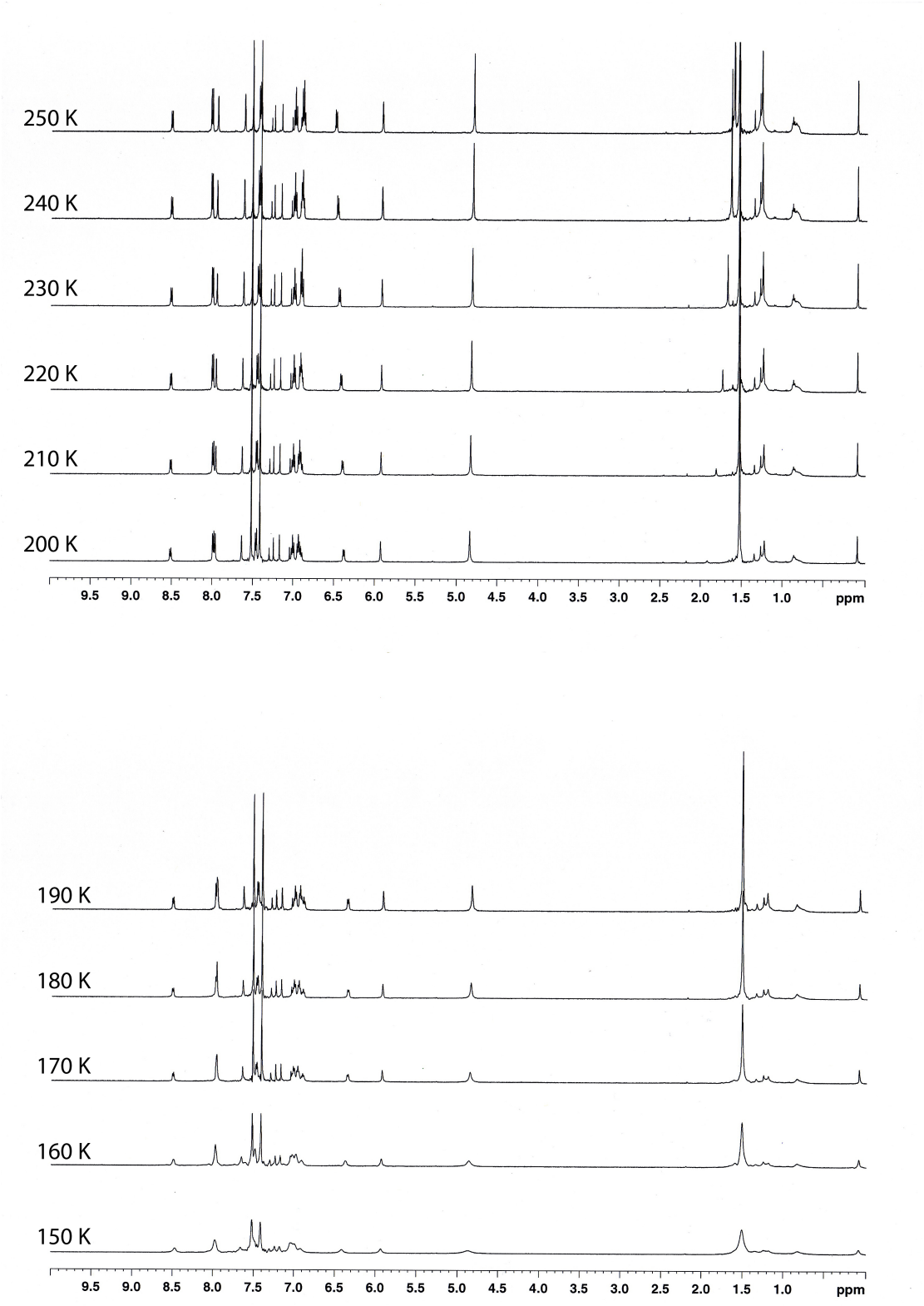

Variable Temperature ^{1}H-NMR Spectra of **65c**.

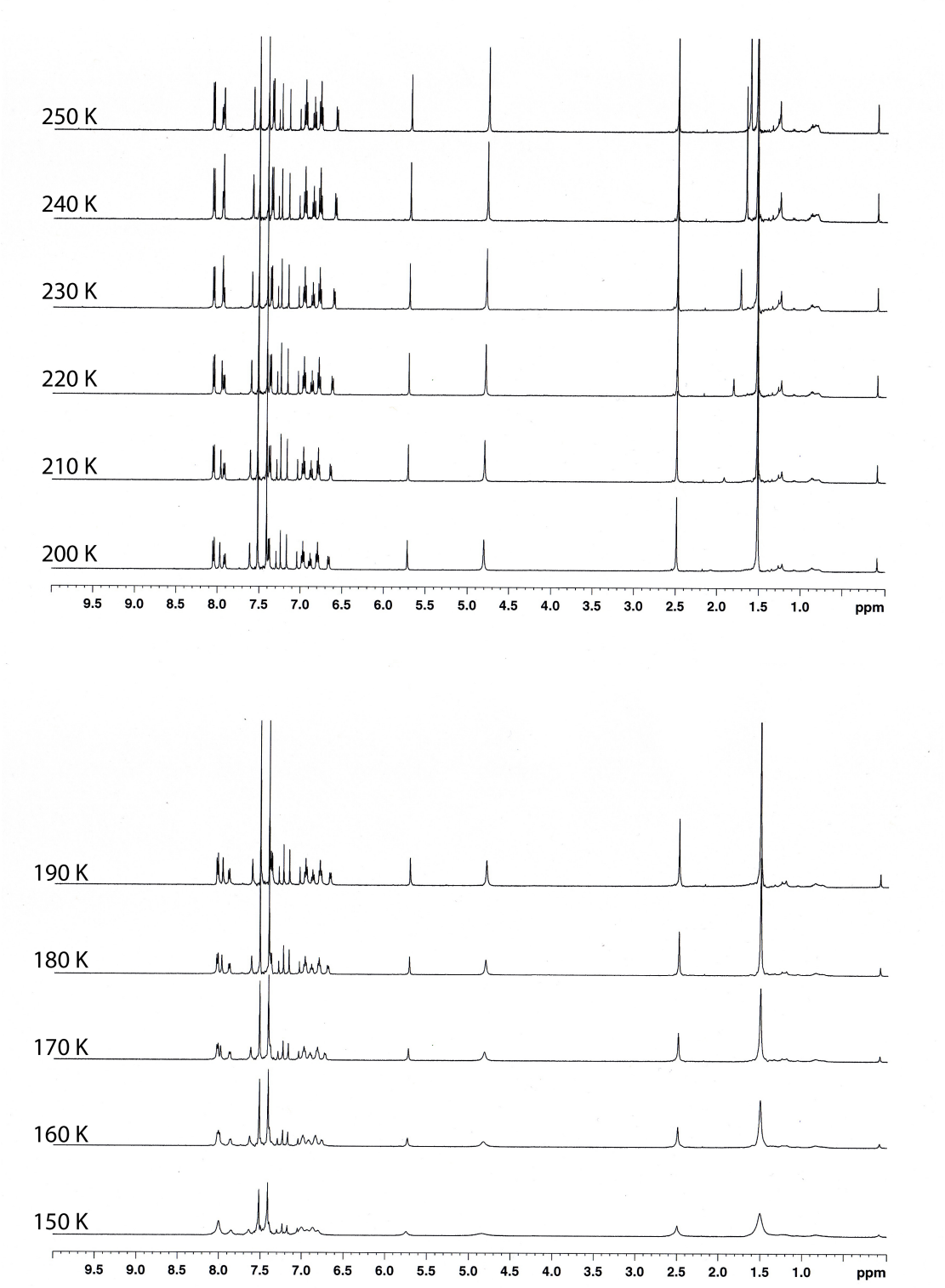

Variable Temperature ^{1}H-NMR Spectra of **69b**.

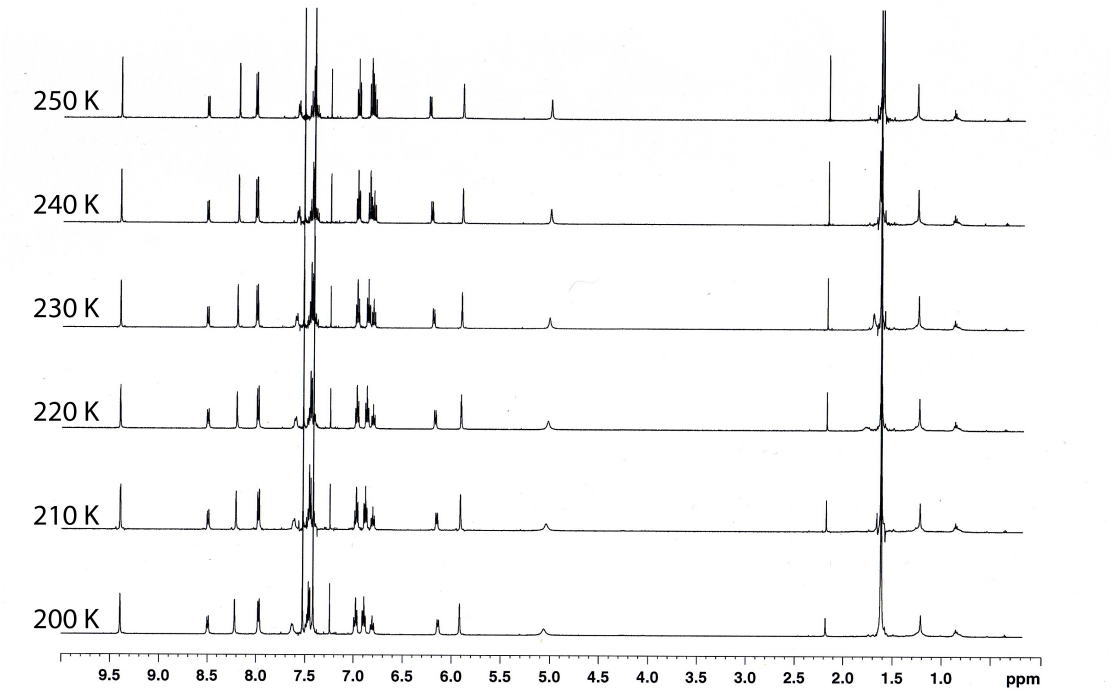

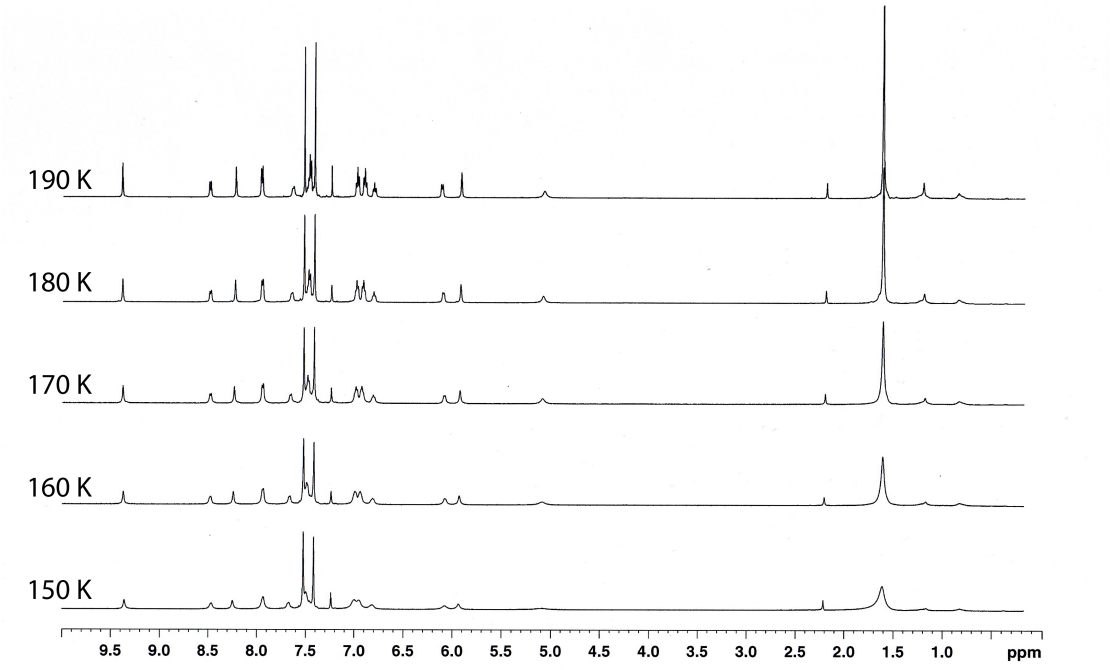

Variable Temperature ^{1}H-NMR Spectra of **69c**.

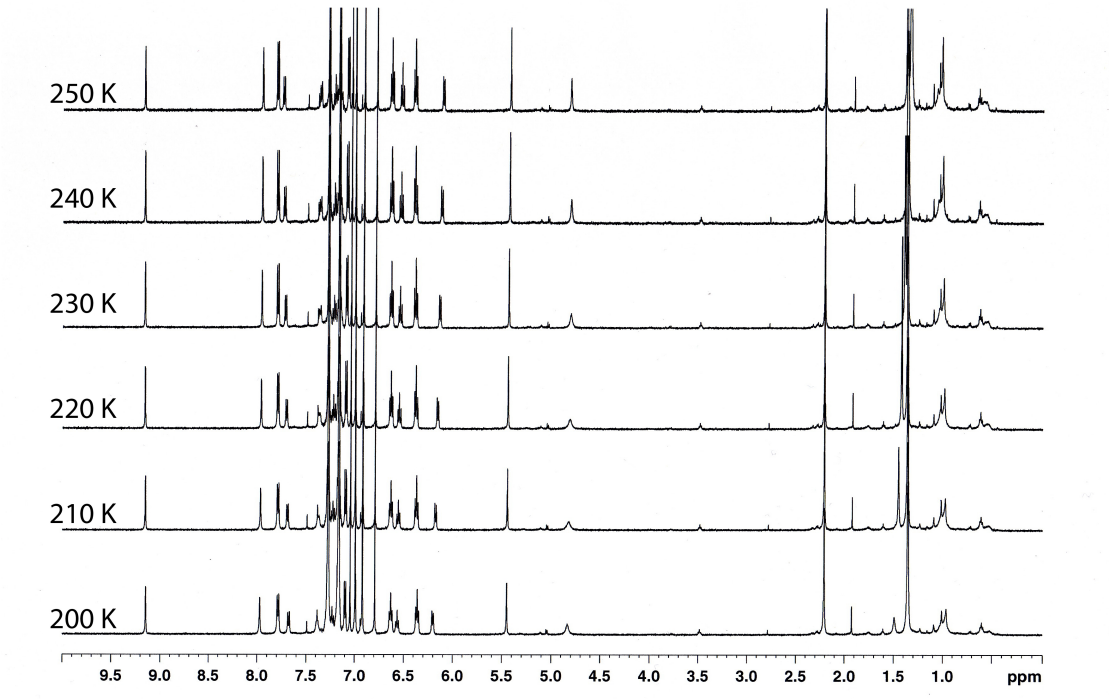

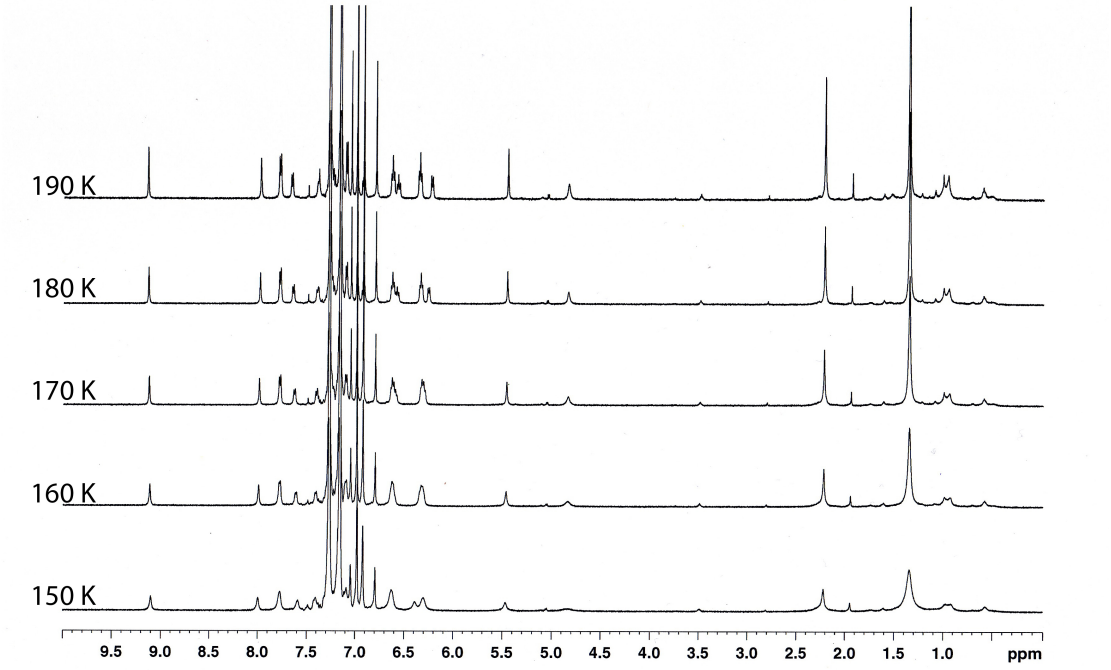

6.1.3. Computational Methods

6.1.3.1. General Remarks

The conformational analyses of the molecular systems described in this study, including structural and orbital arrangements as well as property calculations, were carried out using the GAMESS[245] software package. In the present work, we apply our recently implemented semi-empirically corrected functional, B97-D, according to the ansatz proposed by Grimme (2006).[246] Using an ultrafine grid for evaluation of integrals. The B97-D functional is a special re-parameterization of the original B97 hybrid functional of Becke,[247] which is more neutral to spurious dispersion contamination in the exchange part than the original functional. Both the Dunning-Hay DZV(2d,p)[248] all-electron basis set as well as the Def2-TZVPP basis set[249] were used for all calculations. Full geometry optimizations were performed and uniquely characterized via second derivatives (Hessian) analysis to determine the number of imaginary frequencies (0=minima; 1=transition state). Molecular orbital contour plots and molecular electrostatic potential (MEP) plots, used as an aid in the analysis of results, were generated and depicted using the programs QMView[250] and WebMO.[251]

6.1.3.2. Comparison of Methods

Table 6.1. *Computational Methods for* ***49a*** *(E+ZPE, kcal/mol, and frequencies, cm^{-1}).*

Level of Theory	C_2		C_s		C_{2v}	
	E+ZPE	Hessian	E+ZPE	Hessian	E+ZPE	Hessian
B3LYP/DZV(2d,p)	0.0	PD	3.90	–192.3; –4.4	5.88	–191.7; –8.8; –6.1
BMK/cc-pVDZ	0.0	PD	5.9	–206.6; –20.5	7.8	–207.6
B97-D/DZV(2d,p)	0.0	PD	6.77	MNE	10.85	MNE
B97-D/Def2-TZVP	0.0[c]	PD	7.34	–194.6[a]; –7.5	11.57	–194.1[a]; –20.6
B97-D/Def2-TZVP with Energy perturbation due to Frame Twisting[b]	0.0	--	3.67	TS	7.90	TS
B97-D/Def2-TZVP of **12c**	0.0	PD	--	--	3.67	–194.7

(a) high mode is out-of-plane twisting of CH_2 groups in 2,3-dihydropyrazene moiety at center of stator. (b) Energy difference (C_{2v} – C_2) in model system ***12c*** *(3.67 kcal/mol) was subtracted from B97-D/Def2-TZVP energies to estimate genuine transition state energies. (c) Alternate, diastereomeric C_2 conformation was found to be higher in energy by 0.58 kcal/mol.*

Model System for Twisting Motion of The Frame **49c**

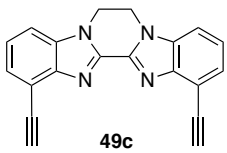

49c

E	–987.8674036	–987.8614267
E+ ZPE	–987.605370	–987.599527

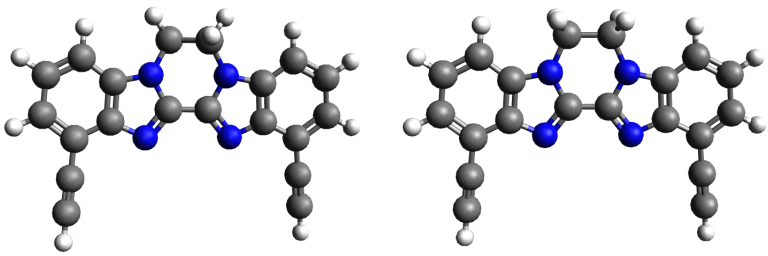

C_2 C_{2v}

Table 6.2. *Computational Methods for* ***49b*** *(E+ZPE, kcal/mol, and frequencies, cm^{-1}).*

Level of Theory	C_2		C_s		C_{2v}	
	E+ZPE	Hessian	E+ZPE	Hessian	E+ZPE	Hessian
B3LYP/DZV(2d,p)	0.0	PD	0.0	-2.4	1.84	-7.3;-5.7
BMK/DZV(2d,p)	0.0	PD	0.73	7.1	3.5	-2.9
M06-2X/cc-pVDZ	0.0	PD	4.2	PD	11.9	-10
B97-D/DZV(2d,p)	0.0	PD	4.11	MNE	9.14	-388.8
B97-D/Def2-TZVP	0.0	PD	3.41	-6.9	7.58	-20.2

6.1.4. X-ray Crystal Structure Information For Compound 65a

Crystal-Structure Determination. – A crystal of $C_{68}H_{52}N_4 \cdot 2C_6H_5Cl$, obtained from chlorobenzene, was mounted on a glass fibre and used for a low-temperature X-ray structure determination. All measurements were made on a *Nonius KappaCCD* area-detector diffractometer[252] using graphite-monochromated Mo *K*α radiation (λ = 0.71073 Å) and an *Oxford Cryosystems Cryostream 700* cooler. The unit cell constants and an orientation matrix for data collection were obtained from a least-squares refinement of the setting angles of 11429 reflections in the range $4° < 2\theta < 50°$. The mosaicity was 0.924(1)°. A total of 559 frames were collected using ω scans with κ offsets, 84 seconds exposure time and a rotation angle of 0.8° per frame, and a crystal-detector distance of 30.0 mm.

Data reduction was performed with *HKL Denzo* and *Scalepack*.[253] The intensities were corrected for Lorentz and polarization effects, but not for absorption. The space group was determined from packing considerations, a statistical analysis of intensity distribution, and the successful solution and refinement of the structure. Equivalent reflections were merged. The data collection and refinement parameters are given in *Table 1*. A view of the molecule is shown in the *Figure*.

The structure was solved by direct methods using *SIR92*,[254] which revealed the positions of all non-hydrogen atoms. The asymmetric unit contains one molecule of the polycyclic compound plus three partially occupied sites for chlorobenzene, which is heavily disordered at each site. Attempts to model the solvent molecules were unsatisfactory. Therefore, the *SQUEEZE* routine[255] of the program *PLATON*[256] was employed. This procedure, which allows the disordered solvent molecules to be omitted entirely from the subsequent refinement model, gave substantially improved refinement results and there were no significant peaks of residual electron density to be found in the voids of the structure. When the solvent molecules are omitted from the model, each unit cell contains one cavity of 1119 Å^3. The electron count in the cavity was calculated to be approximately 214 e although this could be an underbound. As the crystals grew from a chlorobenzene solution and the initial electron density peak distribution looked somewhat like chlorobenzene molecules, it is assumed the cavities contain chlorobenzene. Allowing for four molecule of chlorobenzene per cavity (two

per asymmetric unit, distributed across three sites) yields 232 e and this estimate was used in the subsequent calculation of the empirical formula, formula weight, density, linear absorption coefficient and $F(000)$. Thus the ratio of polycyclic compound to chlorobenzene is approximately 1:2.

The non-hydrogen atoms were refined anisotropically. All of the H-atoms were placed in geometrically calculated positions and refined by using a riding model where each H-atom was assigned a fixed isotropic displacement parameter with a value equal to $1.2U_{eq}$ of its parent atom ($1.5U_{eq}$ for the methyl groups). The refinement of the structure was carried out on F^2 by using full-matrix least-squares procedures, which minimised the function $\Sigma w(F_o^2 - F_c^2)^2$. The weighting scheme was based on counting statistics and included a factor to downweight the intense reflections. Plots of $\Sigma w(F_o^2 - F_c^2)^2$ versus $F_c/F_c(\max)$ and resolution showed no unusual trends. A correction for secondary extinction was applied.

Neutral atom scattering factors for non-hydrogen atoms were taken from Maslen, Fox and O'Keefe,[257a] and the scattering factors for H-atoms were taken from Stewart, Davidson and Simpson[258]. Anomalous dispersion effects were included in F_c;[259] the values for f' and f'' were those of Creagh and McAuley.[8b] The values of the mass attenuation coefficients are those of Creagh and Hubbel.[8c] The *SHELXL97* program[260] was used for all calculations.

*Table 6.3. Crystallographic Data for Compound **65a***

Crystallized from		chlorobenzene
Empirical formula		$C_{80}H_{62}Cl_2N_4$
Formula weight [g mol^{-1}]		1150.30
Crystal color, habit		colorless, prism
Crystal dimensions [mm]		0.15 × 0.23 × 0.30
Temperature [K]		160(1)
Crystal system		triclinic
Space group		$P\bar{1}$ (#2)
Z		2
Reflections for cell determination		11429
2θ range for cell determination [°]		4–50
Unit cell parameters	a [Å]	11.5249(3)
	b [Å]	17.7132(5)
	c [Å]	18.2114(5)
	α [°]	65.750(2)
	β [°]	86.963(2)
	γ [°]	77.082(2)
	V [Å^3]	3300.7(2)
F(000)		1208
D_x [g cm^{-3}]		1.157
μ(Mo $K\alpha$) [mm^{-1}]		0.145
Scan type		ω
2θ(max) [°]		50
Total reflections measured		50971
Symmetry independent reflections		11586
R_{int}		0.071
Reflections with $I > 2\sigma(I)$		7179
Reflections used in refinement		11586
Parameters refined		656
Final $R(F)$ [$I > 2\sigma(I)$ reflections]		0.0788
$wR(F^2)$ (all data)		0.2575
Weights:	$w = [\sigma^2(F_o^2) + (0.1596P)^2]^{-1}$ where $P = (F_o^2 + 2F_c^2)/3$	
Goodness of fit		1.049
Secondary extinction coefficient		0.021(3)
Final Δ_{max}/σ		0.001
$\Delta\rho$ (max; min) [e Å^{-3}]		0.45; –0.29
$\sigma(d(C-C))$ [Å] 0.004 – 0.005		

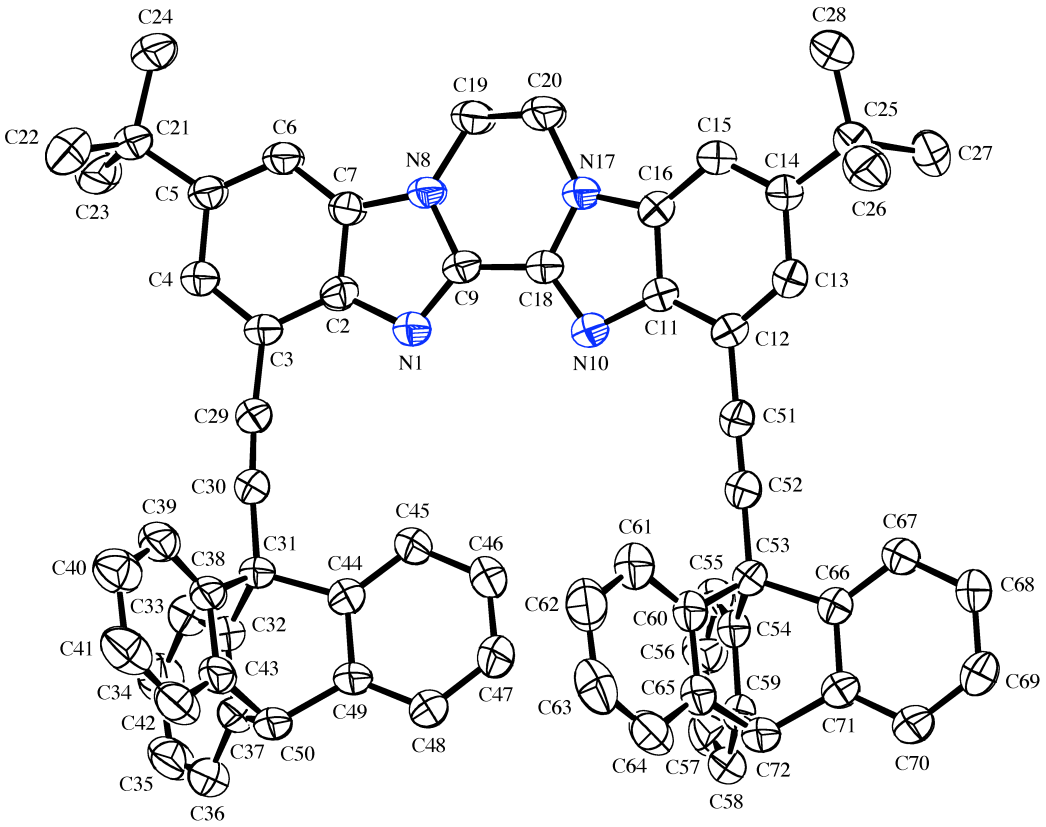

Figure 6.1. *ORTEP Structure (50% Thermal Ellipsoids) of Compound* ***65a****.*

6.2. Experimental Procedures for Section Two

6.2.1. Synthetic Procedures for Compounds in Chapter 4

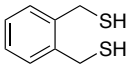

Benzene-1,2-dimethanethiol (**99**): To a solution of 1,2-bis(bromomethyl)benzene (2.00 g, 7.58 mmol) in EtOH (25 mL) was added thiourea (1.44 g 18.9 mmol) and the reaction mixture was heated to reflux for 105 min. The solvent was removed *in vacuo* and a solution of NaOH (1.20 g, 30 mmol) in H_2O (15 mL) was added to the residue. The resulting mixture was heated to reflux for 16 h then cooled to RT. The mixture was acidified to neutral pH with 3 M H_2SO_4 (aq.) and extracted with CH_2Cl_2. The organic phase was washed with sat. NaCl, dried over Na_2SO_4, and concentrated *in vacuo*, affording **99** (1.15 g, 89%) as a colorless solid. Obtained spectra matched literature spectra.[261]

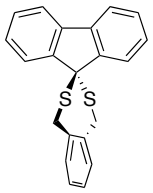

Spiro[(1,5-dihydrobenzo[e][1,3]dithiepane)-2,9'-fluorene] (**86**): To a stirring solution of fluoren-9-one (**83**) (351 mg, 1.95 mmol) and **99** (348 mg, 2.05 mmol) in 1,2-dichloroethane (10 mL) was added $AlCl_3$ (130 mg, 0.975 mmol) and the reaction mixture stirred at RT for 18 h. H_2O was added and the phases were separated. The aqueous phase was extracted with CH_2Cl_2 and the organic phase was dried over Na_2SO_4 and concentrated in vacuo. Trituration in hexane, followed by hot filtration afforded **86** (488 mg, 75%) as a colorless precipitate.

Rf 0.57 (silica, 5:5 CH_2Cl_2–hexane);

mp 247.9–249.2 °C;

1H NMR (500 MHz, acetone-d_6, δ) 8.01 (d, 2H, ^3J = 7.5 Hz), 7.90 (d, 2 H, ^3J = 7.3 Hz), 7.48 (td, 2H, ^3J = 7.5 Hz, ^4J = 1.1 Hz), 7.43–7.34 (m, 4H), 7.31–7.27 (m, 2H), 4.58 (s, 4H);

13C NMR (125 MHz, $CDCl_3$, d) 149.3 (br), 139.2, 138.1, 129.8, 129.2, 128.3, 127.8, 124.2, 120.6, 60.3, 35.7;

MS (EI) 332.0 (<1, $[M]^+$), 196.0 (39, [fluorene]$^+$), 135 (100, [1,3-dihydrobenzo[*c*]thiophene]$^+$).

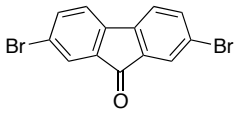

2,7-Dibromofluoren-9-one (**101**): Following a literature procedure,[262] fluoren-9-one (**83**) (15.00 g, 83.3 mmol) was suspended in H_2O (60 mL) and the mixture was heated to reflux, melting the fluoren-9-one in the process. To the hot, biphasic mixture was added Br_2 in three portions: ([A] 5.7 mL, 18 g, 110 mmol), ([B] 4.3 mL, 13 g, 81 mmol), ([C] 2.9 mL, 9.0 g, 51 mmol). Portion (B) was added 2.5 h after portion (A) and portion (C) was added 2 h after portion (B). After portion (C) was added, the reaction mixture was stirred at reflux for an additional 12 h and was subsequently cooled to RT. Aqueous $NaHSO_4$ (20%) was added to quench the excess Br_2 and the precipitate was filtered and washed with H_2O. Recrystallization from toluene/EtOH afforded **101** (16.05 g, 57%) as a bright yellow solid. Obtained spectra matched literature spectra.[193]

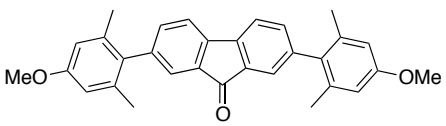

2,7-Bis(4-methoxy-2,6-dimethylphenyl)fluoren-9-one (**103**): To a solution of 4-bromo-3,5-dimethylanisole (5.72 g, 26.6 mmol) in degassed THF (40 mL), cooled to –78 °C, was added *n*-BuLi (1.6 mol/L in hexane, 17 mL, 27 mmol). The reaction mixture was stirred for 30 min then a solution of $ZnCl_2$ (dried by melting *in vacuo*, 4.22 g, 31.1 mmol) in degassed THF (30 mL) was added. The reaction was allowed to

warm to 0 °C while stirring for 45 min. This mixture was added by cannula to a stirring mixture of **101** (3.00 g, 8.88 mmol) and $Pd(PPh_3)_4$ (513 mg, 0.44 mmol) in degassed THF (40 mL). The resulting reaction mixture was heated to 60 °C for 19 h, after which H_2O was added. The phases were separated and the aqueous phase was extracted with EtOAc. The combined organic phase was washed with saturated NaCl solution, dried over Na_2SO_4 and concentrated *in vacuo*. The solid reside was subjected to column chromatography (silica, 8:2 hexane–CH_2Cl_2 → 100% CH_2Cl_2) to afford **103** as a bright orange solid (3.72 g, 93%).

Rf 0.40 (silica, 5:5 CH_2Cl_2–hexane);

mp 219.3–220.9 °C;

^{1}H NMR (400 MHz, CD_2Cl_2, δ) 7.64 (d, 2H, ^3J = 7.5 Hz), 7.41 (d, 2H, ^4J = 1.5 Hz), 7.29 (dd, 2H, ^3J = 7.5 Hz, ^4J = 1.5), 6.68 (s, 4H), 3.81 (s, 6H), 2.06 (s, 12H);

^{13}C NMR (100 MHz, CD_2Cl_2, δ) 194.3, 159.3, 143.4, 142.7, 137.9, 136.8, 135.3, 133.8, 126.1, 120.9;

IR (neat) 3043*w*, 2997*w*, 2951*w*, 2918*w*, 2836*w*, 1716*s*, 1604*s*, 1495*w*, 1462*s*, 1418*m*, 1388*w*, 1315*s*, 1277*w*, 1236*w*, 1192*m*, 1173*s*, 1150*s*, 1119*w*, 1069*s*, 1032*m*, 998*w*, 927*w*, 836*m*, 790*m*, 738*m*, 650*w*, 575*w*, 500*w* cm^{-1};

HRMS (APCI) Calcd for $C_{31}H_{29}O_3$ $[M+H]^+$ 449.2111, found 499.2113.

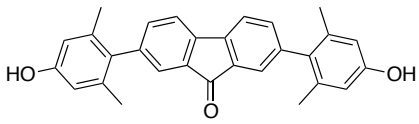

2,7-Bis(4-hydroxy-2,6-dimethylphenyl)fluoren-9-one (**104**): To a thick-walled, sealable reaction flask, fixed with a stirring bar, was added pyridine hydrochloride (18.08 g, 156 mmol). The solid was melted at 165 °C and stirred. Solid **103** (3.50 g, 7.80 mmol) was added and the mixture was heated to 185 °C for 20 h. Additional pyridine hydrochloride (10.0 g, 86 mmol) was then added and the reaction was allowed to stir for 8 h at 185 °C, after which the oil bath was removed and hot water was slowly

added to the reaction mixture, causing a precipitate to form. The mixture was cooled to RT and the precipitate was filtered, washed consecutively with H_2O, 12% NH_4OH solution, and H_2O again, then dried *in vacuo*. The remaining solid residue was used directly in the next step without further purification.

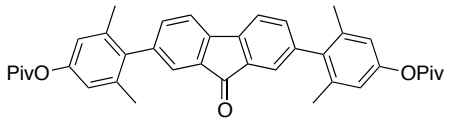

2,7-Bis(4-pivaloyl-2,6-dimethylphenyl)fluoren-9-one (**105**): To a flask containing a mixture of crude **104** from the preceding reaction, Et_3N (3.25 mL, 2.36 g, 23.4 mmol), and DMAP (48 mg, 0.39 mmol), dissolved in CH_2Cl_2 (50 mL), was added pivaloyl chloride (2.10 mL, 2.08 g, 17.6 mmol. The reaction was stirred at RT for 3 h, after which H_2O was added to the mixture and the phases were separated. The aqueous phase was extracted with CH_2Cl_2, and then the combined organic phase was washed with sat. NaCl, dried over Na_2SO_4, and concentrated. The remaining residue was subjected to a short silica column (5:5 CH_2Cl_2–hexane → 100% CH_2Cl_2), affording **105** as a bright yellow solid (3.84 g, 84% over two steps).

Rf 0.43 (silica, 5:5 CH_2Cl_2–hexane);

mp 140.3–141.4 °C;

^{1}H NMR (500 MHz, $CDCl_3$, δ) 7.63 (dd, 2H, ^3J = 7.5 Hz, ^5J = 0.6 Hz), 7.47 (dd, 2H, ^4J = 1.5 Hz, ^5J = 0.6 Hz), 7.29 (dd, 2H, ^3J = 7.5 Hz, ^4J = 1.5), 6.83 (s, 4H), 2.07 (s, 12H), 1.38 (s, 18H);

^{13}C NMR (125 MHz, $CDCl_3$, δ) 194.0, 177.6, 150.2, 143.2, 141.8, 138.1, 137.7, 135.9, 135.0, 125.6, 120.7, 120.5, 39.3, 27.4, 21.0;

IR (neat) 2972*w*, 2931*w*, 2872*w*, 1748*m*, 1720*m*, 1606*w*, 1479*w*, 1461*m*, 1396*w*, 1299*w*, 1274*m*, 1172*m*, 1140*s*, 1110*s*, 1031*m*, 903*w*, 839*w*, 790*w*, 655*w*, 497*w* cm^{-1};

HRMS (ESI) Calcd for $C_{39}H_{40}NaO_5$ $[M+Na]^+$ 611.2768, found 611.2764.

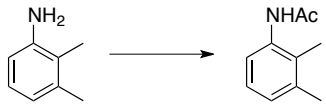

2,3-Dimethylacetanilide (**110**): To a solution of 2,3-dimethylaniline (**109**) (30.0 g, 248 mmol) in CH_2Cl_2 (100 mL), which was open to air, was slowly added acetic anhydride (26 mL, 28 g, 280 mmol) over 15 minutes at RT. The reaction mixture stirred for an additional 15 minutes during which a thick precipitate formed. An additional 50 mL of CH_2Cl_2 was added and the mixture was poured into 800 mL of hexane. The resulting precipitate was filtered, washed with hexane and dried *in vacuo* to afford **110** as a light, colorless solid (34.3 g, 85%). Obtained spectra matched literature spectra.[263]

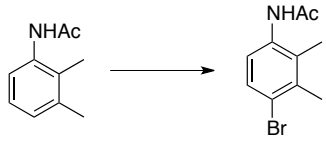

4-Bromo-2,3-dimethylacetanilide (**111**): To a solution of **110** (20.08 g, 123 mmol) in AcOH (400 mL) at 0 °C, which was open to air, was slowly added bromine (6.7 mL, 21 g, 130 mmol). The reaction was stirred at 0 °C for 2h, then the reaction mixture was poured into water and saturated, aqueous $NaHSO_3$. The resulting precipitate was filtered, yielding **111** as a white solid (25.83 g, 87%). Obtained spectra matched literature spectra.

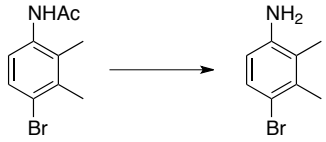

4-Bromo-2,3-dimethylaniline (**112**): To a solution of **111** (12.00 g, 49.6 mmol) in EtOH (60 mL), which was open to the air, was added concentrated, aqueous HCl (32% *w*/*w*). The reaction was stirred at reflux for 3h, then cooled to RT. Water, KOH, and $NaHCO_3$ were added until the solution reached a neutral pH. The aqueous phase was extracted with CH_2Cl_2, washed with saturated, aqueous NaCl, dried over Na_2SO_4, and concentrated *in vacuo* to yield **112** as a yellow oil (7.99 g, 81%). Obtained spectra matched literature spectra. [264]

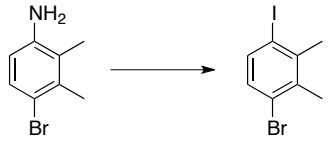

3-Bromo-6-iodo-1,2-xylene (**113**): To a solution of **112** (9.50 g, 47.5 mmol) in acetone (100 mL) at 0 °C in a 1-L, three-neck round-bottom flask was added concentrated, aqueous HCl (32 % *w*/*w*, 11.7 mL, 119 mmol) over 2 min. A thick, white precipitate formed, then a solution of $NaNO_2$ (3.61 g, 52 mmol) in H_2O (25 mL) was added dropwise over 15 minutes, after which the reaction mixture, which became a yellow, transparent solution, was stirred for 45 min at 0 °C. A solution of NaI (15.68 g, 105 mmol) in H_2O (25 mL) was then added to the reaction mixture at –10 °C (NaCl/ice bath) over 20 min and the resulting mixture was stirred at –10 °C for 90 min, then allowed to warm to RT and stirred for an additional 15 min. A solution of NaOAc in H_2O was added and the mixture was concentrated *in vacuo*. The residue was suspended in CH_2Cl_2 and the organic phase was washed with aq. $NaHSO_3$, 2% aq. NaOH, and H_2O; dried over Na_2SO_4; and concentrated *in vacuo*. The residue was subjected to column chromatography (silica 100% hexane) to afford **113** (13.76 g, 93%) as a light brown, low-melting solid.

Rf (silica, hexane) 0.75;

mp 39.3–39.7 °C;

^{1}H NMR (400 MHz, $CDCl_3$, δ) 7.52 (d, 1H, ^3J = 8.5 Hz), 7.09 (d, 1H, ^3J = 8.5 Hz), 2.52 (s, 3H), 2.48 (s, 1H)

^{13}C NMR (125 MHz, $CDCl_3$, δ) 141.4, 137.7, 137.3, 131.7, 126.0, 100.9, 27.1, 21.8

IR (neat) 2923*w*, 1431*m*, 1393*m*, 1256*w*, 1138*s*, 1122*w*, 1004*s*, 826*m*, 797*s*, 531*w* cm^{-1};

MS (EI) 311.9 (96, $[M\{^{81}Br\}]^+$) 309.9 (100, $[M\{^{79}Br\}]^+$), 230.9 (15, $[M–Br]^+$), 184.9 (23, $[M–^{79}Br]^+$), 183.0 (24, $[M–^{81}Br]^+$), 126.9 (10, $I^{\bullet+}$), 104.0 (51, $[M–I,Br]^+$), 103.0 (38, $[M–I,HBr]^+$), 77.0 (26, $[C_6H_5]^+$), 63 (11), 51 (18);

HRMS (EI) Calcd for C_8H_8BrI (M) 309.8854, found 309.8853.

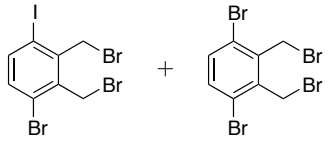

1-bromo-4-iodo-2,3-bis(bromomethyl)benzene (**114**) and **1,4-dibromo-2,3-bis(bromomethyl)benzene** (**115**): To a stirring mixture of **113** (7.00 g, 22.5 mmol) in $CHCl_3$ (100 mL) was added NBS (20.03 g, 113 mmol) and benzoyl peroxide (1.09 g, ~50% mixture in dicyclohexyl phthalate, 2.25 mmol) and the reaction mixture was heated to reflux. Additional portions of NBS and benzoyl peroxide (same amounts as above) were added after 9 h and 24 h. After 71 h of total reaction time, the reaction was cooled to RT and water was added. A solution of 20% aq. $NaHSO_3$ was then added to the stirring mixture until no change of color was observed upon further addition. The phases were separated and the aqueous phase was extracted with CH_2Cl_2. The combined organic phase was dried over Na_2SO_4, and concentrated *in vacuo*. A short column (silica, CH_2Cl_2/hexane = 1:9) afforded a mixture of **114** (52% by 1H-NMR integration) and **115** (48% by 1H-NMR integration) (8.69 g, 87% total yield), which was used in the subsequent steps as a mixture.

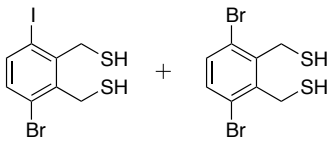

3-Bromo-6-iodobenzene-1,2-dimethanethiol (119) and **3,6-dibromobenzene-1,2-dimethanethiol** (**120**) To a mixture of **114** and **115** (8.00 g, 17.9 mmol total) in EtOH (80 mL) was added thiourea (3.41 g, 44.8 mmol) and the reaction was heated to reflux for 1.5 h. The mixture was cooled to RT and the solvent was removed *in vacuo*. The residue was suspended in H_2O (60 mL) and NaOH (2.87 g, 71.7 mmol) was added and the mixture was heated to reflux for 24 h. The reaction mixture was cooled to RT and brought to neutral pH with 3 mol/L aq. H_2SO_4 and extracted with CH_2Cl_2. The organic phase was dried over Na_2SO_4 and concentrated *in vacuo* to afford a crude mixture of **119** and **120** (6.08 g) which was used directly in the next step.

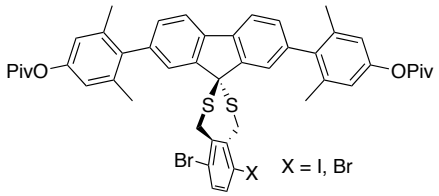

4-{Spiro[(6,7-dibromo-1,5-dihydrobenzo[e][1,3]dithiepane)-2,9'-fluorene]-2',7'-diyl}-bis(3,5-dimethylphen-1-yl) bis(2,2-dimethylpropanoate) (124) and **4-{Spiro[(6-bromo-7-iodo-1,5-dihydrobenzo[e][1,3]dithiepane)-2,9'-fluorene]-2',7'-diyl}-bis(3,5-dimethylphen-1-yl) bis(2,2-dimethylpropanoate)** (**125**): To a stirring solution of **105** (3.84 g, 6.52 mmol) and a mixture **119** (52%) and **120** (48%) (2.76 g total mass, 7.83 total mmol) in CH_2Cl_2 (50 mL) at RT was added solid $AlCl_3$ (434 mg, 3.26 mmol). The reaction mixture was stirred at RT for 15h, then water was added, the phases were separated, and the aqueous phase was extracted with CH_2Cl_2. The combined organic phases were washed with sat. NaCl solution, dried over Na_2SO_4 and concentrated in vacuo. Column chromatography (silica, CH_2Cl_2/hexane 4:6 → 8:2) yielded a mixture of **124** and **125** as a colorless solid (3.43 g, 57% yield of mixture), which was used in the next step.

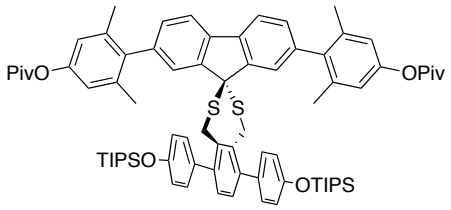

4-{Spiro[(6,7-bis[4-triisopropyloxyphen-1-yl]-1,5-dihydrobenzo[e][1,3]dithiepane)-2,9'-fluorene]-2',7'-diyl}-bis(3,5-dimethylphen-1-yl) bis(2,2-dimethylpropanoate) (**123**): To a solution of 4-bromophenyl triisopropylsilyl ether (4.71 g, 14.3 mmol) in THF (80 mL) at –78 °C was slowly added *n*-BuLi (9.0 mL, 1.6 mol/L in hexane, 14.3 mmol). The mixture stirred for 30 minutes at –78 °C, then $ZnCl_2$ (2.43 g, 17.9 mmol, dried by melting *in vacuo*) in THF (50 mL) was added to the mixture by syringe. The cold bath was removed and the reaction mixture warmed to RT, stirring for a total of 1 h. The mixture was added by cannula to a stirring mixture of **124** and **125** (3.30 g total, 3.58 mmol) and $Pd(PPh_3)_4$ (413 mg, 0.358 mmol) in THF (80 mL) at RT. The

reaction mixture was heated to reflux for 14 h then cooled to RT. Water (200 mL) was added and the phases were separated. The aqueous phase was extracted with EtOAc and the combined organic phases were washed with sat. NaCl, dried over Na_2SO_4, and concentrated *in vacuo*. Colum chromatography (silica, CH_2Cl_2/hexane 4:6) afforded **123** as a colorless solid (3.20 g, 72%).

Rf (silica, 5:5 CH_2Cl_2–hexane) 0.49;

mp (decomp. to red liquid) 253.3–255.4 °C;

^{1}H NMR (500 MHz, $CDCl_3$, δ) 7.80 (d, 2H, ^3J = 7.7 Hz), 7.66 (s, 2H), 7.21–7.18 (m, 8H), 6.90 (d, 4H, ^3J = 8.6 Hz), 6.79 (s, 4H), 4.38 (br s, 4H), 2.07 (s, 12H), 1.37 (s, 18H), 1.26, (sextet, 6H, ^3J = 7.4 Hz), 1.10 (d, 36H, ^3J = 7.4 Hz);

^{13}C NMR (125 MHz, $CDCl_3$, δ) 177.5, 155.4, 150.4, 150.0, 140.4, 139.0, 137.9, 137.8, 136.4, 134.2, 130.8, 130.0, 129.0, 125.8, 120.5, 120.3, 119.9, 59.3, 39.2, 31.7, 27.4, 21.3, 18.1, 12.8;

IR (neat) 2945*w*, 2867*w*, 1747*m*, 1604*w*, 1515*m*, 1481*m*, 1396*w*, 1366*w*, 1264*s*, 1167*w*, 1139*s*, 1113*s*, 1031*w*, 1013*w*, 997*w*, 907*s*, 882*m*, 828*m*, 815*m*, 736*s*, 702*m*, 685*m*, 543*w* cm^{-1};

HRMS (ESI) Calcd for $C_{77}H_{96}NaO_6S_2Si_2$ $[M+Na]^+$ 1259.6079, found 1259.6086.

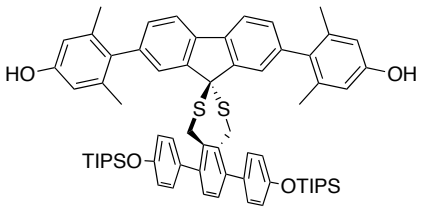

Spiro[(6,7-bis[4-triisopropyloxyphen-1-yl]-1,5-dihydrobenzo[e][1,3]dithiepane)-2,9'-(2',7'-bis[4-hydroxy-2,6-dimethylphenyl]fluorene] (**127**): To a stirring solution of **123** (1.50 g, 1.21 mmol) in Et_2O (100 mL) at –78 °C was added methyllithium (3.2 mL, 1.6 mol/L in Et_2O, 5.1 mmol) dropwise. The reaction was allowed to warm to RT and was stirred for 4 h. Water and EtOAc were added, the phases were separated and the

aqueous phase was extracted with EtOAc. The combined organic phases were dried over Na_2SO_4 and concentrated *in vacuo*. The crude product was triturated in hexane; filtration of the hot mixture afforded **127** (1.08 g, 83%) as a colorless precipitate.

Rf (CH_2Cl_2) 0.37 ;

mp (decomp. to red liquid) 170.5–173.3 °C;

^{1}H NMR (400 MHz, $CDCl_3$, δ) 7.78 (d, 2H, ^3J = 7.8 Hz), 7.65 (s, 2H), 7.26–7.18 (m, 8H), 6.90 (d, 4H, ^3J = 8.6 Hz), 6.59 (s, 4H), 4.55 (s, 2H, O*H*), 4.38 (br s, 4H), 2.03 (s, 12H), 1.26, (sextet, 6H, ^3J = 7.4 Hz), 1.09 (d, 36H, ^3J = 7.4 Hz);

^{13}C NMR (125 MHz, $CDCl_3$, δ) 155.4, 154.5, 150.2, 140.9, 140.7, 138.02, 137.98, 136.2, 134.4, 134.2, 130.7, 130.5, 129.0, 126.2, 120.4, 120.0, 114.2, 59.3, 31.7, 21.3, 18.1, 12.8;

IR (neat) 3500–3100*w* (broad), 2944*m*, 2892*w*, 2866*m*, 1604*m*, 1515*s*, 1461*s*, 1383*w*, 1262*s*, 1168*m*, 1158*m*, 1146*m*, 1025*w*, 1013*w*, 996*w*, 908*s*, 882*s*, 842*m*, 827*s*, 815*m*, 743*s*, 684*s* cm^{-1};

HRMS (ESI) Calcd for $C_{67}H_{80}NaO_6S_2Si_2$ $[M+Na]^+$ 1091.4929, found 1091.4929.

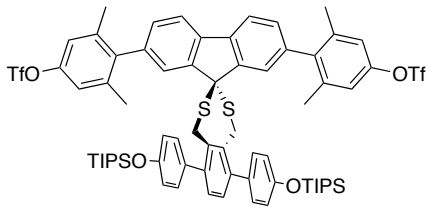

4-{Spiro[(6,7-bis[4-triisopropyloxyphen-1-yl]-1,5-dihydrobenzo[e][1,3]dithiepane) -2,9'-fluorene]-2',7'-diyl}-bis(3,5-dimethylphen-1-yl)bis(trifluoromethanesulfonate) (**128**): To a solution of **127** (900 mg, 0.841 mmol) in CH_2Cl_2 (30 mL) was added ethyldiisopropylamine (0.35 mL, 270 mg, 2.1 mmol) and the resulting mixture was cooled to –40 °C ($CH_3CN/CO_{2(s)}$ bath). A solution of triflic anhydride (1.8 mL, 1.0 mol/L in CH_2Cl_2, 1.8 mmol) was added dropwise and the reaction mixture stirred for 30 min at –40 °C. Water was added and the phases were separated. The aqueous phase

was extracted with CH_2Cl_2. The combined organic phases were dried over Na_2SO_4 and concentrated *in vacuo*. The residue was suspended in hexane and the precipitate was filtered and washed with hexane, 1 N HCl, and water. The precipitate was dried *in vacuo*, affording **128** (641 mg, 57%) as a colorless solid.

Rf (silica, 5:5 CH_2Cl_2–hexane) 0.78;

mp (decomp. to red liquid) 140.7–141.5 °C;

^{1}H NMR (400 MHz, $CDCl_3$, δ) 7.84 (d, 2H, ^3J = 7.8 Hz), 7.60 (s, 2H), 7.21–7.18 (m, 8H), 7.01 (s, 4H), 6.90 (d, 4H, ^3J = 8.6 Hz), 4.38 (br s, 4H), 2.10 (s, 12H), 1.29–1.23, (m, 6H,), 1.10 (d, 36H, ^3J = 7.2 Hz);

^{13}C NMR (125 MHz, $CDCl_3$, δ) 155.5, 150.8 (br), 148.5, 141.9, 141.1, 139.5, 139.2, 137.7, 136.7, 134.2, 130.7, 129.6, 129.1, 125.6, 120.9, 120.0, 119 (q, J_{C-F} = 319 Hz), 59.4, 31.9, 21.4, 18.1, 12.9;

IR (neat) 2945*w*, 2892*w*, 2867*w* 1604*w*, 1516*m*, 1464*m*, 1421*m*, 1264*s*, 1237*s*, 1209*s*, 1170*w*, 1142*s*, 1120*m*, 1013*m*, 954*m*, 910*m*, 882*m*, 872*m*, 826*s*, 766*w*, 745*m*, 686*m*, 662*m*, 611*s*, 586*m*, 509*w* cm^{-1};

HRMS (ESI) Calcd for $C_{69}H_{78}NaF_6O_8S_2Si_2$ $[M+Na]^+$ 1355.3914, found 1355.3918.

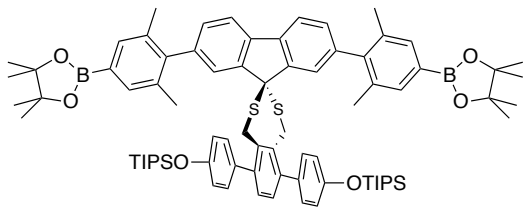

Spiro[(6,7-bis[4-triisopropyloxyphen-1-yl]-1,5-dihydrobenzo[e][1,3]dithiepane)-2,9'-(2',7'-bis[4-{4,4,5,5-tetramethyl-1,3,2-dioxaborolan-2-yl}-2,6-dimethylphenyl] fluorene)] (**129**): To a degassed, solid mixture of **128** (482 mg, 361 μmol), bis(pinacolato)diboron (229 mg, 903 μmol), Pd(dppf)•CH_2Cl_2 (30 mg, 36 μmol), 1,1'-bis(diphenylphosphino)ferrocene (20 mg, 36 μmol), KOAc (197 mg, 2.17 mmol) was added degassed 1,4-dioxane (30 mL) and the resulting mixture was stirred at 90 °C for 19 h. The reaction mixture was cooled to RT and the solvent was removed *in vacuo*.

The remaining residue was subjected to column chromatography (silica, CH_2Cl_2/hexane = 4:6), which afforded **129** as a colorless solid (279 mg, 56%).

Rf (silica, 5:5 CH_2Cl_2–hexane) 0.45;

mp (decomp. to red liquid) 192.4–194.2 °C;

^{1}H NMR (400 MHz, $CDCl_3$, δ) 7.80 (d, 2H, ^3J = 7.8 Hz), 7.66 (s, 2H), 7.56 (s, 4H), 7.20–7.17 (m, 8H), 6.89 (d, 4H ^3J = 8.5 Hz), 4.36 (s, 4H), 2.08 (s, 12H), 1.36 (s, 24H), 1.28–1.21 (m, 6H), 1.09 (d, ^3J = 7.1 Hz);

^{13}C NMR (125 MHz, $CDCl_3$, δ) 155.4, 150.3 (br), 144.8, 141.0, 137.9, 136.4, 135.7, 134.2, 134.0, 129.6, 129.0, 127.7 (br), 125.3, 120.5, 119.9, 83.9, 59.4, 31.7, 25.0, 21.0, 18.1, 12.8.

IR (neat) 2944*w*, 2892*w*, 2867*w*, 1605*m*, 1516*m*, 1468*m*, 1435*m*, 1385*m*, 1363*s*, 1311*m*, 1265*m*, 1230*m*, 1168*m*, 1145*s*, 1125*w*, 995*w*, 967*w*, 910*m*, 883*m*, 852*m*, 828*m*, 816*w*, 745*m*, 702*w*, 685*m*, 663*m*, 651*w* cm^{-1};

HRMS (ESI) Calcd for $C_{79}H_{102}NaB_2O_6S_2Si_2$ $[M+Na]^+$ 1311.6735, found 1311.6754.

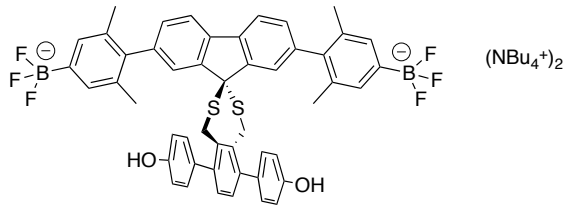

Bis(tetrabutylammonium) 4-{Spiro[(6,7-bis[4-triisopropyloxyphen-1-yl]-1,5-dihydrobenzo[e][1,3]dithiepane)-2,9'-fluorene]-2',7'-diyl}-bis(3,5-dimethylphen-1-yl)bis(trifluoroboronate) (138): To a solution of **129** (44 mg, 34 μmol) in THF (1 ml) in a plastic Eppendorf tube was added TBAF (75 μL, 1.0 mol/L in THF, 75 μmol) and the solution was stirred for 30 min, during which a colorless precipitate formed. MeOH (0.5 mL) was added, dissolving the precipitate, and KHF_2 was added (68 μmol, 4.5 mol/L, 310 μmol) and the reaction was stirred for 4 h. The reaction mixture was

transferred to a one-neck round-bottom flask and the solvent was removed *in vacuo* in a rotatory evaporator. A mixture of H_2O and MeOH (1:1) was added to the residue and the solution was concentrated in the rotatory evaporator to remove pinacol by azeotropic distillation. This distillation procedure was repeated three times and the remaining residue was dissolved in acetone, filtered through celite, and washed with acetone. The solvent was removed, affording **138** (40 mg, 87%) as a colorless solid.

Rf (EtOAc) 0.73;

mp (decomp.) 158.7–161.0 °C;

^{1}H NMR (500 MHz, acetone-d_6, δ) 8.50 (br s, 1.3H), 7.89 (d, 2H, ^3J = 7.7 Hz), 7.80 (s, 2H), 7.27 (s, 4H), 7.22–7.20 (m, 6H), 7.14 (s, 2H), 6.90 (d, 4H, ^3J = 8.4 Hz), 4.60 (s, 4H), 4.43–3.39 (m, 16H), 2.01 (s, 12H), 1.79 (m, 16H), 1.42 (hex, 16H, ^3J = 7.4 Hz), 0.97 (t, 24H, ^3J = 7.4 Hz);

^{13}C NMR (125 MHz, $CDCl_3$, δ) 164.2, 151.4, 143.4, 142.1, 139.0, 138.6, 136.7, 133.1, 132.5, 131.2, 131.0, 129.4, 128.5, 126.8, 120.8, 117.8, 60.3, 59.1, 32.3, 24.5, 21.6, 204, 14.1;

^{19}F NMR (376 MHz, acetone-d_6) –140.50 – –140.56 (m);

IR (neat) 2962*s*, 2936*m*, 2874*m*, 1696*w*, 1608*w*, 1588*w*, 1520*m*, 1483*m*, 1461*s*, 1381*m*, 1274*s*, 1252*m*, 1168*s*, 1150*s*, 1039*s*, 1008*s*, 981*s*, 934*m*, 924*m*, 876*s*, 839*s*, 820*s*, 740*m*, 639*w*, 620*w*, 540*w*, 532*w* cm^{-1};

HRMS (ESI) Calcd for $C_{49}H_{38}B_2F_6O_2S_2$ $[M]^{2-}$ (highest peak) 429.1215, found 429.1216.

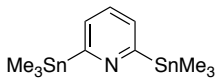

2,6-bis(trimethylstannyl)pyridine (**137**): Trimethyltin chloride (solid, 48.66 g, 244 mmol) was dissolved in dry DME (60 mL) in a round-bottom flask. In another round-bottom flask, sodium metal (~17.0 g, ~73 mmol, cut into small cubes of 1–3 mm length while storing in cyclohexane) was added and suspended in DME (140 mL). The flask containing sodium was cooled to –15 °C (NaCl/ice) bath and the trimethyltin

chloride-containing solution was added by cannula. The resulting mixture was stirred for 4h and temperature range –15 ˚C – –5 ˚C was maintained in the cooling bath. The resulting pistachio green mixture was added to a solution of 2,6-dichloropyridine (14.48 g, 97.8 mmol) in DME (60 mL) at –15 ˚C by using a cannula (most of the sodium pieces remain in their original flask). The resulting reaction mixture was stirred for 2 h at cold temperature (–5 ˚C – –5 ˚C) then an additional 13 h at RT. The contents of the reaction mixture were placed in a large round-bottom flask and the contents were removed by rotatory evaporator in a fume hood in a well-ventilated room. The dark, rock-like residue was broken down into small pieces with a spatula, suspended in Et_2O, filtered through celite and washed with Et_2O until the wash had no color. The organic solution was concentrated *in vacuo*, affording a dark, brown oil, which was subjected to fractional distillation (Vigreaux column installed, weak aspirator pump: ~80 mbar). The first fraction (oil temperature 130 ˚C–140 ˚C, bridge temperature 77 ˚C–78 ˚C) afforded a solid liquid mixture that did not contain the desired product. The second fraction (oil temperature 150 ˚C–170 ˚C, bridge temperature 140 ˚C–143 ˚C) afforded pure **137** (27.43 g, 69%) as a colorless oil. Characterization matched literature.[265]

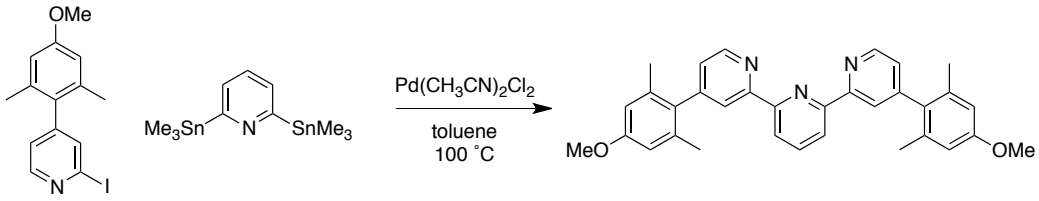

4,4”-bis(4-methoxy-2,6-dimethylphen-1-yl)-2,2’,6’,2”-terpyridine (**136**): Distannylpyridine **137** (413 mg, 1.02 mmol), iodophenylpyridine **135** (761 mg, 2.25 mmol), and $PdCl_2(CH_3CN)_2$ (16 mg, 0.1 mmol) were placed in a round-bottom flask affixed with a condenser. The mixture dissolved in cold, dry toluene and the solution was immediately frozen in a liquid N_2 bath. The solution was degassed by three rounds the freeze-pump-thaw method and the apparatus was refilled with N_2 after completion. After warming to RT, the mixture was heated to 70 ˚C and stirred at that temperature for 48 h, after which the reaction mixture was cooled to RT. Saturated, aqueous KF was added and the resulting black solid was filtered off and washed with EtOAc. The phases were separated and the aqueous phase was extracted with EtOAC. The combined organic phases were washed with saturated NaCl, dried over Na_2SO_4 and

concentrated *in vacuo*. Trituration with hot EtOH (two times) afforded **136** as a colorless powder. Characterization matched literature.[174–176]

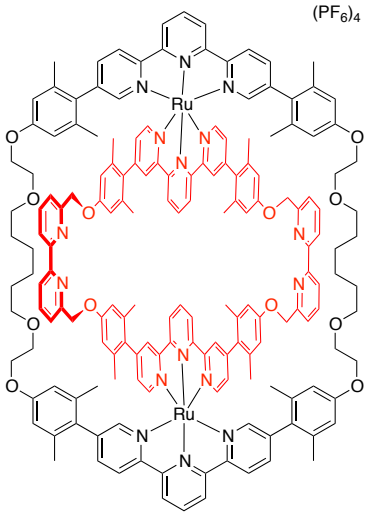

Ring-in-ring compound 76 was prepared following a modified procedure from Loren.[175,176] To a stirring solution of templated ring one [**76** $(PF_6)_4$] (50 mg, 18 μmol) in dry CH_3CN (20 mL, dried by passing through activated, neutral alumina and stored in 3 Å molecular sieves)—containing several 3 Å molecular sieves in the reaction mixture—was added Cs_3CO_3 (29 mg, 88 μmol), triethylene glycol dimethyl ether (20 μL), and 6,6'-bis(bromomethyl)-2,2'-bipyridine (15 mg, 44 μmol). The reaction mixture was heated to reflux and two additional portions of 6,6'-bis(bromomethyl)-2,2'-bipyridine (8 mg, 23 μmol) and (4 mg, 12 μmol) were added after 20 h and 52 h, respectively. After 72 h of total reaction time, the mixture was cooled to RT and filtered over celite to remove the molecular sieves and washed with acetone. The filtrate was concentrated and re-dissolved in a small amount of acetone, precipitated with sat. aq. KPF_6 solution, filtered and washed with water and Et_2O. The precipitate was re-collected by dissolving in acetone and subjected to column chromatography [silica, 100% EtOAc (removes impurities) → 95:5 CH_3CN/sat. aq. KPF_6 solution (flushes out Ru(II)-containing complexes)]. The red residue was suspended in CH_2Cl_2 and filtered. The resulting filtrate was concentrated and suspended in $CHCl_3$ and the suspension was filtered. The precipitate was then suspended in THF and filtered, affording **76** (23 mg, 41%) as a bright red precipitate. Characterization matched literature.[175,176]

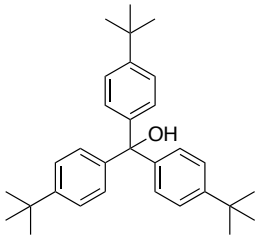

Tris(4-*t*-butylphenyl)methanol (**140**): To a solution of 1-bromo-4-*t*-butylbenzene (2.00 g, 9.39 mmol) in THF (20 mL) at –78 °C was added *n*-BuLi (3.8 mL, 2.5 mol/L in hexane, 9.4 mmol). The mixture was stirred at that temperature for 30 min and a solution of diethyl carbonate (317 mg, 2.68 mmol) in THF (10 mL) was added slowly. The reaction mixture was warmed to RT and stirred for 21 h, then H_2O was added and the phases were separated. The aqueous phase was extracted with EtOAc and the combined organic phase was washed with sat. NaCl, dried over Na_2SO_4 and concentrated *in vacuo*. The residue was recrystallized from hexane, affording **140** (577 mg, 53%) as a colorless solid. Characterization matched literature.[266]

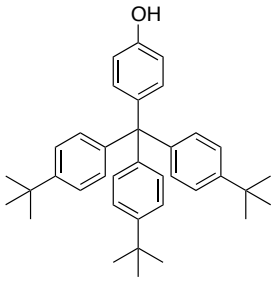

4-[Tris(4-*t*-butylphenyl)methyl]phenol (**140**): Alcohol **143** (500 mg, 1.17 mmol) and phenol (2.00 g, 21 mmol) were placed in a 5-mL round-bottom flask and heated to 80 °C while stirring, melting the phenol in the process. One drop of concentrated H_2SO_4 was added and the mixture immediately turned red. The reaction was stirred at 80 °C for 6 h, and then cooled to RT. The mixture was treated with 10% NaOH in H_2O and the precipitate was collected by filtration, washed with H_2O, and dried *in vacuo*. The residue was purified by column chromatography (silica, 1:9 CH_2Cl_2/hexane), affording **140** (520 mg, 88%) as a colorless solid. Characterization matched literature.[274]

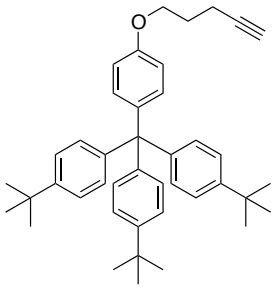

4-[Tris(4-t-butylphenyl)methyl]phenyl pent-4-yne-1-yl ether (**141**): To a solution of **140** (200 mg, 0.396 mmol) in THF (30 mL) was added Cs_2CO_3 (258 mg, 0.792 mmol) and 5-tosylpent-1-yne (141 mg, 0.594 mmol) and the reaction mixture was stirred at 60 °C for 24 h. The reaction mixture was cooled to RT and H_2O was added. The phases were separated and the aqueous phase was extracted with EtOAc. The combined organic phases were dried over Na_2SO_4 and concentrated in vacuo. The residue was purified by column chromatography (silica, 100% hexane → 4:6 CH2Cl2/hexane), which afforded **141** (166 mg, 74%) as a colorless solid. Characterization matched literature.[267]

6.5. Experimental Procedures for Compounds Shown in Chapter 5

6.5.1. Borromean Link Precursors

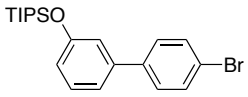

4-Bromo-3-(triisopropylsilyl)biphenyl: To a stirring solution of 3-bromophenyl triisopropylsilyl ether (10.01 g, 30.4 mmol) in THF (50 mL) at –78 °C was added *n*-BuLi (19.0 mL, 1.6 mol/L in hexane, 30.4 mmol) and the resulting mixture stirred for 30 min. A solution of $ZnCl_2$ (dried by melting, 5.12 g, 37.6 mmol) in THF (20 mL) was added to the mixture by syringe, which was subsequently allowed to warm to 0 °C. After 15 additional minutes of stirring at 0 °C, a solution of 1-bromo-4-iodobenzene (8.19 g, 28.9 mmol) and $Pd(PPh_3)_4$ (335 mg, 0.289 mmol) in THF (10 mL) was added. The reaction was warmed at RT and stirred for 15 min. Water was then added and the phases were separated. The aqueous phase was extracted with Et_2O and the combined organic phases were washed with sat. NaCl, dried over Na_2SO_4, and

concentrated *in vacuo*. The remaining residue was subjected to a short silica column (CH_2Cl_2/hexane = 0:10 → 1:9), which afforded 4-Bromo-3-(triisopropylsilyl)biphenyl (11.70 g, 100%) as a colorless oil.

Rf 0.34 (silica, hexane);

^{1}H NMR (300 MHz, $CDCl_3$, δ) 7.55 (d, 2H, ^3J = 8.6 Hz), 7.42 (d, 2H, ^3J = 8.6), 7.27 (t, 1H, ^3J = 8.6 Hz), 7.13–7.10 (m, 1H), 7.06 (t, 1H, ^4J = 2.0 Hz), 6.90–6.85 (m, 1H), 1.34–1.24 (m, 3H), 1.12 (d, 18H, ^3J = 6.9 Hz);

^{13}C NMR (100 MHz, $CDCl_3$, δ) 156.7, 141.6, 140.2, 132.0, 130.0, 128.9, 121.7, 119.9, 119.3, 118.7, 18.1, 12.9;

IR (neat) 2944*m*, 2891*m*, 2866*m*, 1600*m*, 1584*m*, 1473*s*, 1433*m*, 1387*m*, 1305*s*, 1257*m*, 1212*s*, 1074*m*, 1010*m*, 1000*m*, 934*s*, 881*s*, 824*s*, 783*s*, 706*m*, 683*s*, 660*m*, 511*m*, 451*m* cm^{-1};

HRMS (APCI) Calcd for $C_{21}H_{30}BrOSi$ $[M+H]^+$ 405.1244, found 405.1244.

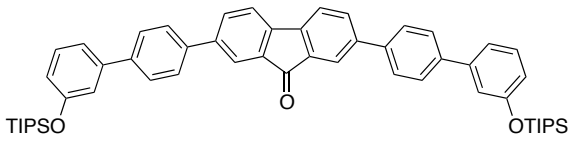

2,7-bis{4-[3-(triisopropylsilyloxy)phen-1-yl]phen-1-yl}fluoren-9-one (**155**): To a solution of 2,7-dibromofluoren-9-one (**100**) (7.66 g, 18.9 mmol) in THF (40 mL) at –78 °C was added *n*-BuLi (11.8 mL, 1.6 mol/L in 18.9 mmol). The reaction mixture was stirred for 30 min at –78 °C and $ZnCl_2$ (dried by melting *in vacuo*, 3.03 g, 22.0 mmol) in THF (20 mL) was added by syringe. The reaction was allowed to warm to 0 °C. A mixture of 2,7-dibromofluoren-9-one (2.10 g, 6.30 mmol) and $Pd(PPh_3)_4$ (367 mg, 0.315 mmol) in THF (35 mL) was added to the reaction mixture by cannula and the reaction was stirred at 60 °C for 2 h. The reaction was cooled to RT and H_2O was added. The phases were separated and the aqueous phase was extracted with EtOAc. The combined organic phases were washed with sat. aq. NaCl, dried over Na_2SO_4, and

concentrated *in vacuo*. Column chromatography (silica, CH_2Cl_2/hexane = 4:6) afforded **155** (3.78 g, 72%) as a bright orange solid.

Rf 0.60 (silica, 5:5 CH_2Cl_2–hexane);

mp 207.8–208.5 °C;

^{1}H NMR (400 MHz, $CDCl_3$, δ) 7.99 (d, 2H, ^4J = 1.4 Hz), 7.79 (dd, 2H, ^3J = 7.8 Hz, ^4J = 1.8 Hz), 7.72 (d, 4H, ^3J = 8.6 Hz), 7.68 (d, 4H, ^3J = 8.6 Hz), 7.63 (d, 2H ^3J = 7.8 Hz), 7.31 (t, 2H, ^3J = 7.7 Hz), 7.23 (dt, 2H, ^3J = 8.1 Hz, ^4J = 1.3 Hz), 7.17 (t, 2H, ^4J = 2.0 Hz), 6.91–6.88 (m, 2H), 1.35–1.26 (m, 6H), 1.15 (d, 36H, ^3J = 7.2 H)

^{13}C NMR (125 MHz, $CDCl_3$, δ) 193.9, 156.7, 143.2, 141.9, 141.8, 140.8, 138.8, 135.4, 133.3, 129.9, 127.8, 127.3, 123.0, 121.0, 119.2, 118.7, 18.2, 12.9.

IR (neat) 2943*m*, 2891*w*, 2866*m*, 1715*m*, 1599*m*, 1580*m*, 1555*w*, 1437*w*, 1424*w*, 1400*m*, 1389*w*, 1365*w*, 1300*m*, 1260*m*, 1213*s*, 1175*w*, 1014*w*, 999*m*, 936*s*, 881*s*, 849*w*, 824*s*, 783*s*, 737*m*, 708*w*, 682*s*, 655*m*, 643*m*, 619*w*, 561*w*, 509*m* cm^{-1};

HRMS (ESI) Calcd for $C_{55}H_{64}NaO_3Si_2$ $[M+Na]^+$ 851.4286, found 851.4283.

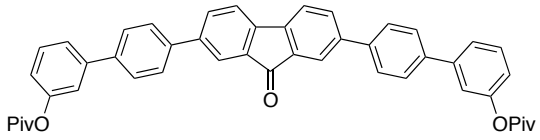

2,7-bis[4-(3-pivaloylphenyl)phen-1-yl]fluoren-9-one (**156**): To a solution of **155** (3.00 g, 3.62 mmol) in CH_2Cl_2 (50 mL) at 0 °C was added tetrabutylammonium fluoride (8.0 mL, 1.0 mol/L in THF, 8.0 mmol) and the reaction was stirred at that temperature for 5 min. PivCl (1.34 mL, 1.31 g, 10.9 mmol) and DMAP (88 mg, 0.72 mmol) were added and the reaction was stirred at RT for 2 h. H_2O was added and the phases were separated. The aqueous phase was extracted with CH_2Cl_2 and the organic phase was washed with sat. aq. NaCl, dried over Na_2SO_4, and concentrated *in vacuo*. The residue was purified by column chromatography (silica, CH_2Cl_2/hexane = 6:4), which afforded **156** (1.77 g, 71%) as a bright orange solid.

Rf 0.51 (silica, CH_2Cl_2);

mp (decomp.) 283.4–287.5 °C (begins to discolor ~275 °C);

^{1}H NMR (500 MHz, $CDCl_3$, δ) 7.98 (d, 2H, ^{4}J = 1.3 Hz), 7.79 (dd, 2H, ^{3}J = 7.7 Hz, ^{4}J = 1.6 Hz), 7.71 (d, 4H, ^{3}J = 8.6 Hz), 7.69 (d, 4H, ^{3}J = 8.6 Hz), 7.63 (d, 2H ^{3}J = 7.8 Hz), 7.51 (t, 2H, ^{3}J = 7.8 Hz), 7.47 (t, 2H, ^{3}J = 7.8 Hz), 7.34 (t, 2H, ^{4}J = 1.8 Hz), 7.09–7.06 (m, 2H), 1.40 (s, 18H);

^{13}C NMR (125 MHz, $CDCl_3$, δ) 193.9, 177.3, 151.7, 143.4, 142.2, 141.8, 140.0, 139.2, 135.5, 133.4, 129.9, 127.3, 124.5, 123.1, 121.1, 120.8, 120.3, 39.3, 27.4;

IR (neat) 2971*w*, 1752*m*, 1704*m*, 1605*w*, 1584*w*, 1465*m*, 1397*w*, 1274*w*, 1176*m*, 1162*m*, 1112*s*, 914*w*, 882*w*, 824*m*, 779*m*, 693*w*, 421*w* cm^{-1};

HRMS (ESI) Calcd for $C_{47}H_{40}NaO_5$ $[M+H]^+$ 685.2949, found 685.2945.

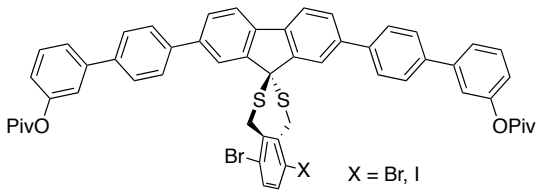

3,3'-{Spiro[(6,7-dibromo-1,5-dihydrobenzo[e][1,3]dithiepane)-2,9'-fluorene]-2',7'-diyl}-bis(3,5-dimethylphen-1-yl) bis(2,2-dimethylpropanoate) (**157**) and **4-{Spiro[(6-iodo-7-bromo-1,5-dihydrobenzo[e][1,3]dithiepane)-2,9'-fluorene]-2',7'-diyl}-bis(3,5-dimethylphen-1-yl) bis(2,2-dimethylpropanoate)** (**158**): To a solution of **156** (1.20 g, 1.75 mmol) and a mixture of **119** (69%) and **120** (31%) (650 mg, 1.81 mmol total) in CH_2Cl_2 (50 mL) was added $AlCl_3$ (118 mg, 0.85 mmol) and the reaction mixture was stirred at RT. After 4 h, an additional portion of $AlCl_3$ (29 mg, 0.22 mmol) was added. The reaction was stirred for an additional 3 h and was subsequently quenched with H_2O. The phases were separated and the aqueous phase was extracted with CH_2Cl_2. The organic phase was dried over Na_2SO_4 and concentrated *in vacuo*. Column chromatography (silica, CH_2Cl_2/hexane 4:6 → 8:2) yielded a mixture of **157** and **158** (1.23 g, 68% total yield) as a colorless solid mixture that was not separated before the next step.

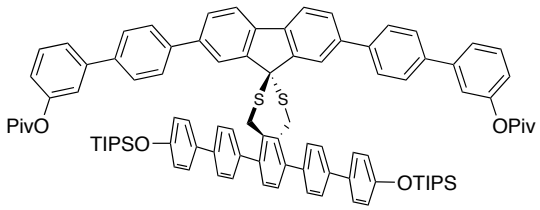

3,3'-{Spiro[4-(6,7-bis[4-triisopropyloxyphen-1-yl)phenyl]-1,5-dihydrobenzo[e][1,3] dithiepane)-2,9'-fluorene]-2',7'-diyl}-bis(3,5-dimethylphen-1-yl) bis(2,2-dimethylpropanoate) (**160**)**:** To a stirring solution of 4-bromo-4-(triisopropylsiloxy)-1,1-biphenyl (632 mg, 1.56 mmol) in THF (5 mL) at –78 °C was added *n*-BuLi (1.00 mL, 1.6 mol/L in hexane, 1.56 mmol) and the reaction mixture was stirred at that temperature for 30 min. A solution of $ZnCl_2$ (265 mg, 1.95 mmol) in THF (5 mL) was added and the reaction mixture was allowed to warm to 0 °C. A mixture of **157** and **158** (400 mg, 0.389 mmol total) and $Pd(PPh_3)_4$ (45 mg, 0.039 mmol) in THF (5 mL) was added to the reaction mixture by syringe and the mixture was then stirred for 22 h at 60 °C. The reaction mixture was cooled to RT and H_2O and CH_2Cl_2 were added. The phases were separated and the aqueous layer was extracted with CH_2Cl_2. The combined organic phases were dried over Na_2SO_4 and concentrated *in vacuo*. The residue was purified by column chromatography (silica, CH_2Cl_2/hexane = 2:8 → 5:5), affording **160** (386 mg, 67%) as a colorless solid.

Rf 0.47 (silica, CH_2Cl_2);

mp >300 °C;

^{1}H NMR (500 MHz, $CDCl_3$, δ) 8.20 (d, 2H, J = 1.0 Hz), 7.84 (d, 2H, 8.0 Hz), 7.73–7.70 (m, 6H), 7.66 (d, 4H, ^3J = 8.4 Hz), 7.61 (d, 4H, ^3J = 8.6 Hz), 7.50–7.53 (m, 12H), 7.39 (s, 2H), 7.31 (t, 2H, 1.9 Hz), 7.06 (dt, 2H, ^3J = 8.4 Hz, ^4J = 1.8 Hz), 6.93 (d, 4H, 8.6 Hz), 4.60 (br s, 4H), 1.39 (s, 18H), 1.31–1.24 (m, 6H), 1.11 (d, 36H, 7.4 Hz)

^{13}C NMR (125 MHz, $CDCl_3$, δ) 177.3, 156.0, 150.8 (br), 151.7, 142.4, 141.4, 140.9, 140.4, 140.0, 139.7, 139.6, 138.3, 136.9, 133.4, 130.1, 129.9, 129.1, 128.2, 128.1, 127.82, 127.79, 126.8, 124.5, 123.4 (br), 121.0, 120.6, 120.4, 120.3, 59.2, 39.3, 32.0, 27.4, 18.1, 12.9;

IR (neat) 2960*w*, 2944*m*, 2891*w*, 2866*m*, 1752*m*, 1604*m*, 1585*w*, 1524*w*, 1499*m*, 1463*s*, 1396*w*, 1366*w*, 1266*s*, 1174*m*, 1162*m*, 1113*s*, 1028*w*, 1014*w*, 1000*w*, 911*s*, 882*m*, 819*s*, 773*m*, 738*w*, 710*m*, 678*m*, 662*m*, 648*w*, 526*w* cm^{-1};

HRMS (ESI) Calcd for $C_{97}H_{104}NaO_6S_2Si_2$ $[M+Na]^+$ 1507.6705, found 1507.6696.

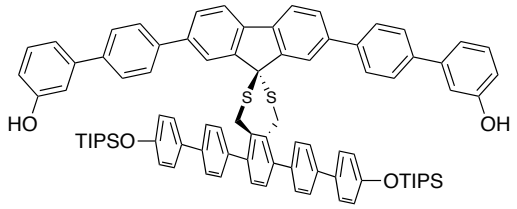

Spiro[(6,7-bis{4-[4-triisopropyloxyphen-1-yl]phenyl}-1,5-dihydrobenzo [e][1,3]dithiepane)-2,9'-(2',7'-bis[4-(3-hydroxyphen-1-yl)phenyl] fluorene)] (162): To a solution of **160** (337 mg, 0.223 mmol) in THF (30 mL) and toluene (30 mL) at –78 °C was added methyllithium (0.57 mL, 1.6 mol/L in Et_2O, 0.92 mmol). The reaction was allowed to warm to RT and stirred for 2.5 h. H_2O was added slowly (under N_2) and the phases were separated. The aqueous phase was extracted with EtOAc and the combined organic phases were dried over Na_2SO_4 and concentrated *in vacuo*. The residue was triturated in hot hexane and filtered while hot, affording **162** (294 mg), which was used in the next step without further purification.

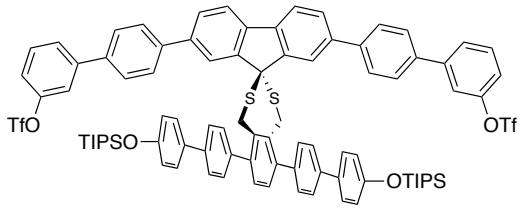

Spiro[(6,7-bis{4-[4-triisopropyloxyphen-1-yl]phenyl}-1,5-dihydrobenzo [e][1,3]dithiepane)-2,9'-(2',7'-bis[4-(3-triflylphen-1-yl)phenyl] fluorene)] (161): To a cloudy suspension of **162** (273 mg, 0.207 mmol) in CH_2Cl_2 (50 mL) was added diisopropylethylamine (0.34 mL, 270 mg, 2.1 mmol), which resulted in a transparent solution. The mixture was cooled to –40 °C (dry ice/CH_3CN) and triflic anhydride (0.46 mL, 1.0 mol/L in CH_2Cl_2, 0.46 mmol) was added over 1 min. The reaction was stirred at –40 °C for 4 h, after which H_2O was added and the phases were separated.

The aqueous phase was extracted with CH_2Cl_2 and the combined organic phases were dried over Na_2SO_4 and concentrated *in vacuo*. The residue was subjected to column chromatography (silica, 5:5 CH_2Cl_2/hexane), affording **161** (253 mg, 75% over two steps) as a colorless solid.

Rf 0.70 (silica, 5:5 CH_2Cl_2/hexane);

mp (decomp. to red liquid) 291.8–292.3 °C;

^{1}H NMR (500 MHz, $CDCl_3$, δ) 8.21 (d, 2H, J = 1.0 Hz), 7.86 (d, 2H, ^3J = 8.0 Hz), 7.76 (d, 4H, ^3J = 8.4 Hz) 7.72 (dd, 2H, ^3J = 8.0 Hz, ^4J = 1.5 Hz), 7.66–7.64 (m, 6H), 7.61 (d, 4H, ^3J = 8.4 Hz), 7.54 (t, 2H, ^3J = 7.56), 7.51 (t, 2H, ^4J = 1.9 Hz), 7.49 (d, 4H, ^3J = 8.4 Hz), 7.46 (d, 4H, ^3J = 8.7 Hz), 7.27 (dd, ^4J = 1.9 Hz, partially obstructed by $CHCl_3$ peak), 6.94 (d, 4H, ^3J = 8.7 Hz), 4.60 (br s, 4H), 1.31-1.26 (m, 6H), 1.11 (d, 36H, ^3J = 7.4 Hz);

^{13}C NMR (125 MHz, $CDCl_3$, δ) 156.1, 150.9 (br), 150.3, 143.6, 141.4, 141.1, 140.7, 140.0, 139.6, 133.4, 130.8, 130.1, 129.1, 128.2, 128.12, 128.09, 127.1, 126.8, 123.4 (br), 121.2, 120.4, 120.1, 120.0, 119.0 (q, J_{C-F} = 319 Hz), 59.2, 32.0, 18.1, 12.9;

IR (neat) 3030*w*, 2945*w*, 2893*w*, 2868*w*, 1604*m*, 1499*m*, 1463*m*, 1424*m*, 1265*m*, 1244*s*, 1210*s*, 1171*m*, 1138*s*, 998*w*, 907*s*, 882*s*, 810*s*, 787*m*, 770*m*, 739*m*, 709*m*, 685*s*, 661*m*, 605*s*, 576*m*, 512*m*, 444*w*;

HRMS (APCI) Calcd for $C_{89}H_{86}F_6NaO_8S_4Si_2$ $[M+Na]^+$ 1603.4540, found 1603.4526.

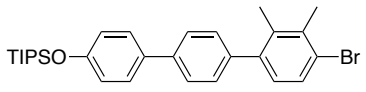

4-bromo-2,3-dimethyl-4"-(triisopropylsilyloxy)[1,1';4',1"]terphenyl (163): To a solution of 4-bromo-4-(triisopropylsiloxy)-1,1-biphenyl (1.87 g, 4.62 mmol) in THF (15 mL) at –78 °C was added *n*-BuLi (2.9 mL, 1.6 mol/L, 4.6 mmol) and the reaction mixture was stirred at that temperature for 30 min. $ZnCl_2$ (777 mg, 5.72 mmol, dried by melting) in THF (10 mL) was added and the stirring mixture was allowed to warm

to 0 °C. A mixture of **113** (1.37 g, 4.40 mmol) and $Pd(PPh_3)_4$ (254 mg, 0.22 mmol) in THF (10 mL) was added and the mixture was stirred at RT for 24 h, after which H_2O was added and the phases were separated. The aqueous phase was extracted with EtOAc and the combined organic phases were washed with sat NaCl, dried over Na_2SO_4, and concentrated *in vacuo*. Column chromatography (silica, hexane) afforded **163** (1.50 g, 67%) as a colorless solid.

Rf 0.15 (hexane);

mp 125.5–126.4 °C;

^{1}H NMR (500 MHz, $CDCl_3$, δ) 7.60 (d, 2H, ^3J = 8.3 Hz), 7.51 (d, 2H, ^3J = 8.6 Hz), 7.46 (d, 1H, ^3J = 8.1 Hz), 7.30 (d, 2H, ^3J = 8.3 Hz), 6.99–6.94 (m, 3H), 2.46 (s, 3H), 2.26 (s, 3H), 1.32–1.25 (m, 3H), 1.13 (d, 18H, 7.0 Hz);

^{13}C NMR (100 MHz, $CDCl_3$, δ) 156.0, 141.6, 140.3, 139.7, 136.7, 136.3, 133.6, 129.81, 129.79, 128.8, 128.1, 126.5, 124.7, 20.4, 18.9, 18.1, 12.9;

IR (neat) 3033*w*, 2943*m*, 2890*w*, 2865*m*, 1601*m*, 1522*m*, 1495*s*, 1461*s*, 1387*m*, 1266*s*, 1192*m*, 1171*m*, 1137*w*, 1105*w*, 917*s*, 881*s*, 830*s*, 810*s*, 660*s*, 619*m*, 589*m*, 542*m*, 452*m*;

HRMS (APCI) Calcd for $C_{29}H_{38}BrOSi$ $[M+H]^+$ 509.1870, found 509.1867.

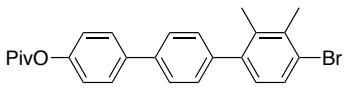

4”-bromo-2”,3”-dimethyl[1,1’;4’,1”]terphen-1-yl pivaloate (164): To a solution of **163** (1.40 g, 2.75 mmol) in CH_2Cl_2 (25 mL) at 0 °C was added tetrabutylammonium fluoride (5.5 mL, 1.0 mol/L in THF, 5.5 mmol) and the resulting mixture was stirred for 15 min. H_2O was then added, the phases were separated and the aqueous phase was extracted with CH_2Cl_2. The combined organic phases were dried over Na_2SO_4 and concentrated *in vacuo*. The residue was dissolved in CH_2Cl_2 (20 mL) and the solution was cooled to 0 °C. Triethylamine (0.46 mL, 330 mg, 3.3 mmol) and pivaloyl chloride (0.38 mL, 370 mg, 3.0 mmol) were added and the reaction was stirred at RT for 14.5

h. H_2O was added, the phases were separated, and the aqueous phase was extracted with CH_2Cl_2. The combined organic phases were dried over Na_2SO_4 and concentrated *in vacuo*. The residue was subjected to column chromatography (silica, CH_2Cl_2/hexane = 2:8) to afford **164** (1.12 g, 93%) as a colorless solid.

Rf 0.60 (silica, 5:5 CH_2Cl_2/hexane);

mp 152.7–153.9 °C;

^{1}H NMR (500 MHz, $CDCl_3$, δ) 7.64 (d, 2H, ^3J = 8.6 Hz), 7.62 (d, 2H, ^3J = 8.3 Hz), 7.48 (d, 1H, ^3J = 8.2 Hz), 7.33 (d, 2H, ^3J = 8.3 Hz), 7.17 (d, 2H, ^3J = 8.6 Hz), 6.98 (d, 1H, ^3J = 8.2 Hz), 2.48 (s, 3H), 2.27 (s, 3H), 1.40 (s, 9H);

^{13}C NMR (100 MHz, $CDCl_3$, δ) 177.3, 150.8, 141.3, 141.0, 139.2, 138.4, 136.8, 136.3, 129.9, 129.8, 128.7, 128.2, 127.0, 124.8, 122.0, 39.3, 27.3, 20.4, 18.9;

IR (neat) 2970*w*, 2870*w*, 1747*m*, 1601*w*, 1496*m*, 1478*m*, 1460*m*, 1392*w*, 1365*w*, 1265*m*, 1232*w*, 1206*m*, 1192*m*, 1167*m*, 1110*s*, 1028*m*, 1004*m*, 942*w*, 897*m*, 840*m*, 813*s*, 795*m*, 737*s*, 704*m*, 610*w*, 570*w*, 531*m* cm^{-1};

HRMS (APCI) Calcd for $C_{25}H_{25}BrNaO$ $[M+Na]^+$ 459.0930, found 459.0928.

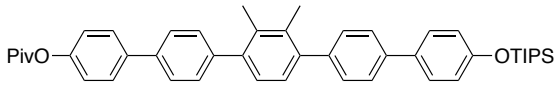

4''''-(triisopropylsilyloxy)-2'',3''-dimehtyl[1,1';4',1'';4'',1''';4''',1'''']quinquephen-1-yl pivaloate (**165**)**:** To a solution of 4-bromo-4-(triisopropylsiloxy)-1,1-biphenyl (204 mg, 0.503 mmol) in THF (5 mL) at –78 °C was added *n*-BuLi (0.31 mL, 1.6 mol/L in hexane, 0.503 mmol) and the reaction mixture was stirred at –78 °C for 30 min. A solution of $ZnCl_2$ (81 mg, 0.595 mmol, dried by melting *in vacuo*) in THF (5 mL) was added and the reaction was allowed to warm to 0 °C. A solution of **164** (200 mg, 0.458 mmol) and $Pd(PPh_3)_4$ (26 mg, 23 μmol) in THF (5 mL) was added and the reaction mixture was heated to 60 °C for 5.5 h, then to 70 °C for another 12 h. The reaction mixture was concentrated and H_2O and CH_2Cl_2 were added. The phases were separated and the aqueous phase was extracted with CH_2Cl_2. The combined organic

phases were dried over Na_2SO_4 and concentrated *in vacuo*. The residue was purified by column chromatography (silica, 2:8 → 5:5 CH_2Cl_2/hexane) to afford **165** (156 mg, 50%) as a colorless solid.

Rf 0.60 (silica, 5:5 CH_2Cl_2/hexane);

mp 179.3–180.1 °C;

^{1}H NMR (400 MHz, $CDCl_3$, δ) 7.67–7.62 (m, 6H), 7.53 (d, 2H, ^3J = 8.7 Hz), 7.44 (d, 2H, ^3J = 8.4 Hz), 7.41 (d, 2H, ^3J = 8.4 Hz), 7.20 (s, 2H), 7.17 (d, 2H, ^3J = 8.7 Hz), 6.97 (d, 2H, ^3J = 8.6 Hz), 2.30 (s, 6H), 1.39 (s, 9H), 1.34–1.27 (m, 3H), 1.14 (d, 18H, ^3J = 4.3 Hz);

^{13}C NMR (125 MHz, $CDCl_3$, δ) 177.4, 141.9, 141.4, 141.1, 141.0, 139.4, 138.9, 138.6, 135.0, 134.9, 133.7, 130.2, 130.1, 128.2, 128.1, 127.4, 127.3, 126.9, 26.5, 122.0, 120.4, 39.3, 27.4, 18.14, 18.11, 18.10, 12.9;

IR (neat) 2945*m*, 2869*m*, 1750*m*, 1603*w*, 1525*w*, 1499*s*, 1472*s*, 1390*w*, 1366*w*, 1266*s*, 1234*w*, 1204*m*, 1192*m*, 1168*m*, 1116*s*, 1027*w*, 1005*m*, 913*m*, 883*m*, 819*s*, 795*w*, 769*m*, 699*m*, 685*m*, 591*w*, 528*w* cm^{-1};

HRMS (APCI) Calcd for $C_{46}H_{55}O_3Si$ $[M+H]^+$ 683.3915, found 683.3907.

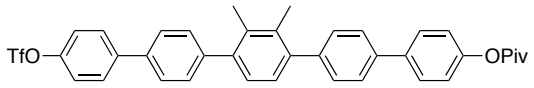

4''''-(pivaloyl)-2'',3''-dimehtyl[1,1';4',1'';4'',1''';4''',1'''']quinquephen-1-yl triflate (166): To a solution of **165** (600 mg, 0.878 mmol) in CH_2Cl_2 (10 mL) at 0 °C was added TBAF (0.97 mL, 1.0 mol/L in THF, 0.97 mmol) over 1 min. After 10 min, triflic anhydride (1.05 mL, 1.0 mol/L in CH_2Cl_2 was added at 0 °C over one min. The reaction stirred at RT for 6 h and H_2O was added. The phases were separated and the aqueous phase was extracted with CH_2Cl_2. The organic phase was dried over Na_2SO_4 and concentrated *in vacuo*. The residue was subjected to column chromatography (silica, 4:6 CH_2Cl_2/hexane), which afforded **166** (65 mg, 11%) as a colorless solid. A

flush of the column with EtOAc afforded the alcohol intermediate (313 mg, 68%) as a colorless solid.

Rf 0.48 (silica, 5:5 CH_2Cl_2/hexane);

mp 259.3–260.5 °C;

^{1}H NMR (500 MHz, $CDCl_3$, δ) 7.72 (d, 2H, ^3J = 8.7 Hz), 7.67–7.63 (m, 6H), 7.47 (d, 2H, ^3J = 8.1 Hz), 7.44 (d, 2H, ^3J = 8.1 Hz), 7.38 (d, 2H, ^3J = 8.7 Hz), 7.213 (s, 1H), 7.207 (s, 1H), 7.17 (d, 2H, ^3J = 8.6 Hz), 2.31 (s, 3H), 2.30 (s, 3H), 1.40 (s, 9H);

^{13}C NMR (125 MHz, $CDCl_3$, δ) 177.4, 150.7, 149.1, 142.6, 141.7, 141.6, 141.4, 140.9, 139.0, 138.6, 137.8, 135.0, 134.9, 130.3, 130.1, 129.0, 128.2, 127.4, 127.3, 127.1, 127.0, 122.0, 121.9, 119.0 (q, J_{C-F} = 319 Hz), 39.3, 27.4, 18.10, 18.09;

IR (neat) 2974*w*, 1750*m*, 1603*w*, 1499*m*, 1473*m*, 1426*m*, 1402*w*, 1278*w*, 1251*m*, 1213*s*, 1192*m*, 1168*m*, 1141*s*, 1113*s*, 1005*w*, 887*m*, 819*m*, 795*w*, 707*w*, 614*w*, 525*w* cm^{-1};

HRMS (APCI) Calcd for $C_{38}H_{34}F_3O_5S$ $[M+H]^+$ 659.2074, found 659.2065.

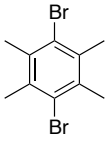

1,4-Dibromo-2,3,4,5-tetramethylbenzene (**173**): To a solution of 1,2,4,5-tetramethylbenzene (2.00 g, 14.9 mmol) in CH_2Cl_2 (20 mL) was added solid I_2 (152 mg, 0.30 mmol). A solution of Br_2 (2.0 mL, 6.2 g, 39 mmol) in CH_2Cl_2 (20 mL) was added to over 10 min and the reaction mixture was then heated to reflux for 90 min. The reaction was cooled to RT and NaOH (aq., 5M) was added. The mixture was filtered, affording **173** (3.11 g, 71%) as a colorless precipitate after washing with H_2O and cold hexane. Characterization matched literature.[240]

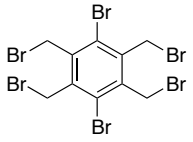

1,4-Dibromo-2,3,5,6-tetrakis(bromomethyl)benzene (**174**): to a solution of **173** (1.02 g, 3.49 mmol) in CCl_4 (10 mL) was added Br_2 (0.74 mL, 2.3 g, 14 mmol) over 10 min and the reaction was irradiated with visible light at 375 Watt for 5 h. The reaction was cooled to RT and the mixture was filtered. The obtained precipitate was recrystallized from $CHCl_3$, affording **173** (1.45 g, 68%) as a colorless solid. Obtained spectra matched literature spectra.[268]

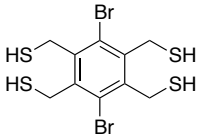

1,4-Dibromobenzene-2,3,5,6-tetramethanethiol (**172**): To a solution of **174** (800 mg, 1.32 mmol) in EtOH (20 mL) was added thiourea (500 mg, 6.58 mmol) and the reaction was heated to reflux for 1.5 h. The mixture was cooled to RT and the solvent was removed *in vacuo*. The residue was suspended in H_2O (10 mL) and NaOH (421 mg, 10.5 mmol) was added and the mixture was heated to reflux for 24 h. The reaction mixture was cooled to RT and brought to neutral pH with 3 mol/L aq. H_2SO_4 and extracted with CH_2Cl_2. The organic phase was dried over Na_2SO_4 and concentrated *in vacuo* to afford a crude mixture that was purified by crystallization from CH_2Cl_2/hexane, affording **172** (203 mg, 37%).

mp 199.9–200.7 °C;

^{1}H NMR (300 MHz, $CDCl_3$, δ) 4.06 (d, 8H, ^3J = 7.7 Hz), 2.15 (t, 4H, ^3J = 7.7 Hz);

^{13}C NMR (125 MHz, $CDCl_3$, δ) 139.9, 127.4, 28.5;

IR (neat) 2985*w*, 2568*w*, 1469*w*, 1433*s*, 1391*m*, 1243*s*, 1197*s*, 1112*m*, 965*s*, 856*w*, 735*m*, 676*m* cm^{-1};

HRMS (EI) Calcd for $C_{10}H_8Br_2S_4$ $[M–(2\ H_2)]^+$ 413.7876, found 413.7872. (disulfide formation during ionization).

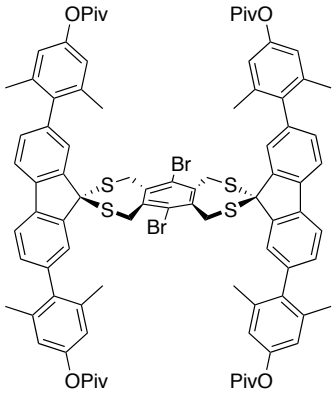

dispiro[(2,7-bis[4-pivaloyl-2,6-dimethylphenyl]fluorene)-9,2'-(6',7'-dibromo-1',5'-dihydrobenzo[e][1,3]dithiepane)-2',9"-(2",7"-bis[4"-pivaloyl-2",6"-dimethylphenyl]fluorene)] (**175**): To a solution of **105** (374 mg, 0.64 mmol) and **172** (133 mg, 0.32 mmol) in CH_2Cl_2 (20 mL) was added $AlCl_3$ (42 mg, 0.32 mmol) and the reaction was stirred at RT for 18 h. H_2O was then added and the phases were separated. The aqueous phase was extracted with CH_2Cl_2 and the combined organic phases were dried over Na_2SO_4 and concentrated *in vacuo*. The crude residue was subjected to column chromatography (silica, 6:4 [yields impurities] → 8:2 [yields product] CH_2Cl_2/hexane), affording **175** (182 mg, 37%) as a colorless solid.

Rf 0.43 (silica, 5:5 CH_2Cl_2/hexane);

mp (decomp. to red liquid) 291.0–292.2 °C;

^{1}H NMR (500 MHz, $CDCl_3$, δ) 7.83 (d, 4H, ^3J = 7.7 Hz), 7.65 (br s, 4H), 7.23 (dd, 4H, ^3J = 7.7 Hz, ^4J = 1.2 Hz), 4.85 (br s, 8H), 2.08 (s, 24H), 1.38 (s, 36H)

^{13}C NMR (100 MHz, $CDCl_3$, δ) 177.5, 150.1, 140.7, 140.1, 138.9, 137.8, 136.4, 130.5, 126.1, 125.4, 120.7, 120.4, 59.8, 39.3, 35.9, 27.4, 21.2;

IR (neat) 2972*w*, 2930*w*, 2871*s*, 1749*m*, 1591*w*, 1479*w*, 1460*m*, 1396*w*, 1272*m*, 1139*s*, 1111*s*, 1031*w*, 902*w*, 823*s* cm^{-1};

HRMS (EI) Calcd for $C_{88}H_{88}Br_2O_8NaS_4$ $[M+Na]^+$ 1581.3621, found 1581.3632.

References

[1] van 't Hoff, J. H. *La chimie dans l'espace*, P. M. Bazendijk: Rotterdam, 1875. For the English translation, see: van 't Hoff, J. H. *The Arrangement of Atoms in Space*, 2nd ed. (A. Eiloart, trans.), Longmans, Green, and Co.: New York, 1898. The discussion of free rotation about a single bond is introduced on p. 54 of this version

[2] The tetrahedral carbon atom was independently described by van 't Hoff and J. A. Le Bel in 1874. See: (a) Ref. 1 (b) van 't Hoff, J. H. *Bull. Soc. Chim. Fr.* **1875**, *23*, 295. (b) Le Bel, J. A. *Bull. Soc. Chim. Fr.* **1874**, *22*, 337.

[3] For an excellent review of van 't Hoff and Le Bel in their historical contexts, see: Riddel, F. G.; Robinson, M. J. T. *Tetrahedron*, **1974**, *30*, 2001.

[4] (a) Balzani, V.; Credi, A.; Raymo, F. M.; Stoddart, J. F. *Angew. Chem., Int. Ed.* **2000**, *39*, 3348. (b) Browne, W. R.; Feringa, B. L. *Nature Nanochem.* **2006**, *1*, 25. (c) Kay, E. R.; Leigh, D. A.; Zerbetto, F. *Angew. Chem., Int. Ed.* **2007**, *46*, 72. (d) Carella, A.; Coudret, C.; Guirado, G.; Rapenne, G.; Vives, G.; Launay, J.-P. *Dalton Trans*. **2007**, 177.

[5] For an excellent review of artificial molecular rotators, see: Kottas, G. S.; Clarke, L. I.; Horinek, D.; Michl, J. *Chem. Rev.* **2005**, *105*, 1281.

[6] Mislow, K. *Chemtracts: Org. Chem.* **1989**, *2*, 151.

[7] (a) (b) Feringa, B. L. *Acc. Chem. Res.* **2001**, *34*, 504. (c) Broer, D. J.; Feringa, B. L. *Nature*, **2006**, *440*, 163.

[8] (a) Khuong, T.-A. V.; Nunez, J. E.; Godinez, C. E.; Garcia-Garibay, M. A. *Acc. Chem. Res.* **2006**, *39*, 423. (b) Godinez, C. E.; Zepeda, G.; Garcia-Garibay, M. A. *J. Am. Chem. Soc.* **2002**, *124*, 4701. and ref. 5.

[9] (a) Clarke, L. I.; Horinek, D.; Kottas, G. S.; Varaska, N.; Magnera, T. F.; Hinderer, T. P.; Horansky, R. D.; Michl, J.; Price, J. C. *Nanotechnology.* **2002**, *13*, 533. (b) Hou, S.; Sagara, T.; Xu, D.; Kelly, T. R.; Ganz, E. *Nanotechnology*, **2003**, *14*, 566. (c) van Delden, R. A.; ter Wiel, M. K. J.; Pollard, M. M.; Vicario, J.; Koumura, N.; Feringa, B. L. *Nature.* **2005**, *437*, 1337.

[10] Magnera, T. F.; Michl, J. *Top. Curr. Chem.* **2006**, *262*, 63. and references cited therein.

[11] Molecular propellers and motors will be discussed in this chapter, but molecular switches will not. For mor information on molecular switches, see: (a) Feringa, B. L., ed. *Molecular Switches*, Wiley–VCH: Weinheim, 2001. and (b) Feringa, B. L. and Browne, W. L., eds. *Molecular Switches: Second, Completely Revised and Enlarged Edition*, Wiley-VCH: Weinheim, 2011. and references cited therein

[12] Dudley, D. W. 'The Evolution of the Gear Art", Dual Printing, Buffalo, **1969**.

[13] Oberg, E.; Johnes, F. D.; Horton, H. L.; Ryffel, H. H. *Machinery's Handbook; A Reference Book for the Mechanical Engineer, Designer, Manufacturing Engineer, Draftsman, Toolmaker, and Machinist*, 26th ed.; Industrial Press: New York, 2000.

[14] Photograph of gear shaft: http://www.cnccookbook.com/CCBlogMar08.htm (accessed February 15, 2012).

[15] Photograph of bevel gear and spur gears courtesy of Emerson Power Transmission Corporation (http://www.emerson-ept.com).

[16] (a) Iverson, D. J.; Hunter, G.; Blount, J. F.; Damewood Jr., J. R.; Mislow, K. *J. Am. Chem. Soc.* **1981**, *103*, 6073. (b) Hunter, G.; Weakley, T. J. R.; Weissensteiner, W. *J. Chem. Soc., Perkin Trans. 2* **1987**, 1633. (c) Hunter, G.; Mislow, K. *J. Chem. Soc., Chem. Commun.* **1984**, 172. (d) Kilway, K. V.; Siegel, J. S. *J. Am. Chem. Soc.* **1991**, *113*, 2332.

[17] Siegel, J.; Gutiérrez, A.; Schweizer, W. B.; Ermer, O.; Mislow, K. *J. Am. Chem. Soc.* **1986**, *108*, 1569.

[18] Hounshell, W. D.; Iroff, L. D.; Iverson, D. J.; Wroczynski, R. J.; Mislow, K. *Isr. J. Chem.* **1980**, *20*, 65.

[19] See Refs. 8 and 9 and references cited therein.

[20] Christie, G. H.; Kenner, J. *J. Chem. Soc.* **1922**, *121*, 614.

[21] Adams, R.; Yuan, H. C. *Chem. Rev.* **1933**, *12*, 261.

[22] Kuhn, R. In *Stereochemie*: Freudenberg, H., Ed.; Franz Deutike: Leipzig-Wien, 1933; pp 803–824.

[23] Ōki, M. *Top. Stereochem.*, **1983**, *14*, 1.

[24] Toyota, S.; Iida, T.; Kunizane, D.; Tanifuji, N.; Yoshida, Y. *Org. Biomol. Chem.* **2003**, *1*, 2298.

[25] Toyota, S.; Makino, T. *Tetrahedron Lett.* **2003**, *44*, 7775.

[26] Fletcher, S. P.; Dumur, F.; Pollard, M. M.; Feringa, B. L. *Science*, **2005**, *310*, 80.

[27] Koumura, N.; Zijlstra, R. W. J.; van Delden, R. A.; Harada, N.; Feringa, B. L. *Nature* **1999**, *401*, 152.

[28] Koumura, N.; Geertsema, E. M.; van Gelder, M. B.; Meetsma, A.; Feringa, B. L. *J. Am. Chem. Soc.* **2002**, *124*, 5037.

[29] van Delden, R. A.; ter Wiel, M. K. J.; Pollard, M. M.; Vicario, J.; Koumura, N.; Feringa, B. L. *Nature* **2005**, 437, 1337–1340.

[30] Kudernac, T.; Ruangsupapichat, N.; Parschau, M.; Maciá, B.; Katsonis, N.; Harutyunyan, S. R.; Ernst, K.-H.; Feringa, B. L. *Nature* **2011**, *479*, 208.

[31] Various news organizations have covered this story, for example Discovery News [*World's Tiniest Electric Vehicle Rolls Out*, http://news.discovery.com/autos/nano-vehicle-111109.html, Nov. 9, 2011 (accessed Feb. 10, 2012).], CNN [*World's Smallest Car Fuels Nanotech Advance*, http://articles.cnn.com/2011-11-18/tech/tech_innovation_nano-car-electric_1_molecule-nanotech-nano-sized?_s=PM:TECH, Nov. 18, 2011 (accessed Feb. 10, 2012).], and Wired [*Molecular Car Drives on Copper Roads with an Electron Burst*, http://www.wired.co.uk/news/archive/2011-11/10/molecular-car, Nov. 10, 2011 (accessed Feb. 10, 2012).].

[32] Allen, M.; Moir, R. Y. *Can. J. Chem.* **1959**, *37*, 1799.

[33] Kwart, H.; Alekman, S. *J. Am. Chem. Soc.* **1968**, *90*, 4482.

[34] Bergman, J. J.; Chandler, W. D. *Can. J. Chem.* **1972**, *50*, 353.

[35] Kessler, H.; Rieker, A.; Rundel, W. *Chem. Commun.* **1968**. 475.

[36] Nelander, B.; Sunner, S. *J. Am. Chem. Soc.* **1972**, *94*, 3576. See also Ref. 35.

[37] Lauer, D.; Staab, H. A. *Chem. Ber.* **1969**, *102*, 1631.

[38] (a) van der Linde, R.; Dornseiffen, J. W.; Veenland, J. U.; de boer, T. J. *Tetrahedron Lett.* **1968**, 525. (b) Montaudo, G.; Caccamese, S; Finocchiaro, P.; Bottino, F. *Tetrahedron Lett*. **1970**, 887. (c) Montaudo, G.; Caccamese, S.; Finocchiaro, P. *J. Am. Chem. Soc*. **1971**, *93*, 4202. (d) Montaudo, G.; Caccamese, S.; Finocchiaro, P. *J. Am. Chem. Soc*. **1971**, *93*, 4208. (e) Montaudo, G.; Caccamese, S.; Finocchiaro, P. *J. Am. Chem. Soc*. **1971**, *93*, 4214. (f) Weissensteiner, W. *Monatsh. Chem.* **1992**, *123*, 1135. (g) Strekowski, L.; Lee, H.; Lin, S.-Y.; Czarny, A.; Van Derveer, D. *J. Org. Chem*. **2000**, *65*, 7703.

[39] (a) Clayden, J.; Pink, J. H. *Angew. Chem. Int. Ed.* **1998**, *37*, 1937. (b) Bragg, R. A.; Clayden, J. *Org. Lett.* **2000**, *2*, 3351. (c) Johnston, E. R.; Fortt, R.; Barborak, J. C. *Magn. Res. Chem.* **2000**, *38*, 932. (d) Bragg, R. A.; Clayden, J.; Morris, G. A.; Pink, J. H. *Chem. Eur. J.* **2002**, *8*, 1279.

[40] (a) Newman, M. S.; Deno, N. C. *J. Am. Chem. Soc.* **1951**, *73*, 3644. (b) Deno, N. C.; Jaruzelski, J. J.; Schriesheim, A. *J. Org. Chem.* **1953**, *18*, 155.

[41] (a) Colter, A. K.; Schuster, I. I.; Kurland, R. J. *J. Am. Chem. Soc.* **1965**, *87*, 2278. (b) Kurland, R. J.; Schuster, I. I.; Colter, A. K. *J. Am. Chem. Soc.* **1965**, *87*, 2279. (c) Schuster, I. I.; Colter, A. K.; Kurland, R. J. *J. Am. Chem. Soc.* **1968**, *90*, 4679.

[42] Mislow, K. *Acc. Chem. Res.* **1976**, *9*, 26. and references cited therein.

[43] Gust, D.; Mislow, K. *J. Am. Chem. Soc.* **1973**, *95*, 1535.

[44] Hummel, J. P.; Gust, D.; Mislow, K. *J. Am. Chem. Soc.* **1974**, *96*, 3679.

[45] (a) Andose, J. D.; Mislow, K. *J. Am. Chem. Soc.* **1974**, *96*, 2168. (b) Finocchiaro, P.; Gust, D.; Mislow, K. *J. Am. Chem. Soc.* **1974**, *96*, 2165.

[46] Finocchiaro, P.; Gust, D.; Mislow, K. *J. Am. Chem. Soc.* **1974**, *96*, 3198.

[47] (a) Rappoport, Z.; Biali, S. E. *Acc. Chem. Res.* **1988**, *21*, 442. (b) Schmittel, M.; Keller, M.; Burghart, A.; Rappoport, Z.; Langels, A. *J. Chem. Soc., Perkin Trans. 2* **1998**, 869

[48] Adams, R.; Campbell, J. *J. Am. Chem. Soc.* **1950**, *72*, 153.

[49] Hutchings, M. G.; Nourse, J. G.; Mislow, K. *Tetrahedron*. **1974**, *30*, 1535.

[50] Hutchings, M. G.; Andose, J. D.; Mislow, K. *J. Am. Chem. Soc.* **1975**, *97*, 4562.

[51] Schlögl, K.; Weissenheimer, W.; Widhalm, M. *J. Org. Chem.* **1982**, *47*, 5025.

[52] Rappoport, Z.; Biali, S. E. *Acc. Chem. Res.* **1997**, *30*, 307.

[53] Patton, A.; Dirks, J. W.; Gust, D. *J. Org. Chem.* **1979**, *44*, 4749.

[54] (a) Gust, D. *J. Am. Chem. Soc.* **1977**, *99*, 6980. (b) Gust, D.; Patton, A. *J. Am. Chem. Soc.* **1978**, *100*, 8175. (c) Pepermans, H.; Willem, R.; Gielen, M.; Hoogzand, C. *J. Org. Chem.* **1986**, *51*, 301.

[55] Brydges, S.; McGlinchey, M. J. *J. Org. Chem.* **2002**, *67*, 7688.

[56] Hrovat, D. A.; Borden, W. T.; Eaton, P. E.; Kahr, B. *J. Am. Chem. Soc.* **2001**, *123*, 1289.

[57] (a) Cozzi, F; Cinquini, M.; Annunziata, R.; Dwyer, T.; Siegel, J. S. *J. Am. Chem. Soc.* **1992**, *114*, 5729. (b) Cozzi, F.; Cinquini, M.; Annunziata, R.; Siegel, J. S. *J. Am. Chem. Soc.* **1993**, *115*, 5330. (c) Cozzi, F.; Ponzini, M.; Cinquini, R.; Annunziata, R.; Siegel, J. S. *Angew. Chem. Int. Ed. Engl.* **1995**, *34*, 1019.

[58] Cozzi, F.; Annunziata, R.; Benaglia, M.; Baldridge, K. K.; Aguirre, G.; Estrada, J.; Sritana-Anant, Y.; Siegel, J. S. *Phys. Chem. Chem. Phys.* **2008**, *10*, 2686.

[59] Bachrach, S. M. *J. Phys. Chem. A.* **2011**, *115*, 2396.

[60] (a) Nakamura, M.; Ōki, M.; Nakashini, H. *J. Am. Chem. Soc.* **1973**, *95*, 7169. (b) Nakamura, M. Ōki, M.; Nakashini, H. *Bull. Chem. Soc. Jpn.* **1974**, *47*, 2415.

[61] Allinger, N. L.; Hirsch, J. A.; Miller, M. A.; Tyminski, I. J.; Van-Catledge, F. A. *J. Am. Chem. Soc.* **1968**, *90*, 1199.

[62] Durig, J. R.; Craven, S. M.; Bragin, J. *J. Chem. Phys.* **1972**, *52*, 2046.

[63] Suzuki, F.; Ōki, M.; Nakanishi, H. *Bull. Chem. Soc. Jpn.* **1974**, *47*, 3114.

[64] Yamamoto, G.; Ōki, M. *Chem. Commun.* **1974**, 713.

[65] Nakamura, M.; Ōki, M. *Bull. Chem. Soc. Jpn.* **1975**, *48*, 2106.

[66] For an account of his work in this field, see: Kelly, T. R. *Acc. Chem. Res.* **2001**, *34*, 514.

[67] Kelly, T. R.; Bowyer, M. C.; Bhaskar, K. V.; Bebbington, D.; Garcia, A.; Lang, F.; Kim, M. H.; Jette, M. P. *J. Am. Chem. Soc.* **1994**, *116*, 3657.

[68] Kelly, T. R.; Tellitu, I.; Sestelo, J. P. *Angew. Chem. Int. Ed.* **1997**, *36*, 1866.

[69] Kelly, T. R.; Sestelo, J. P.; Tellitu, I. *J. Org. Chem.* **1998**, *63*, 3655.

[70] Kelly, T. R.; Silva, R. A.; De Silva, H.; Jasmin, S.; Zhao, Y. *J. Am. Chem. Soc.* **2000**, *122*, 6935.

[71] Kelly, T. R.; Cai, X.; Damkaci, F.; Panicker, S. B.; Tu, B.; Bushell, S. M.; Cornella, I.; Piggott, M. T.; Salives, R.; Cavero, M.; Zhao, Y.; Jasmin, S. *J. Am. Chem. Soc.* **2007**, *129*, 376.

[72] (a) Suzuki, F.; Ōki, M. *Tetrahedron Lett.* **1974**, *15*, 2845. (b) Suzuki, F.; Oki, M. *Bull. Chem. Soc. Jpn.* **1975**, *48*, 596.

[73] Kono, M.; Kihara, H.; Nakamura, N.; Suzuki, F.; Ōki, M. *Bull. Chem. Soc. Jpn.* **1979**, *52*, 1686.

[74] (a) Yamamoto, G.; Ōki, M. *Chem. Lett.* **1979**, 1251. (b) Yamamoto, G.; Oki, M. *Bull. Chem. Soc. Jpn.* **1981**, *54*, 473

[75] Yamamoto, G. *Bull. Chem. Soc. Jpn.* **1989**, *62*, 4058.

[76] Yamamoto, G.; Ōki, M. *Bull. Chem. Soc. Jpn.* **1986**, *59*, 3597.

[77] For an earlier work with only one methyl substituent on the phenyl ring, see: (a) Yamamoto, G.; Ōki, M. *Chem. Lett.* **1979**, 1255. and (c) Yamamoto, G.; Oki, M. *Bull. Chem. Soc. Jpn.* **1981**, *54*, 481.

[78] Yamamoto, G.; Ōki, M. *J. Org. Chem.* **1983**, *48*, 1233.

[79] Nachbar Jr., R. B.; Hounshell, W. D.; Naman, V. A.; Wennerström, O.; Guenzi, A.; Mislow, K. *J. Org. Chem.* **1983**, *48*, 1227.

[80] For the crystal structure of **28**, see Ardebili, M. H. P.; Dougherty, D. A.; Mislow, K.; Schwartz, L. H.; White, J. G. *J. Am. Chem. Soc.* **1978**, *100*, 7994.

[81] Schwartz, L. H.; Koukotas, C.; Yu, C. *J. Am. Chem. Soc.* **1977**, *99*, 7710.

[82] Koo Tze Mew, P.; Vögtle, F. *Angew. Chem. Int. Ed. Engl.* **1979**, *18*, 159.

[83] (a) Toyota, S.; Yamamori, T.; Asakura, M.; Ōki, M. *Bull. Chem. Soc. Jpn.* **2000**, *73*, 205. (b) Toyota, S.; Yamamori, T.; Makino, T.; Ōki, M. *Bull. Chem. Soc. Jpn.* **2000**, *73*, 2591. (c) Toyota, S.; Yamamori, T.; Makino, T. *Tetrahedron* **2001**, *57*, 3521.

[84] Iwamura, H.; Mislow, K. *Acc. Chem. Res.* **1988**, *21*, 175. and references cited therein.

[85] Cozzi, F.; Guenzi, A.; Johnson, C. A.; Mislow, K. *J. Am. Chem. Soc.* **1981**, *103*, 957.

[86] Kawada, Y.; Iwamura, H. *J. Am. Chem. Soc.* **1981**, *103*, 958.

[87] Hounshell, W. D.; Johnson, C. A.; Guenzi, A.; Cozzi, F.; Mislow, K. *Proc. Natl. Acad. Sci.* **1980**, *77*, 6961.

[88] Johnson, C. A.; Guenzi, A.; Nachbar, R. B., Jr.; Blount, J. F.; Wennerstroem, O.; Mislow, K. *J. Am. Chem. Soc.* **1982**, *104*, 5163.

[89] This value assumes a $C(9)_{Tp}$–CH_2 distance of 1.54 Å.

[90] It was calculated that the transition state to gear slippage actually involves C_s conformation that deviates slightly from C_{2v} symmetry. See Bürgi, H.-B.; Hounshell, W. D.; Nachbar, R. B., Jr.; Mislow, K. *J. Am. Chem. Soc.* **1983**, *105*, 1427.

[91] Experimental confirmation of barriers to gear slippage requires analysis of barriers of diastereomerization in phase isomers of desymmetrically labeled Tp rotators. This concept is explained, and data for many desymmetrized systems is supplied, in ref. 84, and references therein. The barrier of gear slippage cannot be calculated for **4** because the three propeller blades are equal by symmetry.

[92] Table 1.1 was copied verbatim from Table 1 in Ref. 84

[93] Thioether (a) Kawada, Y.; Ishikawa, J.; Yamazaki, H.; Koga, G.; Murata, S.; Iwamura, H. *Tetrahedron Lett.* **1987**, *28*, 445. Carbinol Ref 10c. Ketone (b) Johnson, C. A.; Guenzi, A.; Nachbar, Jr., R. B.; Bount, J. F.; Wennerström, O.; Mislow, K. *J. Am. Chem. Soc.* **1982**, *104*, 5163. Silane Ref 5o in Ref 84. Amine (c) Kawada, Y.; Yamazaki, H.; Koga, G.; Murata, S.; Iwamura, H. *J. Org. Chem.* **1986**, *51*, 1472.

[94] Kawada, Y.; Sakai, H.; Oguri, M.; Koga, G. *Tetrahedron Lett.* **1994**, *35*, 139.

[95] Setaka, W.; Nirengi, T.; Kabuto, C.; Kira, M. *J. Am. Chem. Soc.* **2008**, *130*, 15762.

[96] Table 1.2 was modified from Table 2 in reference 84.

[97] Johnson, C. A.; Guenzi, A.; Mislow, K. *J. Am. Chem. Soc.* **1981**, *103*, 6240.

[98] (a) Koga, N.; Kawada, Y.; Iwamura, H. *J. Am. Chem. Soc.* **1983**, *105*, 5498. (b) Koga, N.; Kawada, Y.; Iwamura, H. *Tetrahedron* **1986**, *42*, 1679.

[99] Chance, J. M.; Geiger, J. H.; Mislow, K. *J. Am. Chem. Soc.* **1989**, *111*, 2326.

[100] Yamamoto, G.; Kaneko, M.; Ohkumi, M.; Minoura, M. *Chem. Lett.* **2003**, *32*, 964.

[101] Bryan, J. C.; Sachleben, R. A.; Gakh, A. A.; Bunick, G. J. *J. Chem. Crystallogr.* **1999**, *29*, 513

[102] Gakh, A. A.; Sachleben, R. A.; Bryan, J. C.; Moyer, B. A. *Tetrahedron Lett.* **1995**, *36*, 8163.

[103] For an overview of rope-skipping molecular rotors, see ref. 5, pp. 1335–1338.

[104] Toyota, S.; Shimizu, T.; Iwanaga, T.; Wakamatsu, K. *Chem. Lett.* **2011**, *40*, 312.

[105] Stevens, A. M.; Richards, C. J. *Tetrahedron Lett.* **1997**, *44*, 7805.

[106] Kao, C.-Y.; Hsu, Y.-T.; Lu, H.-F.; Chao, I.; Huang, S.-L.; Lin, Y.-C.; Sun, W.-T.; Yang, J.-S. *J. Org. Chem.* **2011**, *76*, 5782.

[107] Frantz, D. K.; Baldridge, K. K.; Siegel, J. S. *Chimia* **2009**, *63*, 201.

[108] (a) de Silva, A. P.; Gunaratne, H. Q. N.; Gunnlaugsson, T.; Huxley, A. J. M.; McCoy, C. P.; Rademacher, J. T.; Rice, T. E. *Chem. Rev.* **1997**, *97*, 1515. (b) Bell, T. W.; Hext, N. M. *Chem Soc. Rev.* **2004**, *33*, 589.

[109] Dudley, D. W. 'The Evolution of the Gear Art' Dual Printing, Buffalo, **1969**.

[110] Frantz, D. K.; Linden, A.; Baldridge, K. K.; Siegel, J. S. *J. Am. Chem. Soc.* **2012**, *134*, 1528.

[111] Nakamura, M.; Ōki, M.; Nakanishi, H.; Yamamoto, O. *Bull Chem. Soc. Jpn.* **1974**, *47*, 2415.

[112] Imashiro, F.; Takegoshi, K; Terao, T.; Saika, A. *J. Am. Chem. Soc.* **1982**, *104*, 2247.

[113] Cases in which the steric bulk of a group is not well represented by its hydrodynamic radius can often be found in systems that demonstrate interlocking of groups (*e.g.* the rotators in gear constructs **1**–**8**). Other examples include the solid-state structure of a 1:1 mixture of tris(phenylethynyl)benzene and tris[(pentafluorophenyl)ethynyl]benzene, which exhibits interlocked packing alternating molecules (see Ponzini, F.; Zagha, R.; Hardcastle, K.; Siegel, J. S. *Angew. Chem. Int. Ed.* **2000**, *39*, 2323). The structural differences between corannulene, which is well represented as a circular bowl, and 1,3,5,7,9-pentamethylcorannulene, which resembles a pentagon, also illustrate this point (see Bauert, T.; Merz. L.; Bandera, D.; Parschau, M.; Siegel, J. S.; Ernst, K.-H. *J. Am. Chem. Soc.* **2009**, *131*, 3460.).

[114] The point groups given in this discussion assume axles on one side of the rotators that are connected by a stator. By this treatment, a C_{2h} orientation of lone rotators becomes C_2-symmetric, D_{2v} becomes C_{2v}, and C_{2v} becomes C_s. The C_{2v}* orientation positions the blades of each rotator directly toward each other.

[115] Oberg, E.; Johnes, F. D.; Horton, H. L.; Ryffel, H. H. Machinery's Handbook; A Reference Book for the Mechanical Engineer, Designer, Manufacturing Engineer, Draftsman, Toolmaker, and Machinist, 26th ed.; Industrial Press: New York, 2000.

[116] In Figure 2.3, the drawings of Tp from the perspective of looking down on the axis are drawn to scale. The benzene rings have a thickness of 3.40 Å, the van der Waals diameter of a carbon atom. The hydrogen atom at the tip has a van der Waals radius of 1.20 Å. The minimum distance between axes were calculated from van der Waals contacts of inflexible Tp moieties.

[117] In Figure 2.3, the Tp groups are rendered according to the following specifications: the thickness of a benzene ring is 3.4 Å, the van der Waals radius of a carbon atom. The hydrogen atoms at the tips of the benzene rings have a van der Waals radius of 1.2 Å. The minimum distances between axles are calculated from van der Waals contacts of inflexible Tp moieties.

[118] (a) Frantz, D. K.; Sullivan, A. A.; Yasui, Y.; Linden, A.; Baldridge, K. K.; Siegel, J. S. *Org. Biomol. Chem.* **2009**, *7*, 2347. (b) Yasui, Y.; Frantz, D. K.; Siegel, J. S. *Org. Lett.* **2006**, *8*, 4989.

[119] The distances between the 4- and 4'-positions in the X-ray crystal structure of 4,4'diaryl-1,1'-ethylene-bridged derivatives of BBI range from 8.08–8.20 Å (see ref 28a)

[120] Ref. 6a and references cited therein.

[121] There are two diastereomeric C_2 conformations, whose difference in energy is 0.58 kcal/mol, for molecule **12a**. The discussion considers only the lowest energy structure.

[122] 2,3-Dihydropyrazine prefers a twisted conformation. See Wiberg, K. B.; Nakaji, D.; Breneman, C. M. *J. Am. Chem. Soc.* **1989**, *111*, 4178.

[123] Inter-axle distances are measured as the distances between the centroids calculated from the bridgehead carbons at the 9- and 10-positions of the Tp groups.

[124] The values given are based on rates that were calculated from $\Delta G^{\ddagger}_{\text{geared rotation}}$ and $\Delta G^{\ddagger}_{\text{gear slippage}}$ using the Eyring equation.

[125] Preparation of **21** from **17** is reported in: Carpenter, M. S.; Easter, W. M.; Wood, T. F. *J. Org. Chem.* **1951**, *73*, 586.

[126] Holan, G.; Samuel, E. L.; Ennis, B. C.; Hinde, R. W. *J. Chem. Soc. C.* **1967**, 20.

[127] Our synthesis of **14a** closely followed a procedure given in: Kelly, T. R.; Sestelo, J. P.; Tellitu, I. *J. Org. Chem.* **1998**, *63*, 3655.

[128] Corey, E. J.; Fuchs, P. L. *Tetrahedron Lett.* **1972**, 3769.

[129] Godinez, C. E.; Zepeda, G.; Garcia-Garibay, M. *J. Am. Chem. Soc.* **2002**, *124*, 470.

[130] Joyce, R. P.; Gainor, J. A.; Weinreb, S. M. *J. Org. Chem.* **1987**, *52*, 1177.

[131] Zhang, L.; Carroll, P.; Meggers, E. *Org. Lett.* **2004**, *6*, 521.

[132] Austin, W. B.; Bilow, N.; Kelleghan, W. J.; Lau, K. S. *J. Org. Chem.* **1981**, *46*, 2280.

[133] Siegel, J. S.; Anet, F. A. L. *J. Org. Chem.* **1988**, *53*, 2629.

[134] NMR spectra were recorded at 20 K intervals from 250 K to 150 K, then in 10 K intervals from 150 K to 250 K. No hysteresis was observed. All spectra taken from 150 K to 250 K are given in the supplementary information.

[135] A chemical example is bis(2,3-dimethyl-triptycen-9-yl)methanol) in: Guenzi, A.; Johnson, C. A.; Cozzi, F.; Mislow, K. *J. Am. Chem. Soc.* **1983**, *105*, 1438.

[136] Gutowsky, H. S.; Holm, C. H. *J. Chem. Phys.* **1956**, *25*, 1228.

[137] The values used in this discussion are derived from the standard equations for dynamic NMR measurements of interconverting signals with equal populations. If the populations are unequal, the values are quite similar (see Shanan-Atidi, H.; Bar-Eli, K. H. *J. Phys. Chem.* **1970**, *74*, 961.).

[138] Klod, S.; Kleinpeter, E. *J. Chem. Soc., Perkin Trans. 2*, **2001**, 1893.

[139] Tait, P. G. *Trans. Royal. Soc. Edinburgh* **1876**, *28*, 145. in ref. 147.

[140] Naynes, O. *Amer. Math. Monthly* **1993**, *100*, 786.

[141] Lindström, B.; Zetterström, H.-O.; *Amer. Math. Monthly.* **1991**, *98*, 340.

[142] Rolfsen, D. *Knots and Links* Publish or Perish, Berkeley, 1976; second printing with corrections: Publish or Perish, Houston, 1990. Appendix C: Table of knots and links, pp. 339–429.

[143] For a broader discussion of Borromean links in a historical context, see Cromwell, P.; Beltrami, E.; Rampichini, M. *Math. Intelligencer* **1998**, *20(1),* 53.

[144] Didron, M.; Didron, A. N. *Christian Iconography, or the History of Christian Art in the Middle Ages*, George Bell and Sons, London, 1886.

[145] Cromwell, P. *Math. Intelligencer* **1998**, *17(1)*, 3.

[146] "History of Ballantine Beer" <http://ballantineale.com/history/default.aspx>, Feb. 21, 2012.

[147] Wasserman, E. *J. Am. Chem. Soc.* **1960**, *82*, 4433.

[148] Frisch, H. L.; Wasserman, E. *J. Am. Chem. Soc.* **1961**, *83*, 3789.

[149] van Gulick, N. *New J. Chem.* **1993**, *17*, 619.

[150] Walba, D. *New. J. Chem.* **1993**, *17*, 618.

[151] Tauber, S. J. *J. Res. Nat. Bur. Stand.* **1963**, *67A*, 591.

[152] Fox, R. H. "A quick trip through knot theory" in *Topology of 3-manifolds and Related Topics*, ed.: M. K. Fort, Prentice-Hall, Inc., **1962**, 120–167. in ref. 145.

[153] Liang, C.; Mislow, K. *J. Math. Chem.* **1995**, *18*, 1.

[154] Liang, C.; Mislow, K. *J. Math. Chem.* **1994**, *16*, 1.

[155] (a) Sauvage, J.-P. and Dietrich-Buchecker, C., eds. *Molecular Catenanes, Rotaxanes, and Knots: A Journey through the World of Molecular Topology*, Wiley-VCH: Weinheim, 1999. (b) Schill, G. *Catenanes, Rotaxanes, and Knots*, Academic Press: New York, 1971.

[156] Mislow, K. *J. Top Stereochem.* **1999**, *22*, 1.

[157] Walba, D. M.; Homan, T. C.; Richards, R. M.; Haltiwanger, R. C. *New. J. Chem.* **1993**, *17*, 661.

[158] For a recent review on the chemistry of links and knots, see Stoddart, J. F. *Chem. Soc. Rev.* **2009**, *38*, 1802.

[159] Siegel, J. S. *Science* **2004**, *304*, 1256.

[160] Mao, C.; Sun, W. Seeman, N. C. *Nature*, **1997**, *386*, 137.

[161] (a) Seeman, N. C. *Acc. Chem. Res.* **1997**, *30*, 357. (b) Seeman, N. C. *Angew. Chem. Int. Ed.* **1998**, *37*, 3220. (c) Seeman, N. C. *Molec. Biotech.* **2007**, *37*, 246.

[162] Chen, J.; Seeman, N. C. *J. Nature* **1991**, *350*, 631.

[163] Zhang, Y.; Seeman, N. C. *J. Am. Chem. Soc.* **1994**, *116*, 1661.

[164] Cantrill, S.J.; Chichak, K. S.; Peters, A. J.; Stoddart, J. F. *Acc. Chem. Res.* **2005**, *38*, 1.

[165] Chichak, K. S.; Cantrill, S. J.; Rease, A. R.; Chiu, S.-H.; Cave, G. W. V.; Atwood, J. L.; Stoddart, J. F. *Science* **2004**, *304*, 1308.

[166] For a review of reversible imine formation in directed assembly, see Meyer, C. D.; Joiner, C. S.; Stoddart, J. F. *Chem. Soc. Rev.* **2007**, *36*, 1705.

[167] For a recent review of metal-templated synthesis of links and knots, see Beves, J. E.; Blight, B. A.; Campbell, C. J.; Leigh, D. A.; McBurney, R. T. *Angew. Chem. Int. Ed.* **2011**, *50*, 9260.

[168] For a recent article that examines the dynamic behavior of Stoddart's Borromean links, see: Meyer, C. D.; Forgan, R. S. Chichak, K. S.; Peters, A. J.; Tangchaivang, N.;

Cave, G. W. V.; Khan, S. I.; Cantrill, S. J.; Stoddart, J. F. *Chem. Eur. J.* **2010**, *16*, 12570.

[169] (a) Chichak, K. S.; Peters, A. J.; Cantrill, S. J.; Stoddart, J. F. *J. Org. Chem.* **2005**, *70*, 7956. (b) Chichak, K. S.; Cantrill, S. J.; Stoddart, J. F. *Chem. Commun.* **2005**, 3391.

[170] Pentecost, C. D.; Peters, A. J.; Chichak, K. S.; Cave, G. W. V.; Cantrill, S. J.; Stoddart, J. F. *Angew. Chem. Int. Ed.* **2006**, *45*, 4099.

[171] Pentecost, C. D.; Tangchaivang, N.; Cantrill, S. J.; Chichak, K. S.; Peters, A. J.; Stoddart, J. F. *J. Chem. Ed.* **2007**, *84*, 855.

[172] *Chem. Commun.* **2005**, 3394.

[173] Schmittel, M.; He, B.; Fan, J.; Bats, J. W.; Engeser, M.; Schlosser, M.; Deiseroth, H.-J. *Inorg. Chem.* **2009**, *48*, 8192.

[174] Loren, J. C.; Yoshizawa, M.; Haldimann, R. F.; Linden, A.; Siegel, J. S. *Angew. Chem. Int. Ed.* **2003**, *42*, 5702.

[175] Loren, J. C. *Synthesis of Topological Isomers from Manisyl-Substituted Polypyridine Ligands*. Ph.D. Dissertation, University of California, San Diego, La Jolla, CA, 2004.

[176] Klosterman, J. K. *Synthesis and Properties of Manisyl-Substituted Pyridyl-1,10-phenanthrolines and the Chemical Topology of Interlocking Rings*, Ph.D. Dissertation, University of Zurich, Zurich, Switzerland, 2007.

[177] For Stoddarts first ring-in-ring complex, see: Chiu, S.-H.; Pease, A. R.; Stoddart, J. F.; White, A. J. P.; Williams, D. J. M. *Angew. Chem. Int. Ed.* **2002**, *41*, 270.

[178] Forgan, R. S.; Spruell, J. M.; Olsen, J.-C.; Stern, C. L.; Stoddart, J. F. *Mex. Chem. Soc.* **2009**, *53*, 134.

[179] Forgan, R. S.; Wang, C.; Friedman, D. C.; Spruell, J. M.; Stern, C. L.; Sarjeant, A. A.; Cao, D.; Stoddart, J. F. *Chem. Eur. J.* **2012**, *18*, 202.

[180] Carlucci, L.; Ciani, G.; Proserpio, D. M. *Cryst. Eng. Comm.* **2003**, *5*, 269.

[181] Tong, M. L.; Chen, X.-M.; Ye, B.-H.; Ji, L.-N. *Angew. Chem. Int. Ed.* **1999**, *38*, 2237.

[182] (a) Dobrzańska, L.; Raubenheimer, H. G.; Barbour, L. J. *Chem. Commun.* **2005**, 5050. (b) Byrne, P.; Lloyd, G. O.; Clarke, N.; Steed, J. W. *Angew. Chem. Int. Ed.* **2008**, *120*, 5845. (c) Adarsh, N. N.; Dastidar, P. *Cryst. Growth Des.* **2010**, *10*, 483. (d) Zhang, X.-L.; Guo, C.-P.; Yang, Q.-Y.; Wang, W.; Liu, W.-S.; Kang, B.-S.; Su, C.-Y. *Chem. Commun.* **2007**, 4242. (e) Zhang, X.-L.; Guo, C.-P.; Yang, Q.-Y.; Lu, T.-B.; Tong, Y.-X.; Su, C.-S. *Chem. Mater.* **2007**, *19*, 4630. (f) Lü, X.-Q.; Pan, M.; He, J.-R.; Cai, Y.-P.; Kang, B.-S.; Su, C.-Y. *Cryst. Eng. Comm.* **2006**, *8*, 827. (g) Sun, J.-

K.; Yao, Q.-X.; Tian, Y.-T.; Wu, L.; Zhu, G.-S.; Chen, R.-P.; Zhang, J. *Chem. Eur. J.* **2012**, *18*, 1924.

[183] Wu, H.; Brittain, S.; Anderson, J.; Grzybowski, B.; Whitesides, S.; Whitesides, G. M. *J. Am. Chem. Soc.* **2000**, *122*, 12691.

[184] Tkalec, U.; Ravnik, M.; Čopar, S.; Žumer, S.; Muševič, I. *Science* **2011**, *333*, 62.

[185] The *transoid* conformation is preferred over the *cisoid* conformation by ~ 6 kcal/mol. See: Howard, S. T. *J. Am. Chem. Soc.* **1996**, *118*, 10269.

[186] Stenberg, V. I.; Kubik, D. A. *J. Org. Chem.* **1974**, *39*, 2815.

[187] For a review on ketal formation, see Meskens, F. A. J. *Synthesis* **1981**, 501.

[188] Though once abandoned, the term *ketal* has been reinstated as a subclass of *acetal* by IUPAC and the term *thioketal* will be used throughout this Section of the thesis. See "Ketals" *IUPAC Gold Book* http://goldbook.iupac.org/K03376.html, (accessed Jan. 18, 2012).

[189] Greene, T. W.; Wuts, P. G. M. *Protective Groups in Organic Synthesis*, 3rd ed., Wiley-VCH: New York, 1999. and references cited therein.

[190] Arbuzov, B. A.; Strel'nik, D. Y.; Il'yasov, K. A.; Klochkov, V. V.; Klimovitskii, E. N. *J. Gen. Chem. USSR (Engl. Transl.)*, **1988**, *58*, 2409, 2143.

[191] Patney, H. *Synth. Commun.* **1993**, *23*, 1829.

[192] Buemi, G.; Zuccarello, F. *Theochem.* **1995**, *334*, 59.

[193] Zhang, X.; Han, J.-B.; Li, P.-F.; Ji, X. Zhang, Z. *Synth. Commun.* **2009**, *39*, 3804.

[194] Zysman-Colman, E.; Arias, K.; Siegel, J. S. *Can. J. Chem.* **2009**, *87*, 440.

[195] Lai, Y.-H.; Yap, A. H.-T. *J. Chem. Soc. Perkin Trans. 2* **1993**, 1373.

[196] (a) Ref (Lai), (b) Cachia, P.; Wahl, H. *Bull. Soc. Chem. France* **1958**, 1418. (c) Maiereanu, C.; Schmitt, C.; Le Nouen, D.; Defoin, A.; Tarnus, C.; Schifano-Faux, N. *Bioorg. Med. Chem.* **2011**, *19*, 5716.

[197] The Sandmeyer procedure followed that reported in Ito, N.; Watahiki, T.; Maesawa, T.; Maegawa, T.; Sajiki, H. *Synthesis* **2008**, 1467.

[198] See supplementary information for: Wilson, J. N.; Windscheif, P. M.; Evans, U.; Myrick, M. L.; Bunz, U. H. F. *Macromolecules* **2002**, *35*, 8681.

[199] *Carbon tetrachloride*; MSDS No. 319961; Sigma–Aldrich: Buchs, Switzerland, January 9, 2012,http://www.sigmaaldrich.com/MSDS/MSDS/DisplayMSDSPage.do?country=CH&language=en&productNumber=319961&brand=SIAL&PageToGoToURL=http%3A%2F%2Fwww.sigmaaldrich.com%2Fcatalog%2FProductDetail.do%3F

D7%3D0%26N5%3DSEARCH_CONCAT_PNO%257CBRAND_KEY%26N4%3D319961%257CSIAL%26N25%3D0%26QS%3DON%26F%3DSPEC (accessed February 29, 2012).

[200] For the preparation of compound **137**, see page 180.

[201] (a) Ishiyama, T.; Itoh, Y.; Kitano, T.; Miyaura, N. *Tetrahedron Lett.* **1997**, *38*, 3447. (b) Phan, N. T. S.; Van Der Sluys, M.; Jones, C. W. *Adv. Synth. Catal.* **2006**, *348*, 609.

[202] Miyaura, N.; Suzuki, A. *Chem. Rev.* **1995**, *95*, 2457.

[203] (a) Ref. 201a. (b) Takaoka, S.; Nakade, K.; Fukuyama, Y. *Tetrahedron Lett.* **2002**, *43*, 6919. (c) Shim, Y. S.; Kim, K. C.; Chi, D. Y.; Lee, K.-H.; Cho, H. *Bioorg. Med. Chem. Lett.* **2003**, *13*, 2561. (d) Brimble, M. A.; Lai, M. Y. H. *Org. Biomol. Chem.* **2003**, *1*, 2084. (e) Kalinin, A. V.; Reed, M. A.; Norman, B. H.; Snieckus, V. *J. Org. Chem.* **2003**, *68*, 5992. (f) Kamisuki, S.; Takahashi, S.; Mizushina, Y.; Hanashima, S.; Kuramochi, K.; Kobayashi, S.; Sakaguchi, K.; Nakata, T.; Sugawara, F. *Tetrahedron* **2004**, *60*, 5695. (g) Esumi, T.; Wada, M.; Mizushima, E.; Sato, N.; Kodama, M.; Asakawa, Y.; Fukuyama, Y. *Tetrahedron Lett.* **2004**, *45*, 6941. (h) Anemian, R.; Cupertino, D. C.; Mackie, P. R.; Yeates, S. G. *Tetrahedron Lett.* **2005**, *46*, 6717. (i) Yin, H.; Lee, G.-i.; Sedey, K. A.; Kutzki, O.; Park, H. S.; Orner, B. P.; Ernst, J. T.; Wang, H.-G.; Sebti, S. M.; Hamilton, A. D. *J. Am. Chem. Soc.* **2005**, *127*, 10191. (j) Kutzki, O.; Park, H. S.; Ernst, J. T.; Orner, B. P.; Yin, H.; Hamilton, A. D. *J. Am. Chem. Soc.* **2002**, *124*, 11838. (k) Yin, H.; Lee, G.-I.; Hyung, S. P.; Payne, G. A.; Rodriguez, J. M.; Sebti, S. M.; Hamilton, A. D.; *Angew. Chem. Int. Ed.* **2005**, *44*, 2704. (l) (c) Ishikawa, S.; Manabe, K. *Chem. Commun.* **2006**, 2589. (m) Turner, D. J.; Anemian, R.; MacKie, P. R.; Cupertino, D. C.; Yeats, S. G.; Turner, M. L.; Spivey, A. C. *Org. Biomol. Chem.* **2007**, *5*, 1752. (n) Murr, M. D.; Cano, C.; Golding, B. T.; Hardcastle, I. R.; Curtin, N. J.; Griffin, R. J.; Hummersome, M.; Frigerio, M.; Menear, K.; Richardson, C.; Smith, G. C. M. *Bioorg. Med. Chem. Lett.* **2008**, *18*, 4885. (o) Hioki, H.; Shima, N.; Kawaguchi, K.; Harada, K.; Kubo, M.; Esumi, T.; Hashimoto, T.; Asakawa, Y.; Fukuyama, Y.; Nishimaki-Mogami, T.; Sawada, J.-i. *Bioorg. Med. Chem. Lett.* **2009**, *19*, 738. Sangvikar, Y.; Schlüter, A. D.; Sakamoto, J.; Fischer, K.; Schmidt, M. *Org. Lett.* **2009**, *11*, 4112. (p) Kuramochi, K.; Tsubaki, K.; Fukudome, K.; Takeuchi, T.; Sato, Y.; Kamisuki, S.; Sugawara, F.; Kuriyama, I.; Yoshida, H.; Mizushina, Y. *Bioorg Med. Chem.* **2009**, *17*, 7227. (q) Speicher, A.; Groh, M.; Zapp, J.; Schaumlöffel, A.; Bringmann, G. *Synlett* **2009**, 1852. (r) Speicher, A.; Groh, M.; Hennrich, M.; Huynh A.-M. *Eur. J. Org. Chem.* **2010**, 6760. (s) Shetty, R. S.; Lee, Y.; Liu, B.; Husain, A.; Joseph, R. W.; Lu, Y.; Nelson, D.; Mihelcic, J.; Chao, W.; Moffett, K. K.; Schumacher, A.; Flubacher, D.; Stojanovic, A.; Bukhtiyarova, M.; Williams, K.; Lee, K.-J.; Ochman, A. R.; Saporito, M. S.; Moore, W. R.; Flynn, G. A.; Dorsey, B. D.; Spring, E. B.; Fujimoto, T.; Kelly, M. J. *J. Med. Chem.* **2011**, *54*, 179. (t) Clapham, K. M.; Golding, B. T.; Griffin, R. J.; Hardcastle, I. R.; Cano, C.; Bardos, J.; Menear, K. A.; Finlay, M.; Raymond, V.; Griffen, E. J.; Ting, A.; Turner, P. Young, G. L. *Bioorg. Med. Chem. Lett.* **2011**, *21*, 996.

[204] (a) Ref. 201a. (b) Coudret, C.; Mazenc, V. *Tetrahedron Lett.* **1997**, *38*, 5293. (c) Hardcastle, I. R.; Cockcroft, X.; Curtin, N. J.; El-Murr, M. D.; Leahy, J. J. J.;

Stockley, M.; Golding, B. T.; Rigoreau, L.; Richardson, C.; Smith, G. C. M.; Griffin, R. J. *J. Med. Chem.* **2005**, *48*, 7829. (d) Ranta, J.; Kumpulainen, T.; Lemmetyinen, H.; Efimov, A. *J. Org. Chem.* **2010**, *75*, 5178. (e) Kusuma, B. R.; Peterson, L. B.; Zhao, H.; Blagg, B. S. J.; Vielhauer, G.; Holzbeierlein, J. *J. Med. Chem.* **2011**, *54*, 6234.

[205] (a) Ref. 201a. (b) Hangeland, J. J.; Friends, T. J.; Doweyko, A. M.; Mellstroem, K.; Sandberg, J.; Grynfarb, M.; Ryono, D. E. *Bioorg. Med. Chem. Lett.* **2005**, *15*, 4579. (c) Kitamura, Y.; Sakurai, A. Udzu, T.; Maegawa, T.; Monguchi, Y.; Sajiki, H. *Tetrahedron* **2007**, *63*, 10596. (d) Gautrot, J. E.; Hodge, P.; Cupertino, D.; Helliwell, M. *New J. Chem.* **2007**, *31*, 1585. (e) Akwabi-Ameyaw, A.; Bass, J. Y.; Caldwell, R. D.; Deaton, D. N.; Kaldor, I. McFadyen, R. B.; Navas III, F.; Spearing, P. K.; Caravella, J. A.; Madauss, K. P.; Miller, A. B.; Williams, S. P.; Chen, L.; Liu, Y.; Creech, K. L.; Jones, S. A.; Marr, H. B.; Parks, D. J.; Wisely, G. B.; Todd, D. *Bioorg. Med. Chem. Lett.* **2008**, *18*, 4339. (f) Bass, J. Y.; Deaton, D. N.; McFadyen, R. B.; Mills, W. Y.; Navas III, F.; Smalley Jr., T. L.; Spearing, P. K.; Caravella, J. A.; Madauss, K. P.; Miller, A. B.; Williams, S. P.; Chen, L.; Creech, K. L.; Marr, H. B.; Parks, D. J.; Wisely, G. B.; Todd, D. *Bioorg. Med. Chem. Lett.* **2011**, *21*, 1206. (g) Genes, C.; Prado, S.; Michel, S.; Tillequin, F.; Poree, F.-H.; Lenglet, G.; Depauw, S.; Nhili, R.; David-Cordonnier, M.-H. *Eur. J. Med. Chem.* **2011**, *46*, 2117.

[206] (a) Hajduk, P. J.; Dinges, J.; Miknis, M. M.; Middleton, T.; Kempf, D. J.; Egan, D. A.; Walter, K. A.; Robins, T. S.; Shuker, S. B.; Holzman, T. F.; Fesik, S. W. *J. Med. Chem.* **1997**, *40*, 3144. (b) Firooznia, F.; Gude, C.; Chan, K.; Marcopulos, N.; Satoh, Y. *Tetrahedron Lett.* **1999**, *40*, 213. (c) Gong, L.-Z.; Pu, L. *Tetrahedron Lett.* **2001**, *42*, 7337. (d) Berger, D.; Dutia, M.; Powell, D.; Wissner, A.; DeMorin, F.; Raifeld, Y.; Weber, J.; Boschelli, F. *Bioorg. Med. Chem. Lett.* **2002**, *12*, 2989. (e) Hulme, A. N.; Barron, S. A.; Walker, A. J. *Synlett*, **2003**, 1096. (f) Robichaud, J.; Oballa, R.; Prasit, P.; Falgueyret, J.-P.; Percival, M. D.; Wesolowski, G.; Rodan, S. B.; Kimmel, D.; Johnson, C.; Bryant, C.; Venkatraman, S.; Setti, E.; Mendonca, R.; Palmer, J. T. *J. Med. Chem.* **2003**, *46*, 3709. (g) Belletete, M.; Bedard, M.; Bouchard, J.; Leclerc, M.; Durocher, G. *Can. J. Chem.* **2004**, *82*, 1280. (h) Riendeau, D.; Aspiotis, R.; Ethier, D.; Gareau, Y.; Grimm, E. L.; Guay, J.; Guiral, S.; Juteau, H.; Mancini, J. A.; Methot, N.; Rubin, J.; Friesen, R. W. *Biorg. Med. Chem. Lett.* **2005**, *15*, 3352. (i) Mewshaw, R. E.; Edsall, R. J.; Yang, C.; Manas, E. S.; Xu, Z. B.; Henderson, R. A.; Keith, J. C.; Harris, H. A. *J. Med. Chem.* **2005**, *48*, 3953. (j) Ni, A.; France, J. E.; Davies, H. M. L. *J. Org. Chem.* **2006**, *71*, 5594. (k) Trokowski, R.; Akine, S.; Nabeshima, T. *Chem. Commun.* **2008**, 889. (l) Babudri, F.; Farinola, G. M.; Martinelli, C.; Naso, F.; Cardone, A. De Cola, L.; Kottas, G. S. *Synthesis* **2008**, 1580. (m) Karg, E.-M.; Troschütz, R.; Luderer, S.; Pergola, C.; Bühring, U.; Werz, O.; Rossi, A.; Northoff, H.; Sautebin, L. *J. Med. Chem.* **2009**, *52*, 3474.

[207] "PEPPSI Catalysts" http://www.sigmaaldrich.com/chemistry/chemical-synthesis/technology-spotlights/peppsi.html, (accessed Feb. 2, 2012). and references cited therein.

[208] Kobayashi, Y.; Mizojiri, R. *Tetrahedron Lett.* **1996**, *37*, 8531.

[209] (a) Darses, S.; Genet, J.-P. *Chem. Rev.* **2007**, *107*, 288. (b) Molander, G. A.; Petrillo, D. E. *J. Am. Chem. Soc.* **2006**, *128*, 9634. (c) Molander, G. A.; Ham, J. *Org.*

Lett. **2006**, *8*, 2767. (d) Molander, G. A.; Figueroa, R. *J. Org. Chem.* **2006**, *71*, 6135. (e) Molander, G. A.; Ham, J. *Org. Lett.* **2006**, *8*, 2031. (f) Molander, G. A.; Ellis, N. M. *J. Org. Chem.* **2006**, *71*, 7491. (g) Molander, G. A.; Cooper, D. J. *J. Org. Chem.* **2007**, *72*, 3558. (h) Molander, G. A.; Febo-Ayala, W.; Ortega-Guerra, M. *J. Org. Chem.* **2008**, *73*, 6000. (i) Molander, G. A.; Cooper, D. J. *J. Org. Chem.* **2008**, *73*, 3885. (j) Molander, G. A.; Oliveira, *Tetrahedron Lett.* **2008**, *49*, 1266. (k) Molander, G. A.; Febo-Ayala, W.; Jean-Gérard, L. *Org. Lett.* **2009**, *11*, 3830.

[210] (a) Darses, S.; Genet, J.-P.; Brayer, J.-L.; Demoute, J.-P. *Tetrahedron Lett.* **1997**, *38*, 4393. (b) Genet, J.-P.; Darses, S. *Eur. J. Org. Chem.* **2003**, 4313.

[211] (a) Molander, G. A.; Ellis, N. *Acc. Chem. Res.* **2007**, *40*, 275. (b) Molander, G. A.; Canturk, B. *Angew. Chem. Int. Ed.* **2009**, *48*, 9240.

[212] Butters, M.; Harvey, J. N.; Jover, J.; Lennox, A. J. J.; Lloyd-Jones, G. C.; Murray, P. M. *Angew. Chem. Int. Ed.* **2010**, *49*, 5156.

[213] Lennox, A. J. J.; Lloyd-Jones, G. C. *Isr. J. Chem.* **2010**, *50*, 664.

[214] Molander, G. A.; Petrillo, D. E.; Landzberg, N. R.; Rohanna, J. C.; Biolatto, B. *Synlett*, **2005**, 1760.

[215] Yuen A. K. L.; Hutton, C. *Tetrahedron Lett.* **2005**, *46*, 7899.

[216] (a) Skaff, O.; Jolliffe, K. A.; Hutton, C. A. *J. Org. Chem.* **2005**, *70*, 7353. (b) Ting, R.; Adam, M. J.; Ruth, T. J.; Perrin, D. M. *J. Am. Chem. Soc.* **2005**, *127*, 13094. (c) Murphy, J. M.; Tzshucke, C. C.; Hartwig, J. F. *Org. Lett.* **2007**, *9*, 757. (d) Harvey, J. H.; Butler, B. K.; Trauner, D. *Tetrahedron Lett.* **2007**, *48*, 1661. (e) Sakai, N.; Sisson, A. L.; Bhosale, S.; Fürstenberg, A.; Banerji, N.; Vauthey, E.; Matile, S. *Org. Biomol. Chem.* **2007**, *5*, 2560. (f) Scrafton, D. K.; Taylor, J. E.; Mahon, M. F.; Fossey, J. S.; James, T. D. *J. Org. Chem.* **2008**, *73*, 2871. (g) Declamp, J. H.; Brucks, A. P.; White, M. C. *J. Am. Chem. Soc.* **2008**, *34*, 11270. (h) Kabalka, G. W.; Yao, M.-L. *J. Organomet. Chem.* **2009**, *694*, 1638. (i) Inglis, S. R.; Woon, E. C. Y.; Fischer, D. S.; Schofield, C. J.; Zervosen, A.; Gerards, T.; Teller, N.; Luxen, A. *J. Med. Chem.* **2009**, *52*, 6097. (j) Mulla, K.; Dongare, P.; Zhou, N.; Chen, G.; Thompson, D. W.; Zhao, Y. *Org. Biomol. Chem.* **2011**, *9*, 1332. (k) Kim, Y.; Jordan, R. F. *Organometallics* **2011**, *30*, 4250. (l) Fujita, T.; Ichitsuka, T.; Fuchibe, K.; Ichikawa, J. *Chem. Lett.* **2011**, *40*, 986.

[217] Boebel, T. A.; Hartwig, J. F. *J. Am. Chem. Soc.* **2008**, *130*, 7534.

[218] Batey, R. A.; Quach, T. D. *Tetrahedron Lett.* **2001**, *42*, 9099.

[219] Bagutski, V.; Ros, A.; Aggarwal, V. K. *Tetrahedron* **2009**, *65*, 9956.

[220] For a well cited overview of side reactions in transition metal-based cross-coupling reactions, see: Dörwald, F. Z. *Side Reactions in Organic Synthesis*, Wiley-VCH: Weinheim, 2005, pp. 279–308.

[221] (a) Crowley, J. D.; Goldup, S. M.; Lee, A.-L.; Leigh, D. A.; McBurney, R. T. *Chem. Soc. Rev.* **2009**, *38*, 1530. and references cited therein.

[222] Aucagne, V.; Hänni, K. D.; Leigh, D. A.; Lusby, P. J.; Walker, D. B. *J. Am. Chem. Soc.* **2006**, *128*, 2186.

[223] Aucagne, V.; Berná, J.; Crowley, J. D.; Goldup, S. M.; Hänni, K. D.; Leigh, D. A.; Lusby, P. J.; Ronaldson, V. E.; Slawin, A. M. Z.; Viterisi, A.; Walker, D. B. *J. Am. Chem. Soc.* **2007**, *129*, 11950.

[224] (a) Saito, S.; Takahashi, E.; Nakazono, K. *Org. Lett.* **2006**, *8*, 5133. (b) Berná, J.; Goldup, S. M.; Lee, A.-L.; Leigh, D. A.; Symes, M. D.; Teobaldi, G.; Zerbetto, F. *Angew. Chem. Int. Ed.* **2008**, *47*, 4392. (c) Sato, Y.; Yamasaki, R.; Saito, S. *Angew. Chem. Int. Ed.* **2009**, *48*, 504.

[225] Berná, J.; Crowley, J. D.; Goldup, S. M.; Hänni, K. D.; Lee, A.-L.; Leigh, D. A. *Angew. Chem. Int. Ed.* **2007**, *46*, 5709.

[226] Crowley, J. D.; Hänni, K. D.; Lee, A.-L.; Leigh, D. A. *J. Am. Chem. Soc.* **2007**, *129*, 12092.

[227] Goldup, S. M.; Leigh, D. A.; Lusby, P. J.; McBurney, R. T.; Slawin, A. M. Z. *Angew. Chem. Int. Ed.* **2008**, *47*, 3381.

[228] Lahlali, H.; Jobe, K.; Watkinson, M.; Goldup, S. M. *Angew. Chem. Int. Ed.* **2011**, *50*, 4151.

[229] Refs. 174 and 175

[230] Wang, Z.; Reibenspies, J.; Motekaitis, R. J.; Martell, A. E. *J. Chem. Soc. Dalton Trans.* **1995**, 1511.

[231] Breslow, R.; Garratt, Kaplan, L.; LaFollette, D. *J. Am. Chem. Soc.* **1968**, *90*, 4051.

[232] The procedure from the following reference was applied: Sengupta, S.; Purkayastha, P. *Org. Biomol. Chem.* **2003**, *1*, 436.

[233] Zheng, H.; Zhou, W.; Lv, J.; Yin, X.; Li, Y.; Liu, H.; Li, Y. *Chem. Eur. J.* **2009**, *15*, 13253.

[234] (a) Griffiths, K. E.; Stoddart, J. F. *Pure. Appl. Chem.* **2008**, *80*, 485. (b) Arico, F.; Badjic, J. D.; Cantrill, S. J.; Flood, A. H.; Leung, K. C.-F. *Top. Curr. Chem.* **2005**, *249*, 203.

[235] Schill, G. "Directed Synthesis of [2]-Catenanes" in *Catenanes, Rotaxanes, and Knots*, Academic Press: New York, 1971, pp. 77–120. and references cited therein.

[236] Greene, T. W.; Wuts, P. G. M. *Protective Groups in Organic Synthesis* (3rd ed.), John Wiley & Sons: Weinheim, 1999, pp. 329–344.

[237] Gröbel, B.-T.; Seebach, D. *Synthesis* **1977**, 357

[238] Firouzabadi, H.; Iranpoor, N. "Product Subclass 7: Deprotection of S,S-Acetals" in *Science of Synthesis* **2006**, *30*, p. 505.

[239] (a) Pettit, G. R.; van Tamelen, E. E. *Org. React.* **1962**, *12*, 356. (b) Hauptmann, H.; Walter, W. F. *Chem. Rev.* **1962**, *62*, 347.

[240] For preparation of the bromo(triisopropylsilyl)biphenyl from which zincate **154** was prepared, see page 184.

[241] Miller, G. P.; Kaur, I. Soluble, Persistent Nonacene Derivatives. U.S. Patent 20110130593, June 2, 2011.

[242] Hopff, H.; Doswald, P.; Manukian, B. K. *Helv. Chim. Acta* **1961**, *44*, 1231.

[243] Miyaura, N.; Suzuki, A. *Org. Synth.* **1990**, *68*, 130.

[244] Prepared according to a procedure from: Joyce, R. P.; Gainor, J. A.; Weinreb, S. M. *J. Org. Chem.* **1987**, *52*, 1177.

[245] Schmidt M; Baldridge, K. K.; Boatz, J. A.; Elbert, S.; Gordon, M.; Jenson, J. S.; Koeski, S.; Matsunaga, N.; Nguyen, K. A.; Su, S. J.; Windus, T. L.; Dupuis, M.; Montgomery, J. A. *J. Comp. Chem.* **1993**, *14*, 1347.

[246] Grimme, S. *J. Comput. Chem.* **2006**, *27*, 1787.

[247] Becke, A.D. *Phys. Rev. A.* **1988**, *38*, 3098.

[248] Dunning Jr., T. H.; Hay, P. J. in *Methods of Electronic Structure Theory*, ed. H. F. Schaefer III, Ed., Plenum Press, New York, 1977.

[249] Weigend, F.; Ahlrichs, R. *Phys. Chem. Chem. Phys.* **2005**, *7*, 3297.

[250] Baldridge, K. K.; Greenberg, J. P. *J. Mol. Graphics*, **1995**, *13*, 63.

[251] http://www.webmo.net/index.html.

[252] Hooft, R. *KappaCCD Collect Software*, Nonius BV, Delft, The Netherlands, 1999.

[253] Otwinowski, Z.; Minor, W. in *Methods in Enzymology*, Vol. 276, *Macromolecular Crystallography*, Part A, Eds. Carter Jr., C. W.; Sweet, R. M. Academic Press, New York, 1997, pp. 307-326.

[254] Altomare, A.; Cascarano, G.; Giacovazzo, C.; Guagliardi, A.; Burla, M. C.; Polidori, G.; Camalli, M. *SIR92*, *J. Appl. Crystallogr.* **1994**, *27*, 435.

[255] van der Sluis, P.; Spek, A. L. *Acta Crystallogr.* **1990**, *A46*, 194-201.

[256] Spek, A. L. *PLATON*, *Program for the Analysis of Molecular Geometry*, University of Utrecht, The Netherlands, 2008.

[257] (a) Maslen, E. N.; Fox, A. G.; O'Keefe, M. A. in 'International Tables for Crystallography', Ed. A.J.C. Wilson, Kluwer Academic Publishers, Dordrecht, 1992, Vol. C, Table 6.1.1.1, pp. 477-486; (b) Creagh, D. C.; McAuley, W. J. *ibid*. Table 4.2.6.8, pp. 219-222; (c) Creagh, D. C.; Hubbell, J. H. *ibid*. Table 4.2.4.3, pp. 200-206.

[258] Stewart, R. F.; Davidson, E. R.; Simpson, W. T. *J. Chem. Phys.* **1965**, *42*, 3175-3187.

[259] Ibers, J. A.; Hamilton, W. C. *Acta Crystallogr.* **1964**, *17*, 781-782.

[260] Sheldrick, G. M. *SHELXL97, Program for the Refinement of Crystal Structures*, University of Göttingen, Germany, 1997.

[261] Boyd, D. R.; Sharma, N. D.; King, A. W. T.; Shepherd, S. D.; Allen, C. C. R.; Hold, R. A.; Luckarift, H. R.; Dalton, H. *Org. Biomol. Chem.* **2004**, *2*, 554.

[262] Zhang, X.; Han, J.-B.; Li, P.-F.; Ji, X.; Zhang, Z. *Synth. Commun.* **2009**, *21*, 3804.

[263] Mousseau, J. J.; Xing, L.; Tang, N.; Cuccia, L. A. *Chem. Eur. J.* **2009**, *15*, 10030.

[264] Lai, Y.-H.; Yap, A. H.-T. *J. Chem. Soc., Perkin 2*. **1993**, *7*, 1373.

[265] Silbestri, G. F.; Lo Fiego, M. J.; Lockhart, M. T.; Chopa, A. B. *J. Organomet. Chem.* **2010**, *695*, 2578.

[266] Ashton, P. R.; Ballardini, R.; Balzani, V.; Bělohradsky, M.; Gandolfi, M. T.; Philp, D.; Prodi, L.; Raymo, F. M.; Reddington, M. V.; Spencer, M.; Stoddart, J. F.; Venturi, M.; Williams, D. J. *J. Am. Chem. Soc.* **1996**, *118*, 4931.

[267] Refs. 221 and 223.

[268] Facchetti, A.; Marks, T. J.; Wang, Z. M. Acene-based organic semiconductor materials and methods of preparing and using the same. U.S. Patent 20080185555, August 7, 2008.

Derik K. Frantz

Personal Information

Address	OCI, Universität Zürich, Winterthurerstrasse 100, 8057 Zürich, Switzerland
Date/Place of Birth	26 June 1982 / Lancaster, PA, USA
Nationality	USA
Languages:	English (native speaker), German (satisfactory)

Education

Bachelor of Science (with distinction)	**Juniata College,** Huntingdon, Pennsylvania, USA Graduation Date: May 2005 Major: Chemistry Grade Point Average: 3.6 (4.0 Scale)
Master of Science	**University of Zurich,** Zurich, Switzerland Graduation Date: January 2008 Organic Chemistry Grade Point Average: 5.5 (6.0 Scale) Research Advisor: Prof. Dr. Jay S. Siegel
PhD Student	**University of Zurich,** Zurich, Switzerland Dates: January 2008–present Organic Chemistry Research Advisor: Prof. Dr. Jay S. Siegel

Chemistry Work Experience

January 2006–present	**Research Assistant**, University of Zurich, Zurich Switzerland *Organic chemistry* research as a guest student, an MSc student and a PhD student
Fall 2007–Spring 2011	**Teaching Assistant**, University of Zurich, Zurich, Switzerland Fall Semester, 2007: Teaching assistant for "Principles of Chemistry" Spring and Fall Semesters, 2008 and 2009: Practicum assistant for "Organic Chemistry Practicum I & II" (750 total hours) Spring Semester, 2010: Teaching assistant for "Principles of Chemistry" Spring Semester, 2011: Teaching assistant for "Principles of Chemistry"
July 2005–August 2005	**Graduate Summer Intern in Chemistry**, University of Illinois at Urbana-Champaign, Department of Chemistry, Urbana, IL, USA An organic chemistry methodology research project was conducted under the supervision of Prof. Dr. Jeffrey S. Moore.
Summer 2003 & Summer 2004	**William von Liebig Undergraduate Research Fellow**, Juniata College, Huntingdon, PA, USA A project entitled "Progress in the synthesis of 1,5-methylenesemibullvalene" was undertaken under the supervision of Prof. I David Reingold.

Participation at Chemical Conferences

Oral Presentations

2009: Fall Meeting of the Swiss Chemical Society, Lausanne, Switzerland
2011: "Doktorandentag" Organic Chemistry Institute, University of Zurich
2011: Fall Meeting of the Swiss Chemical Society, Lausanne, Switzerland

Posters

2003: National Organic Symposium, Bloomington, IN, USA
2005: 229th ACS National Meeting, San Diego, CA, USA
2006, 2007, 2008, 2009, 2010: Dorothy Crowfoot Hodgkin Symposium, Zurich, Switzerland
2006, 2007, 2009, 2010: Swiss Chemical Society Meetings, Zurich and Lausanne, Switzerland
2008: EuCheMS Chemistry Congress, Torino, Italy
2009: Gordon Conference on Physical Organic Chemistry, Holderness, NH, USA
2010: EuCheMS Chemistry Congress, Nuremburg, Germany
2011: International Symposium on Novel Aromatics, Eugene, OR, USA

Honors & Awards

2001: Calvert Ellis Scholarship, Juniata College
2003: National Organic Symposium Travel Award
2004: American Chemical Society Organic Chemistry Award, Juniata College
2005: The Rockwell Chemistry Prize, Juniata College
2005: Runner-up for Fulbright Scholarship
2008: Poster Prize at Swiss Chemical Society Fall Meeting
2011: CMSZH Travel Award to ISNA Conference in Eugene, OR, USA

Service Positions

September 2008 – June 2010: Organic Chemistry Institute PhD Student Representative

June 2009 & June 2010: Organizer of Doktorandentag (chemistry symposium lead by students of the Organic Chemistry Institute, UZH); Head Organizer in 2009

Interests & Hobbies

Fitness (CrossFit), Reading (non-fiction), Film